NASA Contractor Report 3866

The Mechanisms of Flame Holding in the Wake of a Bluff Body

Roger A. Strehlow and Sarmad Malik

GRANT NAG3-60
MARCH 1985

NASA

NASA Contractor Report 3866

The Mechanisms of Flame Holding in the Wake of a Bluff Body

Roger A. Strehlow and Sarmad Malik
University of Illinois at Urbana-Champaign
Urbana, Illinois

Prepared for
Lewis Research Center
under Grant NAG3-60

National Aeronautics
and Space Administration

**Scientific and Technical
Information Branch**

1985

TABLE OF CONTENTS

LIST OF SYMBOLS

A	area
Cp	heat capacity
D_{AB}	diffusion coefficient
E	activation energy
H	enthalpy
i	indices
[I]	concentration of i^{th} species
j	indices
K	karlovitz number
L	flame thickness
l	length
Le	Lewis number
m	mass
Mw	molecular weight
N	molecular concentration
n	number of moles
P	pressure
q	heat
r	radius of curvature
r_{crit}	radius of curvature at incipient blow-off
R	gas constant
s	component along the flame direction
Su	burning velocity
S_b	velocity of burned gas

t	time
T	temperature
T_{ad}	adiabatic temperature
T_f	flame temperature
Tu	unburned mixture temperature
U_o	approach flow velocity
V	blow-off velocity
V_i	diffusion velocity
X_i	mole fraction of i^{th} species

Subscript

j	indices
k	indices
l	indices
i	indices
b	burned
u	unburned
m	mixture

Greek Symbols

α	angle
ε	reaction zone thickness
η_c	preheat zone thickness
k	thermal conductivity
ρ	density
τ	nondimensional temperature
ϕ	Equivalence ratio
Z	correction factor in Wilke's formula

CHAPTER I

Introduction

Flame stabilization is of fundamental importance in the design, efficient performance and reliable operation of high speed propulsion systems. In gas turbines and other combustion equipment, the velocities at which gases flow are much higher than the maximum flame speeds of practical fuels. Therefore regions of low velocity must be provided within the combustor to stabilize or anchor the flame. In the industrial design of combustors one can provide several techniques for anchoring the flames. Most flame stabilizing techniques use bluff bodies (such as Vee gutters and disks) placed in the main flow and such methods exploit a recirculating type of flow for anchoring the flame. All these techniques are the result of experimental work together with empirical formulations, and much work is still being done. However a clear understanding of flame holding is still needed.

In problems like these, the most logical way of tackling the problem is to simplify the flame holding process, so that many variables are removed and the flame holding mechanism can be observed in its purest form. The purpose of this study is to examine flame holding under conditions where the recirculation zone is absent, thus eliminating the complications introduced by

recirculation. This can be achieved by simply placing a streamlined thin obstacle in the flow field. If a thin metal plate is placed into a gas stream parallel to the flow, then the boundary layer on this plate produces a region of low velocity which extends into the wake of the plate. Now, if the stream is a combustible gas mixture, then a flame which ordinarily would be carried away by the high stream velocity can attach itself in the wake of the strip since the velocity in this region is much less than the stream itself. The flame will remain stationary in this region and it is said to be stabilized at a location in the plane of the center of the plate, where the gas velocity equals the burning velocity (stabilization point). This region serves as a continuous source of ignition for the neighboring gas elements whose velocity exceeds the burning velocity. As the combustion zone propagates from the holding region it assumes an angle to the direction of gas flow so that everywhere the normal component of the gas velocity equals the burning velocity. In summary, low flow velocities near the flame holder produce a laminar boundary layer which creates a velocity gradient and low velocity region that holds the flame in the wake of the obstacle.

Therefore, steady (or time average steady) combustion of fuel-air mixtures cannot be stabilized in a high velocity flow ($\bar{U} > S_u$, where S_u is the normal burning velocity and $\bar{U}$ is the time average approach flow velocity), unless the flow contains a "holding region" whose properties are adequate to continually

ignite and provide regions of low velocity in order to stabilize or anchor the flame. In essence the "holding" process is the fundamental process that determines whether or not a flame can be stabilized (in a time average sense) at a specified location in any specific apparatus for any specified approach conditions.

Due to the absence of a recirculation zone in this study, the blow-off mechanism of the inverted premixed flame that was investigated, is entirely different from the flame stabilized by bluff bodies. However, this problem is still quite involved and complex because of the coupling of fluid flow and gas expansion at the base of the flame front. Since the flame can be stabilized only at a relatively low approach velocity (U_o < 2.0 m/sec), the presence of the flame affects the structure of the approach flow.

There have been studies of the holding problem of inverted flames originally reported by Lewis and von Elbe [1], Edmondson and Heap [2], and most recently Kawamura et al [3]. Blow-off for rim held flames for a laminar approach flow has been correlated to the critical velocity gradient $\left(\partial u/\partial y\right)_{crit}$ and it has been shown empirically that the correlation can be extended to premixed fuel-air systems with different combustion properties by forming the dimensionless correlation factor $K = \partial u/\partial y \cdot \eta_o/S_u$, where η_o is the preheat zone thickness of a laminar flame, Reed [4]. While this empirical correlation is interesting and

useful, its functional similarity to the flame stretch Karlovitz number has led to the interpretation that laminar flame blow-off is due to flame stretch processes. Virtually all the experimental work to be found in the literature consists mainly of measurements of blow-off and flashback limits. In order to correlate the data, critical properties like boundary velocity gradient ($g = {}^{du}/_{dy}$), Karlovitz number, or Peclet number were introduced. These different properties are based on conflicting theories for the blow-off mechanism, Reed [5]. It would be a very useful if it were possible to show unequivocally that such a simple correlation as that provided by the flame stretch theory was adequate to describe the apparently complex problem of premixed flame stability.

The main objective of this work is to study the holding process (flame stabilization) in detail in an attempt to determine the mechanism of flame holding and also the conditions where this mechanism is viable and when it fails and blow-off occurs. In order to determine in detail the mechanisms that are operative in the flame holding region, detailed knowldge of the flow field velocity near the flame holder is required. The reason for such a study is to attempt to produce an unambiguous understanding of flame holding in at least one simple geometry. Inverted flames held in the wake of a flat strip were studied rather than rim held flames because entrainment of the surrounding air greatly complicates the rim held flame studies.

Experiments with different sizes of flame holders have been performed. The experimental set-up provides a strictly laminar flow with a constant velocity profile from a burner mouth of square cross section. The flame holders are thin enough to ensure the absence of a recirculation zone. The velocity field was determined using a non-intrusive technique, Laser Doppler Velocimetry. A "built-in" Digital RT-11 computer was linked with the electronics of the Laser Doppler Velocimeter system for data acquisition purposes to allow direct computer manipulation of the data. Additionally, observations of the inverted flame itself were obtained using schilieren and direct photography.

CHAPTER II

Fundamentals of Premixed Flames

The combustion processes that involve flames can be divided into two main categories: diffusion flames, where the rate of the combustion process is mainly controlled by the rate of inter-diffusion of oxygen and fuel; and premixed flames where the fuel and air or oxygen are premixed and the rate of combustion is controlled by a coupling of transport properties and chemical kinetics. The best example of this type of flame is the common bunsen burner flame. In burner flames the flame is propagating against the flow of the reactants and its position is stationary to an observer. Variation in input conditions such as fuel-air flow rate, or boundary conditions such as unstable holding can cause the flame to become non-stationary or unstable. A burner flame or any flame stabilized over a flame holder is usually stable over a range of velocity and composition if such variations do not cause the flame to blow-off or flashback into the burner.

One of the basic concepts in premixed flame theory is the concept of flame propagation. To discuss this consider the strictly one dimensional propagation of a combustion wave through a combustible mixture. Conceptually the laminar flow of a combustible gas, containing a thin flame sheet normal to the flow

results in a steady flow when the rate of propagation of the flame (the normal burning velocity usually refered to as S_u in literature) is exactly balanced by the normal component of the gas velocity ahead of the flame. The major purpose of any laminar premixed flame theory is to determine this velocity as well as the temperature and concentration species profiles. The absolute value of S_u depends on the oxidizer-fuel combination, but for any oxidizer-fuel combination the basic dependency of burning velocity on mixture composition is about the same. The dependence of S_u on the mixture composition for methane-air and propane-air flames are shown in figure II-1 [6]. At times it is convenient to work with the equivalence ratio ϕ rather than the mixture composition. The equivalence ratio ϕ in this figure is defined by

$$\phi = \frac{X_{fuel} / X_{ox}}{\left(X_{fuel} / X_{ox} \right)_{stoich.}} \qquad 2.1$$

where X is the mole fraction. By definition ϕ < 1.0 is a (fuel) lean mixture and ϕ > 1.0 is a (fuel) rich mixture. Observe that the curves exhibit a maximum around ϕ = 1.0 and decrease for other values of ϕ.

The adiabatic flame temperature of a flame is, strictly speaking, the temperature that would be attained by the given combustible mixture if it were allowed to approach chemical equilibrium at constant pressure with no heat loss to the surroundings. Therefore T_{ad} is the maximum temperature of the

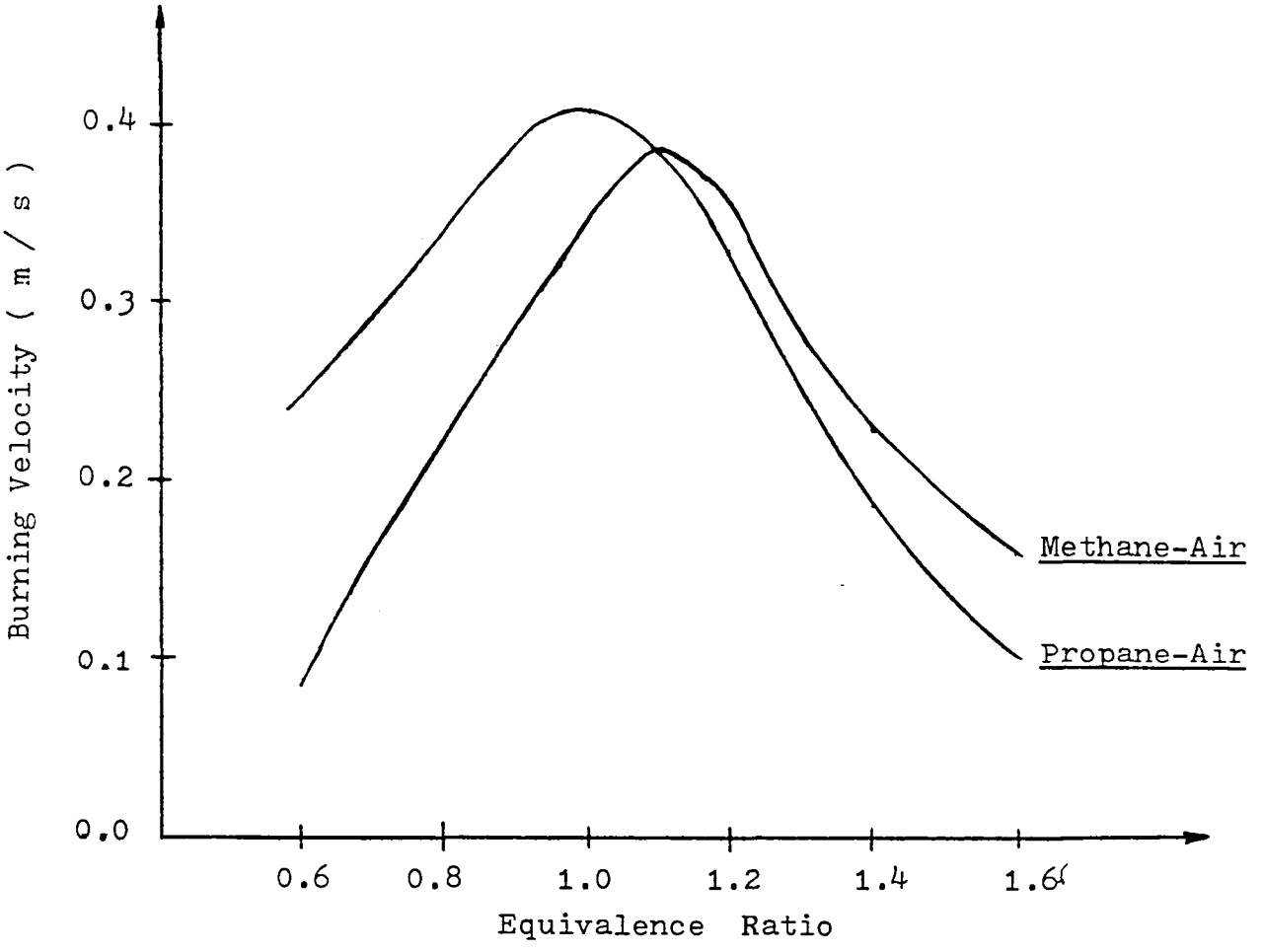

Fig. II-1. Measured Burning Velocity vs Equivalence Ratio

combustion products at chemical equilibrium. Curves of T_{ad} versus the equivalence ratio ϕ for both methane and propane are shown in figure II-2 [7].

Another important parameter of intertest for premixed flames is the flame thickness L. Typically it is determined from the measured or calculated temperature profile versus distance through a one-dimensional flame. This is shown in figure II-3, where T_u is the unburned or ambient gas temperature. A rough estimate for flame front thickness can be obtained from the empirical relation for flames in air or oxygen given by Fristrom and Westenberg [8].

$$L = \frac{2 \cdot 5}{P \cdot S_u} \; [cm]; \quad S_u \left[cm/s \right]$$

where P is the pressure in atmospheres. Linked with this parameter is the preheat zone thickness η_o . This is the region ahead of the reaction zone where the temperature increase is almost entirely due to energy transport from the reaction zone. Schematically this zone is shown in figure II-4. In this region no chemical reaction occurs, and therefore no significant heat is produced. The reaction zone thickness δ is that region of the flame where the major portion of the reaction takes place. This can be determined from the temperature profile as that region from the inflection point to the point where $T = 0.99 \times T_{ad}$ or by the intercept method shown in figure II-4.

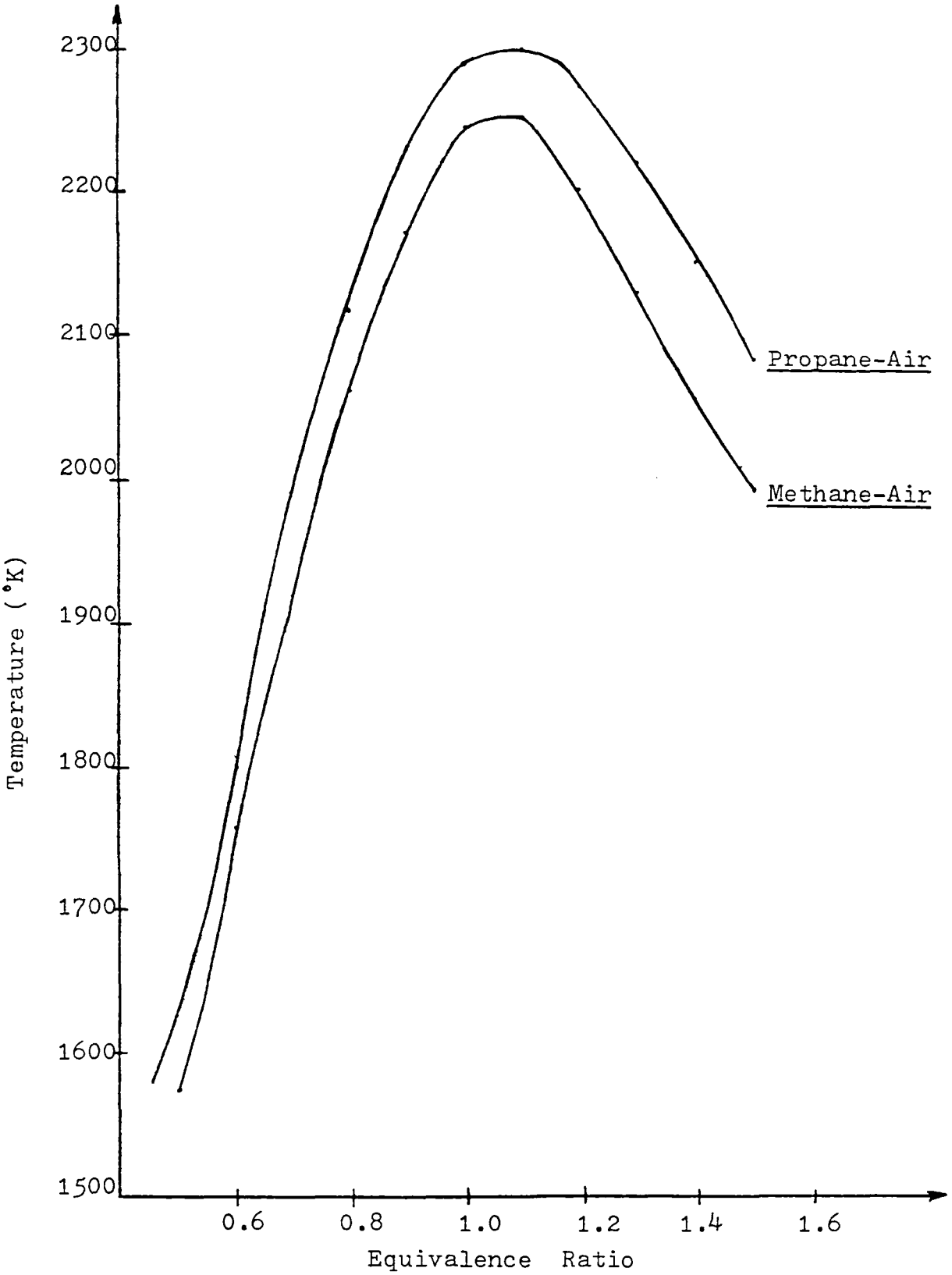

Fig. II-2. Adiabatic Flame Temperature vs Equivalence Ratio (7).

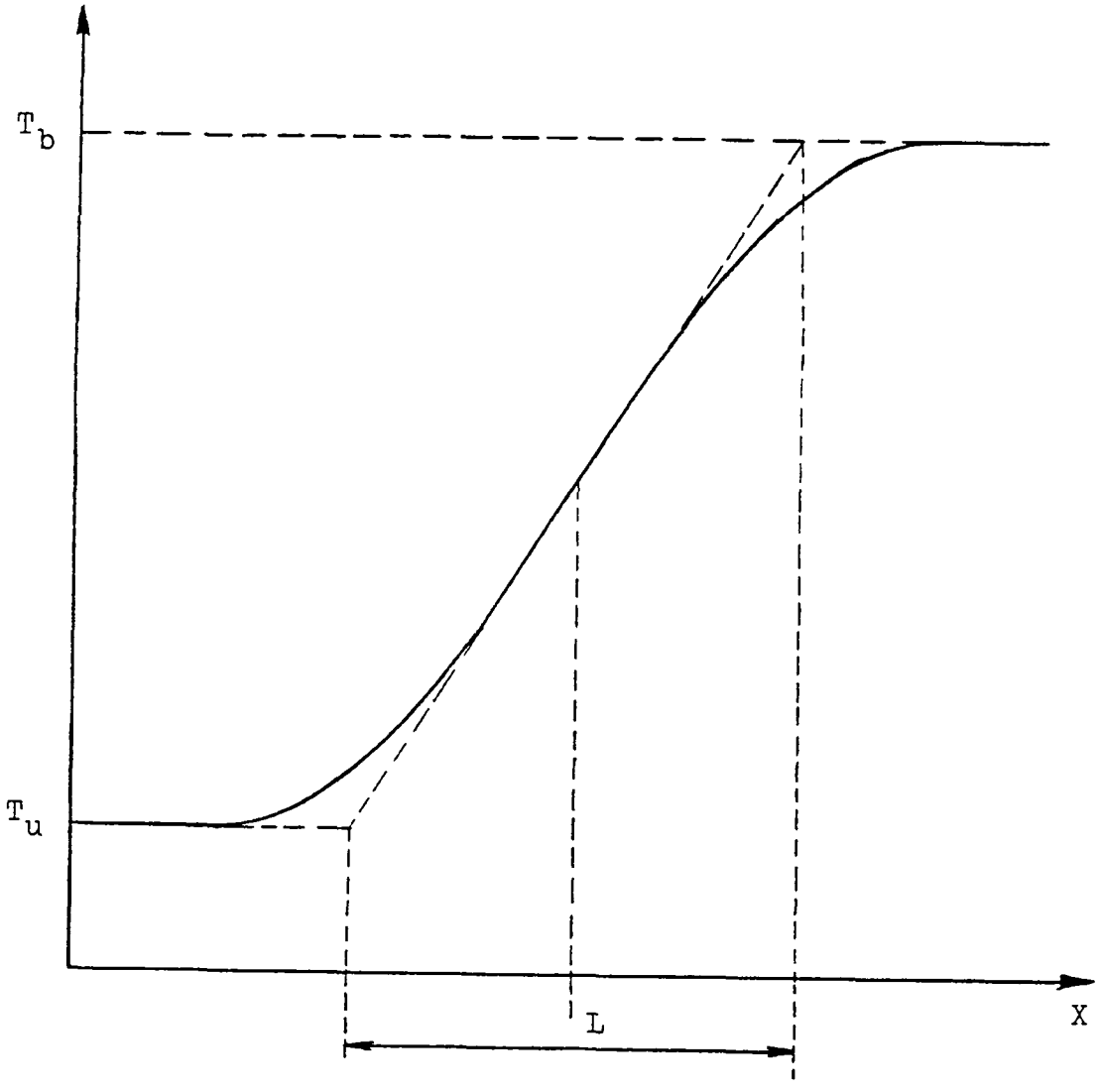

Fig. II-3. Flame Front Thickness

In view of the interdependence of the parameters in premixed flames, it should be pointed out that in the case of lean flames one should expect low burning velocity, low flame temperature and large flame thickness (~ 5-10 mm). The phenomenological behavior of these parameters is important for understanding the macroscopic behavior of laminar premixed flames, though a full understanding of the mechanism of flame propagation can be gained only by studying appropriate laminar premixed flame models.

The earlier laminar premixed flame theories were used to predict only the burning velocity. These theories were based on intuitive reasoning supported by gross physical observations, Mallard and Le Chatelier [9] developed a theory of burning velocity based entirely on heat conduction. In 1947 Tanford and Pease [10] observed that there was a strong correlation between the calculated equilibrium hydrogen atom concentration and the burning velocity in CO-air flames at various equivalence ratios. In a subsequent paper by Tanford [11] a theory based on diffusion of hydrogen atoms was compared with a thermal theory based on conduction and heat release by chemical reaction. It was concluded in this work that heat conduction was not important compared to the diffusion of hydrogen radicals (at least in CO-air flames).

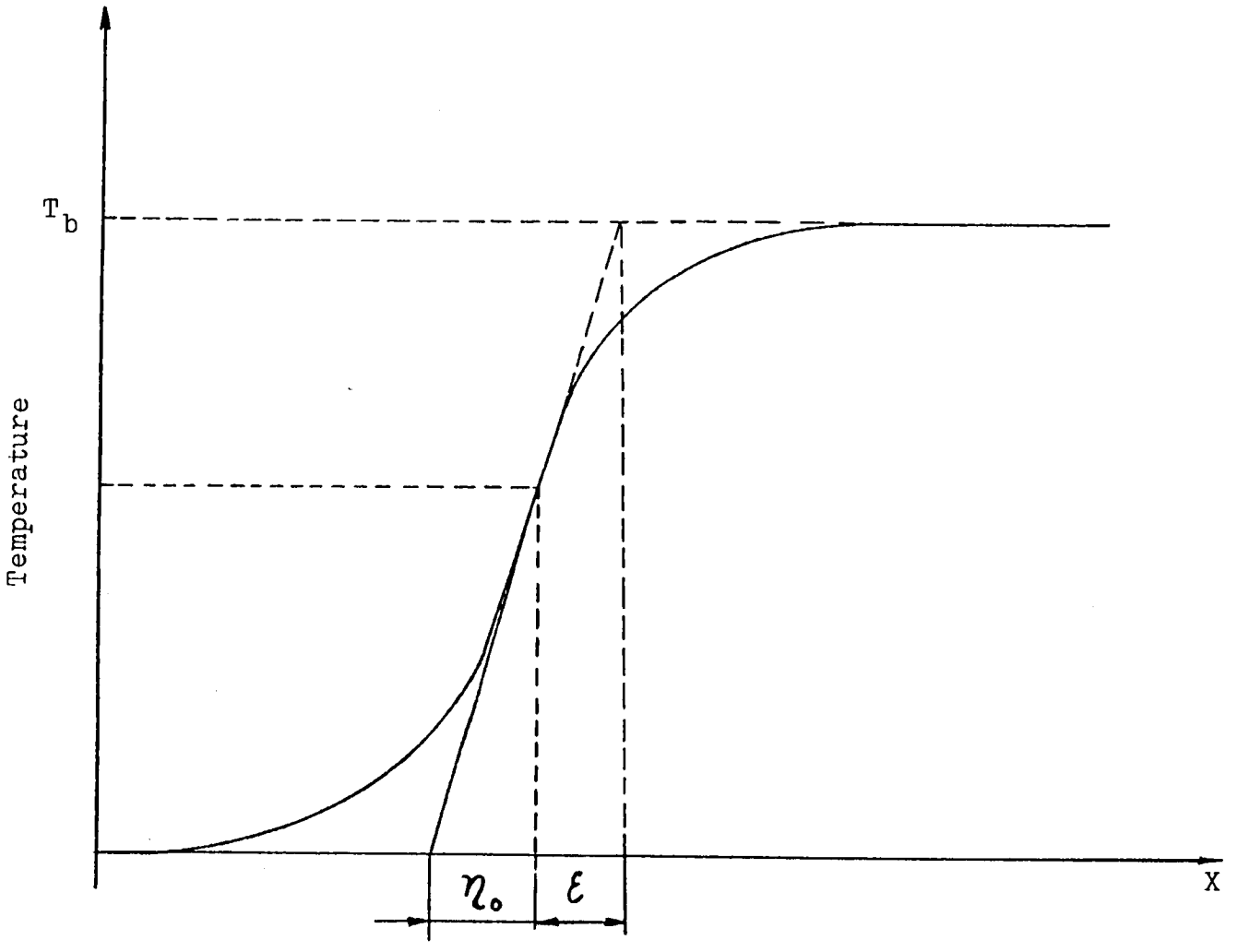

Fig. II-4. Schematic Diagram Showing the Preheat-Zone Thickness

The first attempt to model a laminar premixed flame from a continuum mechanics point of view was undertaken by Hirschfelder and Curtis [12]. In this work the hydrodynamic equations were first generalized to include diffusion and chemical kinetics and then simplifications were made by considering only the conditions appropriate for a steady one-dimensional adiabatic flame. The momentum equation can be neglected because the pressure change across the flame is very low. This can be seen by considering the Mach number, based on the burning velocity, in the one- dimensional mommentum equation given by Strehlow [13],

$$P_b - P_u = P_u \cdot \gamma \cdot \left(1 - \frac{v_b}{v_u}\right) M_{su}^2 \qquad 2.2$$

where P_b and P_u are the burned and unburned gas pressures, respectively, and v_b and v_u are the specific volumes. Substituting typical values of $v_b/v_u<15$, $\gamma \leq 1.67$ and $M_{su} <0.02$ into 2.2, we obtain $P_u-P_b \leq 0.01xP$. Hence the pressure change across a combustion wave is generally very small compared to the total pressure. Such changes in pressure have no significant effect on the processes occuring within the combustion wave, but give rise to gas motions which can affect the flow pattern ahead of the flame in two or three dimensional situations. It is important to mention here that the kinetic energy of the flow can also be neglected because the flow has such a low subsonic velocity.

The approach used by Hirschfelder and Curtis included heat conduction, diffusion, and rapid exothermic chemical reaction, which play an important part in an ordinary one-dimensional flame propagation mechanism. On the other hand the effects of radiative heat transfer, and second-order (i.e., coupled) transport effects, such as thermal diffusion were neglected in their theory.

In their theory the gas in any wave layer enclosed by planes x and x+dx is composed of various molecular species (molecules of reactants and final products, as well as intermediate products such as atoms and free radicals), which may be labelled 1,2,.... i, respectively. The number of moles of i that flow across unit area of plane x in unit time is

$$n_i (S+V_i) \qquad 2.3$$

where n_i is the number of moles i per unit volume, S is the net mass flow velocity, and V_i is the diffusion velocity of component i. The mass flow across the plane x is

$$\sum_i n_i m_i (S+V_i) = \sum_i n_i m_i S = \rho S = M \qquad 2.4$$

where m_i is the molecular weight and the symbol M denotes the steady mass rate of flow with units of gm-cm^{-2} -sec^{-1} . Equations 2.4 yields an expression relating the diffusion velocities of the individual species

$$\sum n_i m_i V_i = 0 \qquad 2.5$$

It is important to note that V_i is positive or negative depending upon the sign of the concentration gradient of component i. The only process that causes formation or dissapearence of molecules is chemical reaction, so that

$$\frac{d(n_i(S+V_i))}{dx} = K_i = \left(\frac{\partial n_i}{\partial t}\right)_{chem} \qquad 2.6$$

The term K_i is the rate at which n_i would change due to chemical causes alone under the conditions of temperature, density, and composition that exist in the volume dx. Note that if $(\partial n_i/\partial t)$ is not identically zero throughout the flame, concentration gradients will exist and cause diffusion of individual species to be superimposed on the net motion of the flame. It is in this term that the mechanism of the chemical reaction is taken into account in the continuity equation 2.6 with the reaction kinetic equations for all the K_i (i.e for each component).

For conservation of energy, an energy balance is written in the flame. As the pressure across the flame is essentially constant and the flame is a low speed subsonic wave, one can write an enthalpy balance. The enthalpy of the i-th species is

$$H_i = H_i^{\circ} + \int_{T_0}^{T} C_{p_i}\, dT \qquad 2.7$$

where $H_i^{\bullet}$ is the heat of formation at 298.16 K and. C_{pi} the heat capacity per mole. When writing the energy equation, Hirschfelder and Curtis assumed that the flame is adiabatic and that kinetic energy storage is negligible so that all chemical energy is transferred only into potential energy in the fluid.

Since in this steady state theory, the energy in the control volume does not change with time, there is an energy loss of equal magnitude. This is represented by the heat flux

$$q_v = k\frac{dT}{dx} \qquad 2.8$$

across the plane x, so that for adiabatic combustion the equation of conservation of energy becomes

$$q_v = \sum_i n_i (S + V_i) H_i - \sum_i n_i (S H_i)_b \qquad 2.9$$

After assuming that the heat flux is due only to thermal conduction and energy transport by diffusion, equation 2.7 becomes

$$\sum_{i=1} (n_i S H_i)_b = \sum_{i=1} n_i S H_i + \sum_{i=1} n_i V_i H_i - k\frac{dT}{dx} \qquad 2.10$$

The diffusion velocity can be defined in terms of a diffusion coefficient, after which the equation may be written as

$$\left(\sum_i n_i S H_i \right)_b = \sum_i \left(n_i S H_i \right) - N \sum_i D_i \frac{dx_i}{dx} - k\frac{dT}{dx} \qquad 2.11$$

where D_i is the diffusion coefficient. N is the total molar concentration of the mixture. The three terms on the right in equation 2.11 are energy fluxes due respectively to convection, diffusion, and conduction in the flame zone. The above equation can also be expressed in the differential form

$$\frac{d}{dx}\sum n_i S H_i - \frac{d}{dx}\left(N \sum D_i \frac{dx_i}{dx} \right) - \frac{d}{dx}\left(k\frac{dT}{dx} \right) = 0 \qquad 2.12$$

The i-th mass balance equation is expressed in the form

$$\rho \sum_{j=1}^{K} \nu_{ij} \frac{d\lambda_j}{dt} = \frac{d}{dx}\left(n_i S \right) - \frac{d}{dx}\left(N D_i \frac{dx_i}{dx} \right) \qquad 2.13$$

where there are k chemical reactions occuring, each with their reaction coordinate λ_j and rate $\frac{d\lambda_j}{dt}$. The reaction rate k_i of the i-th reaction is given by an Arrhenius expression

$$K_i = A_i T^{\alpha_i} e^{-E_i/RT} \qquad 2.14$$

where the activation energy is E_i, the exponent α_i represents an additional weak temperature dependence and the frequency factor is A_i . The rate constant expression 2.14 was deduced from simple arguments by Arrhenius many years ago and is now known to apply to the elementary steps that cause the chain reaction mechanisms that occur during combustion. The frequency factor A is sometimes referred to as the preexponential factor. The constants A_i, α_i, and E_i, are usually determined experimentally.

Equation 2.11, the mass flow equation 2.13 and relationships defining reaction rates, diffusion coefficients, thermal conductivities and enthalpies can be used to determine the burning velocity and detailed structure of any premixed gas flame. The burning velocity S_u is the eigenvalue of this mathematical problem. The boundary conditions are:

At the hot boundary

$$\frac{dT}{dx} = 0, \quad \frac{dX_i}{dx} = 0, \quad \frac{d\left(n_i(S+V_i)\right)}{dx} = 0$$

At the cold boundary

$$T = T_u, \quad X_i = X_{iu}$$

The cold boundary condition represents a problem, because equation 2.12 predicts a finite reaction rate for $T = T_u$. This problem of the cold boundary can be solved by not allowing the products to diffuse past a certain point in the cold boundary, or by making the reaction rate go to zero at room temperature. The latter technique is more physically satisfying.

The cold boundary problem was solved by using a technique introduced by Friedman and Burke [14]. The model developed by them is a rather simplified model suitable to show basic trends rather than to obtain precise quantitative results. It considers the flame reaction to be an irreversible first order decomposition of pure A yielding only B as product.

$$A \longrightarrow B$$

with molecular weights

$$M_{W_A} = M_{W_B} = M_W$$

and enthalpies

$$H_A = c_p(T - T_u) \; ; \quad H_B = c_p(T - T_b)$$

where C_p = constant. This means that the enthalpy is zero at both boundaries. The first order rate equation is written as

$$\frac{d(NX_B)}{dt} = K_1 N X_A \exp\left(-E/R\tau T_b\right)$$

where $$\tau = \frac{T - T_u}{T_b - T_u}$$

In this case at the cold boundary $\tau = 0$, and thus the reaction rate is also zero.

Here, although the Friedman-Burke model is rather simple it does provide a useful description of flame structure. Figures II-5a and II-5b are solutions to the Friedman-Burke model for Le = 1.0 and Le = 0.0 respectively. Here the expresion for Lewis number is taken to be

$$Le = \frac{c_p \cdot D_{AB} \cdot \rho}{k}$$

and Z represents the mass due to flow and diffusion combined. These solutions indicate that there is a preheat zone with very little reaction and a reaction zone in the high temperature region where almost all the reaction occurs. For Le = 1.0 when diffusion is included the flame is thicker and has a lower burning velocity. According to Friedman-Burke this is due to the back diffusion of products which dilute the reactants in the reaction zone and therefore reduce the reaction rate. But Strehlow [13] points out that diffusion of radicals in the flame model would increase S_u by allowing the radicals to diffuse into the preheat zone. However the Friedman-Burke model does not include reacting radicals and this is its major weakness. Nevertheless it is valuable because it shows the main structural features of a flame.

It has often been assumed that there is really only one rate determining reaction and therefore that the Friedman-Burke model is reasonable. In the work of Smoot et al [15], it was found that there are at least three and in some cases 7 important reactions. This means that when using this model, care must be

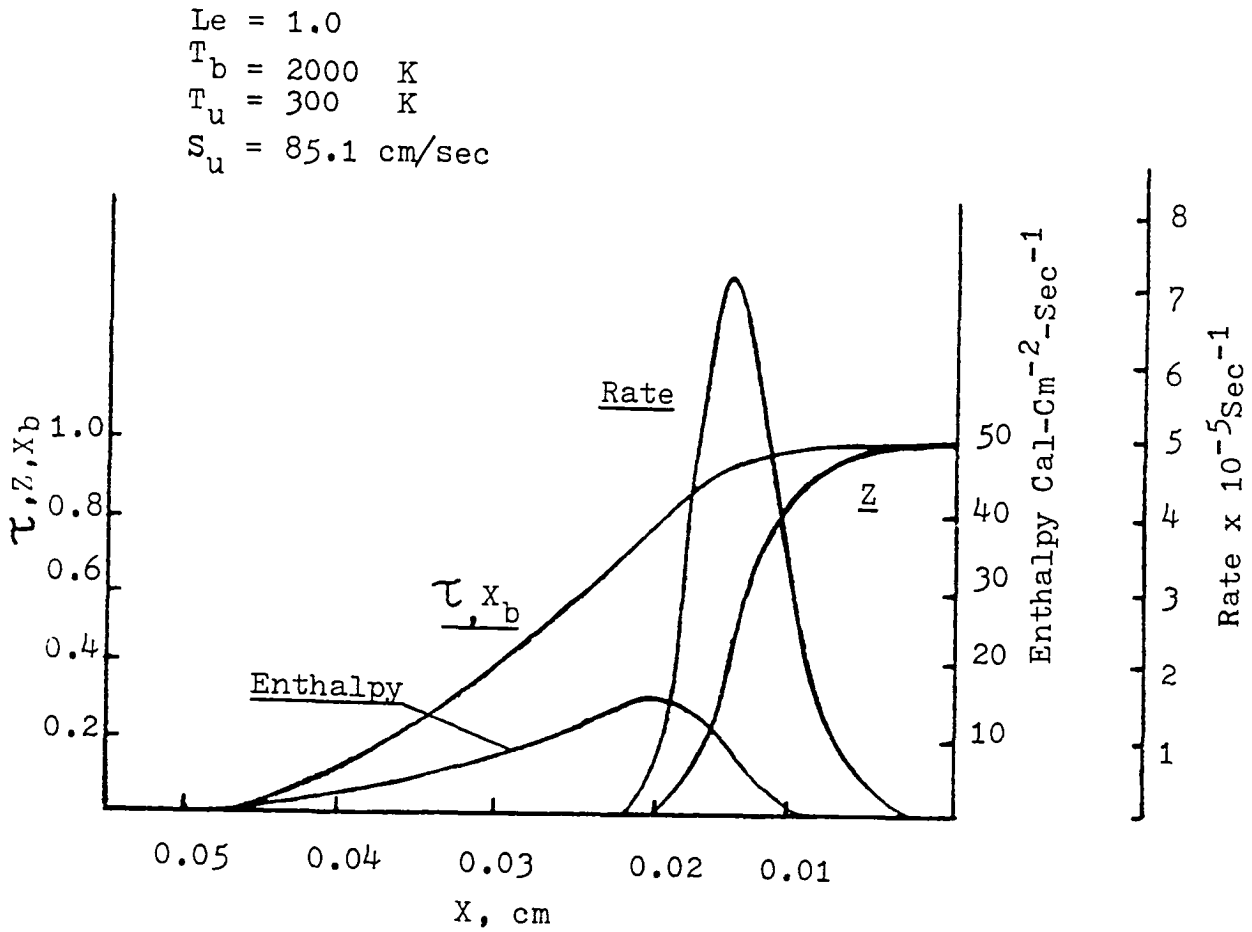

Fig. II-5a. Flame Structure for a Flame with Lewis Number = 1.0 (13).

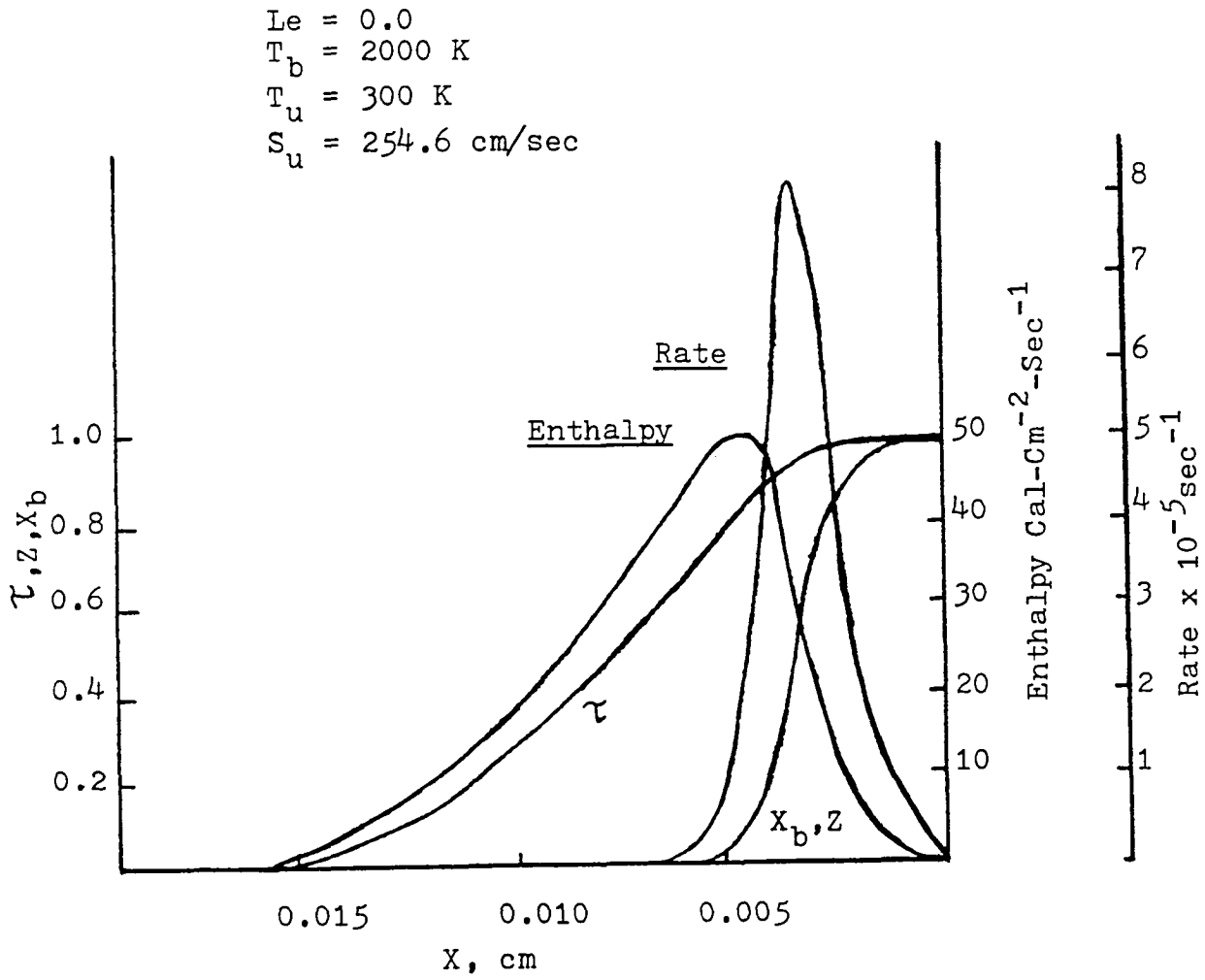

Fig. II-5b. Flame Structure for a flame with Lewis Number = 0.0 (13).

taken when extrapolating kinetic parameters. Levy and Weinberg [16] experimentally determined that in the low temperature zones of the flame the one step reaction mechanism is not valid.

Considerable work has been done in the theoretical description of flame structure for a large value of the reduced activation energy and for a Lewis number close to unity. This approach in solving the problem of finding laminar flame burning velocity was taken by Bush and Fendell [17,18]. They invoked the method of matched asymptotic expansions in determining the structure of a steady one - dimensional isobaric deflagration wave. A model was used for the case of first order one-step exothermic unimolecular decomposition using Arrhenius kinetics [19]. Basically the same governing equations were obtained as in the Friedman- Burke model.

The large activation energy asymptotics approach can be applied to any three dimensional non steady reactive flow in which the chemical reaction is observed to be confined to a narrow zone. Referring to figure II-5 the region of rapid reaction is confined to that part of the flame where the dimensionless temperature, τ , is greater than 0.8, thus the lower temperature or preheat zone of this flame is essentially an unreactive flow. As the effective activation energy of the chemical reaction is increased the length of the reaction zone becomes smaller relative to the length of the preheat zone and

the temperature change in the reaction zone becomes smaller. In fact, as the activation energy $E \to \infty$, the length of the reaction zone approaches zero. Many of the reactions occuring in combustion do have large activation energies and the reaction rate is strongly temperature-dependent; this causes the chemical reaction to be confined to a thin reactive diffusive layer. Typical flames have reaction zones $\sim 10^{-3}$ mm and transport zones $\sim 10^{-1}$ mm. Figure II-6 is a sketch of the flame front showing the reaction zone. The key features of matched asymptotics and singular perturbation techniques lie in solving the governing equations independently in the preheat zone (where the chemical source term is zero at all algebraic orders in powers of $1/\varepsilon$). The boundary conditions in the unburned and in the burned gases are then matched for the external solutions (preheat zone) and the internal solution (reaction zone) respectively.

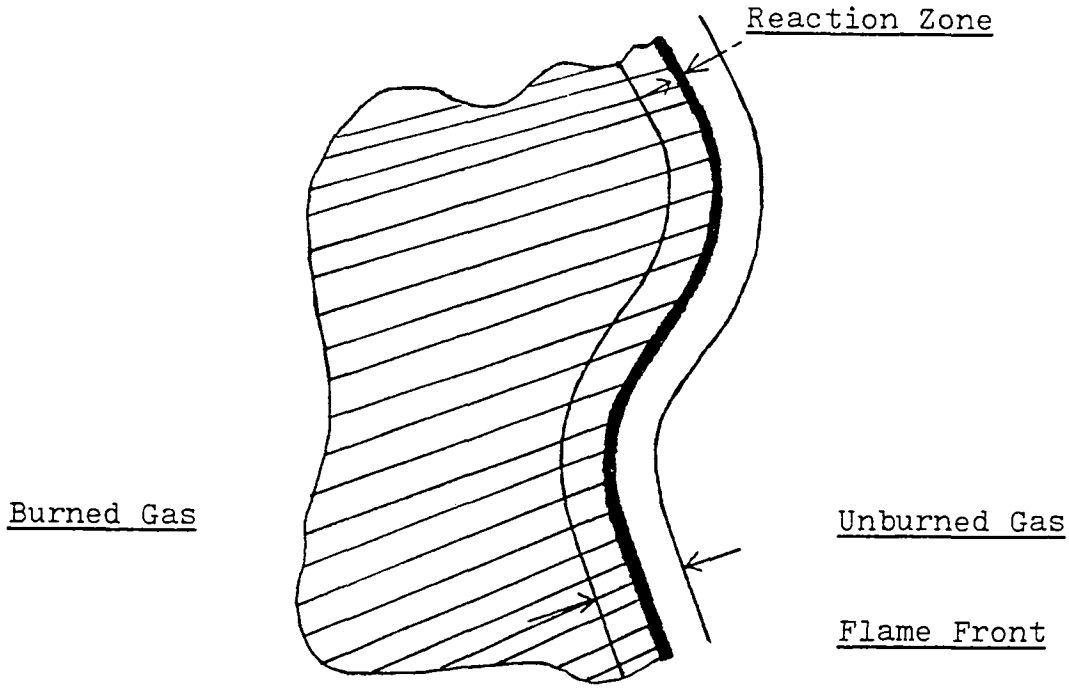

Fig. II-6. Schematic Diagram Showing that the Reaction Takes Place only in a Thin Zone.

CHAPTER III

Combustion Aerodynamics of Flames

In this chapter attention will be given only to a particular aspect of deflagration waves (laminar flames), where the interaction of a combustion wave with a flow field containing velocity gradients occurs, i.e., the combustion aerodynamics of flames in a velocity gradient. This combustion problem requires the simultaneous consideration of both fluid dynamics and chemical kinetics for its study. Normal laminar flame propagation is specified by heat transmission by molecular heat conduction and diffusion of reactive species from the hotter layers of the flame to the cooler layers; the normal flame propagation rate is highly subsonic, of the order of several tens of centimeters per second for ordinary hydrocarbons in air. The combustion is accompanied by small pressure changes and in the majority of cases it can be considered to be isobaric.

Laminar premixed gas flames may be observed as steady waves in a variety of laminar flow situations, and have the property that any element of the flame front propagates normal to itself in any flow situation. These flames will exhibit a steady wave nature only if the flow velocity of the main stream is well above the normal burning velocity of the mixture. Therefore all attached laminar flames (as is the case for the problem being

studied here) are oriented obliquely to the flow. This kind of flow situation is shown in figure III-1. From this figure it is seen that even though a flame of this geometry appears steady to an observer, an element of this flame is, in reality propagating along the flame at a velocity S_{11} . Thus the flame can exist only as an apparently steady flame at some time t_2 at the point 2, if at some earlier time t_1 it appeared steady at a point 1 whose distance from point 2 (along the flame in the upstream direction) is given by the expression,

$$S_2 - S_1 = (t_2 - t_1) S_u \qquad 3.1\,a$$

This implies that all the steady flames must have an attachment region at the most downstream location of the flame which continually reignites the oblique flame sheet. The normal burning velocity S_u is given by the expression, where α is the angle between the flame and the flow direction and U is the local flow velocity.

$$S_u = U \sin\alpha \qquad 3.1\,b$$

Note from figure III-1 that the flow velocity vector is deflected by the flame due to the oblique position of the flame and the expansion of the gases as they pass through the flame.

As has been mentioned earlier, flames are rather thick, and there are many flow situations where the equations for strictly one dimensional flow through the flame are not applicable. Under these conditions the flame is said to exhibit

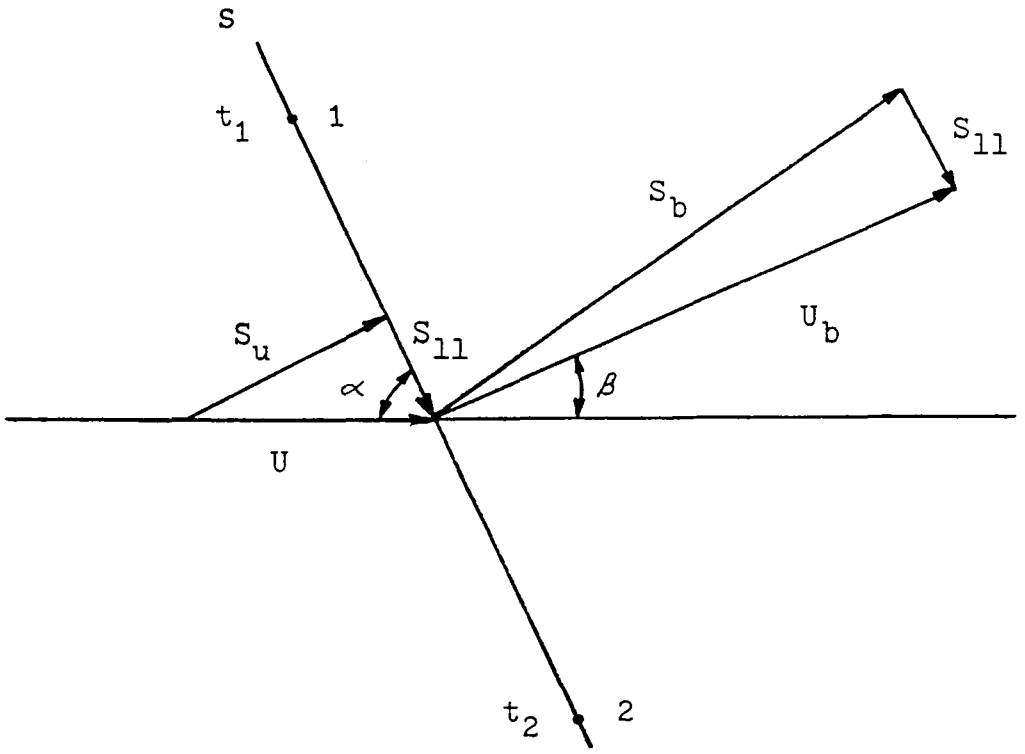

Fig. III-1. Oblique Flame Orientation and Flow - Velocity Vectors.

stretch (either positive or negative). The first attempt to calculate the positive stretch factor for curved flames was made by Karlovitz et al [20].

Flame stretch is observed in steady oblique flames and highly curved flames, when the approach flow contains a velocity gradient. This situation is illustrated in figure III-2. In this case the approach flow is assumed to have a velocity vector U, which lies in the x direction only and which contains a gradient dU/dY. The infinitely thin flame is assumed to have an orientation which makes it appear steady at every location. Each element of this flame is slipping along the sheet at the velocity U_{11} . As the flow gradient exists in this case ahead of the flame, U_{11} is not constant with time and the frontal area of the flame increases as it propagates. In the literature it is reffered to as positive stretch if its frontal area increases with time due to flow geometry and negative stretch if it decreases with time. Under these conditions one can form a dimensionless parameter,

$$K = \frac{\partial(\ln \Delta A)}{\partial t} \cdot \eta_o / S_u \qquad 3.2$$

which is defined as the Karlovitz number.

$$\frac{\partial(\ln \Delta A)}{\partial t}$$

is a fractional rate of flame area increase with units of inverse seconds and η_o / S_u is a characteristic time of propagation

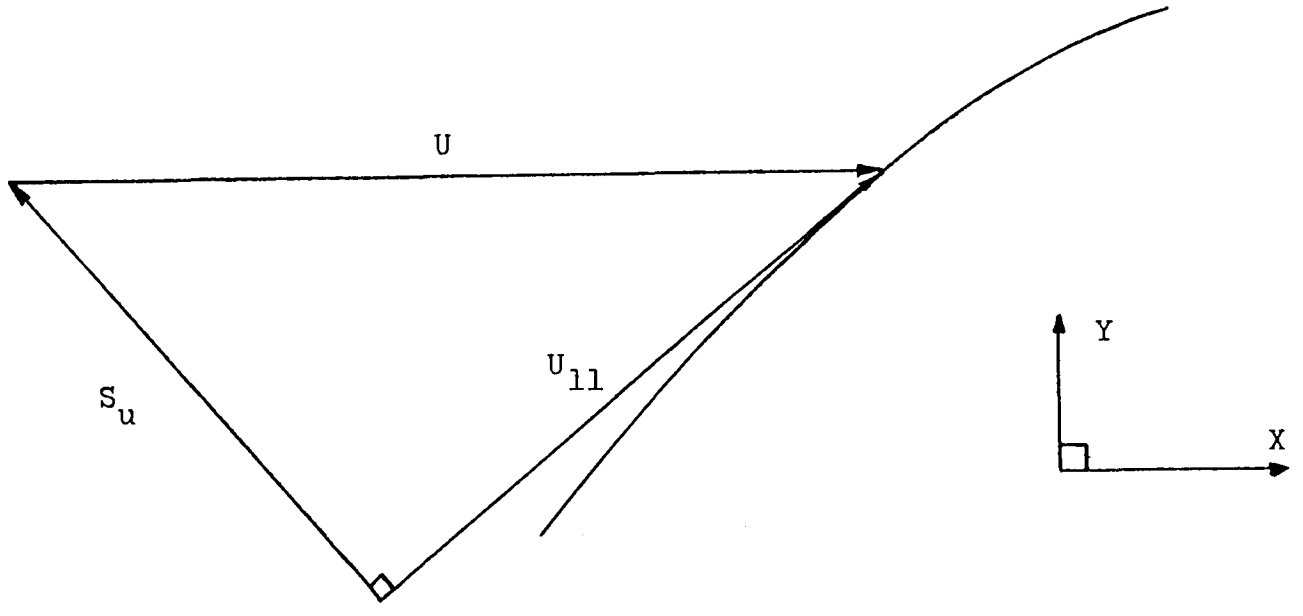

Fig. III-2. Vector Diagram for a Stretched Oblique Flame in Steady Flow.

through the preheat zone with units of seconds, and is sketched in figure II-4. This parameter can be calculated from the expression,

$$\eta_o = \frac{k}{c_p \rho S_u} \qquad 3.3$$

where k is the mixture thermal conductivity, ρ is the density and C_p is the mixture specific heat at constant pressure, while S_u is the normal burning velocity. Equation 3.2 represents a logical definition of the Karlovitz number, K, based on the behavior of an element of the wave front.

A second effect produced by the interaction of a velocity gradient with a flame is that of preferential diffusion. This causes the local stratification of a premixed flame due to the higher diffusivity of the deficient species. Since the diffusion coefficient for lighter species is larger than for heavier species, the effects of such diffusion will occur in lean mixtures where the fuel is lighter than the oxidizer and in rich mixtures where the fuel is heavier than the oxidizer. Within the combustion wave, heat flows from the burned to the unburned gas and the reactants and reaction products interdiffuse at certain diffusion velocities V_i for each molecular species i. The direction of the diffusion velocities is determined by the gradient of species concentration, $G_i=[I].V_i=-D_i \text{grad}[I]$. It was found by Markstein [21] that changes of composition by diffusion can occur in a gas flow only if the concentration

gradients are not parallel to the flow lines, i.e if grad[I] is not parallel to U, where U is the unburned mixture flow velocity. This can be conceptually understood by looking at figure III-3 where a small segment of the curved shape flame is shown. Since the diffusive transport is normal to the flame along the centerline, there the velocity U is parallel to the diffusion velocity V_i and as we travel along the flame front these two vectors diverge more and more. As a consequence of this, lighter species either fuel or oxidizer diffuse to the curved part of the flame (grad[I] $\not\parallel$ U) and the mixture becomes leaner. Thus preferential diffusion of the lighter species either fuel or oxidizer towards the reaction zone can alter the equivalence ratio locally in the preheat zone by enriching the concentration of the lighter species there. This in turn will alter the burning velocity due to a shift in the equivalence ratio. It is important to note that curved shape of the flame front is neither a sufficient nor a necessary condition for transport across the flow and the effects of preferential diffusion cannot depend on the flame curvature alone but also depend on the flow field (converging or diverging flow lines) in the immediate vicinity upstream of the flame front.

In order to fully understand any flame holding mechanism, the effect of flame stretch and preferential diffusion have to be taken into consideration. This is due to the change of flow pattern in the region of flame attachment above the stabilizing

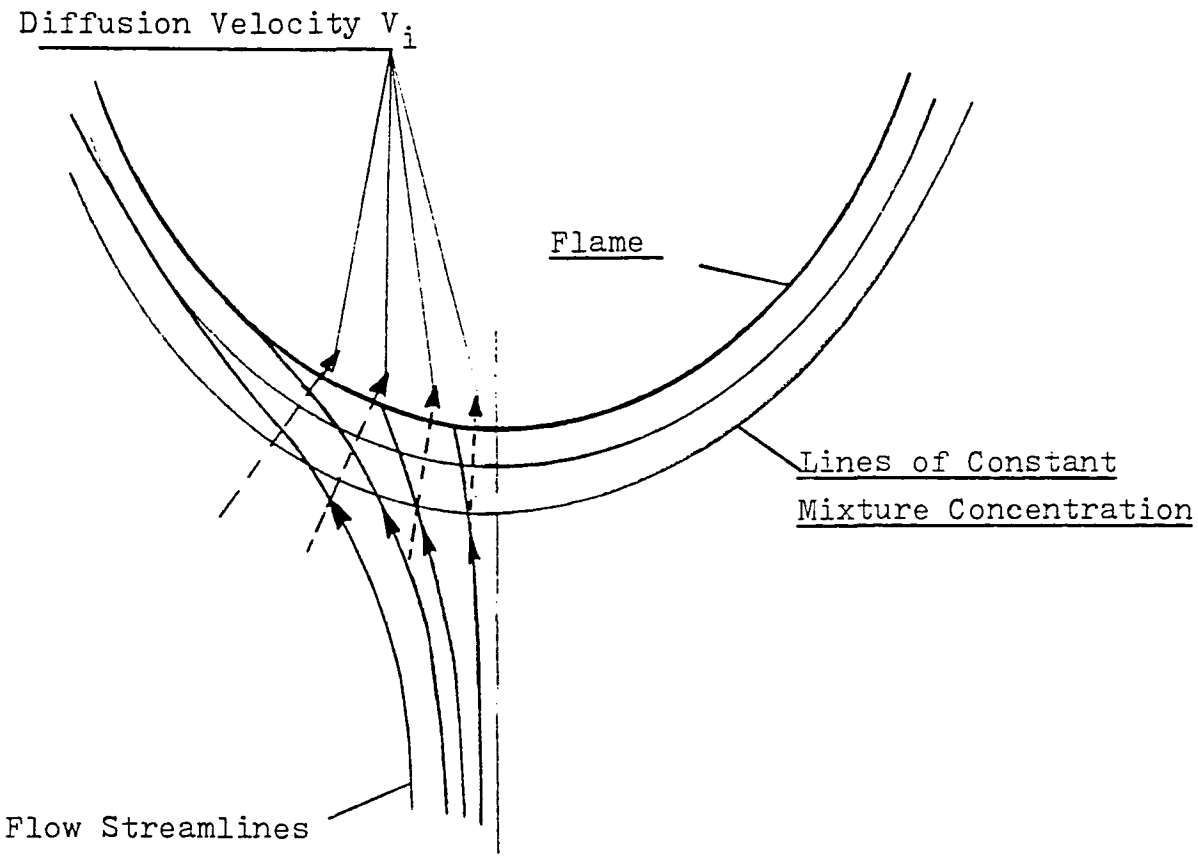

Fig. III-3. Schematic Illustration of the Effects of Preferential Diffusion.

plate. In this region, flow lines close to the side of the flame holder (stabilizing plate) bend inward towards the centerline axis whereas flowlines farther away are deflected outward by the back pressure of the flame. In figure III-4 is illustrated the qualitative effect of velocity gradient leading to the shearing (stretching) of the flame element. At point 1 the combustion wave enters the segment 1-2 with the small velocity component $U_1 \cos\alpha_1$ parallel to the wave surface; at point 2 it leaves with the large velocity component $U_2 \cos\alpha_2$. Thus new flame surface is produced continually as the flame traverses the velocity gradient. As a result of this "stretching" of the flame surface, the amount of heat flowing from the reaction zone of the flame into the unburned gas is distributed over increased volume of gas. Thus at this point one can see that the influence of flow on the structure of flame leads to the appearance of heat extraction and mass transfer along the front. Along every isothermal plane inside the front the flow velocity increases linearly and this causes the divergence of heat flux in the preheat zone.

In the following pages of this chapter an attempt is made to carry out a brief review on different trends and approaches to the understanding of the flame holding mechanism viz a viz shearing effects caused by the gradient in the approach flow velocity.

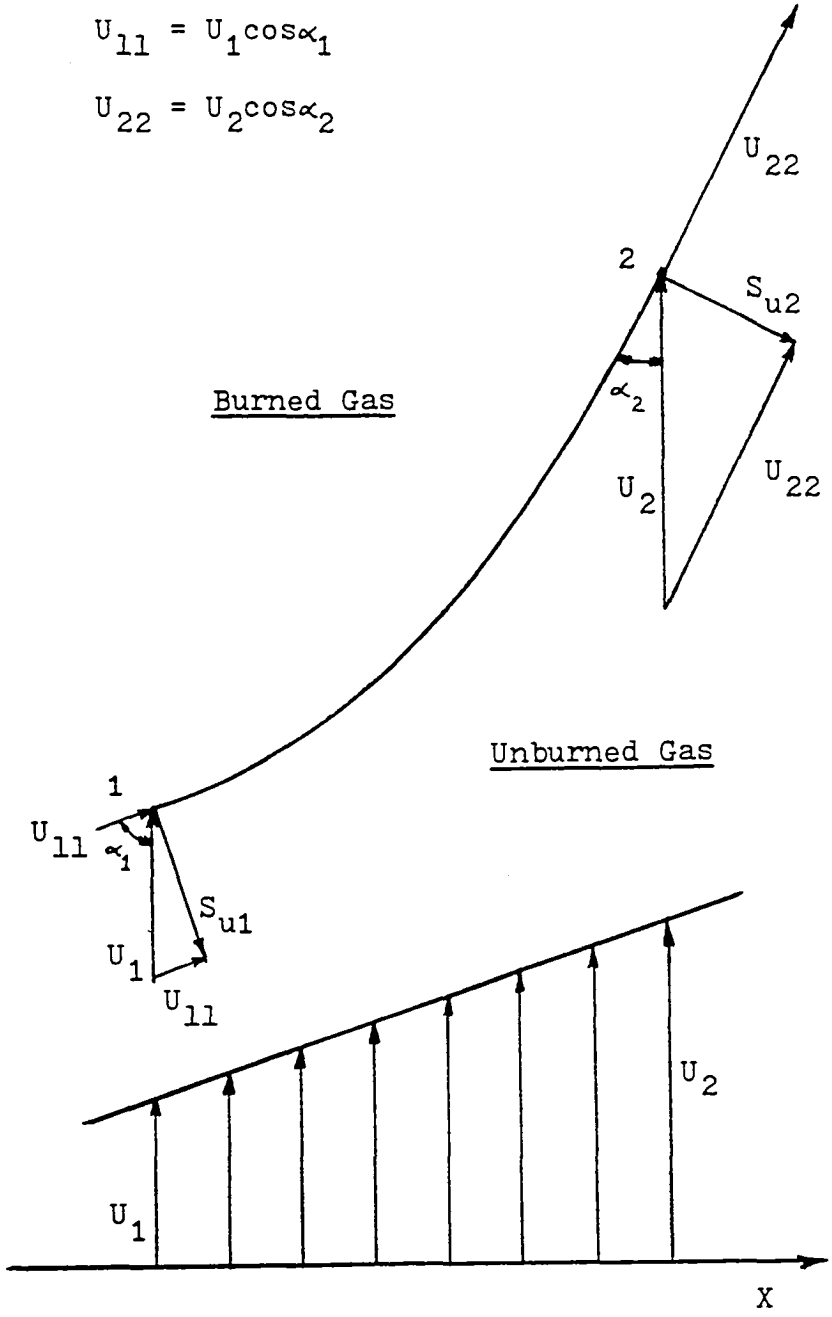

Fig III-4. Velocity Diagram of a Laminar Flame in a Flow with Velocity Gradient.

Pioneering work of flame propagation across velocity gradients has been done by Karlovitz et al [20]. Karlovitz attempted to develop a relationship between the burning velocity and the velocity gradient. A parameter β was expressed in the form

$$\beta = 1 + a \cdot \eta_0$$

where $$\eta_0 = \frac{k}{c_p \rho S_u}$$

is the length characteristic of the preheat zone defined earlier, and a is

$$a = \frac{1}{U} + \frac{dU}{dy}$$

where U is the approach flow velocity. The value of β characterizes the velocity increase over the distance η_0. Calculation of increased values of β correspond to respective reductions in the burning velocity caused by the effect of the velocity gradient, if the approach flow velocity increases considerably. If the burning velocity is reduced to a small fraction of its normal value, propagation of the flame may be entirely interrupted by small velocity fluctuations. Closer to the wall the value of β is even larger, and the burning velocity is reduced further. Karlovitz presented an approximate theory which cannot predict the exact limit where flame propagation will be interrupted, but it can give the stability region to some extent beyond which the danger of flame interruption exists.

It is assumed that when a premixed flame is stabilized in space, in general there must exist a "stabilization point". At this furthest upstream point of a steady flame, the local flow velocity vector and the local flame velocity vector must be equal in magnitude, coincident in direction, and of opposite sign. The importance of flame stabilization in high speed flow makes it necessary to investigate the propagation of combustion waves across velocity gradients.

A common example related to stabilization of a combustion wave in a gas stream is given by Bunsen burner flame. The mechanism by which the inner cone of the Bunsen burner flame maintains a fixed position with respect to the burner rim was originally examined by Lewis and von Elbe [22,23]. In their book [1] a working model describing the stability of flames held over a burner rim in a flow field with velocity gradients was presented. A schematic illustration of this kind of working model is shown in figure III-5. Straight lines 1 through 5 presented in figure III-5a represent typical velocity profiles corresponding to different range of flow rates. The curves b,c and d represent lateral distributions of the burning velocity for arbitrary flame positions 2,3 and 4 shown in figure III-5b. The model presented in this figure covers the extreme cases of flame positions where the flow velocity exceeds the burning velocity everywhere in the field (blow-off represented by the velocity gradient 1) and conversely the case when the burning velocity

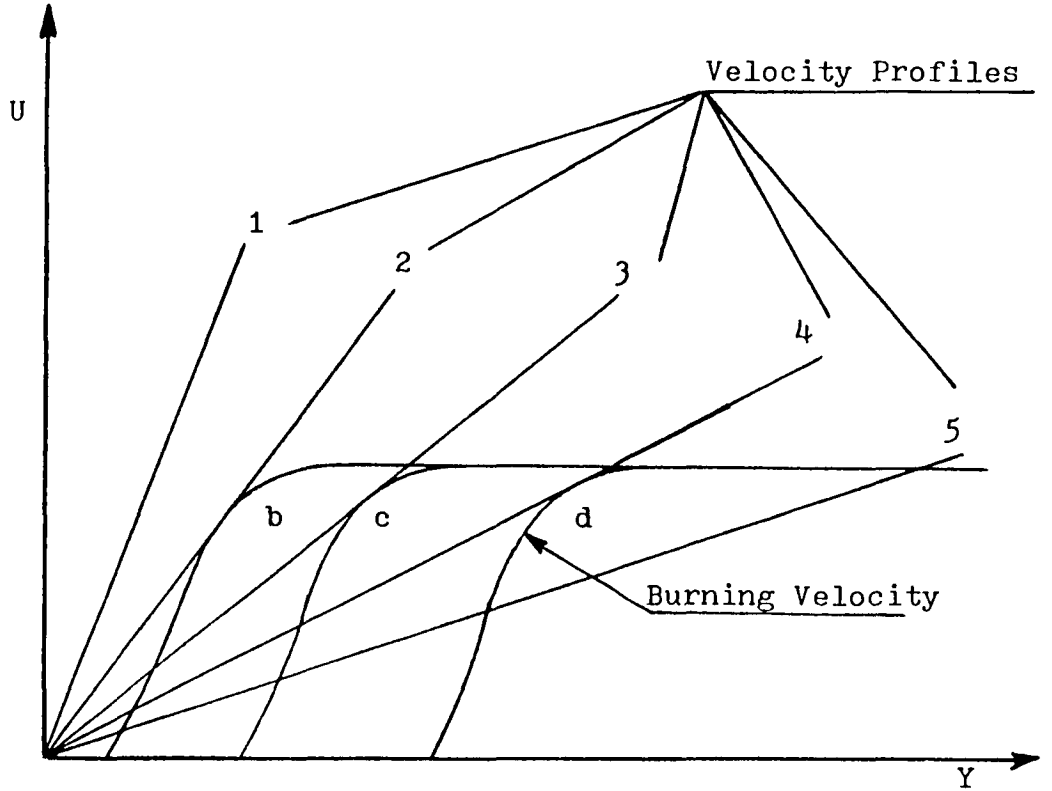

Fig. III-5a

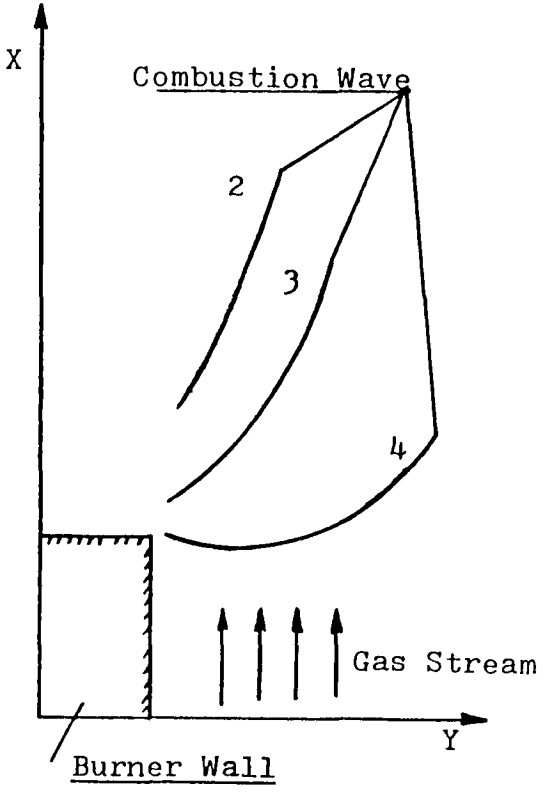

Fig. III-5b

Fig. III-5. Schematic Diagram of Holding Behavior.

exceeds the flow velocity (flashback, represented by the velocity gradient 5). Between the flow rates corresponding to 2 and 4, which are limits for blow-off and flash back respectively, the flame will be stable. When the combustion wave is closest to the wall of the obstacle, a reduction in burning velocity occurs due to the heat sink (heat loss) effect of the wall. If the flame is originally stabilized in position 4 and the flow rate is increased to produce the velocity gradient 3 (represented by straight line 3), the flame will move downstream, but will now stabilize in position 3 because of the increase in burning velocity, which occurs due to the reduction in quenching effect of the rim, as the flame moves downstream to a new position. This will happen again as the gradient is increased to its limiting value 2. Beyond this position, however, there is no further increase in burning velocity because the dilution of the flame gases by the surrounding gas becomes effective at some distance from the rim. Thus as the flow velocity is increasesd the flame will shift to higher positions. This would lead to local burning velocity falling below the local flow velocity at all points in the flow and blow-off will occur. On the other hand if the flow velocity is decreased to a lower velocity gradient such as 5, this allows the local burning velocity to exceed the local flow velocity, and therefore, this would lead to the occurance of flashback.

This kind of conceptual approach predicts that blow-off and flashback could be correlated with the velocity gradient. This correlation has been verified experimentally. The effect of velocity gradient on flame stability for natural-gas mixtures [1] is shown in figure III-6. The critical boundary velocity gradient g_f and g_b are the lower and upper critical values between which the flame is stable. Subscripts f and b refer to the flashback and blow-off condition, respectively. It is worthwhile to note here that essentially the velocity gradients in the stream have no effect on the process of propagation within the combustion wave if, over distances comparable to the wave width, the change of velocity is slight. On the other hand the above justification will not be valid if the combustion wave enters a flow field, where, over distances of this order the velocity changes substantially.

Lewis and von Elbe have also made study of blow-off of inverted natural gas-air flames which were anchored at the end of wires or rods mounted in the axis of cylindrical tubes. A similiar kind of working model as described above (figure III-5) can be adapted for describing the stability of flames held over the end of wires or rods and at the trailing edge of a thin strip of plate.

While discussing in general the concept of flame stretch, Lewis and von Elbe suggested that the curvature of the flame

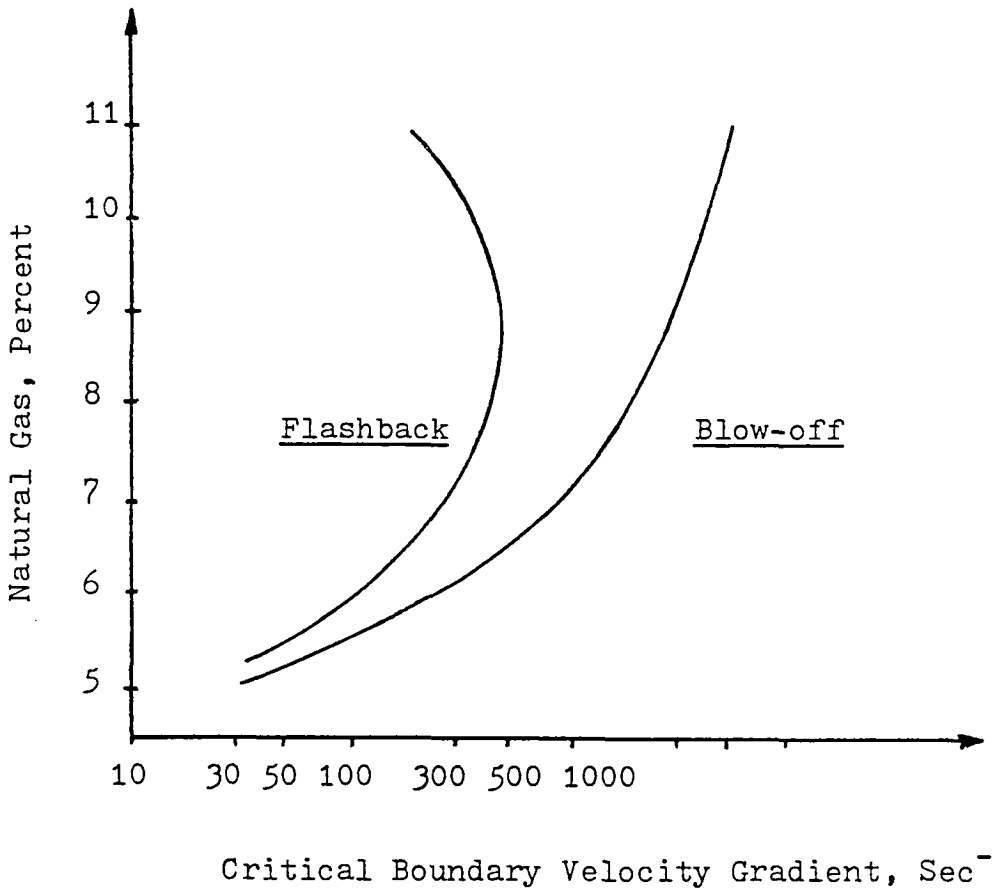

Fig. III-6. Flashback and Blow-off Critical Velocity Gradient for a Natural Gas Air Flame, (1).

surface which occurs with laminar flame propagation in non-uniform velocity fields leads to local reaction zone inbalances in the flux of energy and reactive species. For certain particular types of flow, Lewis and von Elbe believed that excessive stretching of the flame surface could lead to local quenching of the reaction, even in the absence of any external heat sinks, and they showed that a critical value of the Karlovitz factor correlated to the blow-off of flames stabilized on wires. However it turns out that a similiar criterion could not be established for flames stabilized on burner ports.

In recent years, Reed [4,5] has attempted to extend the Karlovitz flame stretch concept to flames stabilized on burner ports. In his work, an argument is put forward that flame blow-off results from an excessive enthalpy loss from the stabilizing region rather than because the velocity of the unburnt gas every where exceeds the local burning velocity. The effect of excessive shear in the flame stabilizing region has been regarded as the sole factor in bringing about the blow-off of flames. It is important to indicate here, that all the parameters needed to determine the non-dimensional Karlovitz flame stretch factor ($K = \frac{dv}{dy} \cdot \frac{\eta_o}{v}$) must be evaluated at conditions prevailing in the freestream. In order to evaluate this factor at local conditions, Reed and some other co-workers substituted S_u for U which means that their correlation variable $\frac{\partial u}{\partial y} \cdot \frac{\eta_o}{S_u}$ is no longer a Karlovitz stretch factor. According to Reed's

interpretation of his extensive data, the values of $\frac{\partial u}{\partial y} \cdot \frac{r_o}{S_u}$, a dimensionless correlation parameter, for the fuel-rich flames burning in an inert atmosphere remain at around a critical value of 0.23 characteristic of fuel-lean flames, while the values of this parameter for the fuel-rich flames burning in air increase rapidly once the stoichiometric fraction reaches approximately unity. Further more, Reed's suggestion that diffusion of the surrounding air into the holding region significantly influences the local mixture at the flame base (for flames stabilized at burner ports), such that the burning velocity at the conditions prevailing in the free stream is not representative locally, appears to be a valid obervation. This is why this study used flames held on the trailing edge of a flat plate, where this type of diffusion cannot occur. Such data and interpretation essentially supports the view that blow-off is a highly localised phenomenon which will prove difficult to test if measurement is restricted to the average, free stream conditions. It is also worth while to note that the relationship between the burning velocity and mixture composition is not single-valued but is dependent on flame curvature. It is apparent that on the basis of 'free stream' burning velocity alone, it should be difficult to predict blow-off uniquely.

Reed [4,24] has suggested that the strength of his correlation lies in the considerable range of measured parameters incorporated in his analysis. Reed himself accepts a sufficient

number of qualifications and exceptions in his analysis that the correlation does not work for (richer mixtures, light fuels and pure oxygen as an oxidant). Thus his flame stretch correlation appear to be quite limited as a "unifying principle". The correlations are however valuable as an empirical correlation.

Edmondson and Heap [25] suggested that Reed did not have data of high enough accuracy when he provided his correlation results. Although Edmondson and Heap aimed at greater accuracy in their measurements and their results are more self-consistent, Reed's compilation of data is much more comprehensive and has formed the basis for the unified interpretation of blow-off data in terms of flame stretch. One can conclude from the previous discussion that this particular approach to flame stretch correlation is only partially successful in describing blow-off. Edmondson and Heap [26] tend to ignore Reed's extensive ethylene-air flame data which provides the main evidence for the apparent success of the flame stretch correlation.

Thus so far 'flame stretch' is described by these authors through their correlation of data obtained from their experiments. In some of these papers the correlation was done by plotting parameters like S_u versus $g_b \cdot \eta_o$. Although Kawamura et al [3,27] refute flame stretch on the basis of the Karlovitz number they merely put forward a different version of the

Karlovitz factor. They said that at the base of the inverted flame, where the flame propagation is divergent, the flow of heat from the reaction zone to the preheat zone may also be divergent, and hence the area increase factor at the very base of the inverted flame is taken to be the leading or controlling factor η_0/R , where R is the inverted flame radius.

The description of a wide variety of flame extinction and blow-off situations in these earlier papers have been expressed simply in terms of the dynamic balance between laminar flame speed and flow velocity. In view of flame stretch concept, active species and energy are passed through the flame front more rapidly then they are supplied by reaction, and the flame is extinguished. Melvin and Moss [28] in their work put forward the argument that blow-off is a local interaction of both the reaction zone and the outer diffusion flame with the burner port and ambient atmosphere. Development in understanding this interaction can be possible if it is treated as a problem which involves reaction kinetic quenching of the base of the flame by the flow field and burner port itself. In other words for blow-off or more generally, extinction, there exists a certain critical value which is a ratio of the residence time in the reaction zone to a time characteristic of chemical reaction, this ratio is the Damköhler number.

Haniff and Melvin [29] in their paper discuss the "inadequacy" of the traditional qualitative approach of using "flame stretch". They state that blow-off can be considered as an extinction process and its mechanism ascribed to Damköhler number. In their theoretical approach which is some what heuristic in approach, they define the Damköhler number to be the ratio of overall frequency factor, density and potential flow parameters. Similarly Sivashinsky [30] when discussing Karlovitz's approach states that the reaction rate depends not only on the heat transfer to the surrounding gas, but also on the intensity with which the limiting reactant diffuses into the reaction zone. Some progress has been made in this direction through the Damköhler number approach in the papers of Tsuji, Sato [31,32,33] and Law [34] for the case of extinction of diffusion and premixed flames in a forward stagnation point flow.

Tsuji and Yamaoka in their paper [32] discuss the structure and extinction of near-limit rich-and lean-methane/air and propane/air premixed flames using counter flow twin flames established in the forward stagnation region of a porus cylinder. In their observation, they confirmed that two distinct modes of flame extinction exist: one is flame extinction at which the two flame zones are close to each other and the other is flame extinction at which the two flame zones are separated by a much larger distance. Both the flames are stretched because of the nature of the stagnation point flow and eventually at some

critical lean or rich composition the flames blow out.Experimentally it was observed that near the limit rich methane or lean propane flames stand at distance apart while lean methane or rich propane flames approach each other very closely. This is illustrated in figure III-7 [35]. Furthermore it can be concluded from their work that if the counter flow of heat by conduction from the reaction zone toward the unburnt mixture outweighs the inflow of the deficient reactant by diffusion from the unburnt mixture in to the reaction zone (Le <1), the temperature of reaction zone is reduced, and finally the flame is extinguished at a finite distance from the stagnation surface (flame stretch extinction). In this case, the flame extinction is not caused by incomplete combustion of the reactants. The extinction of lean propane/air and rich methane/air flames belong to this category of extinction On the other hand, if the inflow of the deficient reactant into the reaction zone outweighs the outflow of heat from the reaction zone (Le >1), the flame temperature increases with stagnation velocity gradient and the flames can approach each other without extinction. In this case the flame extinction occurs as the result of incomplete combustion in the reaction zone, and to this category of extinction belongs rich propane/air and lean methane/air flames. In the table below are shown the thermal diffusivities, the diffusion coefficients of the deficient reactants and the lewis number estimated for methane/air and propane/air mixtures near the lean-and rich-extinction limits [32].

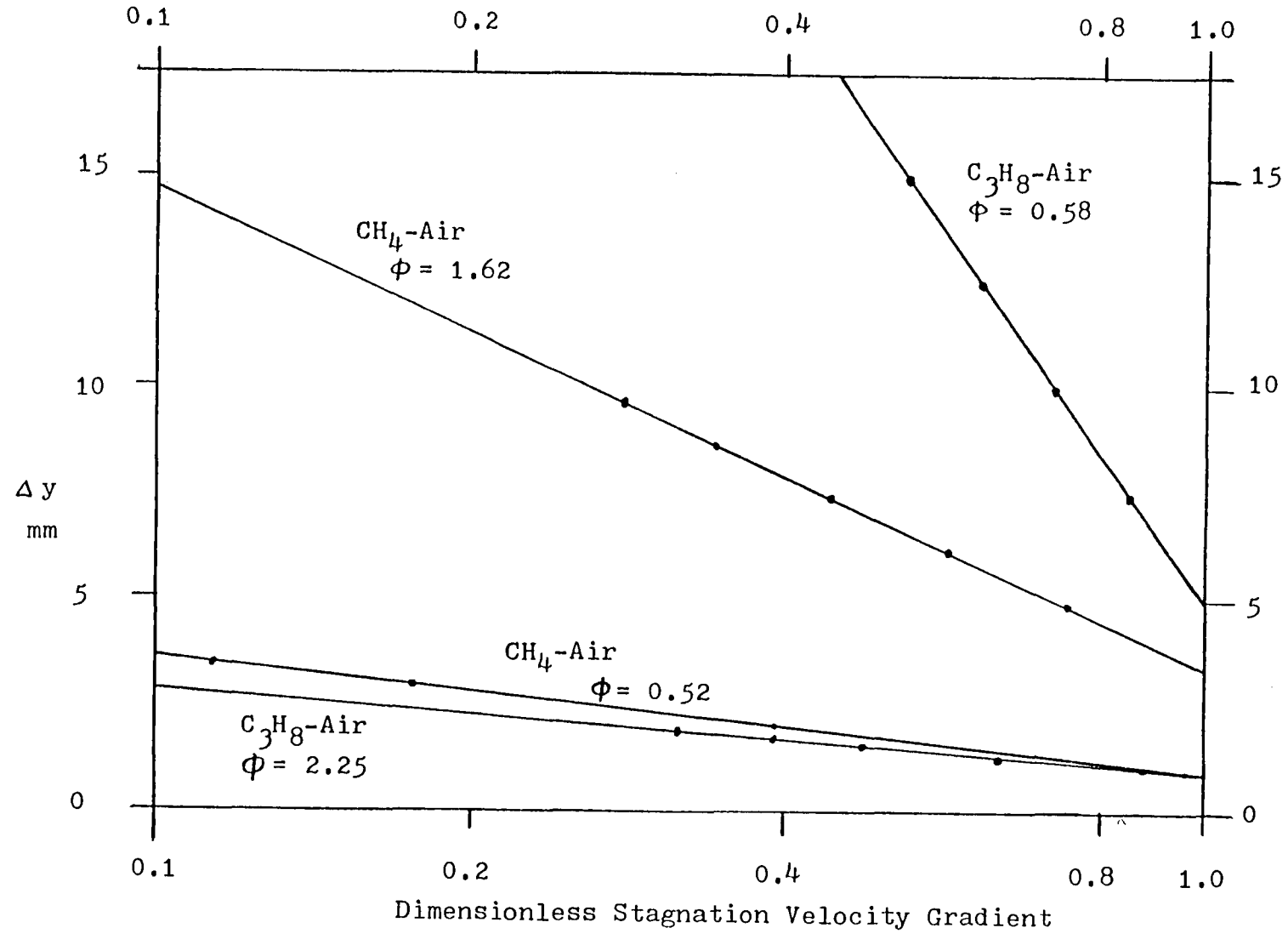

Fig. III-7. The Separation Distance between the two Flames.

Table 3.1 *

Deficient Reactant	Equivalence Ratio	Thermal Diffusivity (cm^2/sec)	Diffusion Coffecient (cm^2/sec)	Lewis number
CH_4	0.51	0.213	0.220	1.03
O_2	1.60	0.213	0.207	0.97
C_3H_8	0.55	0.208	0.114	0.55
O_2	2.25	0.197	0.207	1.05

*- Taken from (32)

Here the binary diffusion coefficients of the deficient reactants with nitrogen are used as the diffusion coefficients, because the nitrogen concentration in all mixtuires considered is very high as compared with concentrations of other species.

CHAPTER IV

Experimental Technique for Observing Fuel-Air Inverted Flames Held Over Various Flame Holders.

This chapter is devoted to a description of the experimental set-up for observing the behavior of lean limit fuel-air inverted flames.

The experimental study was divided into the following steps:

1. DESIGN OF THE APPARATUS.
    1. Burner design.
    2. Types of flame holders.
2. DESIGN OF THE FLOW SYSTEM.
    1. Particle injector.
    2. Flow velocity measurement and flow configuration with the particle injector
3. LASER DOPPLER VELOCIMETRY (LDV) ARRANGEMENT.
    1. Adaptation of the LDV system to the present study.
    2. Description of the LDV system.
4. SCHLIEREN AND VISIBLE LIGHT PHOTOGRAPHY.
5. THE PROCEDURE USED FOR COLLECTING BLOW-OFF DATA.

DESIGN OF THE APPARATUS.

Burner design.

In order to quantitatively observe the blow-off behavior of lean limit flames, the approach flow velocity must be strictly controlled, using a constant velocity profile at the burner mouth. Therefore the burner was designed to provide uniform flow with no irregularity in the flow, and great care was taken to avoid creating small disturbances that trigger transition from laminar to turbulent flow.

The burner consists of three main parts:

1. Lower Section.
2. Middle Section.
3. Upper Section.

The lower section consists of a circular tube with diffusers attached to both ends. The lower diffuser, circular tube and the back diffuser are shown in figures IV-1,IV-2 and IV-3 respectively. The diffuser was designed to reduce irregularities due to the sudden enlargement of the cross-sectional area. Attaching the long rectangular chamber at the other end of the back diffuser stabilizes the flow and a constant velocity profile is obtained.

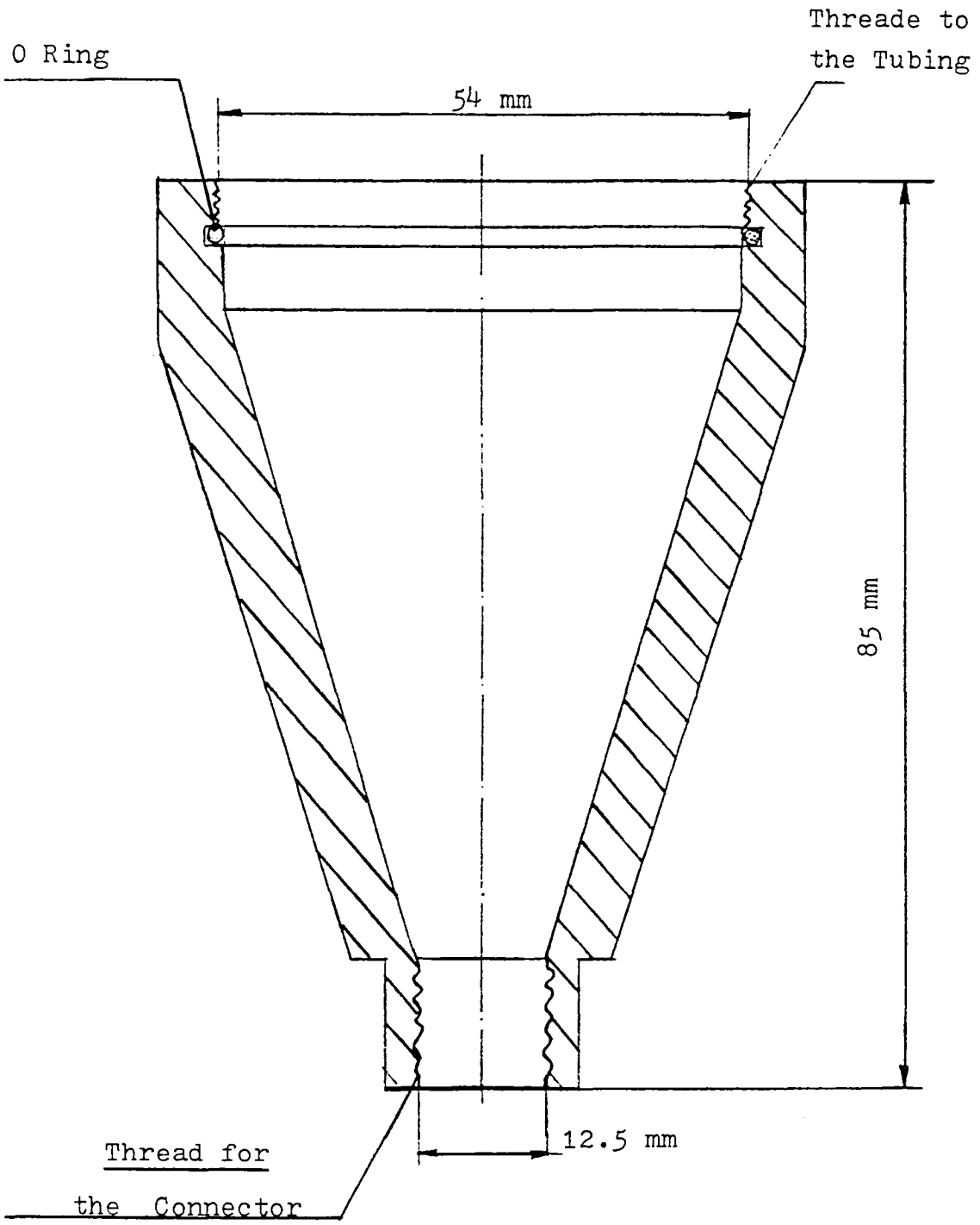

Fig. IV-1. Lower Diffuser of the Burner.

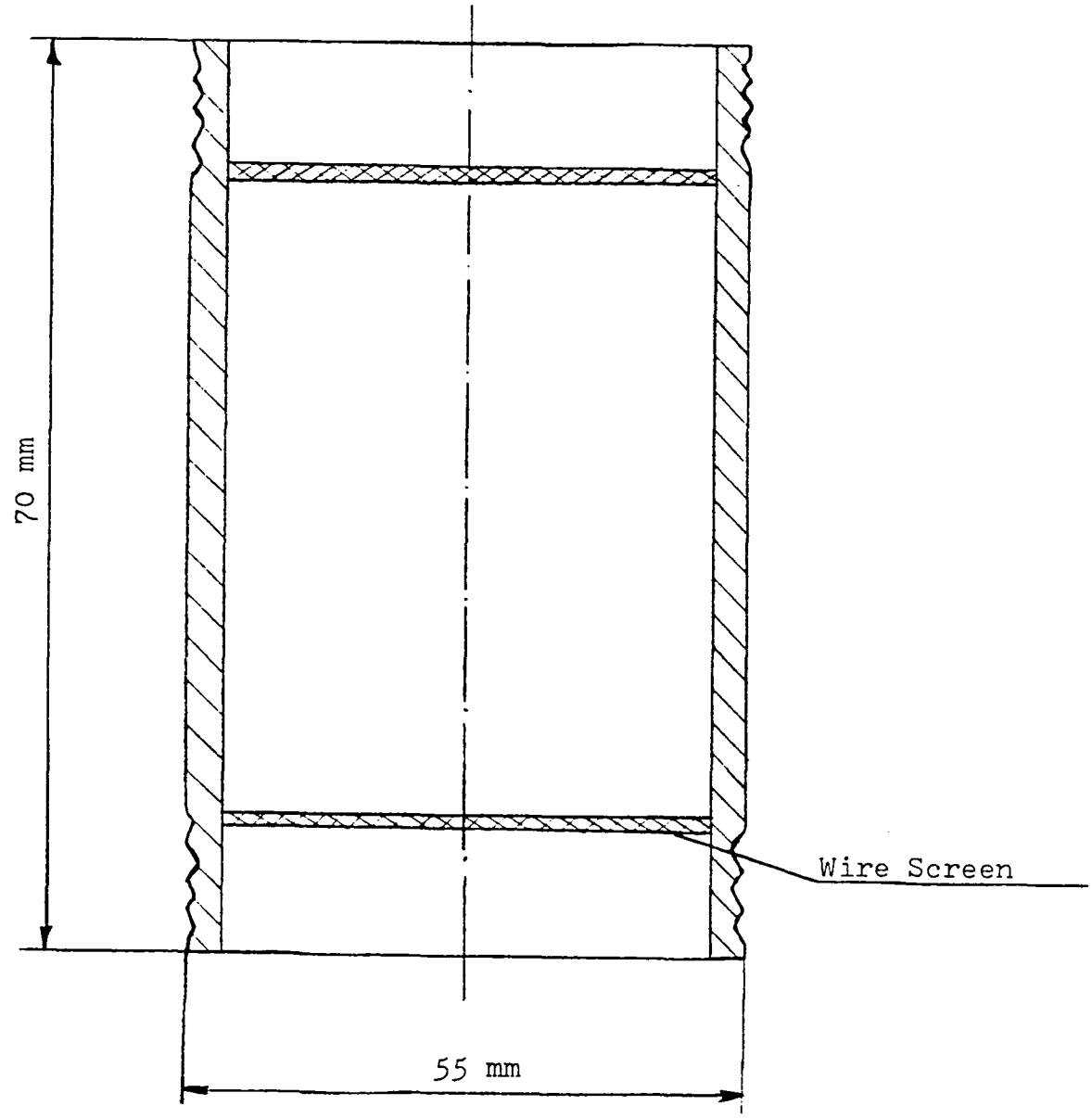

Fig. IV-2. Circular Tube with Wire Screens

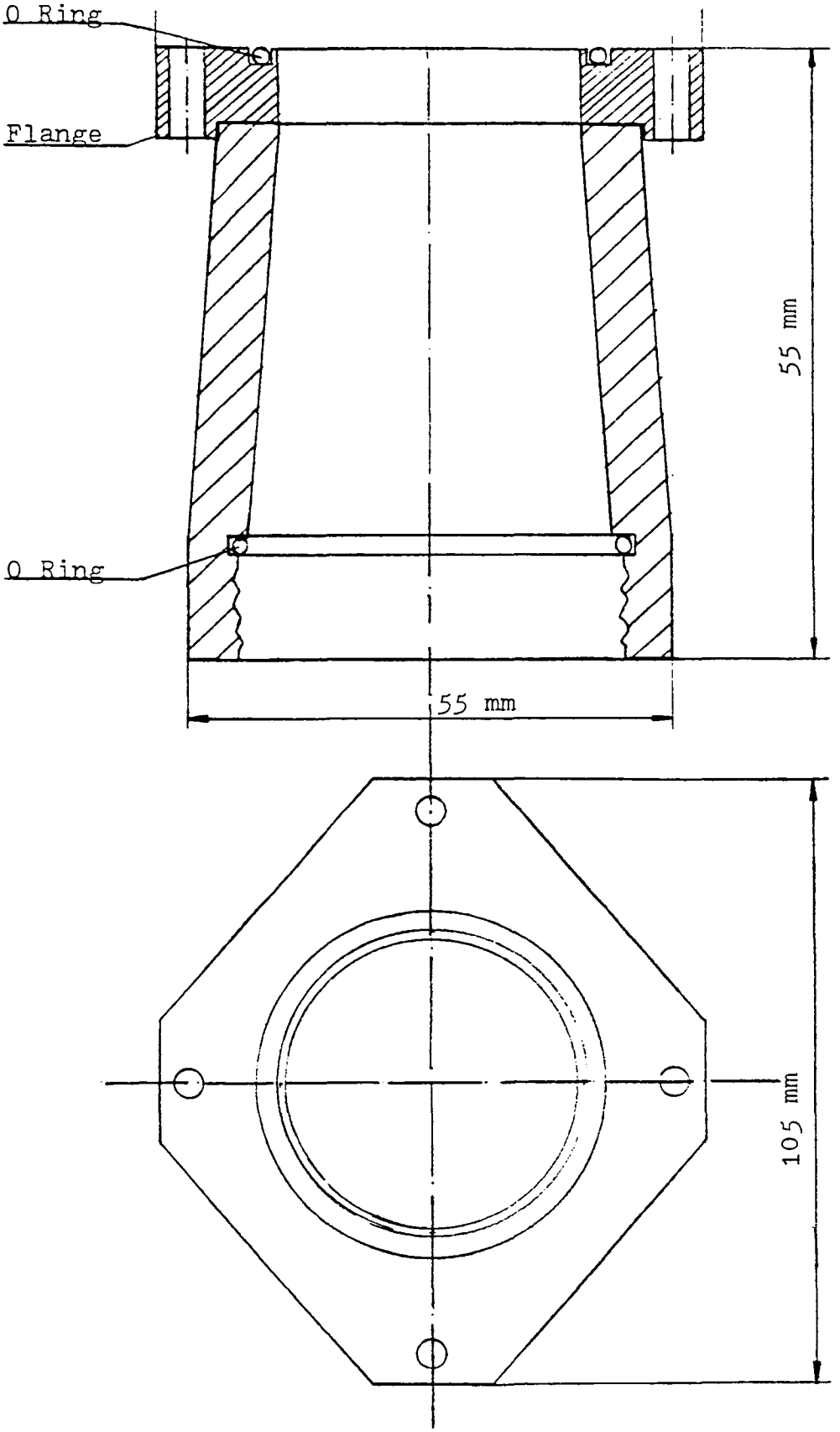

Fig. IV-3. Back Diffuser

The diffuser in figure IV-1 is machined from plexiglass. The smaller ID is 1.1 cm and the bottom of this component is threaded to a connector which is joined to polypropylene tubing of 0.635 cm ID. A plexiglass tube of 3.0 mm wall thickness with an outer diameter of 5.5 cm is threaded to the top portion of the diffuser. An O-ring is placed between the two edges of the components to form a proper seal. Figure IV-2 shows the circular tube and two wire screens of mesh size 1.0 mm, which are snuggly fitted in both the ends of the tube so that good mixing is achieved before the mixture enters the main portion of the burner. Figure IV-3 shows the back diffuser which is attached to the rest of the burner with the help of a plexiglass flange, permanently joined to the back diffuser and attached to the base of the burner (middle section) with four allen types screws. All the components have O-rings placed at the attachment points to properly seal the system.

The main base of the burner (middle section), Figure IV-4, which is rectangular in shape is joined on one end to the back-diffuser and on the other to the long rectangular cross-secton burner head. A support for the flame holders is attached to one side of the burner. The base of the middle section of the burner is made of stainless steel. The entrance to the middle section is the same diameter as the lower component of the burner. A fine meshed screen is located at this entrance. This insures proper mixing of the fuel-air mixture. The middle

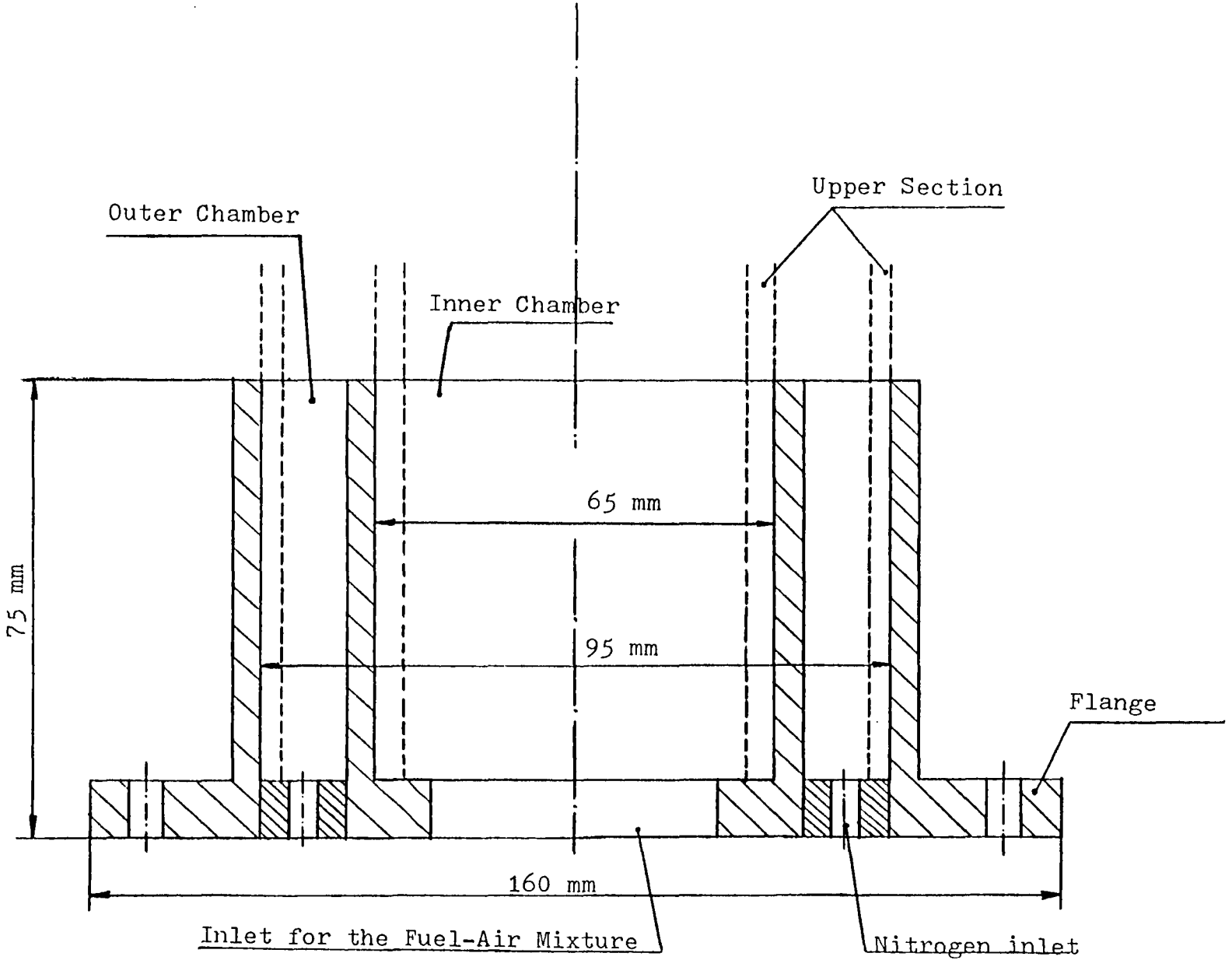

Fig. IV-4. Main Base of the Burner

section has flanges protruding from two opposite sides, which are used to mount the burner. This section of the burner has two chambers, the inner and outer for the fuel-air mixture and nitrogen respectively. Nitrogen gas was introduced to the surrounding flow to reduce the effect of air on blow-off of the inverted flame. The upper section of the burner (burner head) is designed to fit the inner and outer chamber of the middle section (base of the burner). The dimensions of the inner and outer chambers are 50.0x75.0 mm and 90.0x115.0 mm respectively. The length of this section is 80.0 mm. There are connectors threaded into the four inlets for nitrogen, positioned on each of the corners of outlet chamber. In this manner fuel-air gas mixture is surrounded by an approximately 20.0 mm wide channel of parallel nitrogen flow. The burner is enclosed by a removable transparent plexiglass chimney connencted to the exhaust hood. The rectangular geometry makes it simpler to use both the Laser Doppler Velocimetry apparatus and Schlieren optics.

The top part of the burner contains nozzles which insure flat velocity profiles. This section of the burner is shown in figure IV-5. The dimensions at the exit of the inner and outer zones are 28.0x28.0 mm and 60.0x60.0 mm respectively.

This section of the burner is made of sheet aluminium. There are two fine wire screens placed at the beginning of the nozzle and one at the exit of the burner mouth. This helps to

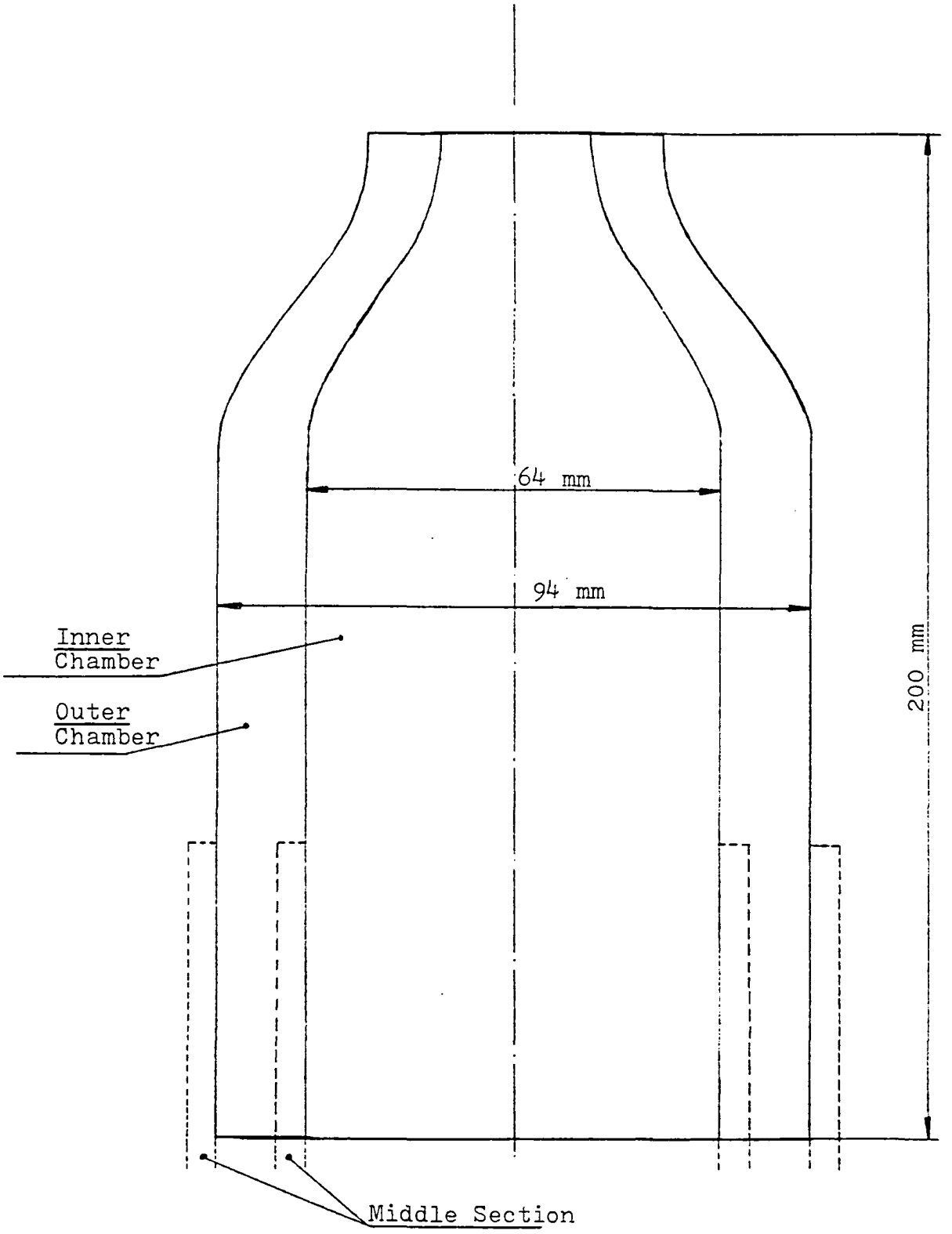

Fig. IV-5. Top Part of the Burner

prevent flashback. This component is fixed to the inner and outer compartments of the middle section (the base) of the burner as shown by dashed lines in figure IV-4.

Types of flame holders.

In the experimental study different types and sizes of flame holders were used. All together four different curved flame holders were used. The reason for making the flame holders curved is to observe only a portion of flame sheet of the inverted flame tangentially. Figure IV-6 is an isometric representation of the flame sheet held over a curved flame holder. Initially, straight brass strips were used as flame holders. This lead to the observation of a bushy flame sheet because the ends of the flame never remaining exactly stationary. This fluttering of the edge of the flame caused both the schlieren and the visible light photographs to be not well defined. The extreme flame edges could be expected to be unstable because this portion of the flame is at the perimeter of the burner mouth where surrounding disturbances affect the flame sheet most.

The flame holders were made from brass strips. For one flame holder the trailing edge was machined to be a knife-edged. All the other flame holders were thin enough to avoid any bluff body recirculation.The flame holder cross-sections are shown in

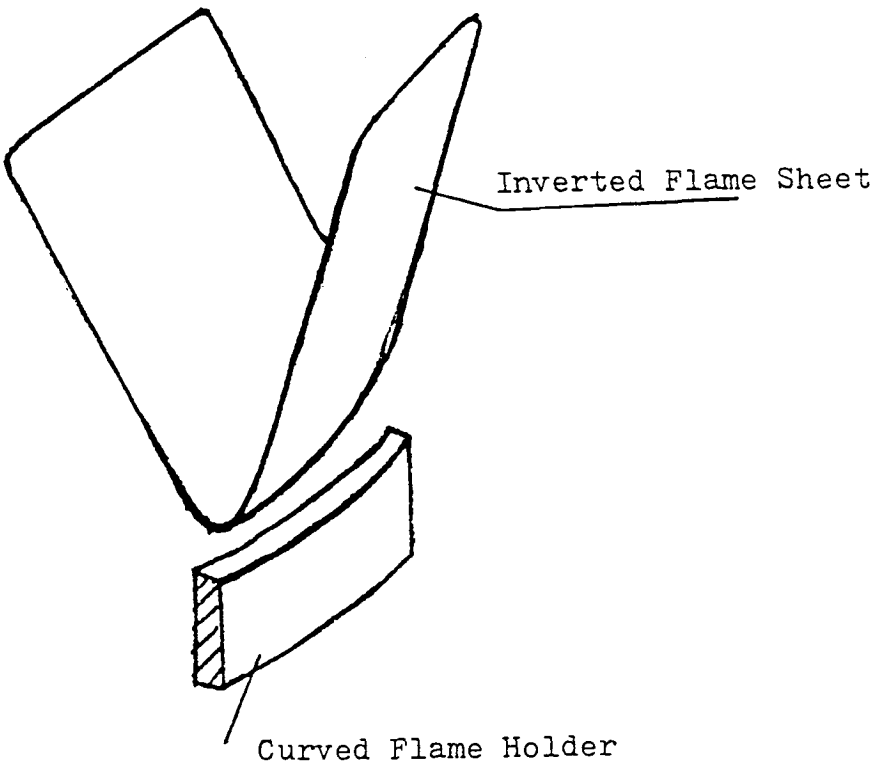

Fig. IV-6 Isometric Representation of the Flame Sheet.

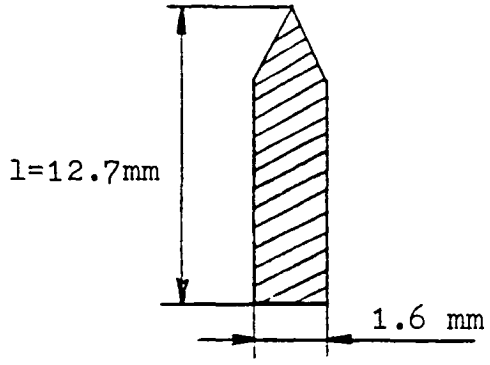

Flame Holder A

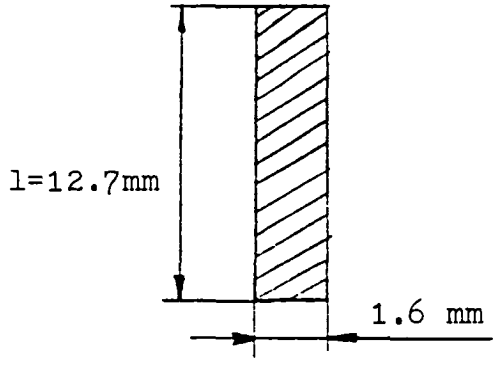

Flame Holder B

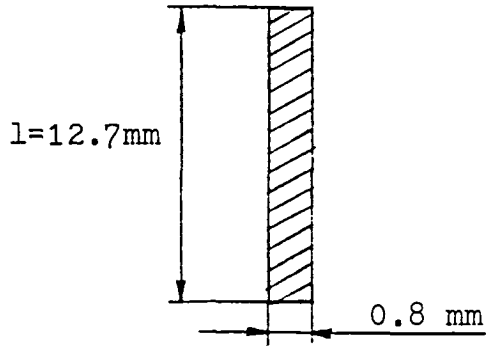

Flame Holder C

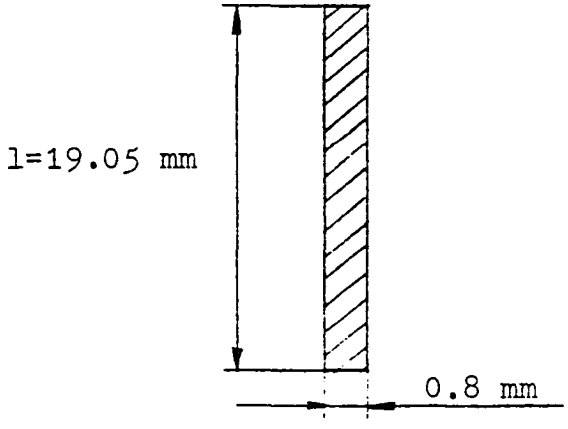

Flame Holder D

Fig. IV-7. Dimensions of Flame Holders

figure IV-7, and each flame holder is referenced as A,B,C and D for convenience. The radius of curvature is approximately equal to 65.0 mm. The distance between the burner mouth and the forward edge of the flame holder was always somewhere between 10.0 mm to 15.0 mm. A plain aluminium sheet of 10.0 mm thickness was attached to the side of the burner base and had two slots in the top edge where the two ends of the circular shaped flame holders were mounted. In figure IV-8a is an assembly drawing of the flame holder mounted on the burner and the mounting plate, and figure IV-8b is a photograph of the whole burner assembly.

DESIGN OF THE FLOW SYSTEM.

Particle injector.

One of the many possible means of seeding with solid particles is by dispersing a powder from a fluidized bed; this technique has been employed in a number of LDV experiments [36]. Particular difficulties, were however, found with regard to maintaining a controlled particle size and uniform delivery rate from fluidized beds. Although Kunii, D., and Levenspiel, O., [37] have provided a methodical approach to this problem, still the design and optimization of fluidized beds tends to be a matter of experience which is tailored according to the need of the experimental work. A further discussion of the importance of particle seeding will be presented in the LDV measurement

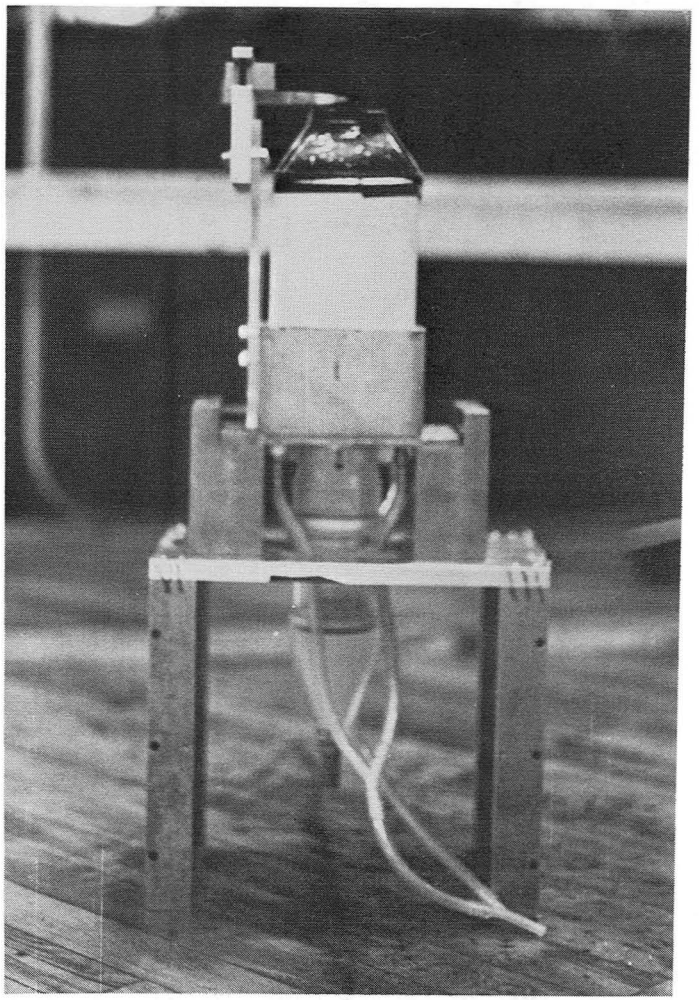

Fig. IV-8b. Photograph of the Burner Assembly.

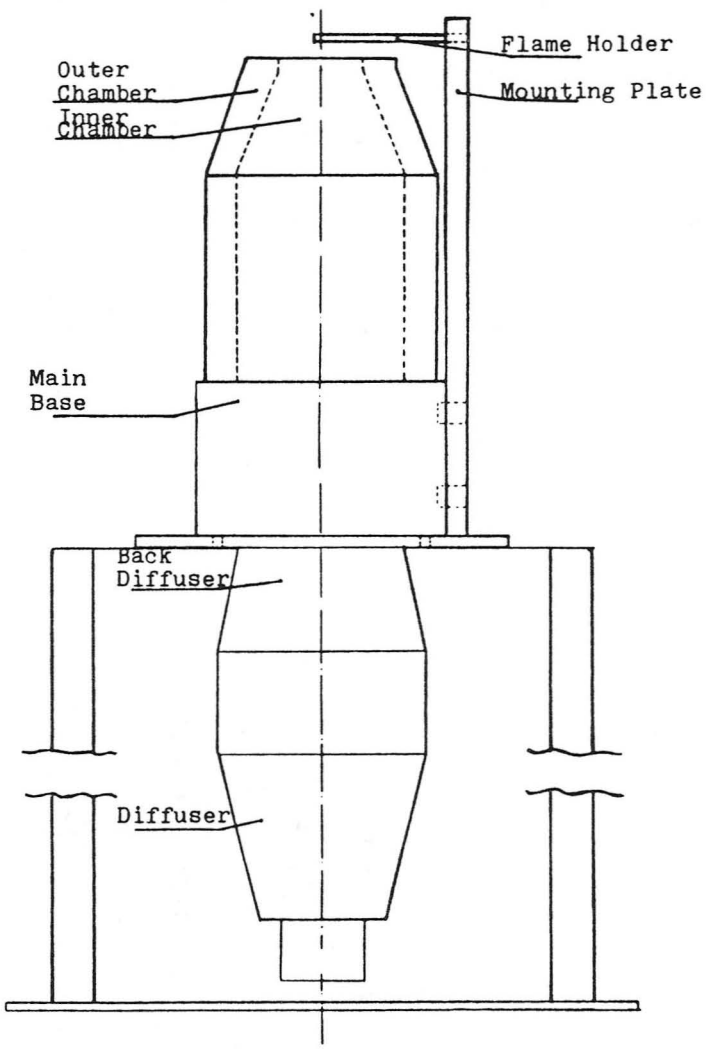

Fig. IV-8a. Assembly Drawing of the Burner.

section.

A schematic of the particle feed system used for this study is illustrated in figure IV-9. This system was developed earlier by Reuss D., [38]. Some changes were made in the particle seeder from the earlier version after analysis of the results obtained from preliminary LDV measurements. The fluidized bed has been changed to be similiar to the "Puldoulit" fluidized bed described by Guichard [39]. In this technique the powder to be fluidized is mixed with relatively large glass beads, which allows a clear passage for the fluidizing air without the formation of bubbles. Also, friction between the beads decreases the aggregation of particles, which coat the beads, thereby contributing to the stability of the particle concentration and size distribution.

The dimension of the fluidized bed is 20.0 mm diameter and 140.0 mm long. After passage through the bed particle laden air passes through a settling tube into a hypodermic tube 1.25 mm ID and 100.0 mm long. Up to this point the suspended powder still contains agglomerates which can be up to 1.0 mm in diameter. The jet formed at the hypodermic tube exit creates a region of high shear which breaks up the agglomerates. This flow containing fine particles enters the upper large settling chamber. During the experiments the filter at the top of the large settling chamber was not used.

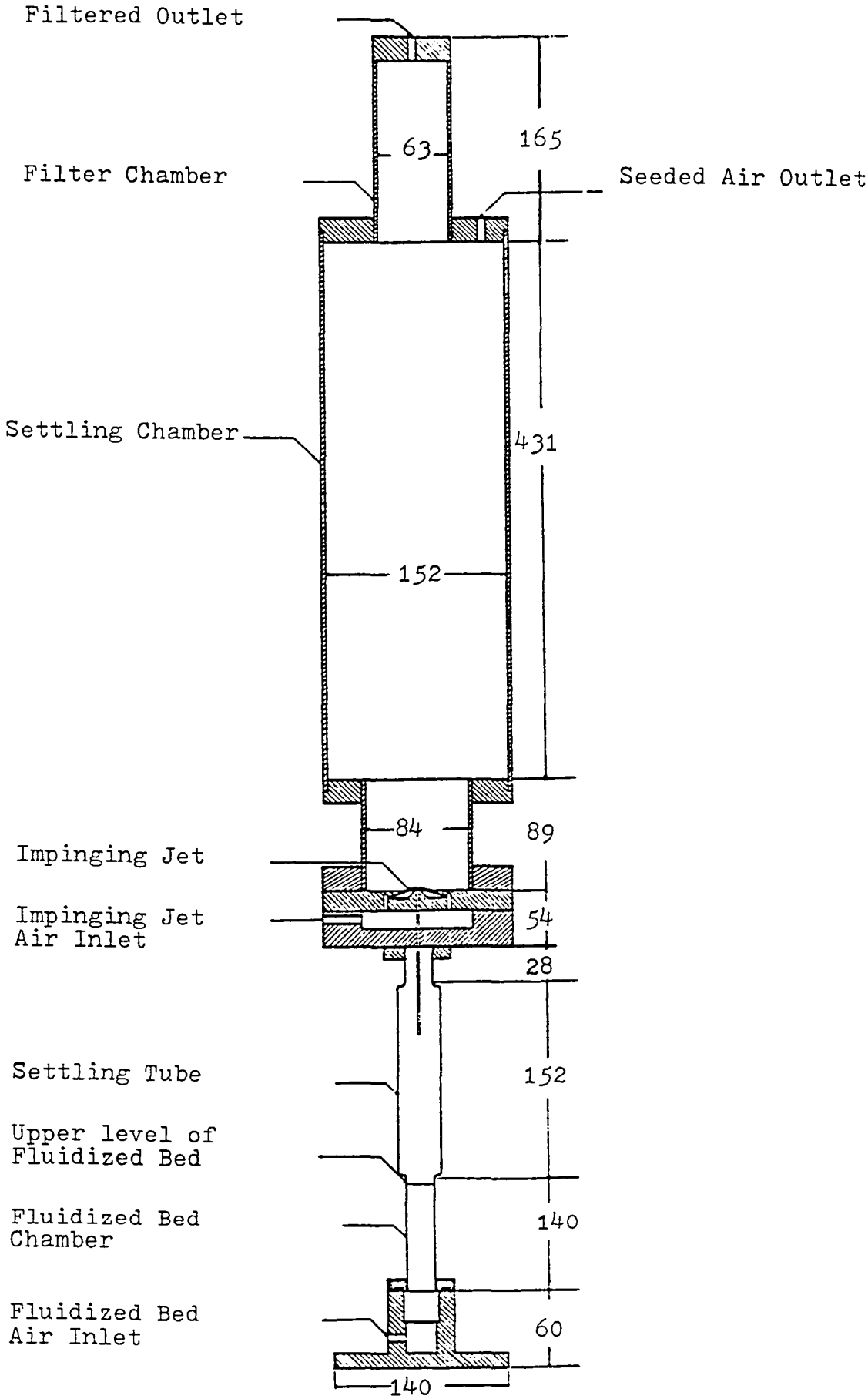

Fig. IV-9. Particle Injector.

Only part of the air that entered the burner was passed through the fluidized bed as can be seen in figure IV-10, and it exited through the outlet at the top (right hand side of the settling chamber). The particle laden flow then passed through a piece of 6.4 mm polypropylene tubing to the mixing chamber where it was mixed with the fuel.

Flow velocity measurement and
Flow configuration with the particle injector.

The flow velocity measurements were taken with the help of laser doppler velocimetry system. More about the LDV system will be presented in the pages ahead. Here it will be suffice to mention that the amount of fuel-air mixture exiting from the burner outlet was controlled by rotameters placed in the flow line. Calibration curves for respective fuels were used in order to convert the rotameter reading to the actual flow rate. These rotameters were made by Matheson Gas products.

Figure IV-10 is a schematic sketch of the flow system showing the particle injector and mixing chamber. A pressure gauge was placed in the fuel line to keep a check on the line pressure. The air supply line was divided before entering the particle injector. The reason being to let only part of the whole air supply go through the particle injector system. This enabled the experimentor to control the concentration of the

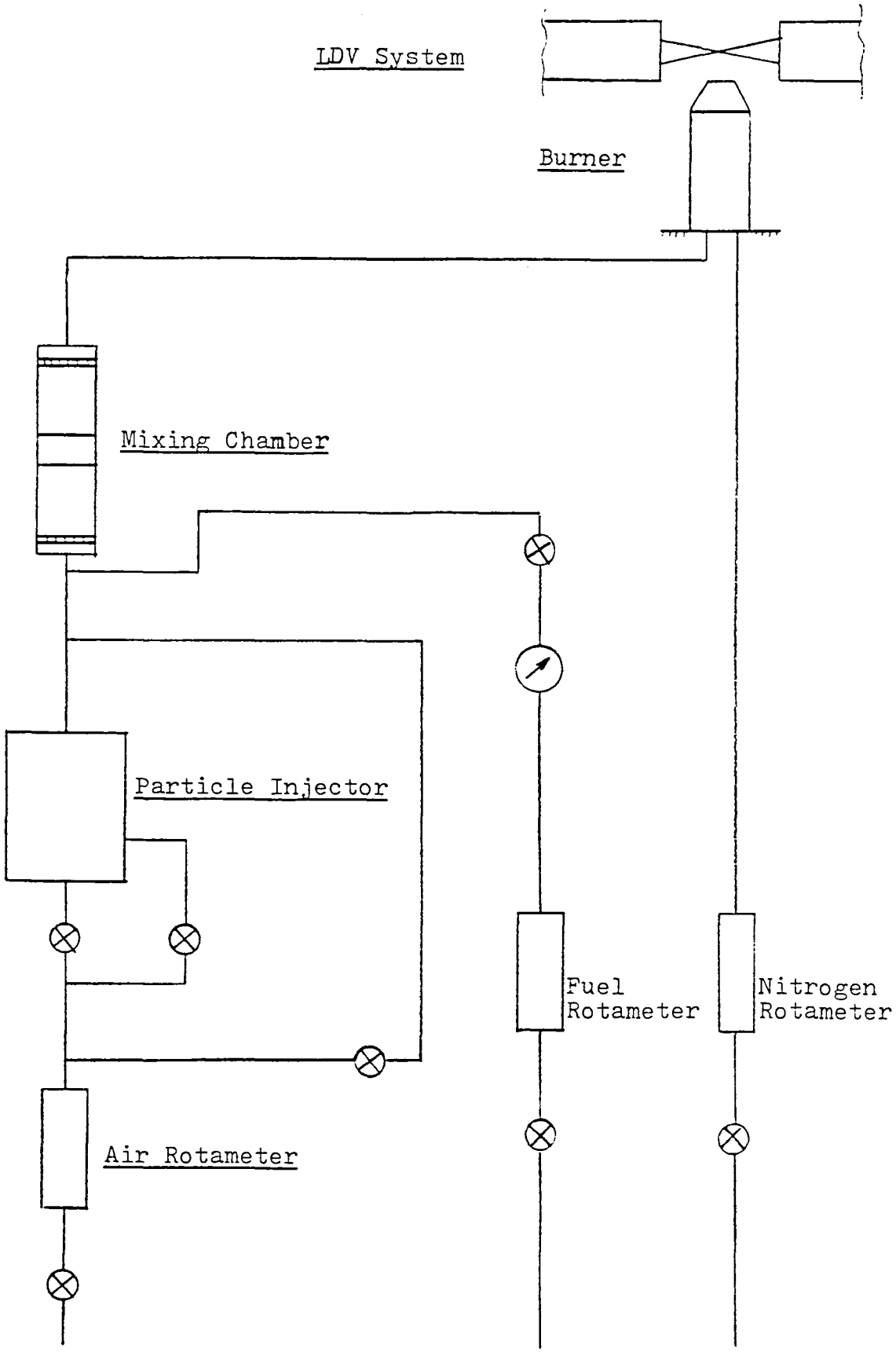

Fig. IV-10. Schematic Sketch of the Flow System.

particles in the air. From the experimental observations it was found best to keep the surrounding flow rate of nitrogen to 0.2 - 0.3 per second.

LASER DOPPLER VELOCIMETRY (LDV) ARRANGEMENT.

Adaptation of the LDV system to the present study.

Laser Doppler Velocimetry systems have been used for making measurements in flames under both laboratory and industrial conditions, in flames using gaseous, liquid, and solid particle fuels. The flow situation prevailing in the flame, particularly in the wake of a flame holder, are essentially inaccessible to conventional intrusive measuring methods and this justifies the use of LDV. The flame measurements provide information about local fluid velocities, particularly in the vicinity and across the flame front. This kind of information is of fundamental importance to the understanding of flame stabilization and flame behavior near blowoff.

In selecting the components of the LDV system for this particular application, considerable attention was given to:

1. Forward or Back Scattering.
2. Laser Power.
3. Particle Seeding.
4. Measurement of the Probe Volume.

The question of selecting forward or back scattering is generally dictated by the degree of access to the test section. In this study the burner was surrounded by a chimney of plexiglass which had two windows on two opposite sides which were fitted with high quality glass viewing ports. Thus the test section was accessible from both sides and one could easily use the better and more efficient forward scattering mode.

Combustion systems are more likely to have particulate matter in the flow system than many other wind tunnel or aerodynamic systems. Although there may be some particulate matter in flows involving reactive gas mixtures, in this experiment these particles were not suitable for the desired LDV measurements. Thus artificial seeding had to be used to study this flow. Furthermore, it was necessary to choose an inert material which would not be destroyed in the flame. The two limits set on artificial seeding are dictated by the fact that the particles should be of small enough diameter to follow the flow but on the other hand large enough to give a good signal; therefore, a compromise had to be made in the selection of the particle size. As far as the concentration of the particles is concerned, it is sufficient to maintain at least one particle in the probe volume most of the time. The probe volume with the transmitting (focusing) lens system are shown in figure IV-11. As illustrated the measuring volume is approximately an ellipsoid. The edges of the ellipsoid are defined as the point

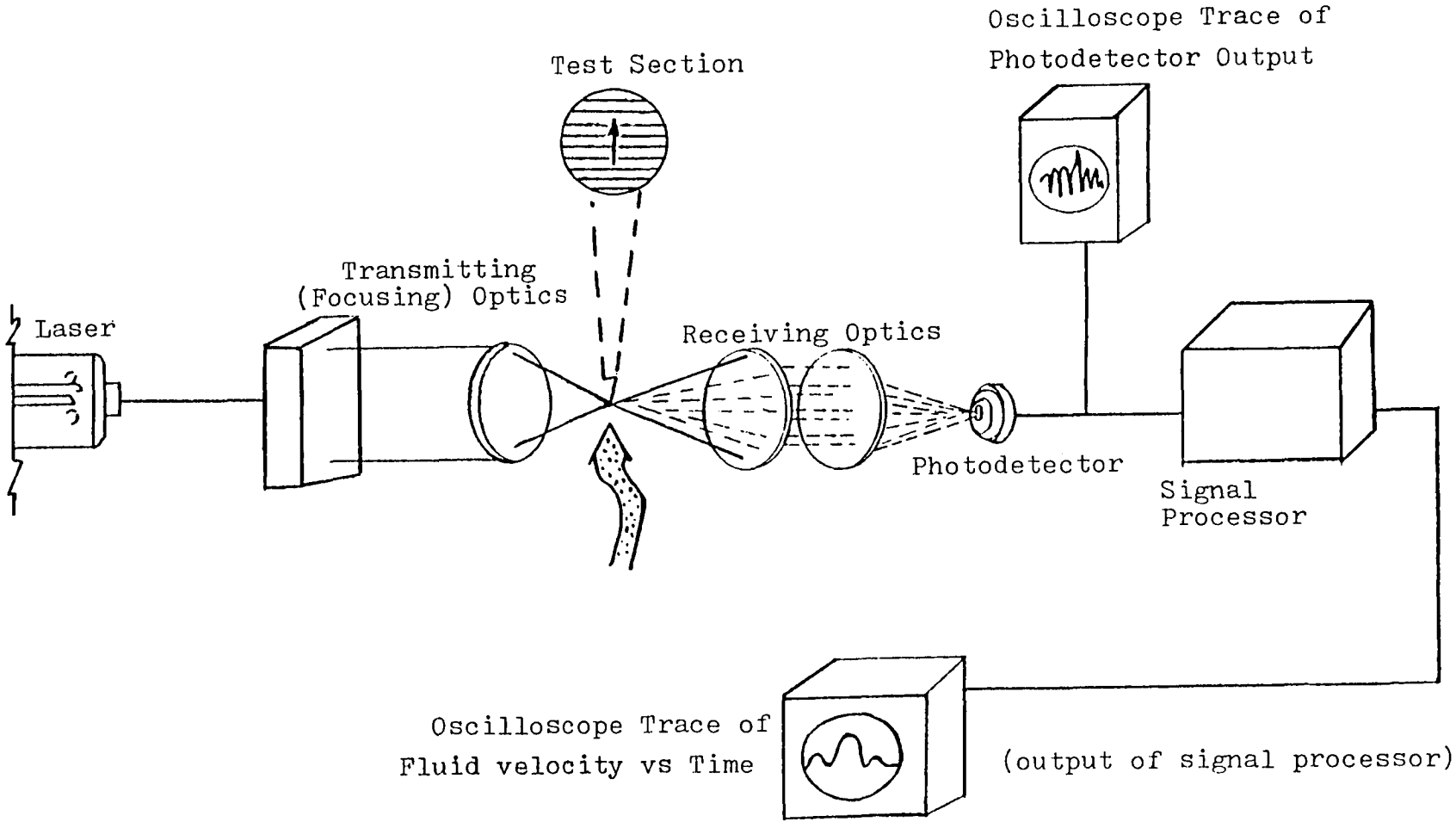

Fig. IV-11. Complete Dual Beam LDV System.

where the amplitude of the doppler signal is e^{-2} of its centerline value. This is a convenient definition for reference purposes.

For this study Aluminium Oxide (Al_2O_3) polishing powder was used since it met the criteria and was readily available. A particle size of one micron was used. The specifications are given in table 5.1.

Table 5.1

Specification of Powder

used for Particle Seeding

Microgrit GB, Aluminium Oxide Polishing Powder, 98%

From: Micro Abrasives Corporation, Westfield, MA

Specific Gravity	3.6
Particle Size #	# 2000
Average Size	1
Color	White
pH	8.5
Hardness, Mho	9.0

This powder was choosen because it has about the correct size and because the particles are approximately spherical (as opposed to oblong - like for some particles). Special experiments were not

conducted to find out whether or not the particles are non-intrusive, but when the blow-off data obtained during schlieren photography (without seeding) were compared to the LDV measurements (with seeding), it was observed that the lean blow-off limit of methane - air and propane - air flames are altered by the presence of particles. It was seen that the seeded blow-off lean limit mixture composition is richer than the unseeded mixture. This can be explained by the fact that presence of particles increase the effective heat capacity of the fluid and therefore lowers the flame temperature and normal burning velocity slightly. The data from LDV measurements, blow-off data and the schlieren pictures are presented in the next chapter.

Another difficulty should be noted at this stage concerning the artificial seeding. A bias can result from non-uniform particle number density in the flow. The condition of non uniform seeding could arise when seeded and unseeded gas streams, are mixed e.g. a seeded air jet discharging into ambient air, or in a gas in which an initially uniform seeding density becomes non-uniform as a result of local density changes, e.g. from passage through a flame [40]. This phenomena is illustrated in figure IV-12. Across the flame front of a reacting mixture, the ratio of the densities of unburnt and burnt gas may be as high as 7.0, and as the unburned gas approach the flame front the temperature gradients are very high. Hence in a

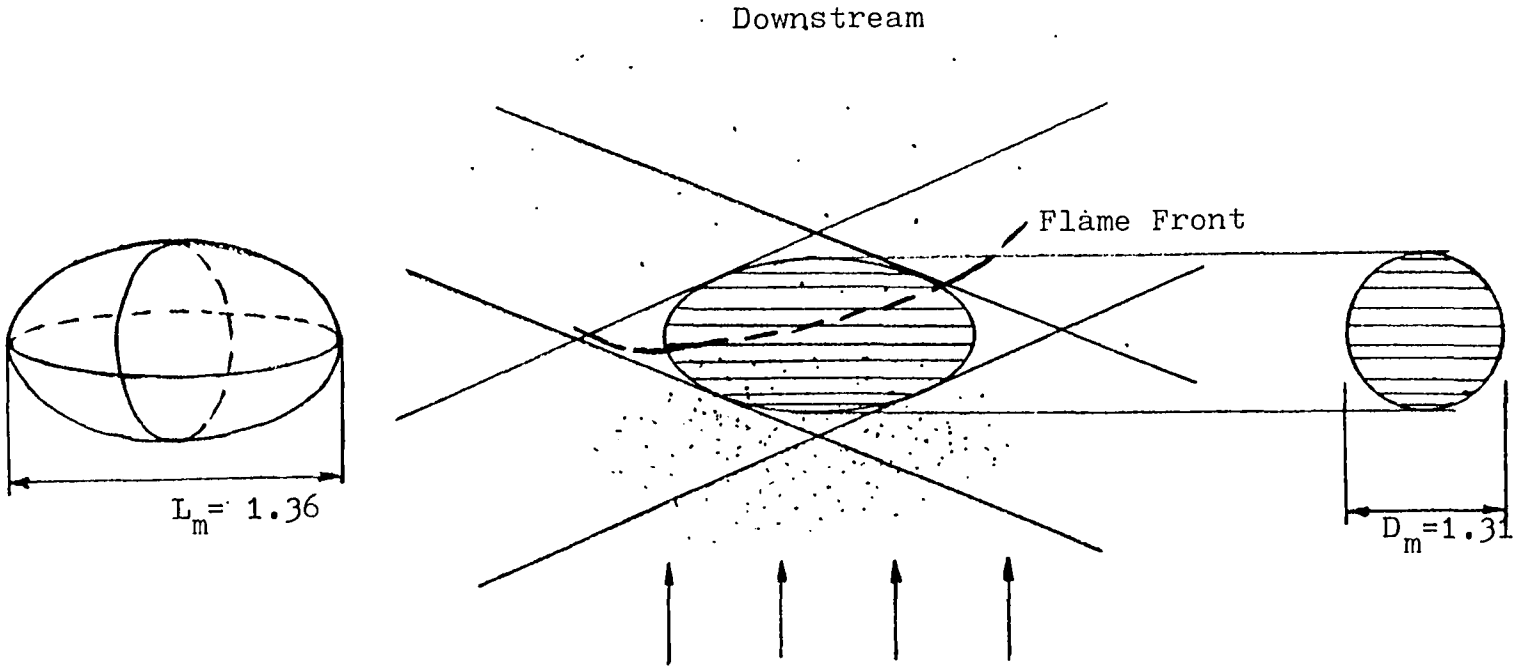

Area of Scattering Volume Normal to Flow = $L_m \cdot D_m$

Fig. IV-12. Non-Uniform Particle Concentration.

measuring volume, the proportion of doppler signals received per unit time from the unburned gas will be several times as great as that from the burned gas, due to thermal expansion of the gases. To solve this problem the concentration of the particles was carefully increased when measurements were made inside the flame front. This was done by diverting less air flow around the particle generator, keeping the total flow constant.

A simple LDV system has a 180 degrees directional ambiguity so that, if no special devices are used, the sense (negative or positive) of the flow direction cannot be distinguished. In the current study directional ambiguity was not a problem and therefore the introduction of frequency shifting was not considered necessary. The main reason behind this was that there was one main predominant vertical velocity component which was always directed upward. The horizontal component of velocity was almost zero. The major portion of the data was gathered for this single channel vertical component. Two sets of data for the knife edge flame holder using two different fuels: methane and propane has been gathered with the help of the two - channel data acquisition program. For this portion of the study, the two measured components were oriented at 45 degrees to the right and left of the vertical axis. The reason for taking measurements in this manner is the fact that the horizontal component has an almost negligible magnitude. A direct measurement of this very small velocity component would

require frequency shifting to remove the zero frequency post which would over-power the very low frequency signal associated with the low horizontal velocity component. Since the maximum flow deflections are much less than 45 degrees to either side of the vertical axis. There is no directional ambiguity and the two measured velocity components could be resolved to determine the actual horizontal components of velocity.

The LDV system is linked with the RT-11 computer for data acquisition purposes.

Brief description of the LDV system.

The Laser used in this study was a Spectra - Physics model 164-06 two watt argon-ion laser. It was powered by a Spectra - Physics model 265 exciter. While examining the laser power it was found that only a portion of the total laser power was emitted at wave-lengths of 488 nm (~ 45% of total power) and 514.5 nm (~ 35% of total power), corresponding to the colors blue and green respectively. Power losses through units of the LDV system were observed to be 15% to 20%. Also repeated checks were needed to keep the optical system aligned and surfaces of the mirrors clean in order to maintain beam power. It was found that the laser power should be at least in the range of 0.5 to 1.0 Watts in the forward scatter mode in order to obtain good signal - to - noise ratios using seeding particles in the one micron

range. The exciter provided current to the plasma tube solenoid and controlled the ion discharge in the plasma tube so that a constant laser output was maintained.

The beam leaving the laser was first checked for its collimation so that the probe volume fringes were parallel and the beam "waist" or minimum diameter occured at the point of velocity measurement. Collimation was performed after the LDV optical system was assembled. Collimation can be accomplished indirectly by making the fringes in the probe volume parallel. This was checked by translating the rotating disk along the long axis of the probe volume and adjusting the collimation until the frequency output (and thus the fringe spacing) was nearly constant. A schematic sketch of the LDV system is shown in figure IV-13. The beam was resolved into its component colors by a TSI model 901 dispersion prism. Plane mirrors (TSI model 907) directed the green beam down the main optical axis and blue beam down a parallel axis to bypass the green beam splitter. The beam displacer (TSI model 973) realigned the blue beam along the main optical axis at 90^{o} degrees to the green beam. Polarization rotators (901 and 902 for green and blue) were used to rotate the polarity of the beams perpendicular to the plane of the beam splitter. In this way, the beams were resolved into two perpendicular components of equal intensity. The green beams were separated by 50.0 mm at 45^{o} to the horizontal plane and the blue beam by 50.0 mm at 45^{o} to the verical plane. Two achromatic

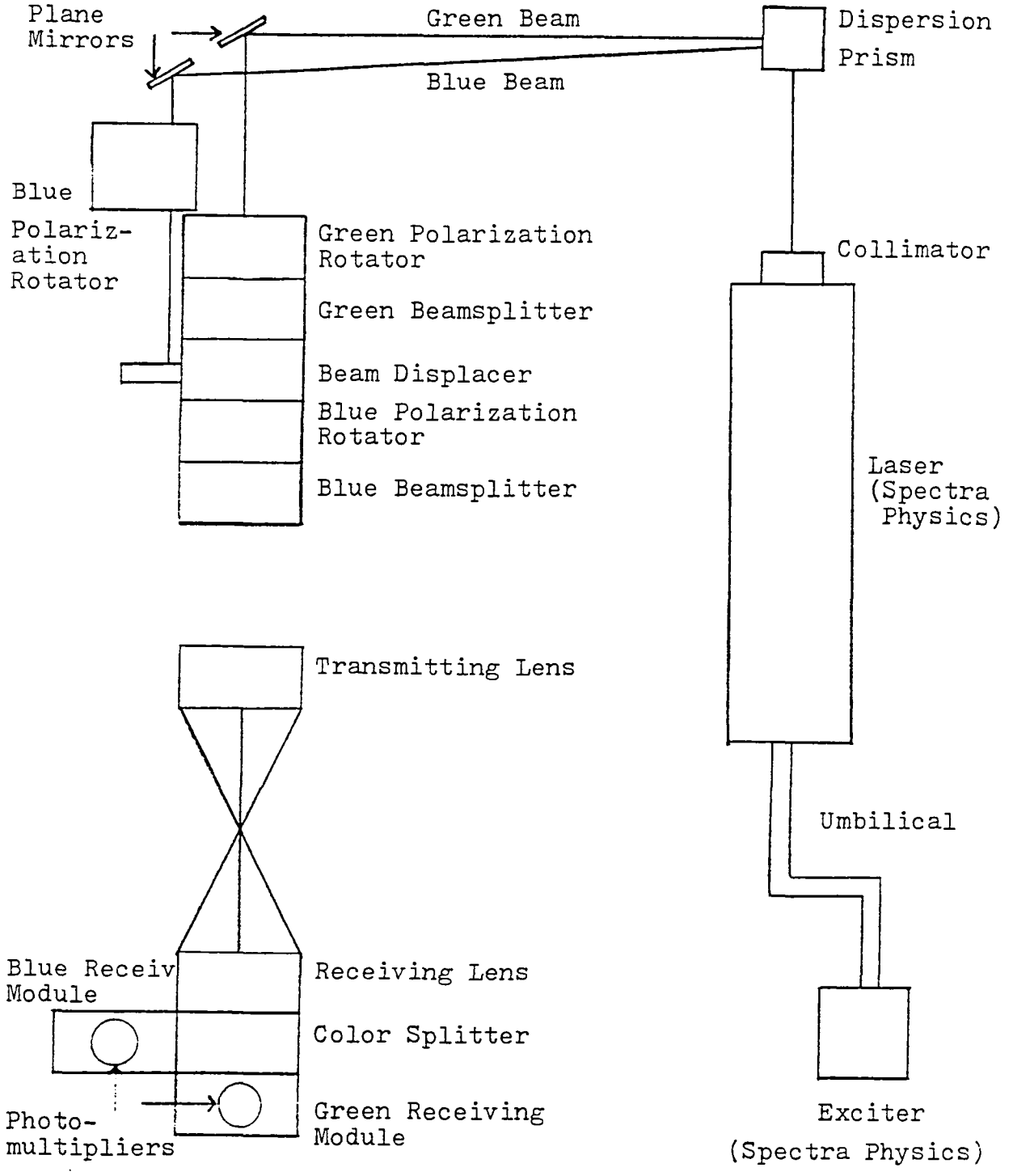

Fig. IV-13. LDV Assembly for Forward Scatter Collection.

lenses of focal lengths 250.0 mm were used, one to focus the laser beams at the receiving volume, the other to collect light for the receiving optics, to pick up the doppler burst signals with the photomultipliers.

The receiving optics consisted of color splitters with dichoric mirrors for both green and blue beams. The scattered light from the particles in the probe volume was focused onto the photomultiplier. Each receiving module had a narrow band - pass filter; one passed only blue light, the other only green. This helped to eliminate noise from other light sources such as flame radiation. The components of the LDV system and signal processing unit are illustrated in figure IV-13. Green beam fringe spacing for a lens of 250.0 mm focal length was calculated to be 2.682x10E-06 m. The diameter of ellipsoid shaped probe volume was D_m =0.131 mm and the length of the probe volume L_m =1.36 mm. The blue beam fringe spacing was D_f =2.544x10E-06 m. The dimension of D_m is small enough so that there is no appreciable gradient in this distance.

The whole LDV system i.e. LDV table plus the burner table had 3 degrees of freedom. The directions of various movements are shown in figure IV-14. The burner assembly was mounted inside the laser table between the transmitting and receiving platforms.

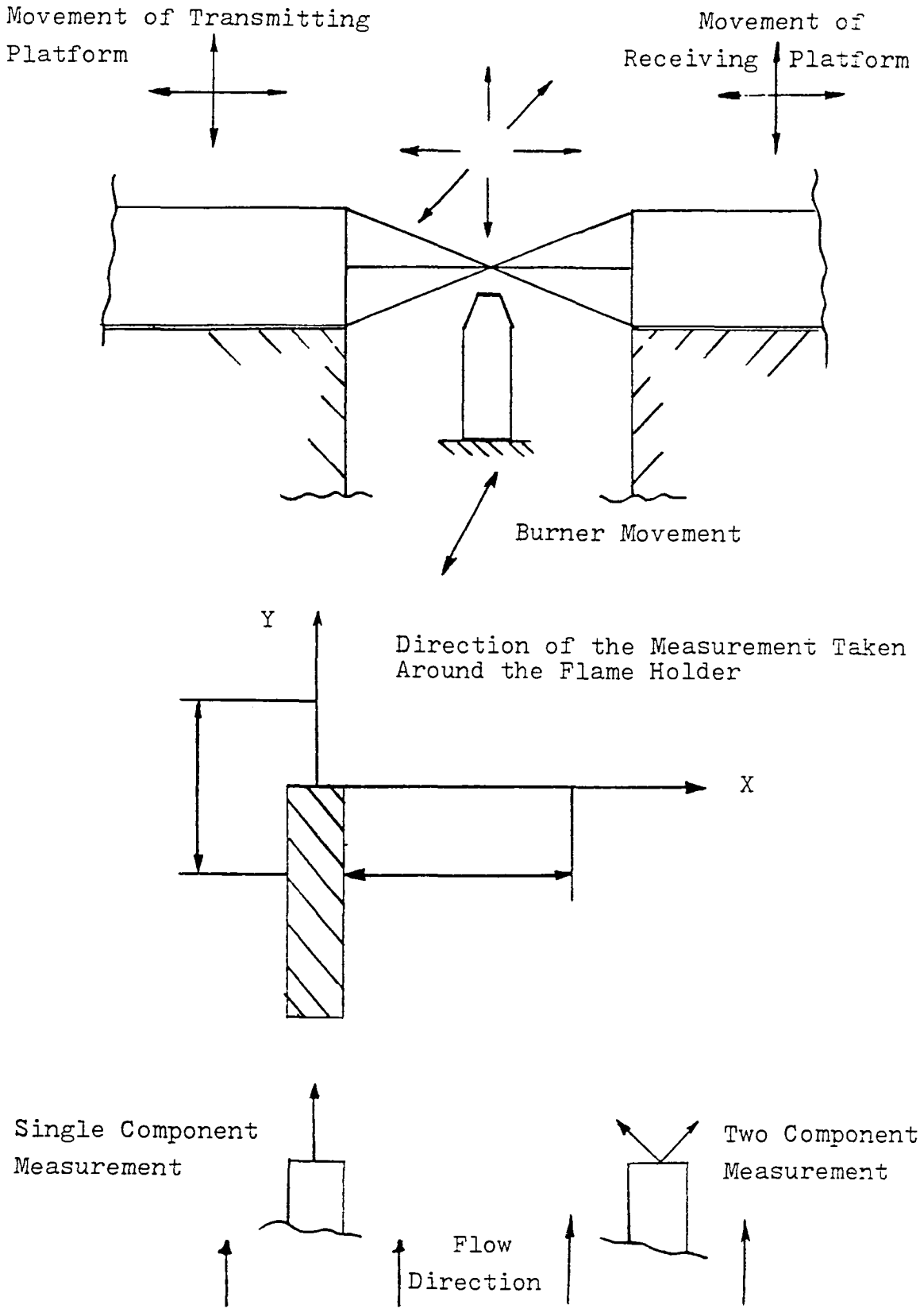

Fig. IV-14. Movement of the LDV table Plus Burner table.

SCHLIEREN AND VISIBLE LIGHT PHOTOGRAPHY.

One aspect of this experimental study was concerned with collecting the data for the blow-off limits of the inverted flame plus taking the schlieren photographs of the flames near the blow-off limit.

"Schliere" is a German word meaning the inhomogeneous regions in otherwise homogeneous matter, i.e regions in a fluid medium that has a density and hence a refracive index differing from that of the bulk of the medium. These schlieren effects can easily be observed when hot air rises above a hot body. When gases in case of combustion approach the rection zone of the flame, the gases are heated, and the increase in temperature causes changes in their density, and refractive index. In a flame, the refractive index varies due to changes in temperature and in composition, though the predominant effect is due to the temperature change. In figure IV-15 is illustrated the working principle of schlieren system. Parallel light rays emitted from the source pass through the test region, E, those which are not deflected are brought to a point focus by the "schlieren lens", D. The corresponding points of focus for deflected rays are displaced, as shown by dashed lines. The "projection lens", G, is positioned so that in conjuction with D, it images E on the screen H. In the absence of knife edge F, a normal image of E would be produced. The knife edge used with an absolutely

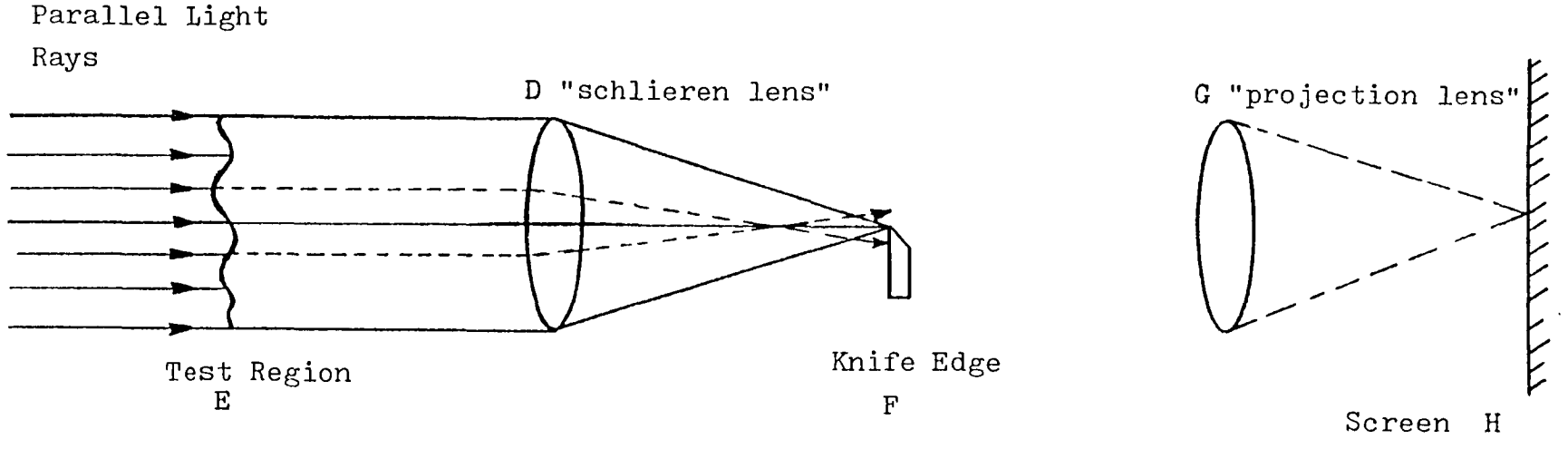

Fig. IV-15. The Working Principle of
Schlieren System.

parallel incident beam deprives the image of all light in zones corresponding to downward deflection, while allowing passage to rays deflecting upward.

Figure IV-16 illustrates a schematic set up of the schlieren system used for the present experiments. A is the real source, C is the aperture confining the "effective source" (slit opening between two knife edges). D are the concave mirrors of approximately 100.0 mm diameter and 750.0 mm focal length. E is the test section with the curved flame holder placed tangentially to the line of the two mirrors. F is the second knife edge and G is the projection lens of the camera.

Concave mirrors are used instead of expensive lenses, and the astigmatism may be overcome, by focusing so that the image is drawn out parallel to the direction of the knife edge. Coma is kept to a minimum by keeping the angle between the parallel beam and the light source the same as the angle between the parallel beam and the camera (see Figure IV-16). The camera used for schilieren pictures was Cannon AE-1 with the lens removed.

The visible light photograph helped in determining the position of the luminous zone of the flame front with respect to the trailing edge of the flame holder. The same camera (Cannon AE-1) was used with combination of two lenses attached to the camera. It is worthwhile to mention here the importance of

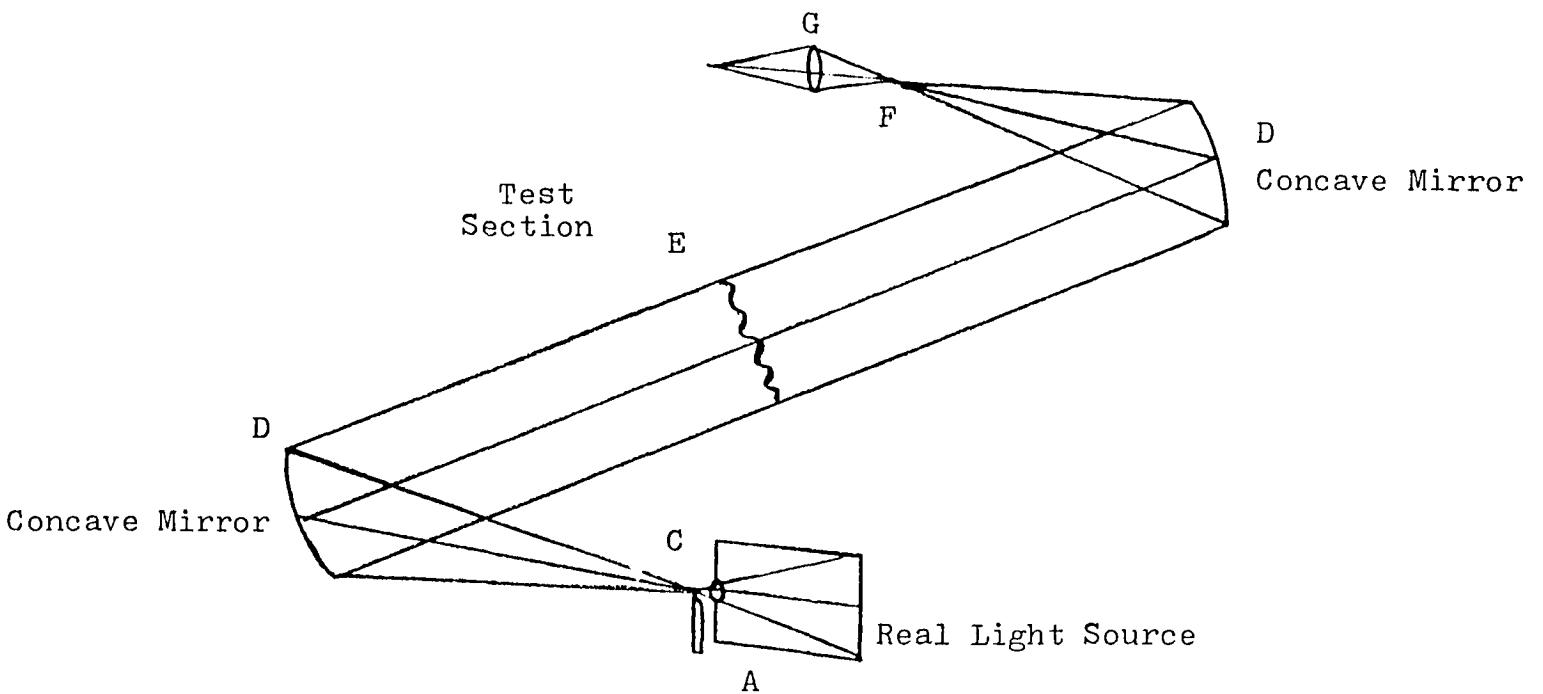

Fig. IV-16. Schematic Set-up of the Schlieren System for the Present Experiments.

having the test object in focus on the plate of the camera for both schilieren and visible light photography. In order to focus on the test section a wire grid was placed perpendicular to the tangent of the curved flame holder, and illuminated with a flood light.

THE PROCEDURE USED FOR COLLECTION OF BLOW-OFF DATA.

Blow-off data was collected by keeping the approach flow velocity for air at a particular value and slowly decreasing the approach flow concentration of the fuel. In this manner the data was collected for approach flow velocities varying from 50 cm per second to 155 cm per second. For every setting of air two schlieren photographs were taken, one when the flame was stable over the flame holder and the other when the flame was about to lift-off.

CHAPTER V

Experimental Results and Their Analysis.

In the previous chapter the experimental set-up and apparatus were described. In the current chapter experimental results and their analysis will be presented.

As has been discussed in the previous chapter, the Laser Doppler Velocimetry technique was used to determine the velocity flow field around the trailing edge of various sizes of flame holders. Table 5.1 indicates the referenced flame holders that were used and the fuels used with each (see figure IV-7).

Table 5.1

Type of Experiments	Flame Holders using Methane	Flameholders using Propane
Blow-Off Data	A,B,C,D	A,D
Schlieren Pictures	A,B,C,D	A,D
Direct Pictures	A,D	A,D
LDV Measurements (single component)	A,B,C	A
LDV Measurements (two components)	D	D

For certain flame holders both the fuels methane and propane were used in order to obtain the effect of lighter and heavier fuel on the shape of the flame and blow-off velocity and for comparison to the extinction studies of Tsuji [32].

The blow-off data was taken for methane and propane by fixing the air flow rate and slowly varying the fuel flow rate untill blow-off occured. Air flow rates were varied from 0.4 liter per second to 1.0 liter per second, with an interval of 0.04 liter per second. The blow-off velocities were calculated by dividing the total flow rate exiting from the burner outlet by the area of the burner outlet, which was 2.65x2.65 square cm. This yielded flow velocities at the burner mouth that changed from 55.0 cm per second to 152 cm per second.

The blow-off data for various flame holders is illustrated in figures V-1 to V-4. The flame holders used for obtaining this data are the same that were used in the case of velocity measurements using the LDV technique. The blow-off data shows that there is not much change in the blow-off criteria for the different flame holders using both the fuels methane and propane. The blow-off velocity curves for flame holders A and B in the case of methane-air mixtures are shown in figures V-1a and V-2 which have similiar behaviors, although in the intermediate range of 5.25% to 5.65% fuel concentration, the flame stabilized over the flame holder B blows off at a relatively leaner fuel

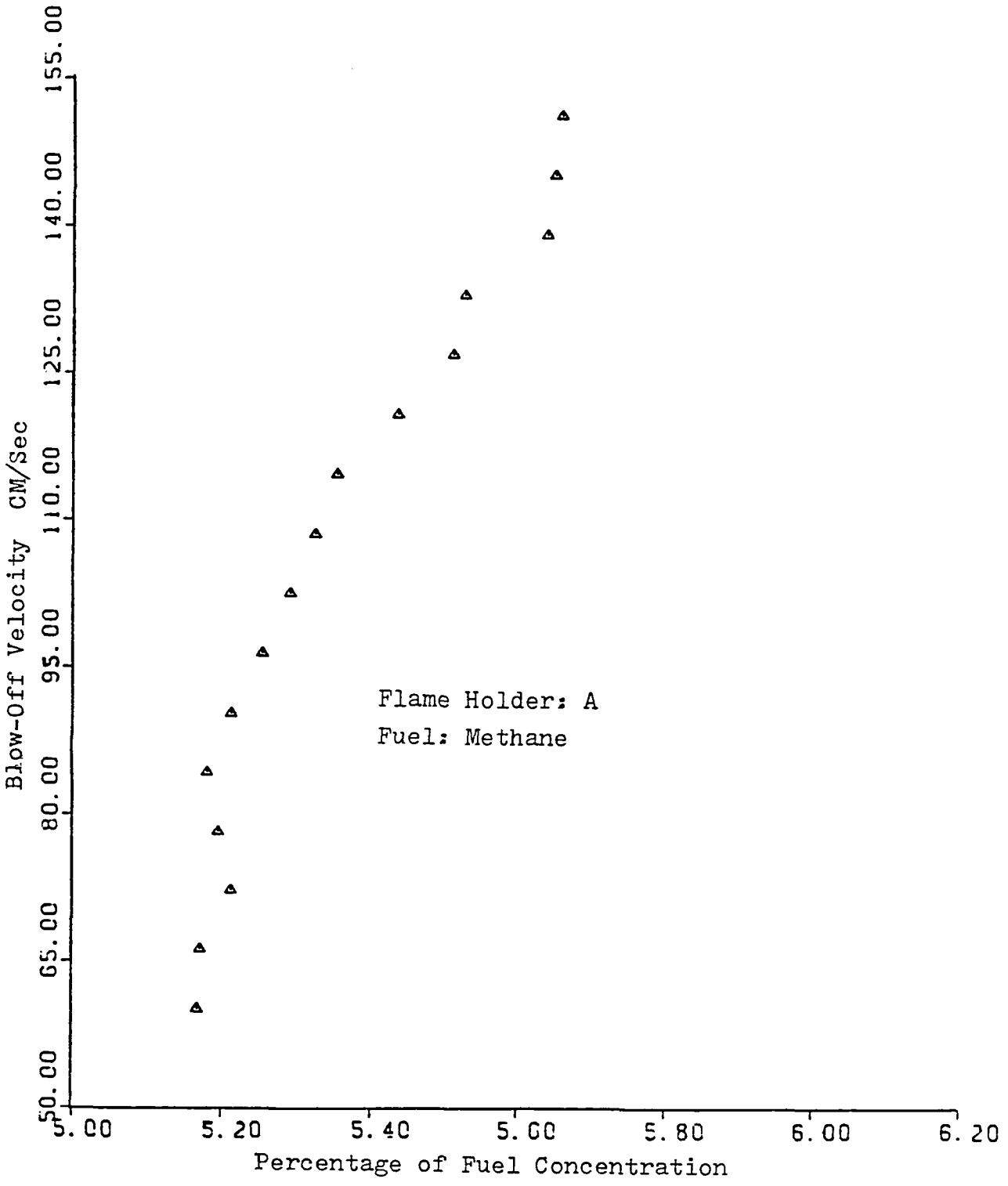

Fig.V-1a. Blow-Off Velocity versus Fuel Concentration.

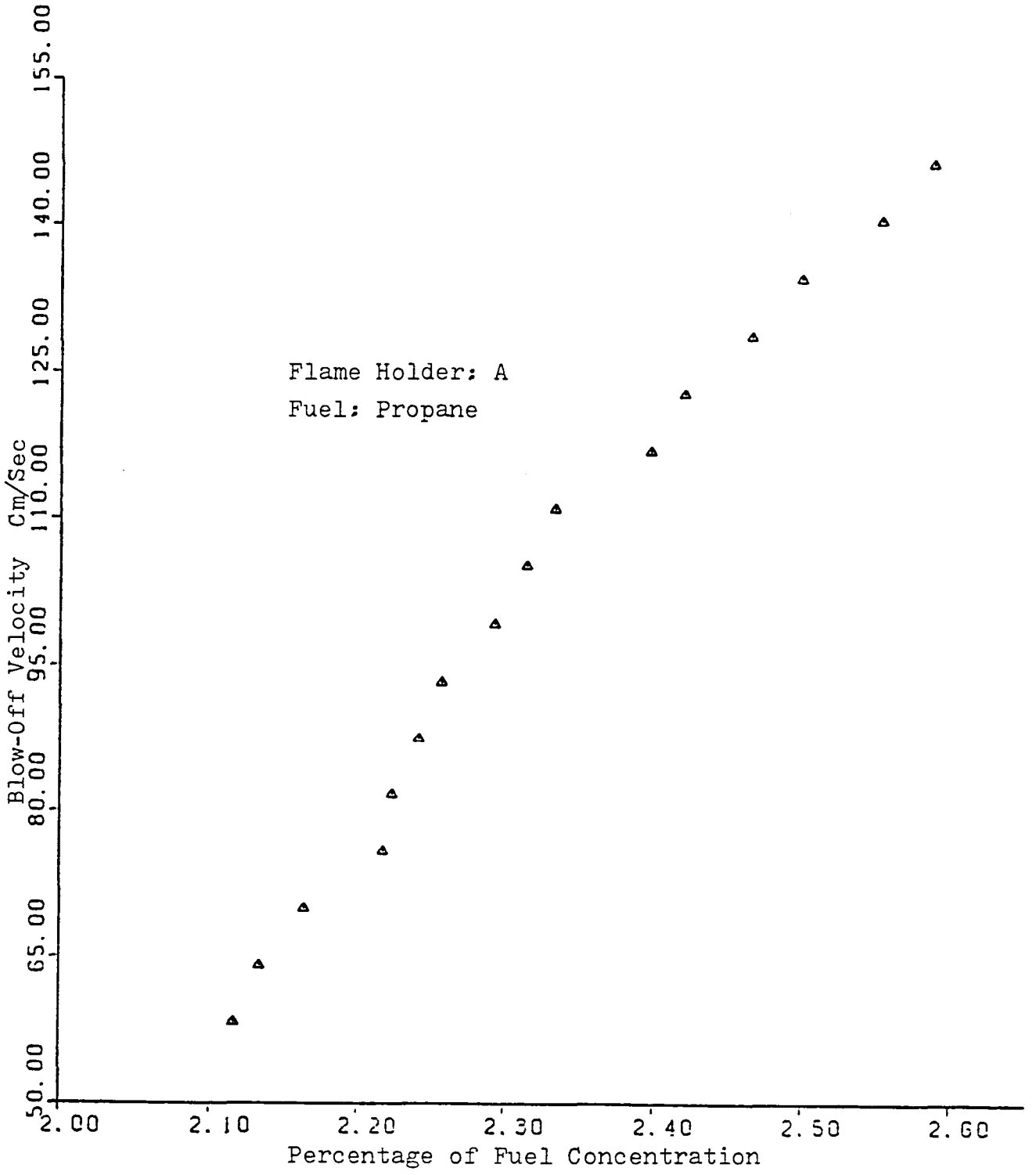

Fig.V-1b. Blow-Off Velocity versus Fuel Concentration.

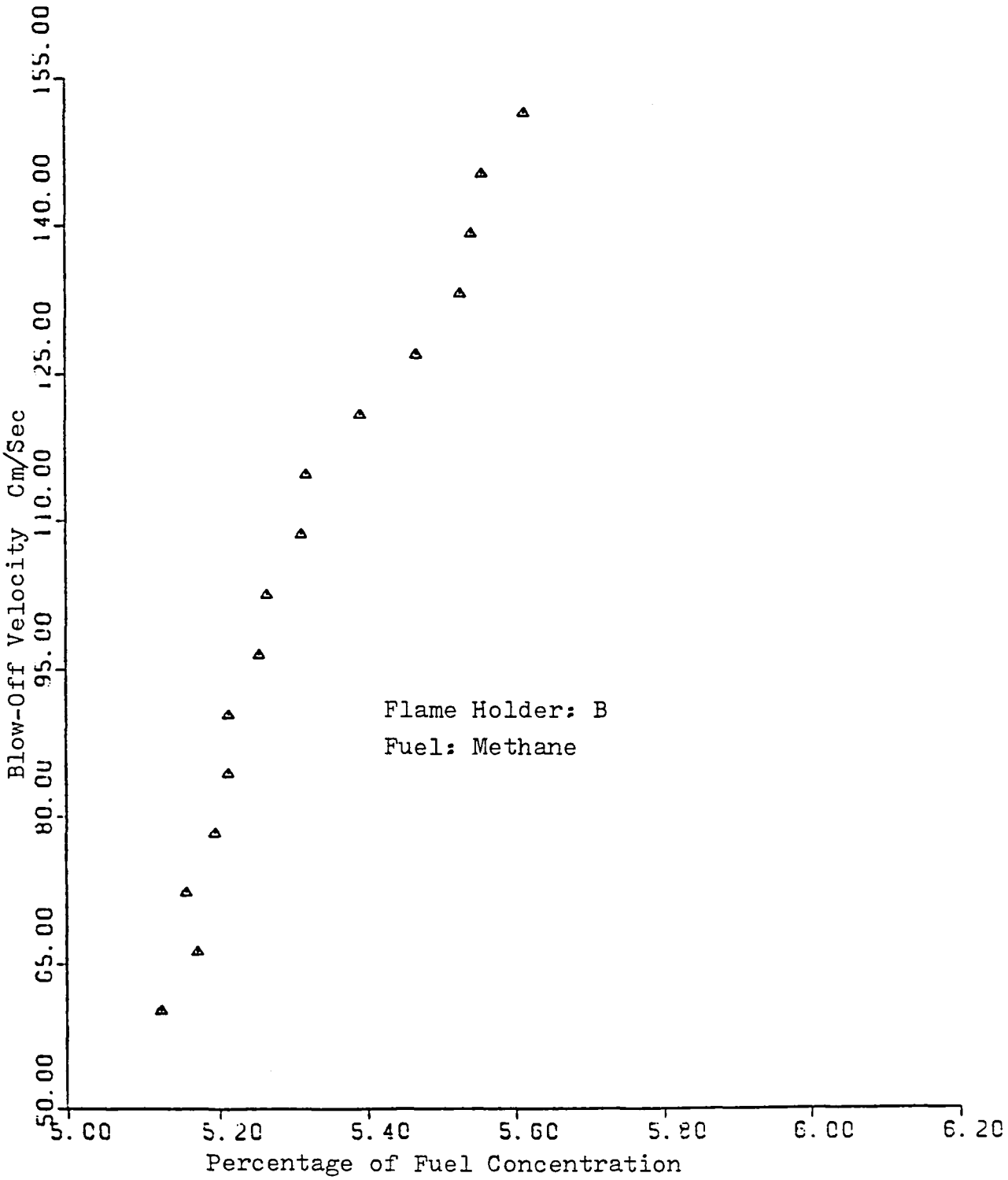

Fig.V-2. Blow-Off Velocity versus Fuel Concentration.

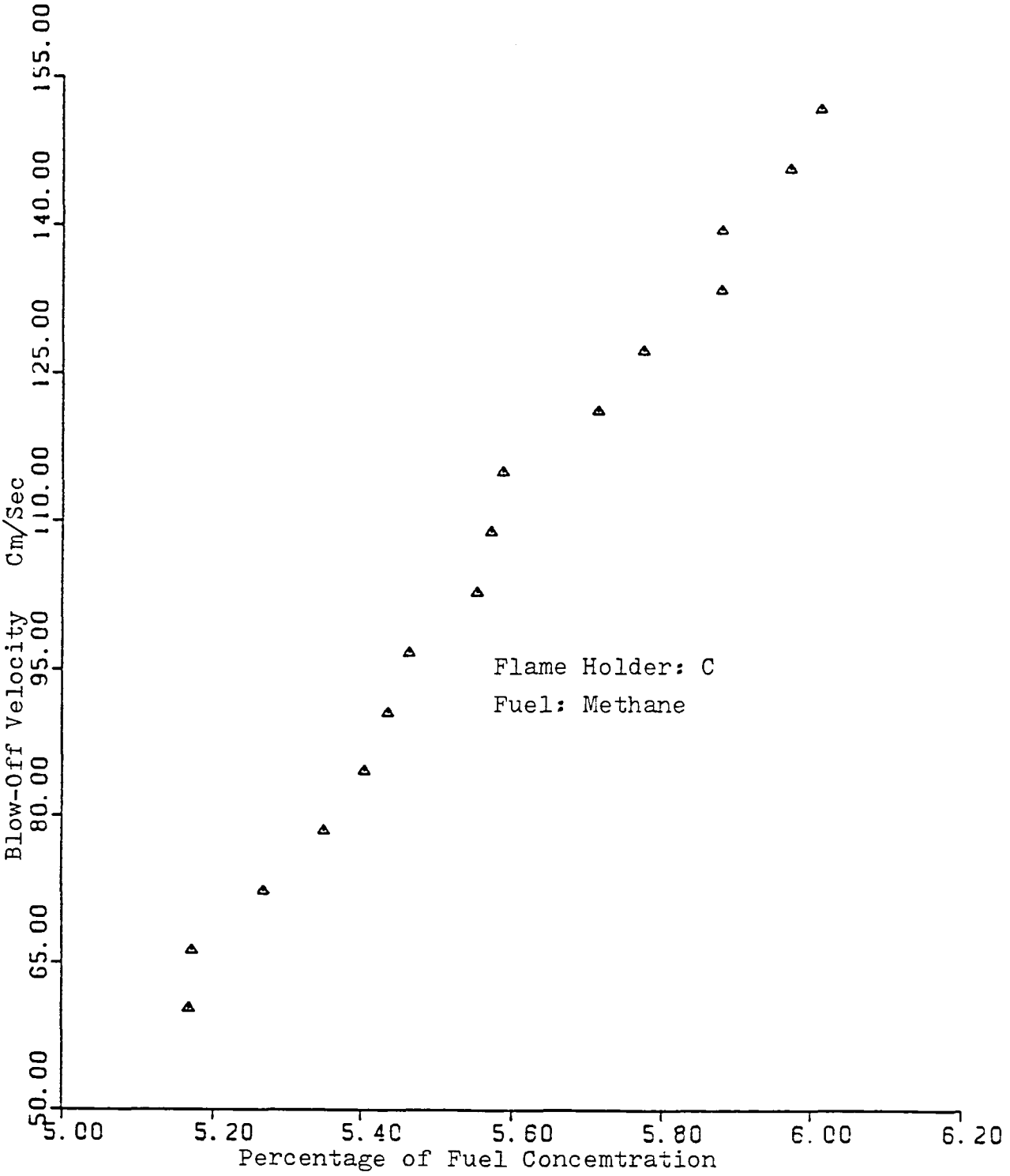

Fig.V-3. Blow-Off Velocity versus Fuel Concentration.

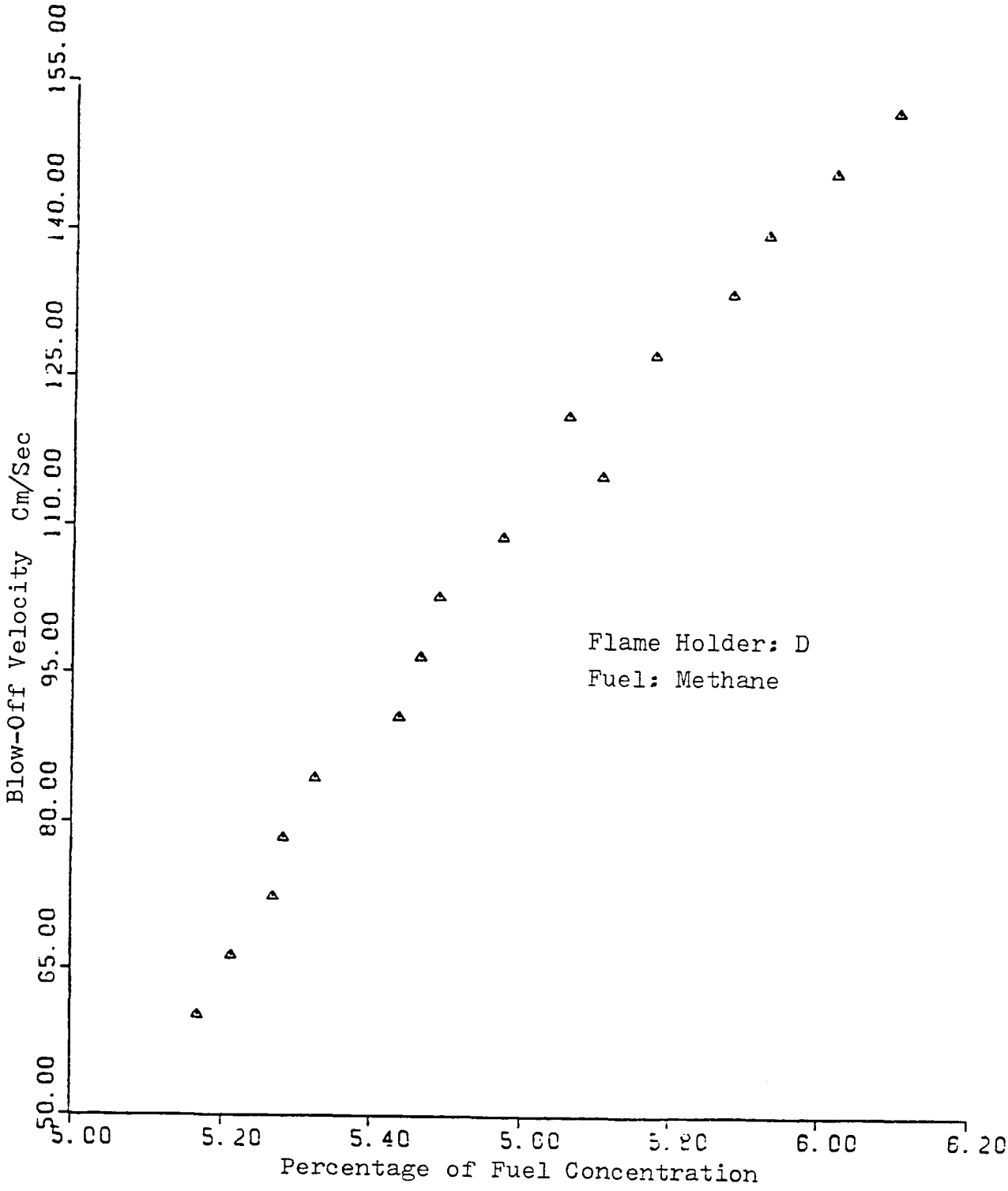

Fig.V-4a. Blow-Off Velocity versus Fuel Concentration.

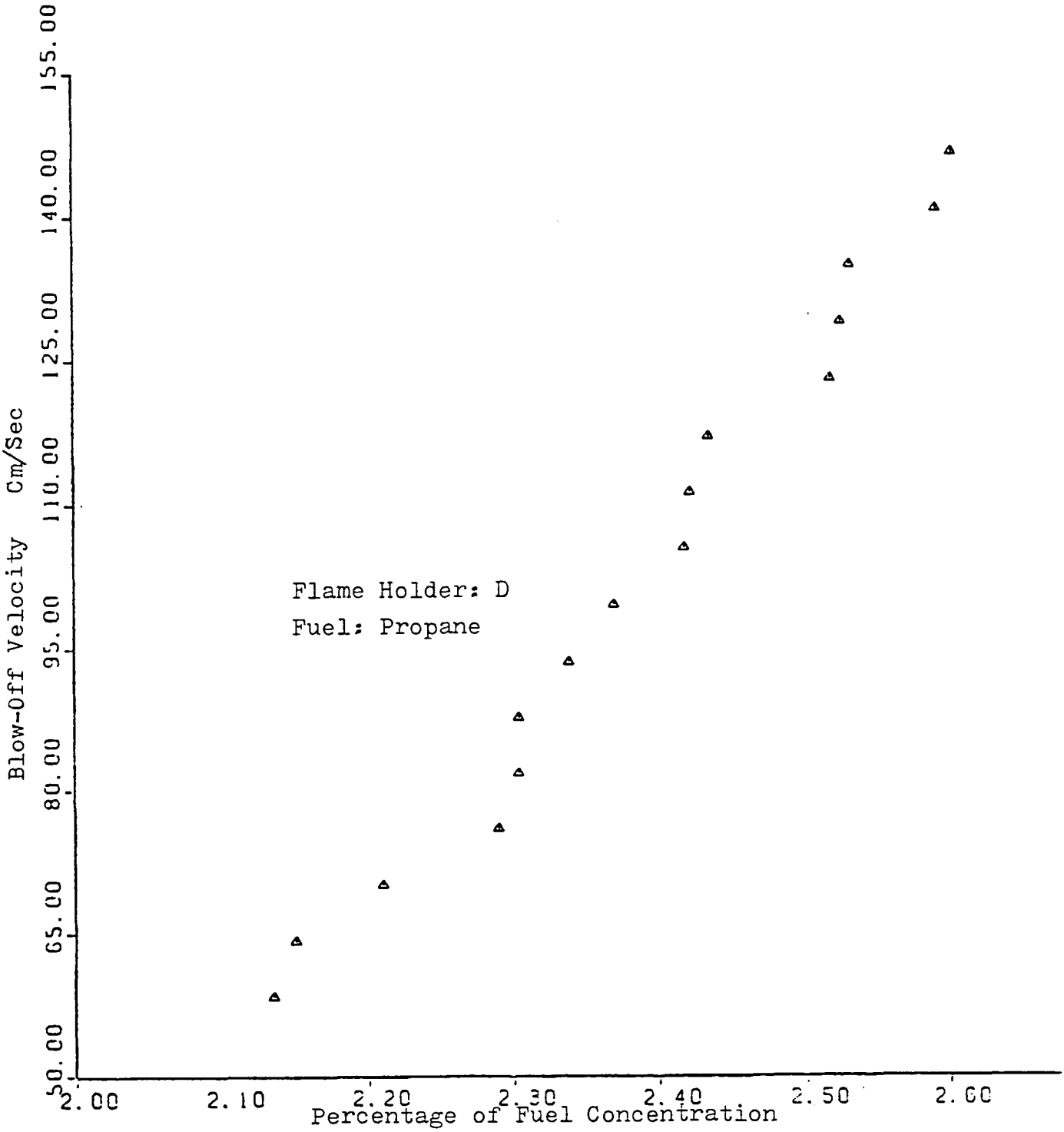

Fig.V-4b. Blow-Off Velocity versus Fuel Concentration

concentration. Figure V-1b corresponds to the case of propane-air mixture using flame holder A. The trend in the blow-off velocity curves for the flame holders C can be observed in figure V-3 and figures V-4a,b show the velocity curves for flame holder D using methane- and propane-air mixtures respectively. As can be seen from these figures the variation in the length of the flame holders C and D from 12.7 mm (figure V-3) to 19.0 mm (figure V-4a) does not have any significant effect on the blow-off velocity of a methane-air flame. On the other hand there is some variation in the blow-off velocity curves for different thickness flame holders using methane and propane, as illustrated in figures V-1a,b and V-4a,b. Here one observes for both methane- and propane-air mixtures that at lower velocities the flame blow-off occurs at almost the same fuel concentration for both the different thickness flame holders. But as the velocity of the fuel-air mixture increases the blow-off of the flame held over the 1.6 mm thick flame holder, A, tends to occur at leaner fuel concentration as compared to 0.8 mm thick flame holder, D.

Comparing the blow-off behaviors of methane and propane it was observed that methane flames were easier to stabilize near the blow-off limit and could tolerate more variations in the flow rate as compared to propane. In case of the propane flame it was more difficult to anchor the flame and the flame was very sensitive to the changes in the flow rate. The occurence of

flash back was more frequent and in order to avoid such a situation the flame was stabilized at a higher flow rate of air. At the point of blow-off the radius of curvature was much larger for propane and the process of blow-off was much faster as compared to methane, because one could visually keep track of the methane flame as it slowly lifted off and this could not be done for the propane flame.

Two schlieren pictures for each setting of the air flow rate were taken; one picture was taken very near the blow-off position, the other one corresponded to a "well-held" position. This was done in order to observe the change of shape and position of the preheat zone region of an inverted flame with respect to the trailing edge of the flame holder and the fuel type. In each figure from V-5 to V-8 there are four pairs of pictures presented which correspond to air flow rate setting of 0.4, 0.6, 0.8 and 1.0 liter per second. In each of these figures, pictures on the left hand side were taken near blow-off conditions, while those on the right were taken at a fuel concentration where the flame is stable. Pictures presented in figures V-5a,6,7 and 8a are of methane flames while figures V-5b and V-8b are of propane flames. Comparing the two positions of the flame: near the blow-off limit, the flame is moved further downstream as compared to the well held condition. Also the flame is more curved at higher blow-off velocities. It is also evident from these figures and blow-off data presented earlier

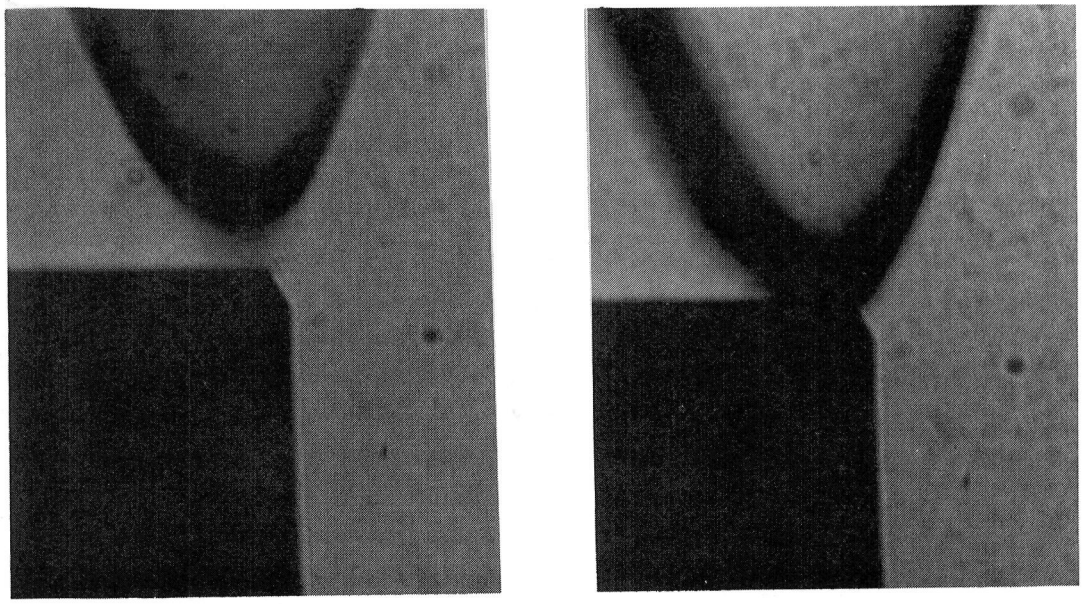

Air Flow Rate = 0.4 liter/sec
Fuel Concentration = 5.17% ; V = 60.0 Cm/Sec

5 mm

Air Flow Rate = 0.6 liter/sec
Fuel Concentration = 5.21% ; V = 90.43 Cm/Sec

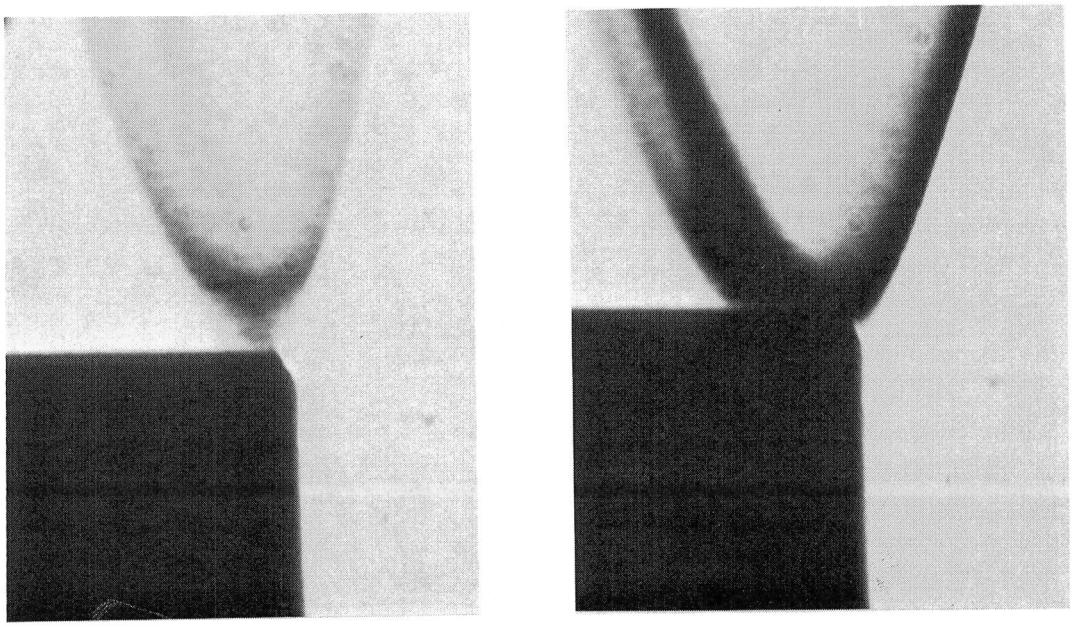

Fig.V-5a. Schlieren Pictures of Methane-Air Flame

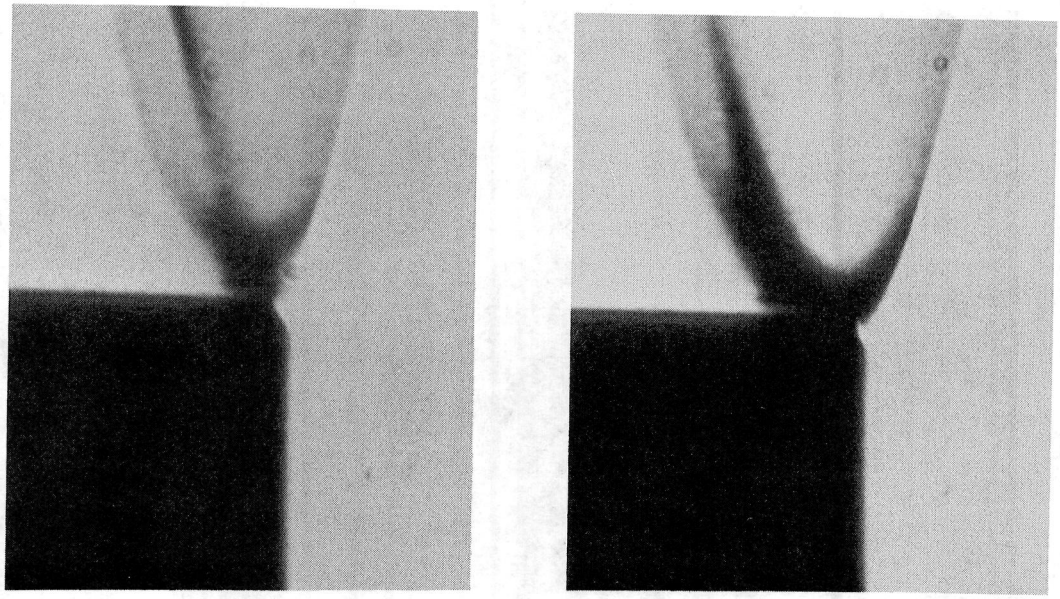

Air Flow Rate = 0.8 liter/sec;
Fuel Concentration = 5.44% ; V = 120.8 Cm/Sec

5 mm

Air Flow Rate = 1.0 liter/sec;
Fuel Concentration = 5.66% ; V = 151.4 Cm/Sec

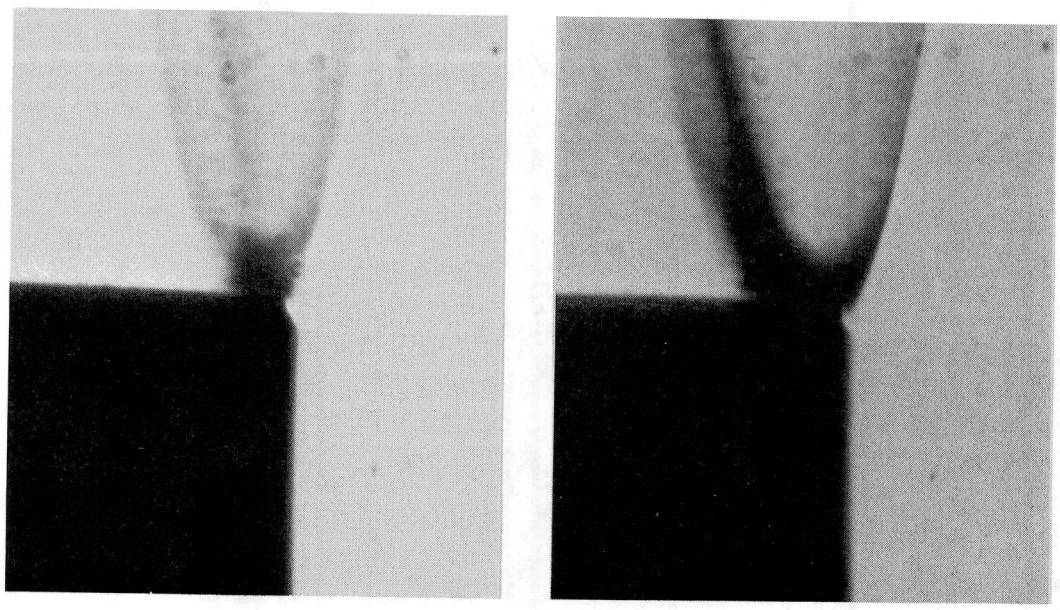

Fig.V-5a (contd.) Schlieren Pictures of Methane-Air Flame.

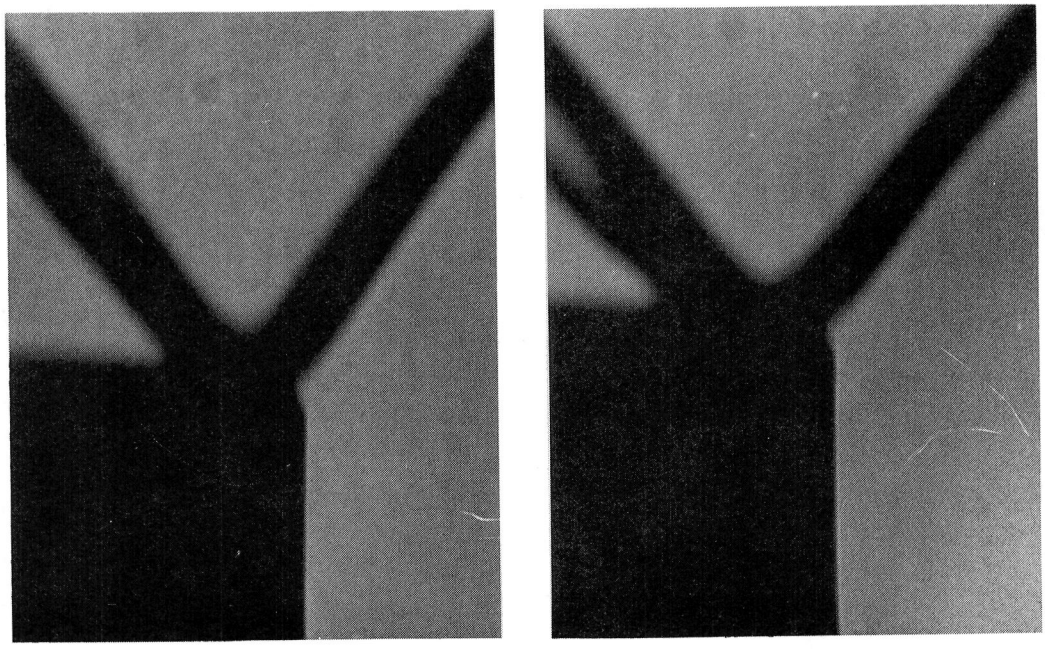

Air Flow Rate = 0.4 liter/sec;
Fuel Concentration = 2.12% ; V= 57.0 Cm/Sec

5mm

Air Flow Rate = 0.6 liter/sec;
Fuel Concentration = 2.24% ; V = 87.5 Cm/Sec

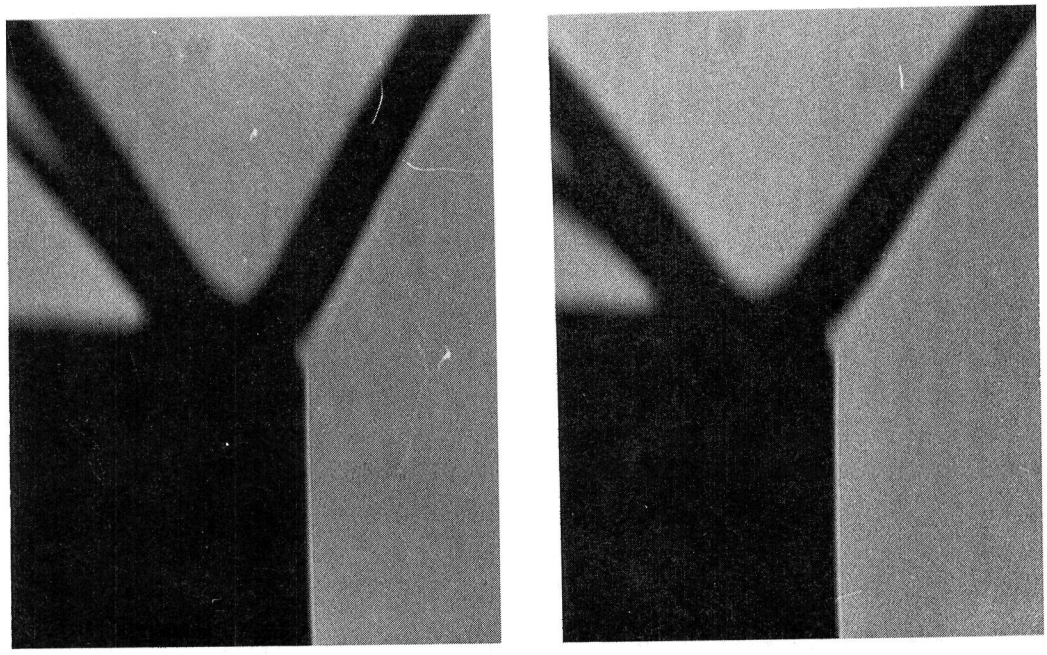

Fig.V-5b. Schlieren Pictures of Propane-Air Flame Stabilized Over Flame Holder A.

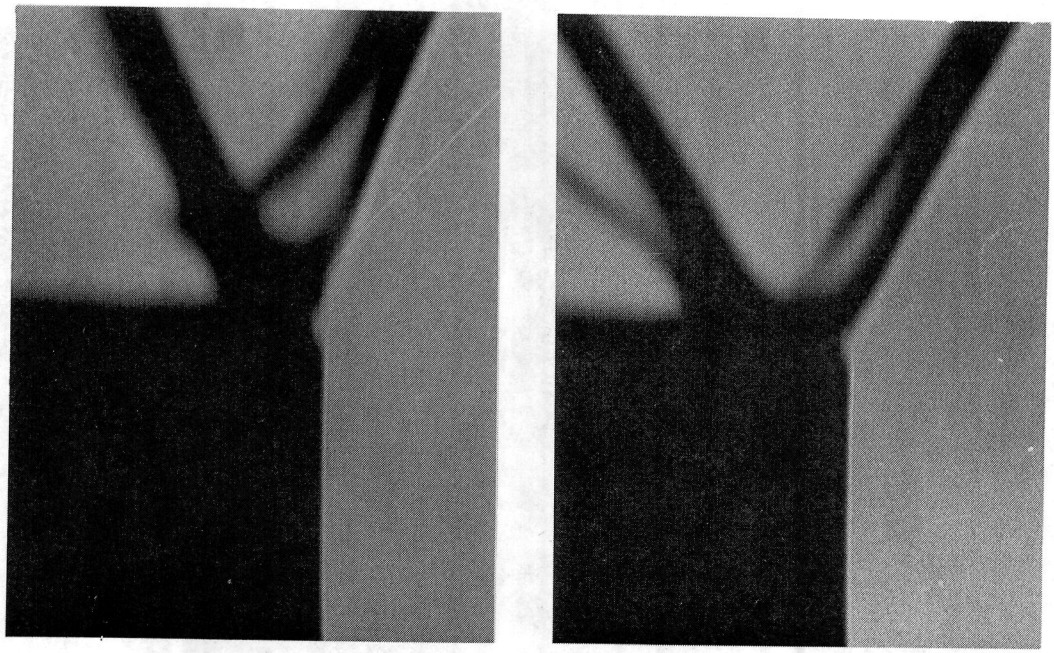

Air Flow Rate = 0.8 liter/sec;
Fuel Concentration = 2.4% ; V = 117.0 Cm/Sec

5mm

Air Flow Rate = 1.0 liter/sec;
Fuel Concentration = 2.6% ; V = 147.3 Cm/Sec

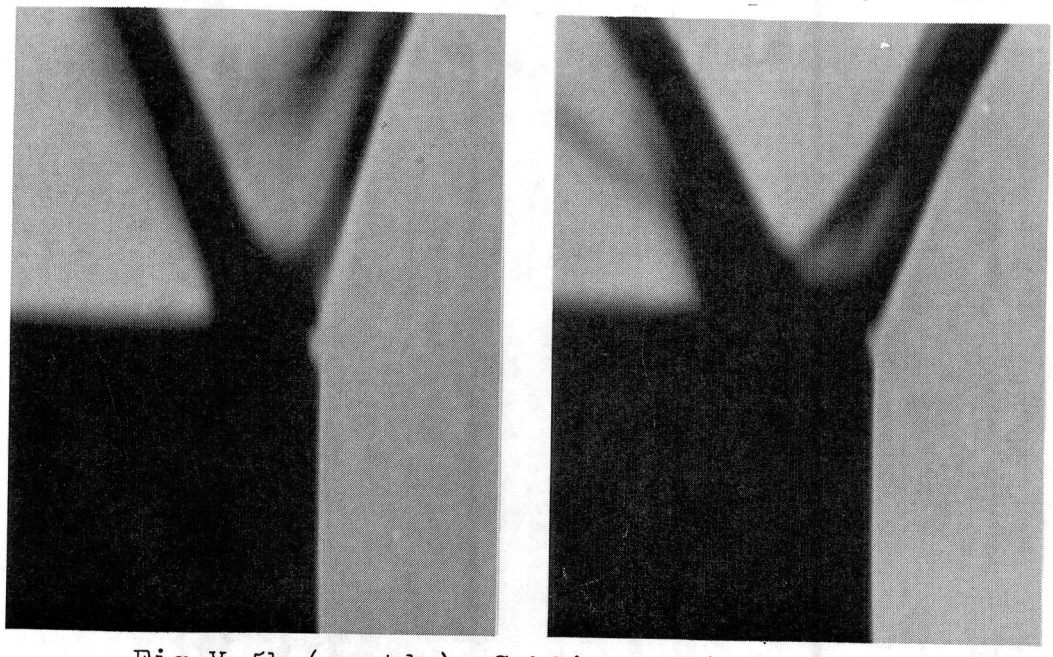

Fig.V-5b (contd.) Schlieren Pictures for Propane-Air Flame Stabilized Over Flame Holder A

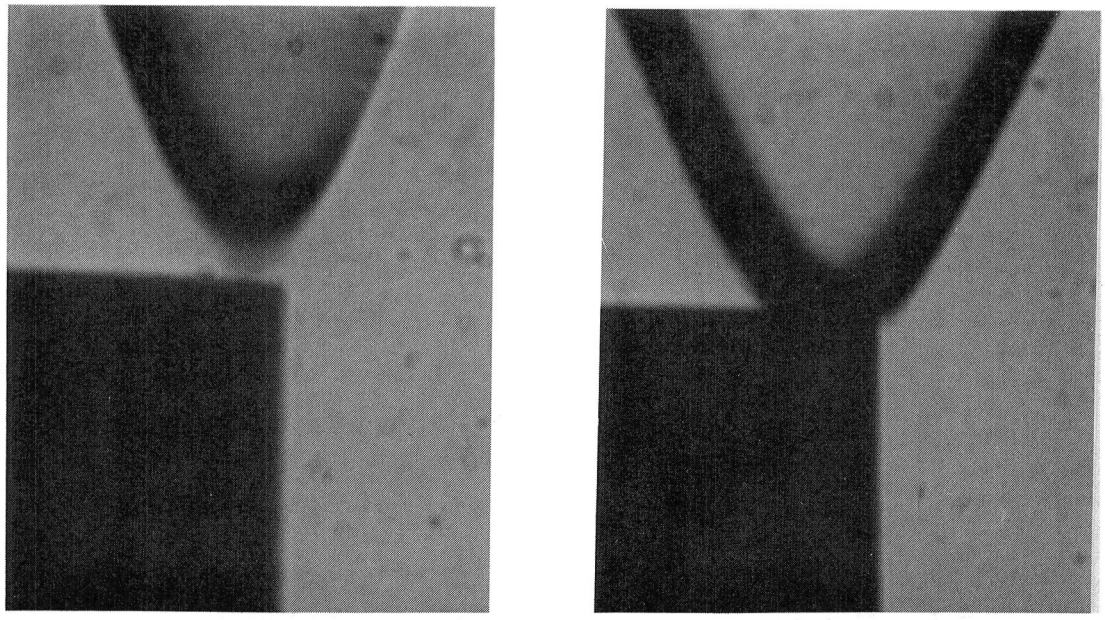

Air Flow Rate = 0.4 liter/sec;
Fuel Concentration = 5.12% ; V = 60.0 Cm/Sec

5 mm

Air Flow Rate = 0.6 liter/sec;
Fuel Concentration = 5.21% ; V = 90.43 Cm/Sec

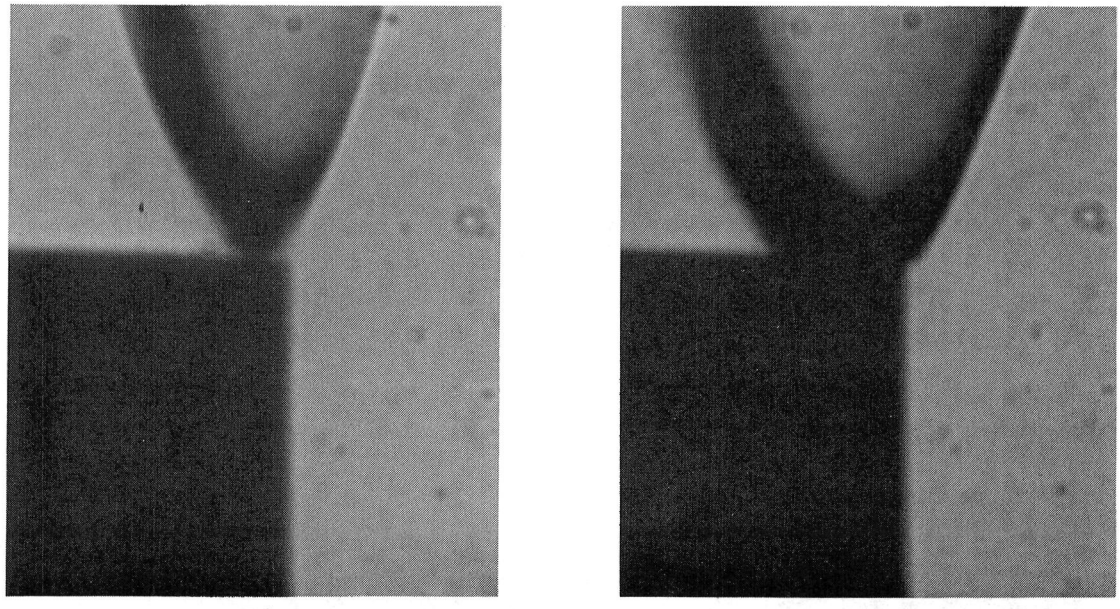

Fig.V-6. Schlieren Pictures of Methane-Air Flame Stabilized over Flame Holder B.

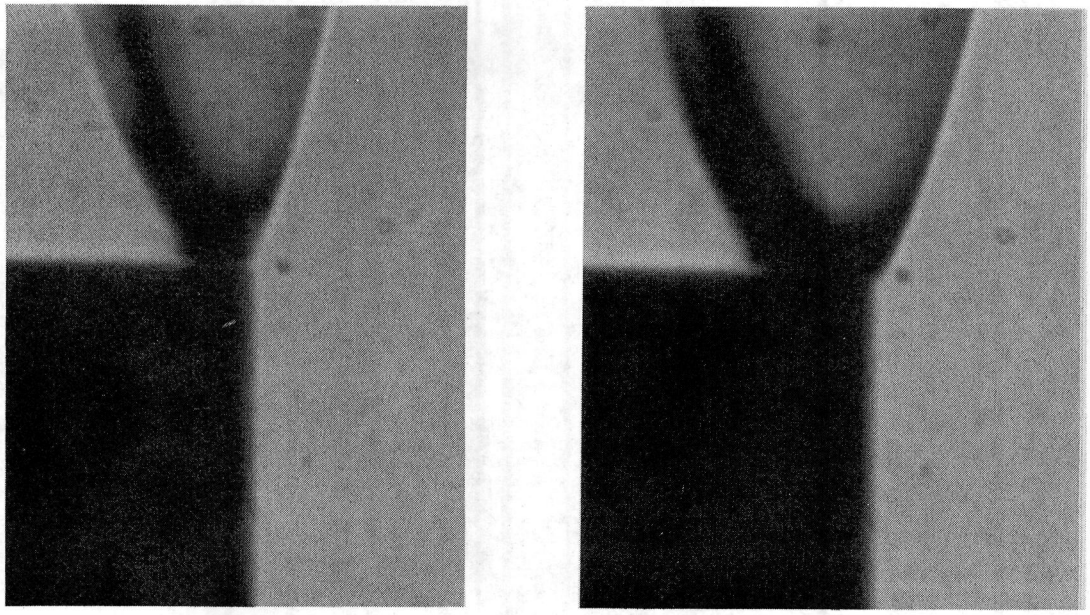

Air Flow Rate = 0.8 liter/sec;
Fuel Concentration = 5.4%; V = 120.7 Cm/Sec

5 mm

Air Flow Rate = 1.0 liter/sec;
Fuel Concentration = 5.61%; V = 151.4 Cm/sec

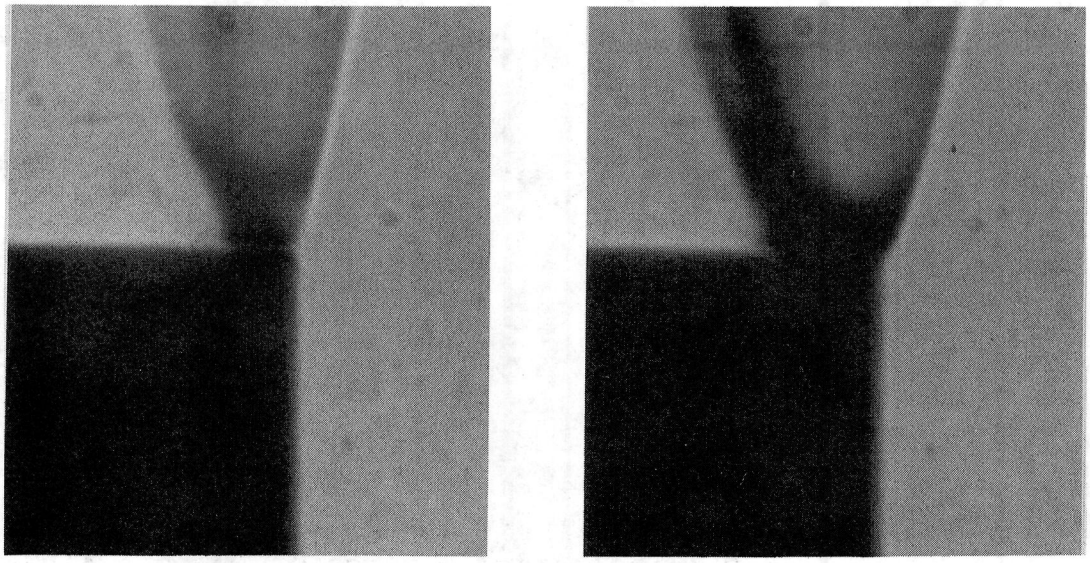

Fig.V-6 (contd.) Schlieren Pictures of Methane-Air Flame Stabilized Over Flame Holder B.

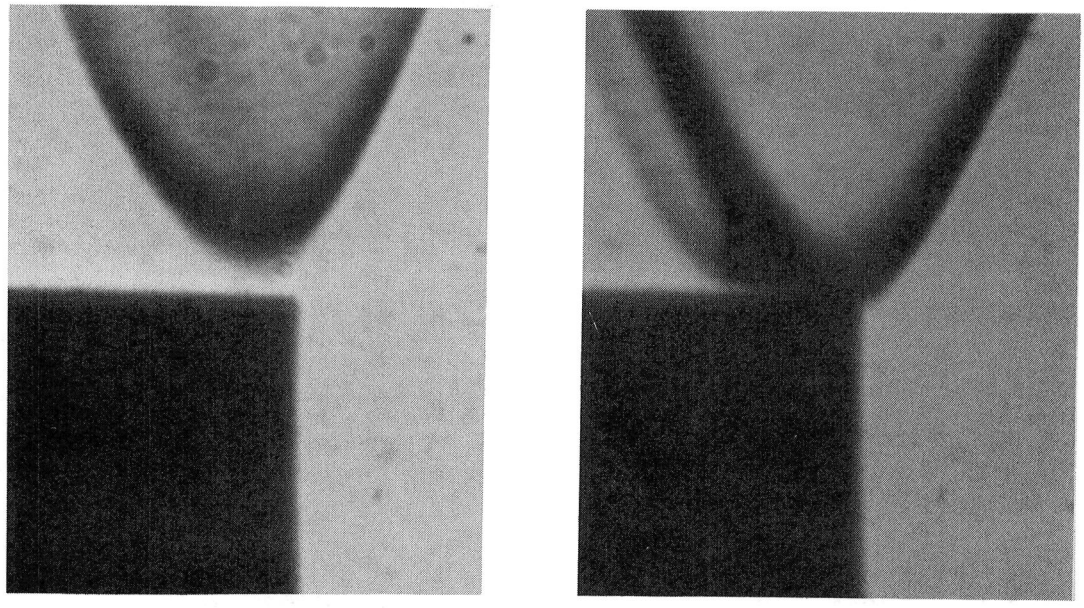

Air Flow Rate = 0.4 liter/sec;
Fuel Concentration = 5.17%; V = 60.0 Cm/Sec

5 mm

Air Flow Rate = 0.6 liter/sec;
Fuel Concentration = 5.44%; V = 90.6 Cm/Sec

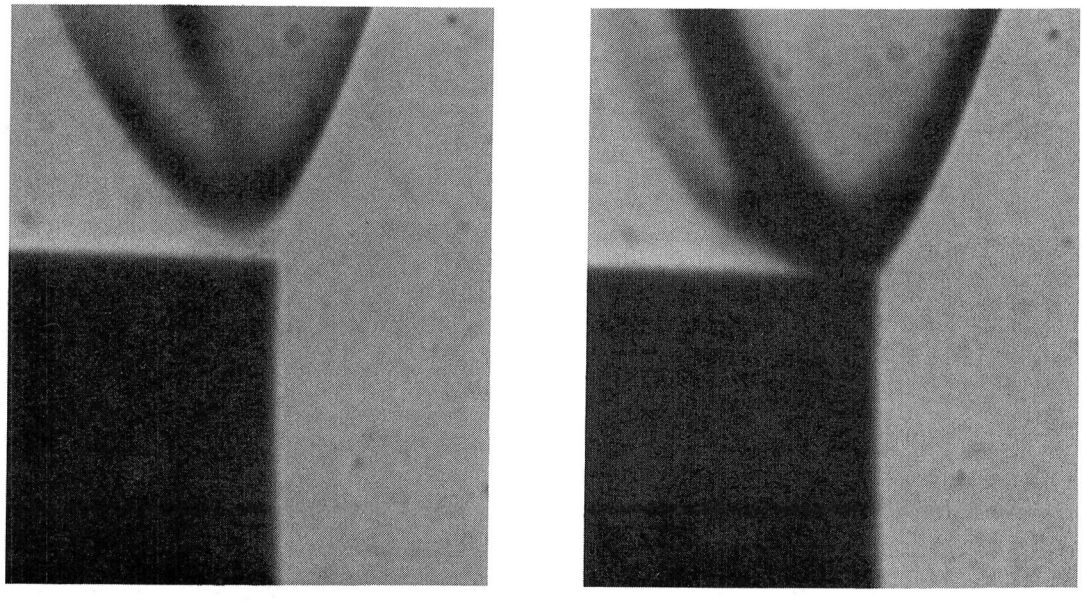

Fig.V-7. Schlieren Pictures of Methane-Air Flame Stabilized Over Flame Holder C.

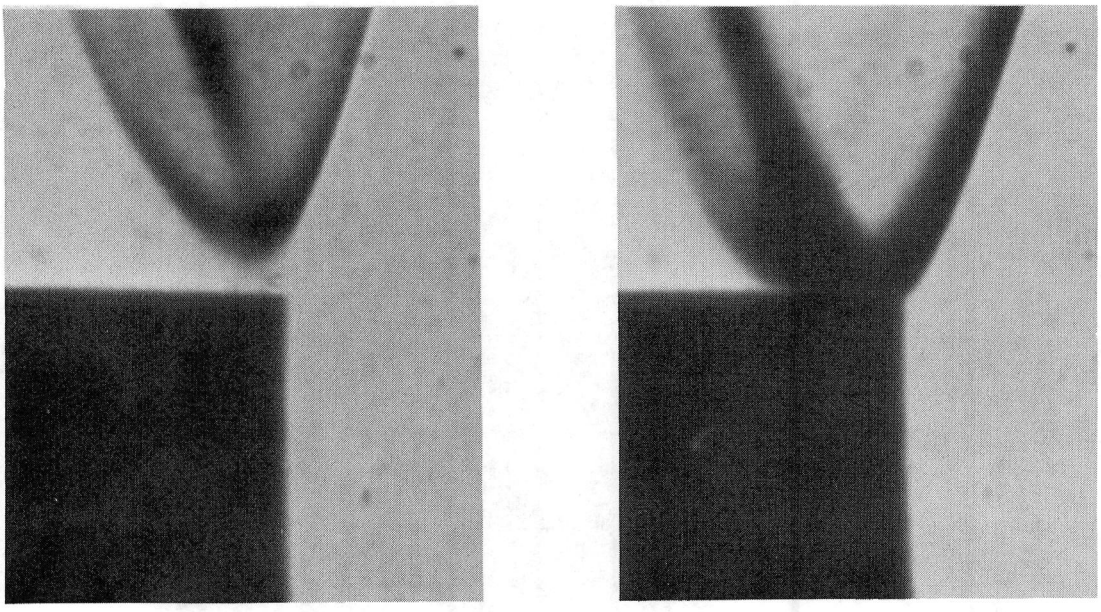

Air Flow Rate = 0.8 liter/sec;
Fuel Concentration = 5.71%; V = 121.3 Cm/Sec

5 mm

Air Flow Rate = 1.0 liter/sec;
Fuel Concentration = 6.0%; V = 152 Cm/Sec

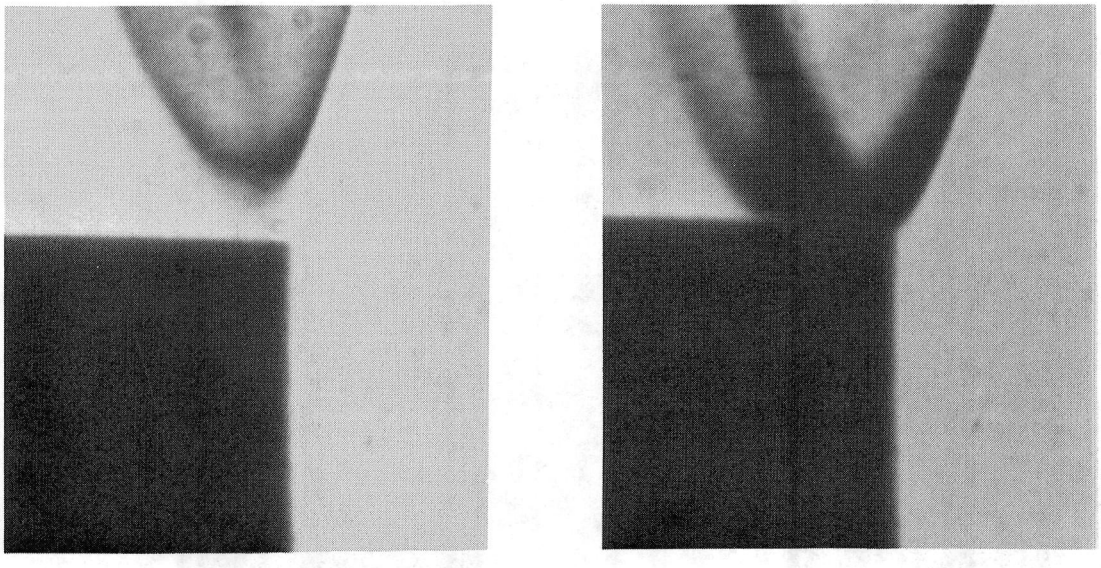

Fig.V-7 (contd.) Schlieren Pictures of Methane-Air Flame Stabilized Over Flame Holder C.

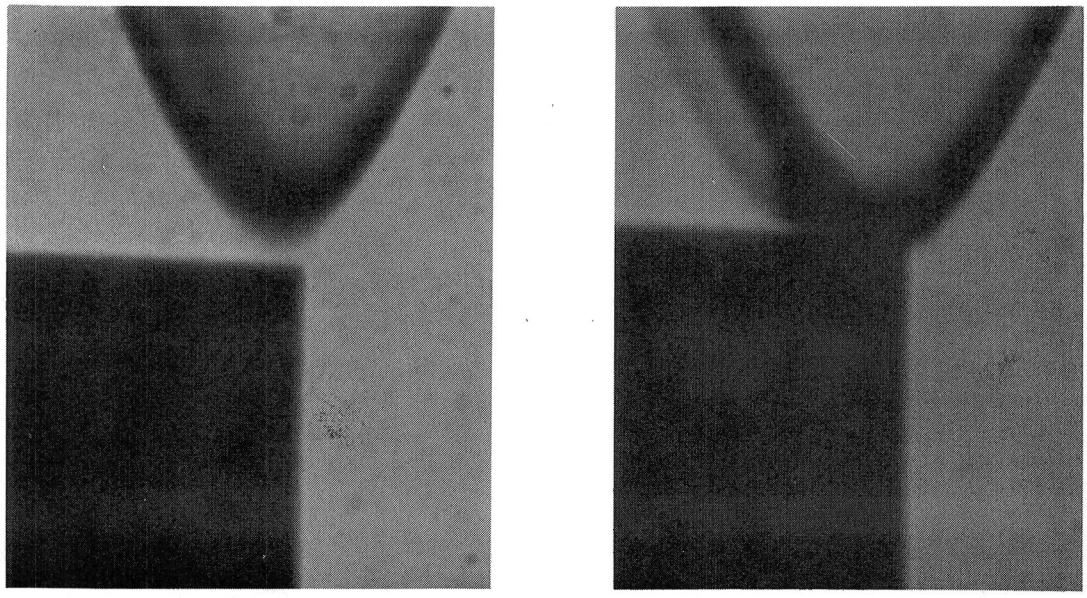

Air Flow Rate = 0.4 liter/sec;
Fuel Concentration = 5.17%; V = 60.0 Cm/Sec

5mm

Air Flow Rate = 0.6 liter/sec;
Fuel Concentration = 5.44% V = 90.6 Cm/Sec

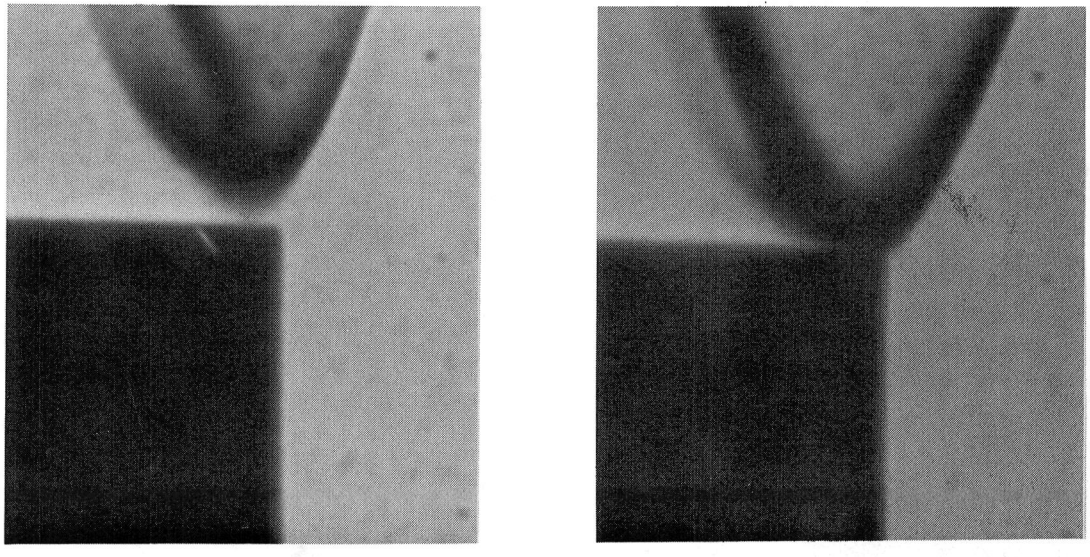

Fig.V-8a. Schlieren Pictures of Methane-Air Flame Stabilized Over Flame Holder D.

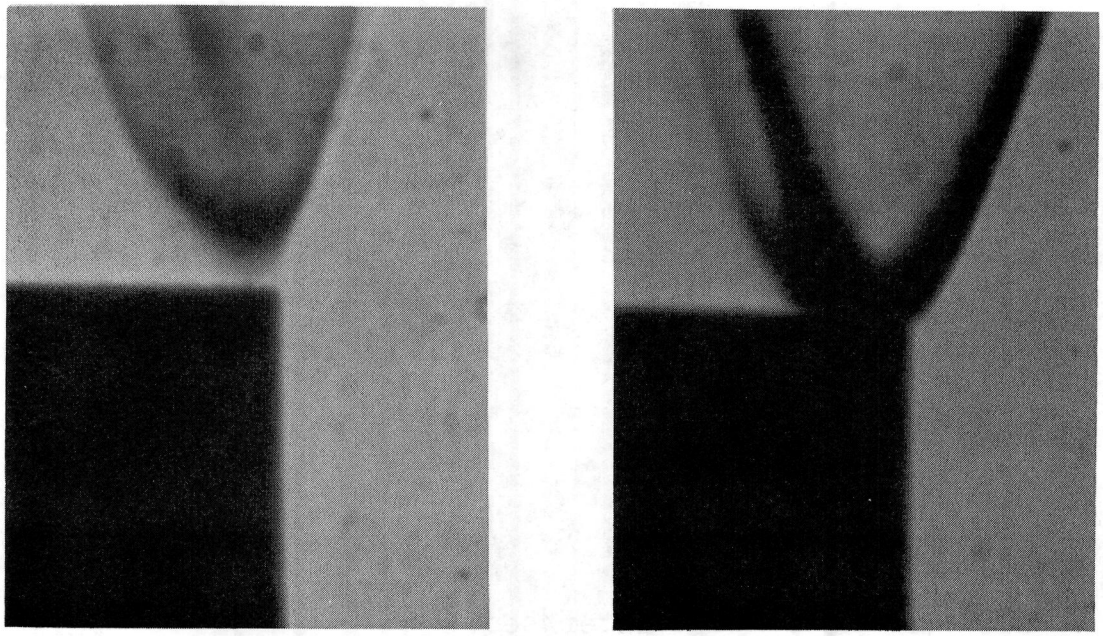

Air Flow Rate = 0.8 liter/sec;
Fuel Concentration = 5.66%; V = 121.1 Cm/Sec

5 mm

Air Flow Rate = 1.0 liter/sec;
Fuel Concentration = 6.10%; V = 152 Cm/Sec

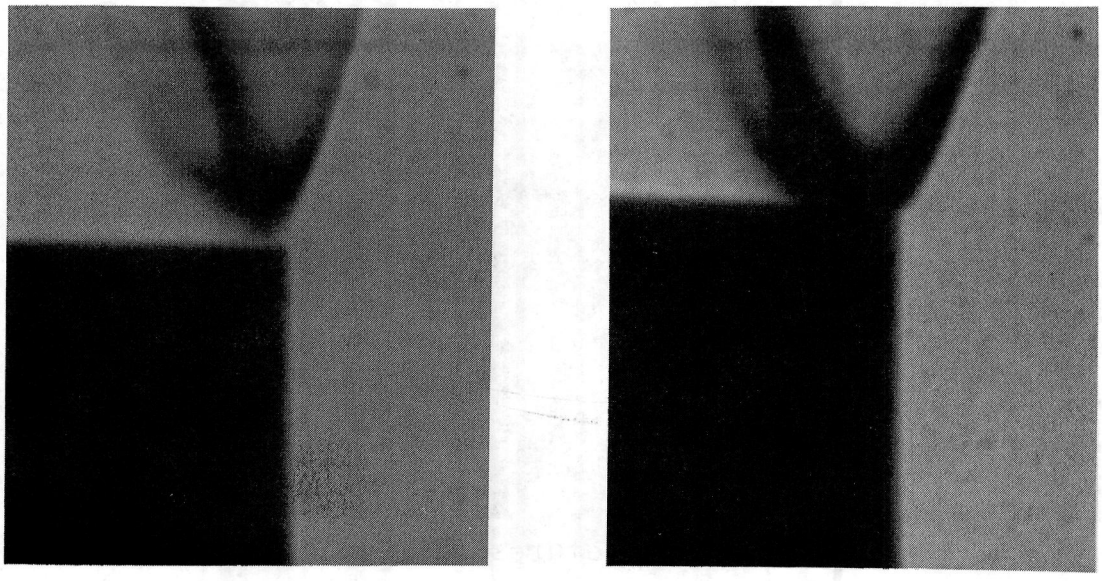

Fig.V-8a (contd.) Schlieren Pictures of Methane-Air Flame Stabilized Over Flame Holder D.

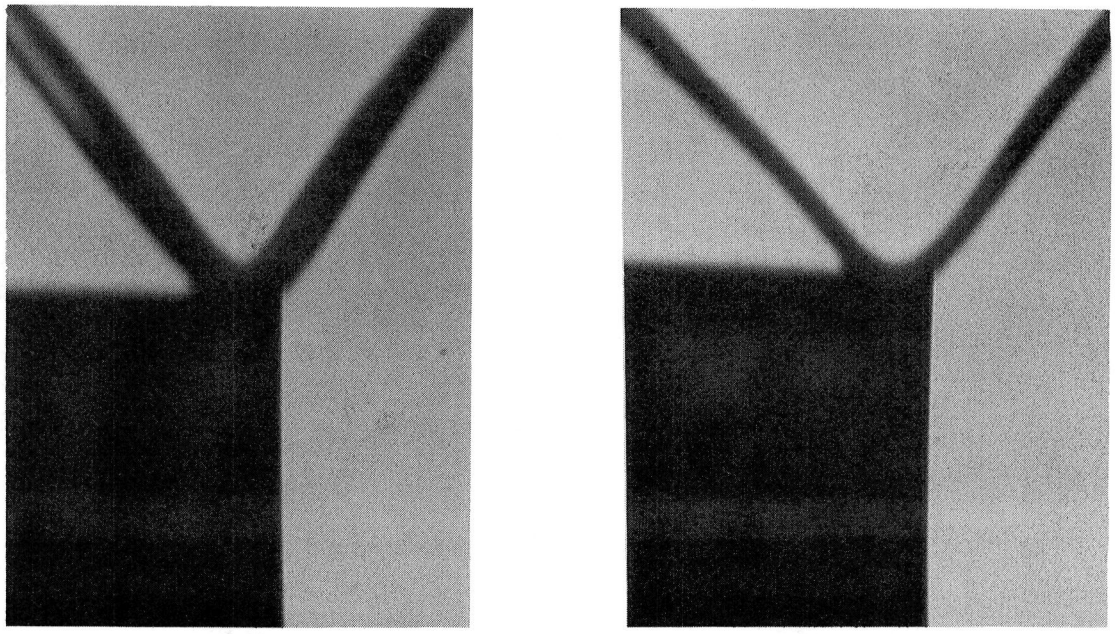

Air Flow Rate = 0.4 liter/sec;
Fuel Concentration = 2.13%; V = 58.0 Cm/Sec

5 mm

Air Flow Rate = 0.6 liter/sec;
Fuel Concentration = 2.3%; V = 88.4 Cm/Sec

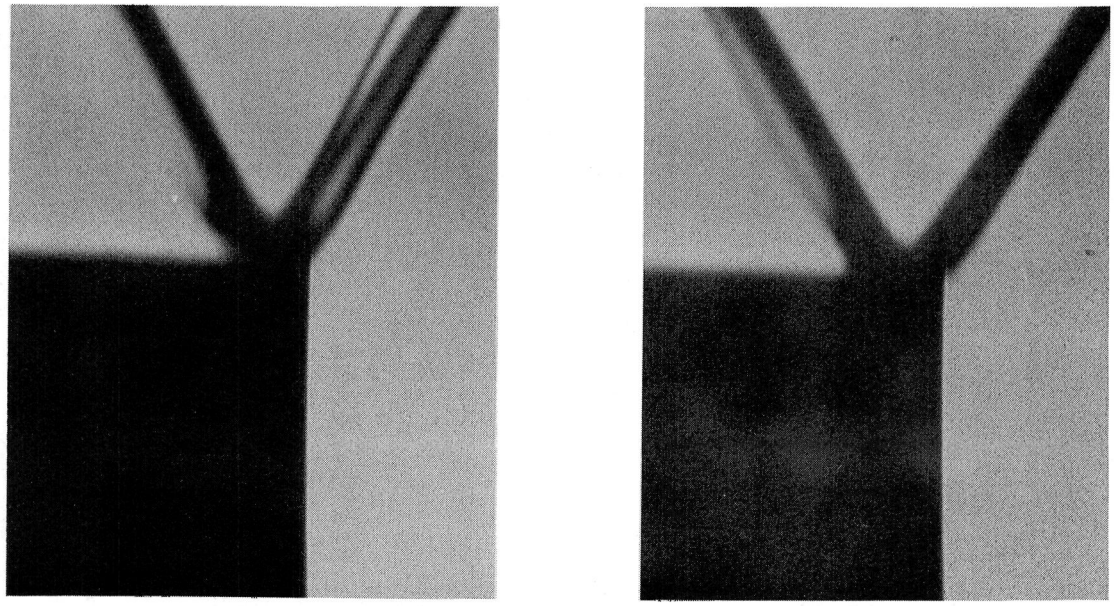

Fig.V-8b. Schlieren Pictures of Propane-Air Flame Stabilized Over Flame Holder D.

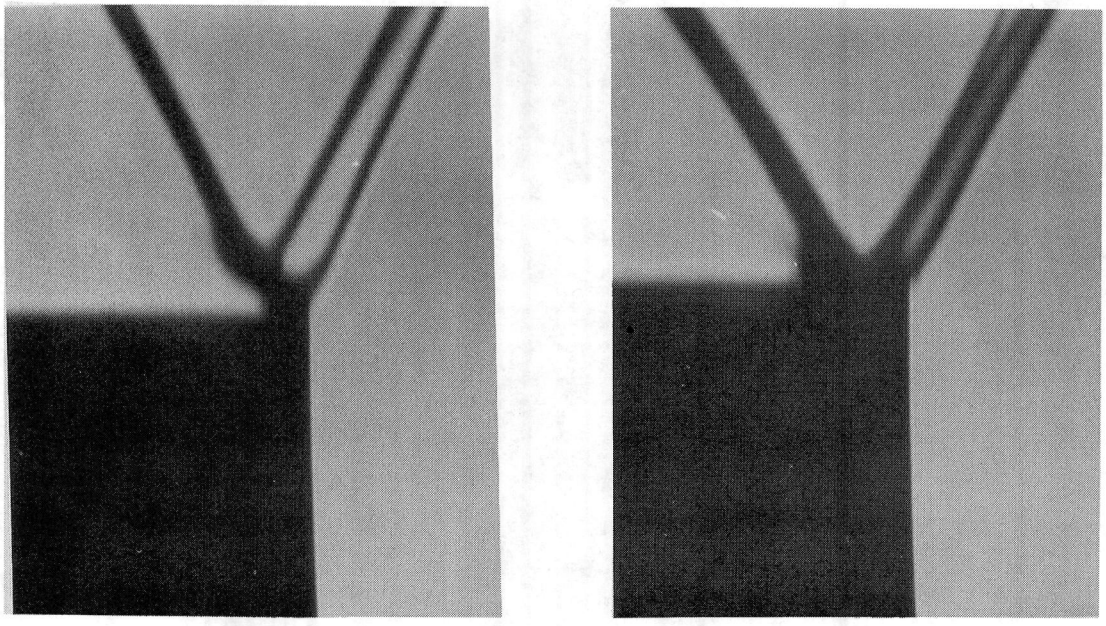

Air Flow Rate = 0.8 liter/sec;
Fuel Concentration = 2.44%; V = 117.0 Cm/Sec

5 mm

Air Flow Rate = 1.0 liter/sec;
Fuel Concentration = 2.6%; V = 147.4 Cm/Sec

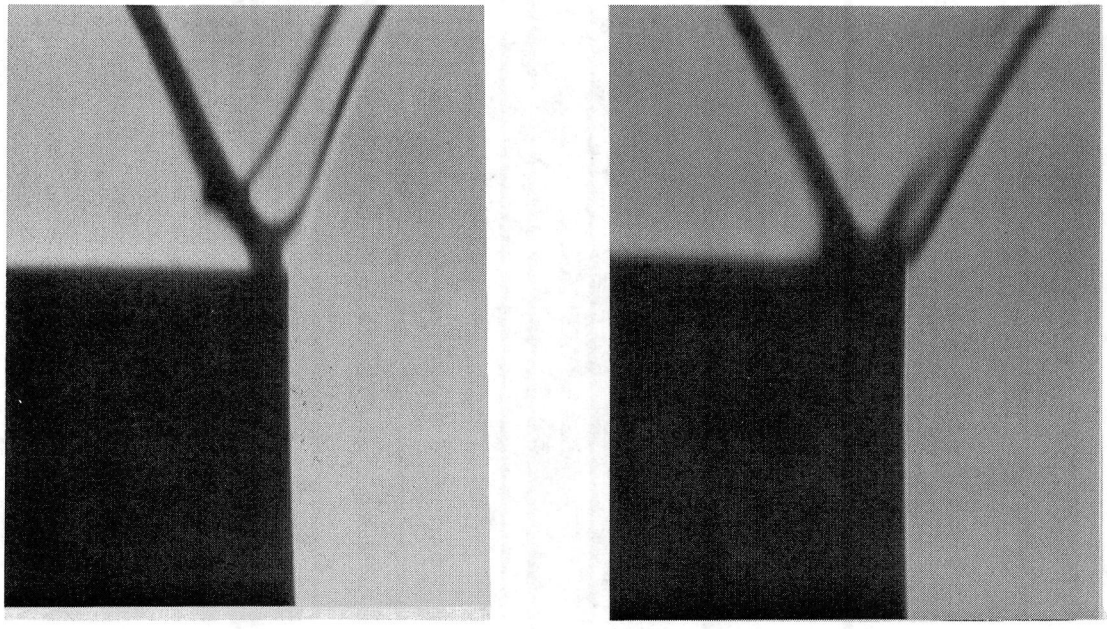

Fig.V-8b (contd.) Schlieren Pictures of Propane-Air Flame Stabilized Over Flame Holder D.

that for each fuel used there is not much variation in the blow-off criteria for all the flame holders tried. As the approach flow velocity is increased the radius of curvature decreases untill blow-off occurs. One can observe from the pictures (figures V-5a,6,7,8a) of the methane flames, that the schlieren image of the preheat zone for the blow-off condition just touches the trailing edge of the flame holder and does not go further upstream of the trailing edge. In case of the propane flame (figures V-5b, 8b) the preheat zone approaches much closer to the flame holder, and the base of the inverted flame has a larger radius of curvature than the methane flames. Since the flame holders used are curved, therefore in some pictures one sees parts of flame which happen to be located in front and rear of the plane perpendicular to the tangent of the flame holders. In order to locate the true image of the schlieren image one should examine only that part of the flame which is stabilized over the outermost part of the flame holder. For propane there are sometimes double images on this side of the flame holder. This is because these flames were more unstable than the methane flames.

The visible light pictures are presented in figures V-9 and V-10, for holder A & D. Figures V-9a,10a are of methane flames, while V-9b and 10b are of propane flames. These pictures show that the visible region of methane flame also has a smaller radius of curvatue when compared to that of a propane flame. The position of the trailing edge of the flame holder is

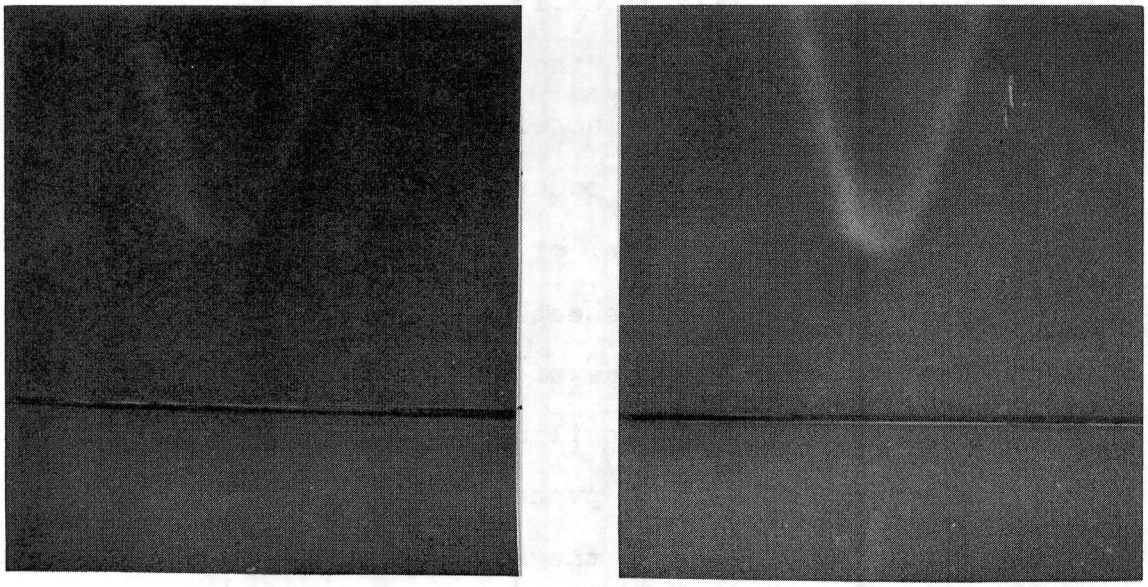

V=60.0 cm/sec

V=90.43 cm/sec

2 mm

V=120.8 cm/sec

V=151.4 cm/sec

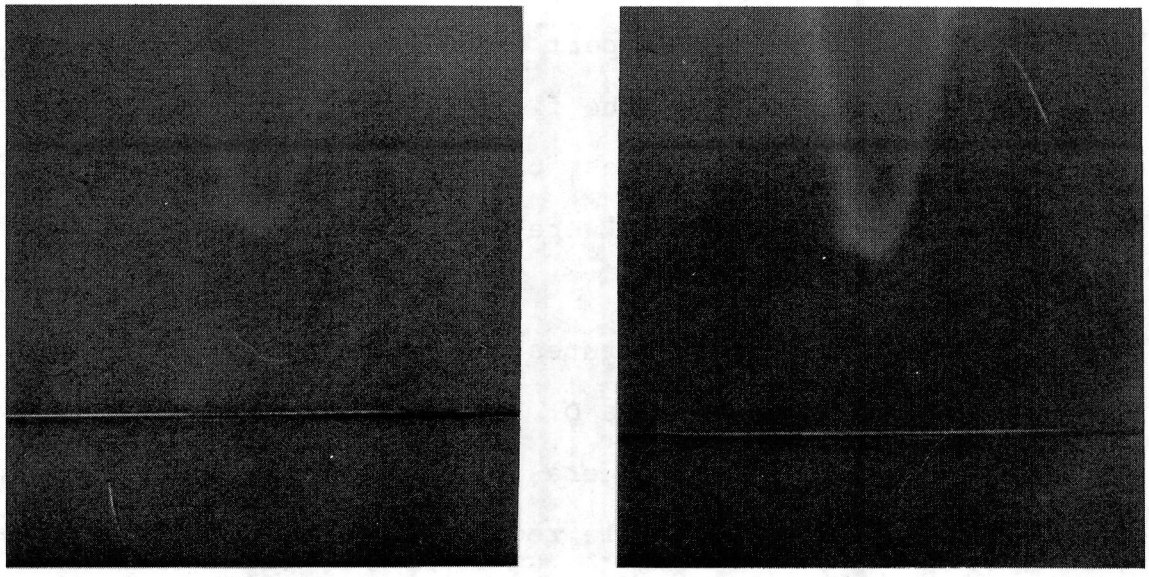

Fig.V-9a. Visible Light Pictures of Methane-Air Flame Stabilized Over Flame Holder A.

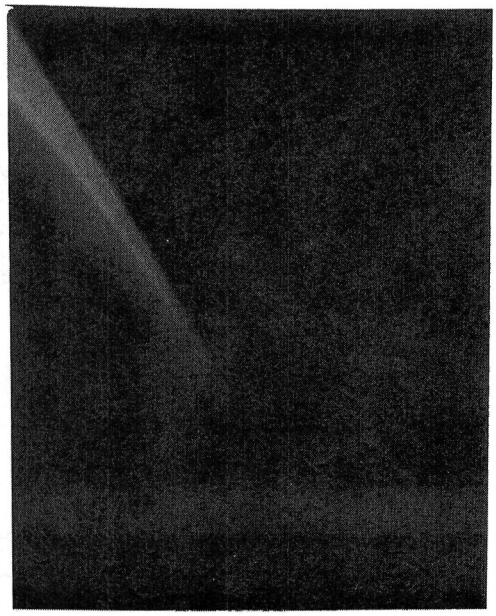

V=57.0 cm/sec

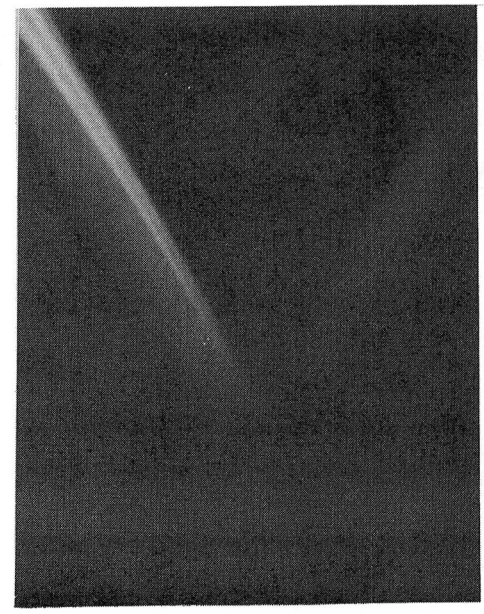

V=87.5 cm/sec

2 mm

V=117.0 cm/sec

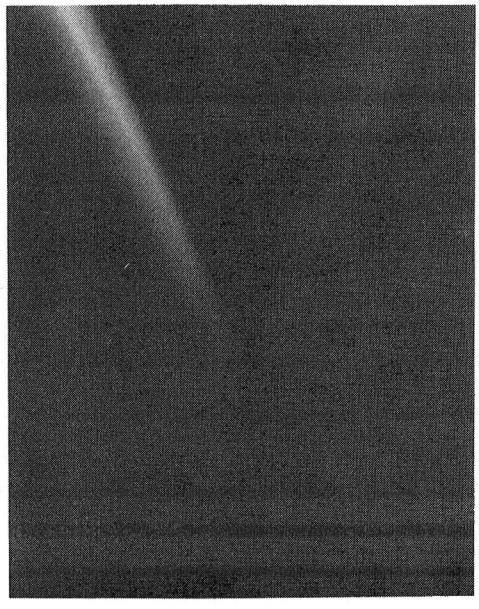

V=147.3 cm/sec

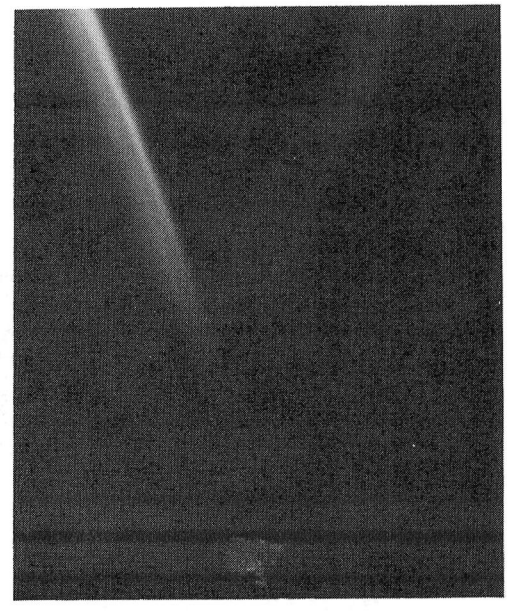

Fig.V-9b. Visible Light Pictures of Propane-Air Flame Stabilized Over Flame Holder A.

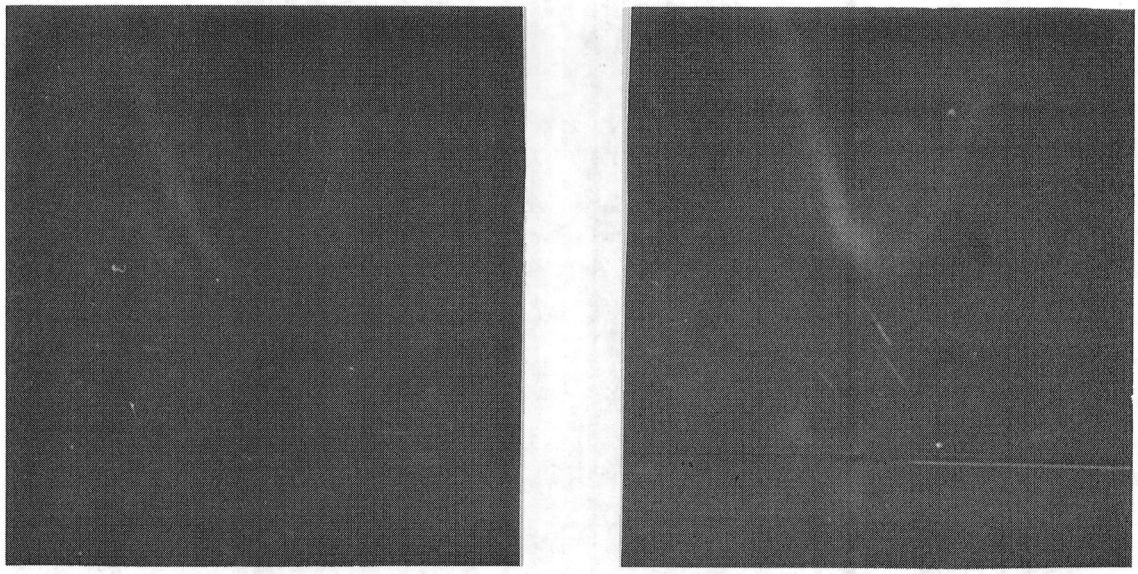

Fig.V-10a. Visible Light Pictures of Methane-Air Flame Stabilized Over Flame Holder D.

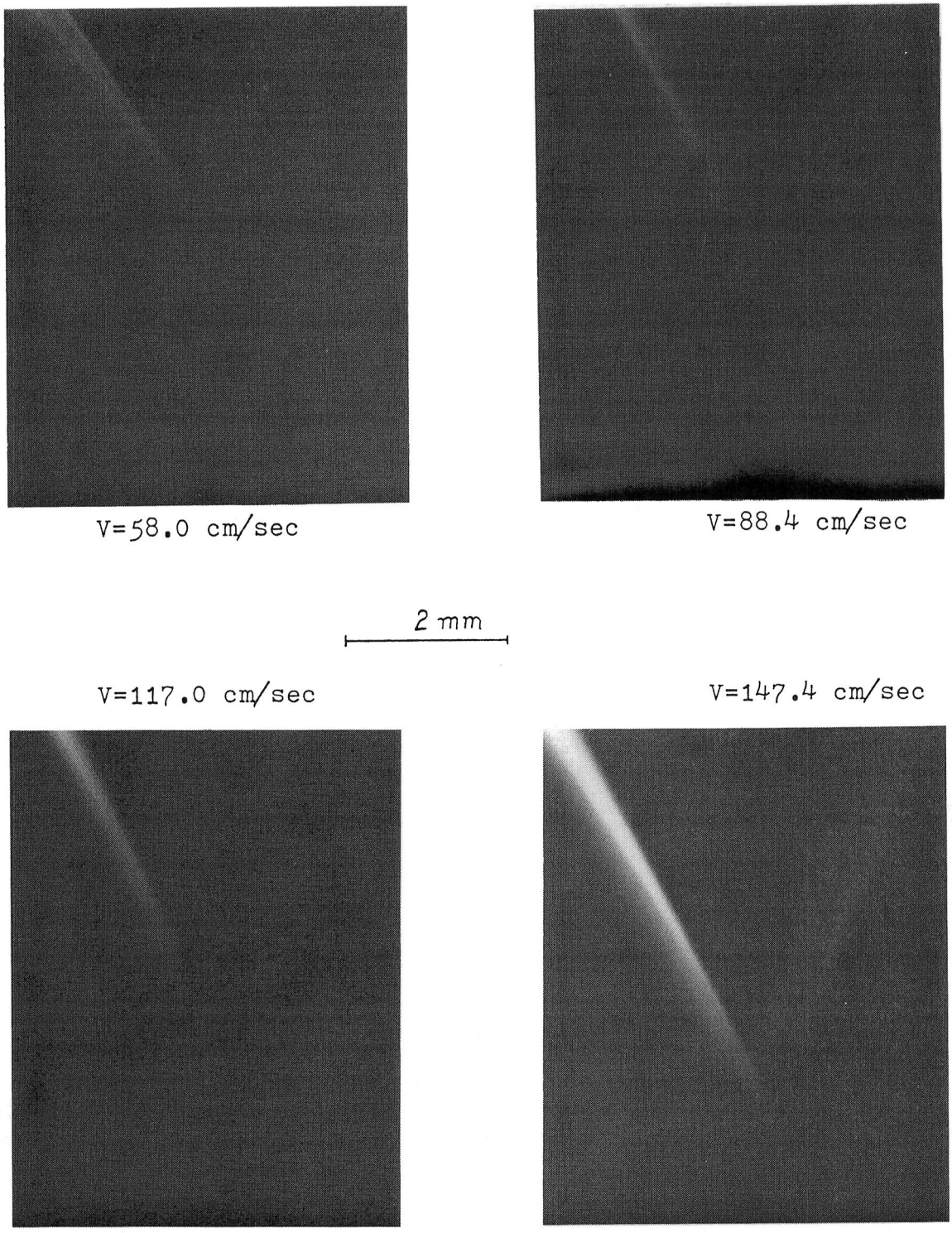

Fig.V-10b. Visible Light Pictures of Propane-Air Flame Stabilized Over Flame Holder D.

indicated by the black lines on the pictures. For both fuels the radius of curvature of the base of the flame decreases as the flow rate is increased.

Now referring back to the velocity measurements, using the Laser Doppler Velocimetry technique, the size of the regions where the velocity of the flow field was measured for the four flame holders for both the fuels are indicated in figure V-11. The solid and dashed lines indicate the measured flow field dimension for methane and propane respectively. As seen from figure V-11, the reference coordinate system was fixed at the trailing edge. Two sets of LDV data were taken, one without the flame present, the other with the flame present. This enabled one to observe the deflections in the flow-field due to the presence of the flame. All the experimental data has been gathered for lean flames near blow-off conditions. Initially, velocity profiles for methane-air mixtures for the knife edge flame holder A will be presented in detail. Data was also taken for propane using the same flame holder.

In this experimental run the air flow rate was set to 0.36 liters per second and the fuel flow rate was set to 0.024 liters per second, i.e methane concentration was 6.25% (an equivalence ratio of 0.635). Figures V-12 to V-21 contain the velocity profiles with and without flame. Measurements were taken with a step of 1.0 mm starting from 4.0 mm below the trailing edge

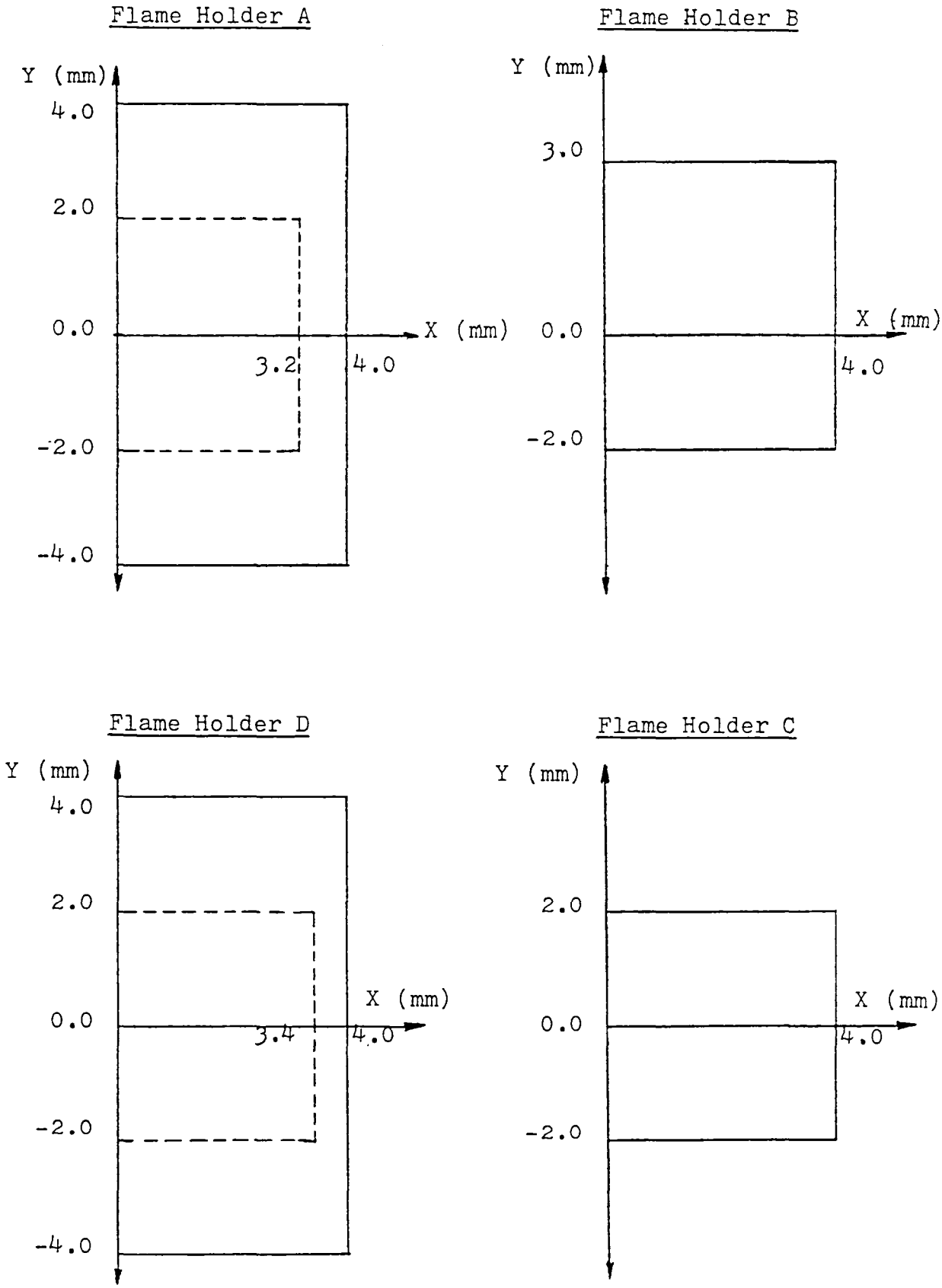

Fig.V-11. Dimensions of the Regions Measured by LDV.

(origin of the coordinate system). Since the flow configuration and the inverted flame sitting on the trailing knife edge of the flame holder are symmetrical, only one half of the profile was measured. The width of this non-uniform region increases with increasing vertical distance and the velocity profile very close to the body is evidently determined by the developing boundary layer.

In this two dimensional problem, illustrated in the above mentioned figures, it is assumed that the wall of the flame holder is perfectly flat and coincides with the Y direction. The reference velocity U_o is the free stream velocity. The parallel component U in the boundary layer tends asymptotically to U_o of the approach flow velocity as one travels away from the wall.

The direction of the streamlines near the flame holder and the base of the inverted flame is influenced by the back pressure of the flame. The pressure gradient between the inside of the stabilized inverted flame base and the surrounding atmosphere is normal to the flow direction exiting from the burner mouth. Therefore the pressure gradient tends to bend the streams outward. Due to the effects of the pressure gradient in the flame and widening of the stream-tubes the velocity along the flow direction decreases at first and then increases in the flame front. This behavior is seen in figures V-19 to V-21. The velocity profile in the boundary layer of the flame holder with

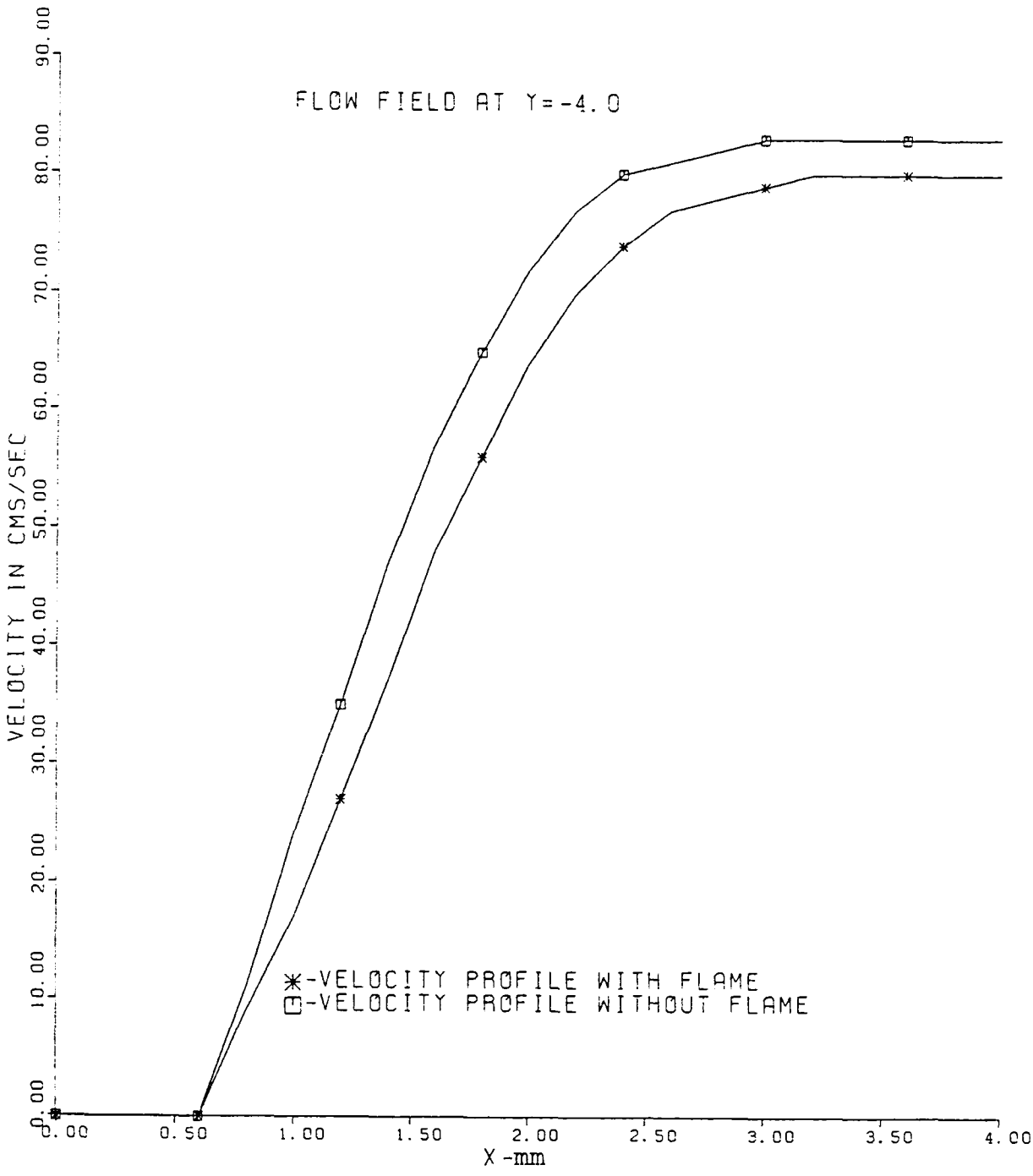

Fig.V-12. Velocity Profile of Methane-Air Mixture Along Flame Holder A.

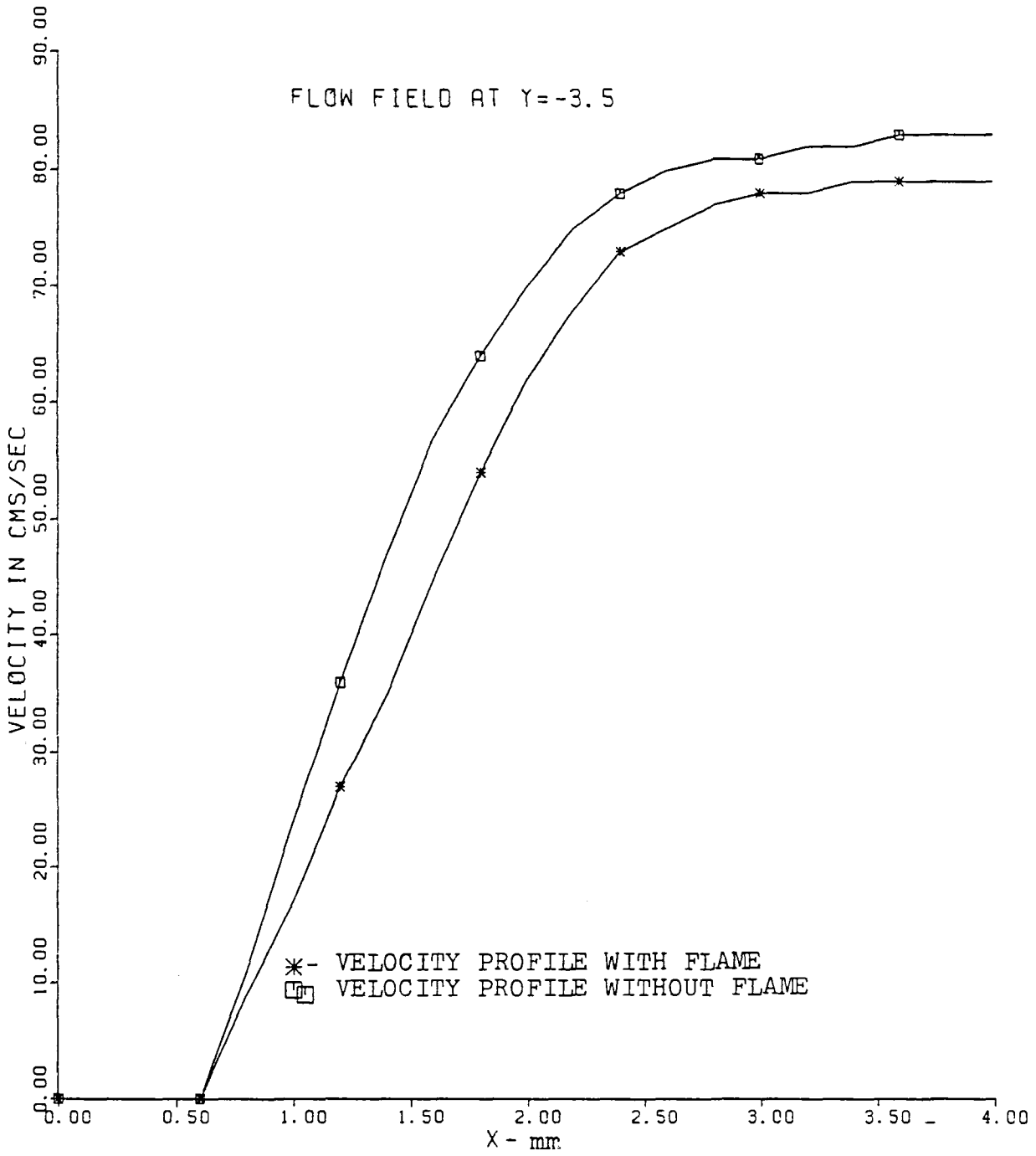

Fig.V-13. Velocity Profile of Methane-Air Mixture Along Flame Holder A.

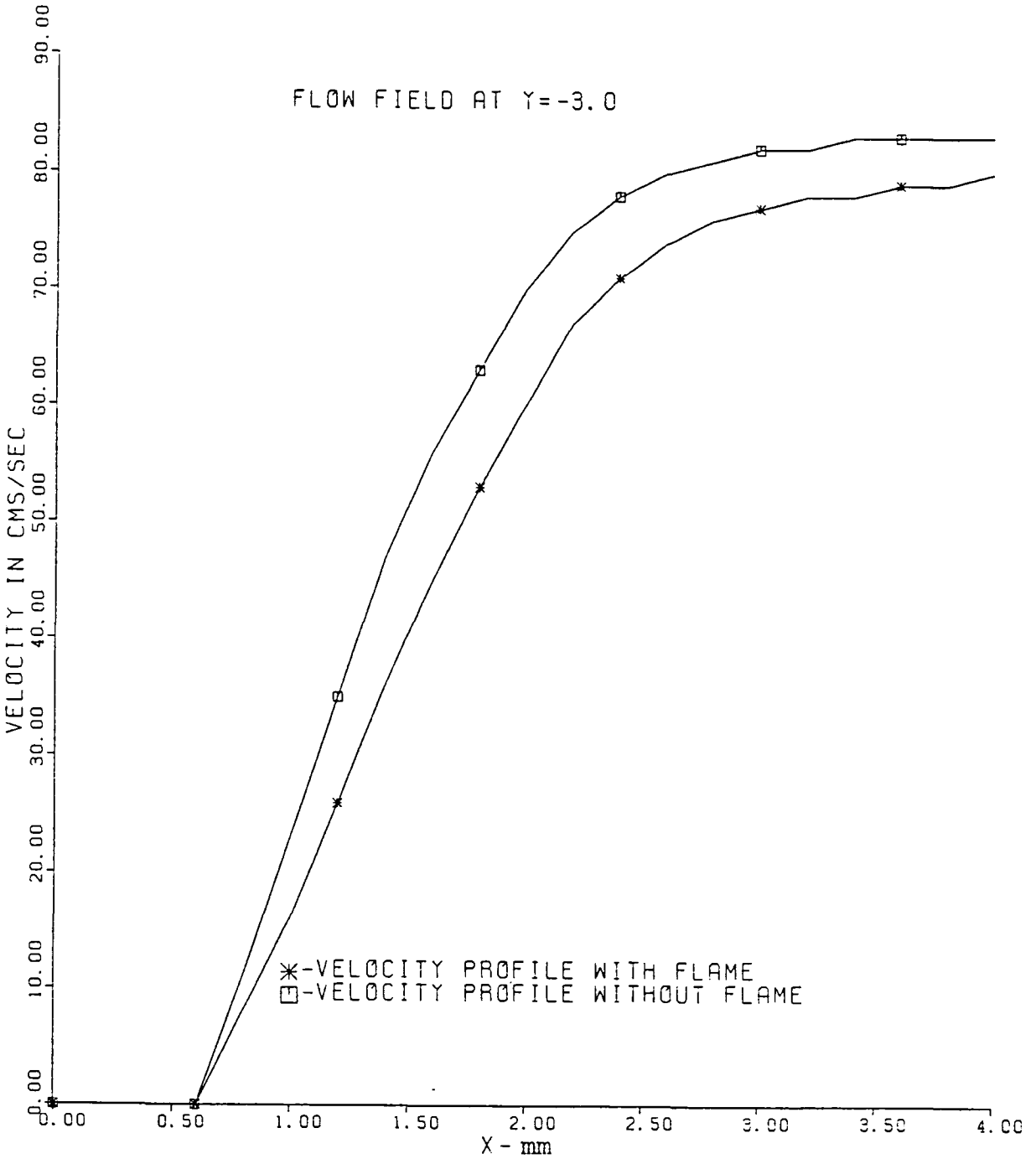

Fig.V-14. Velocity Profile of Methane-Air Mixture Along Flame Holder A.

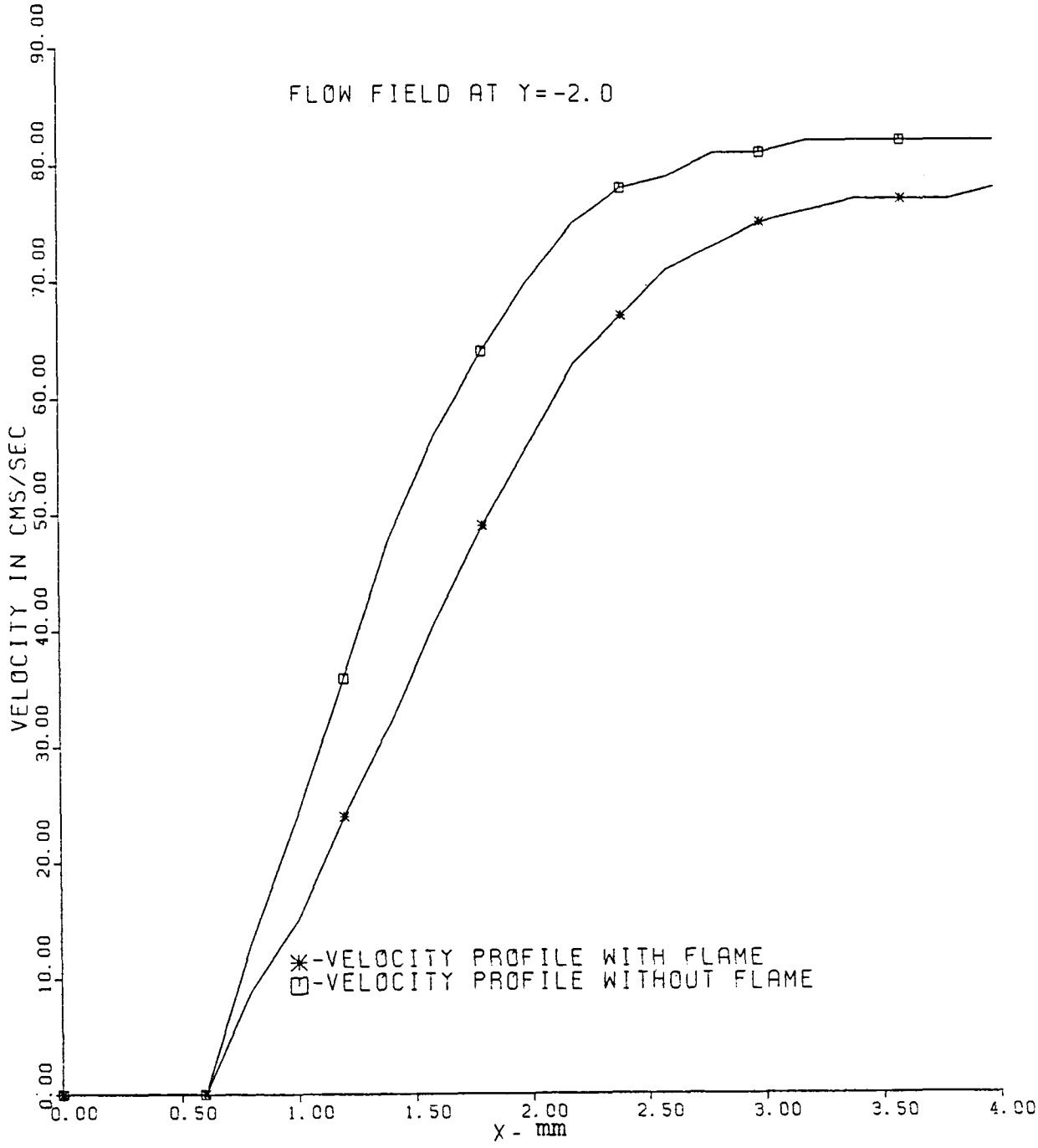

Fig.V-15. Velocity Profile of Methane-Air Mixture Along Flame Holder A.

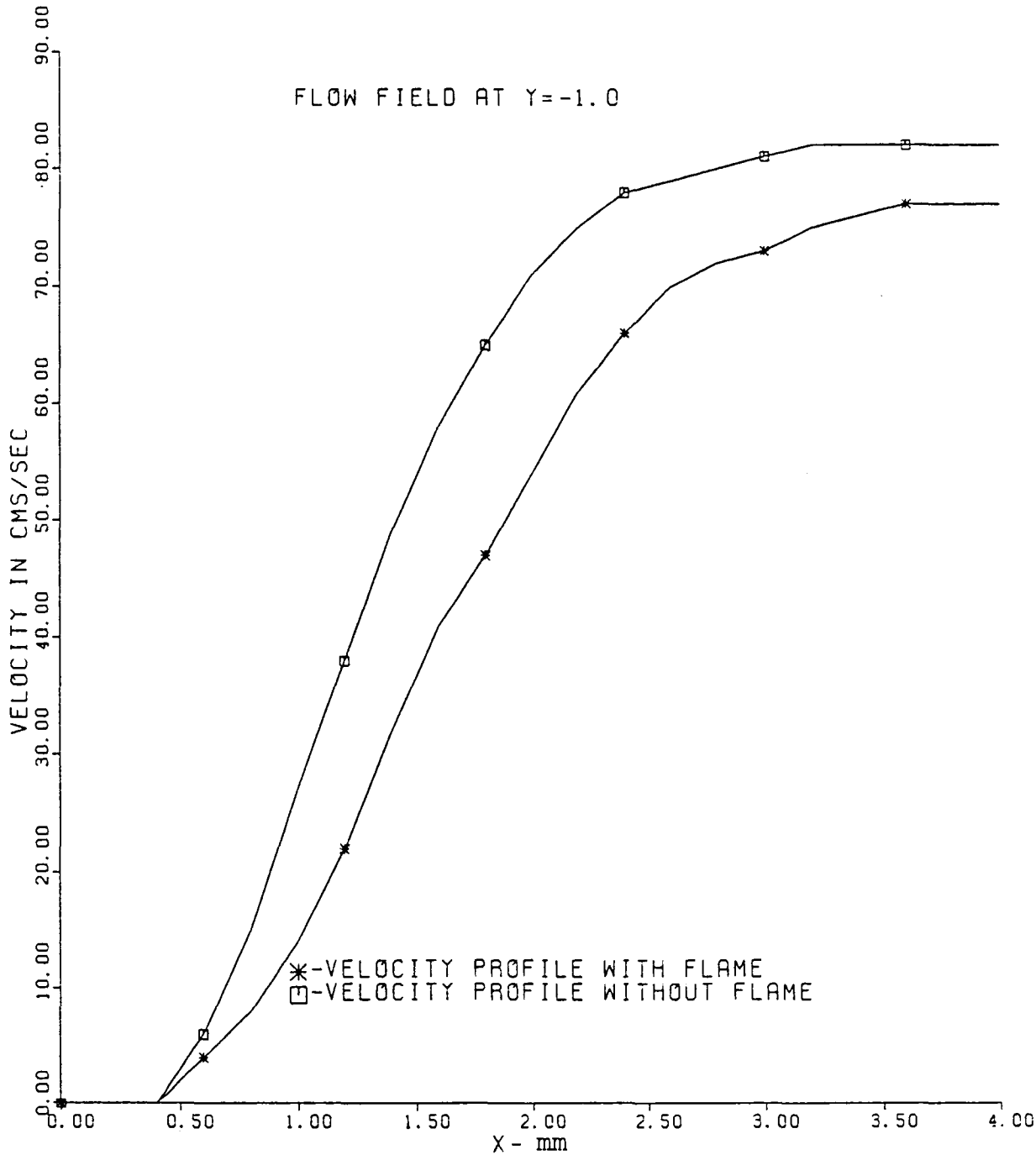

Fig.V-16. Velocity Profile of Methane-Air Mixture Along Flame Holder A.

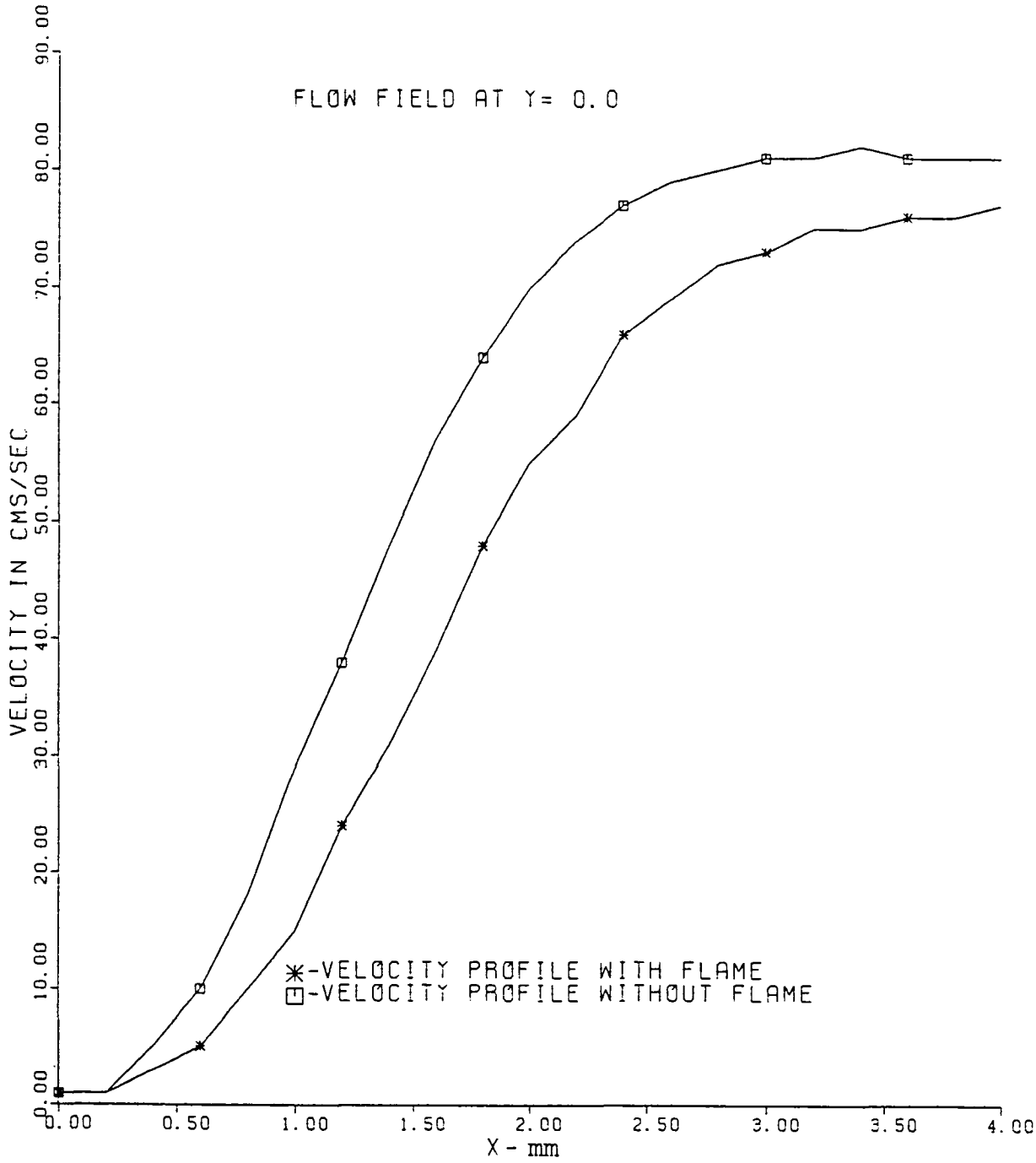

Fig.V-17. Velocity Profile of Methane-Air Mixture Along Flame Holder A.

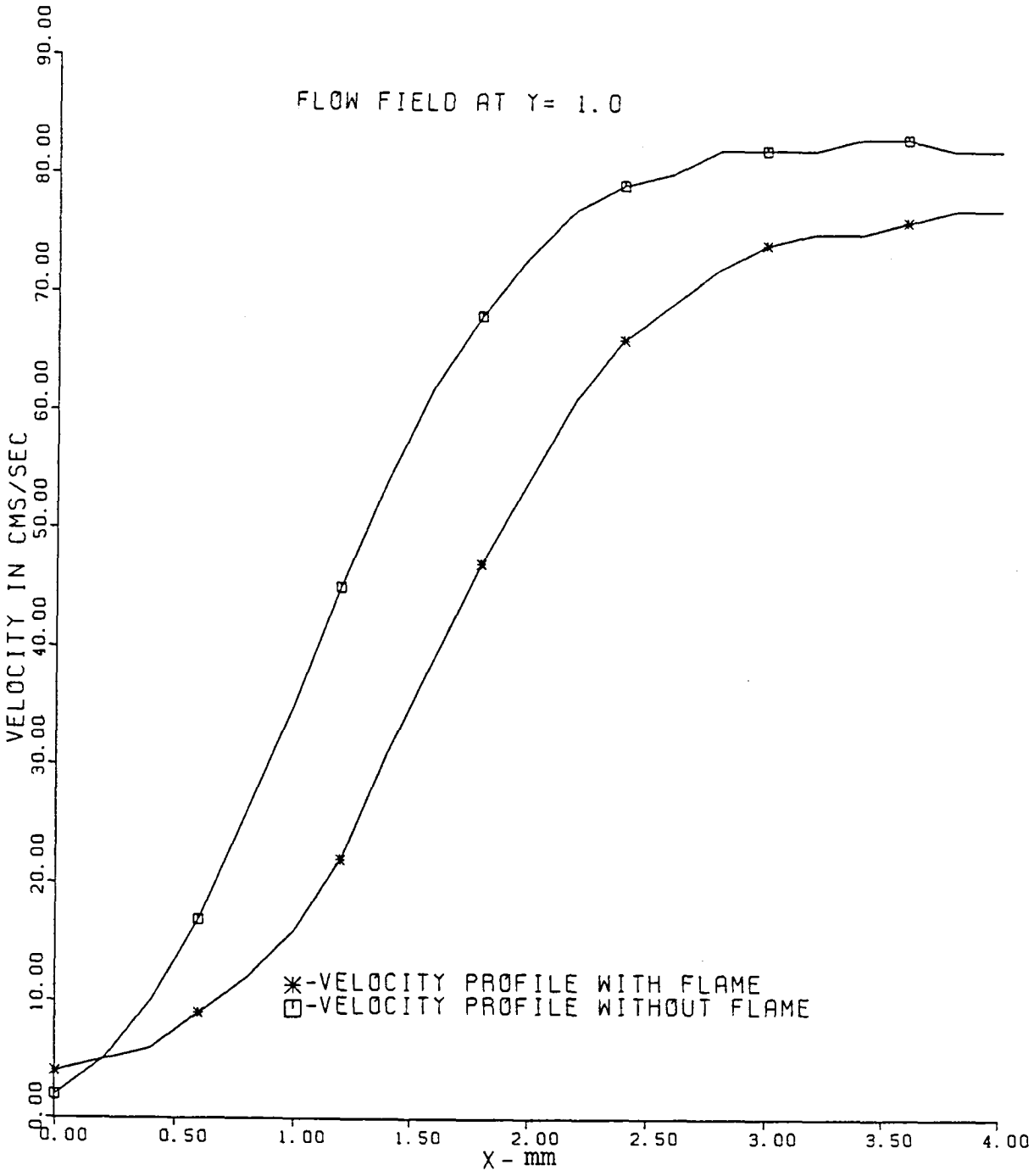

Fig.V-18. Velocity Profile of Methane-Air Mixture Along Flame Holder A.

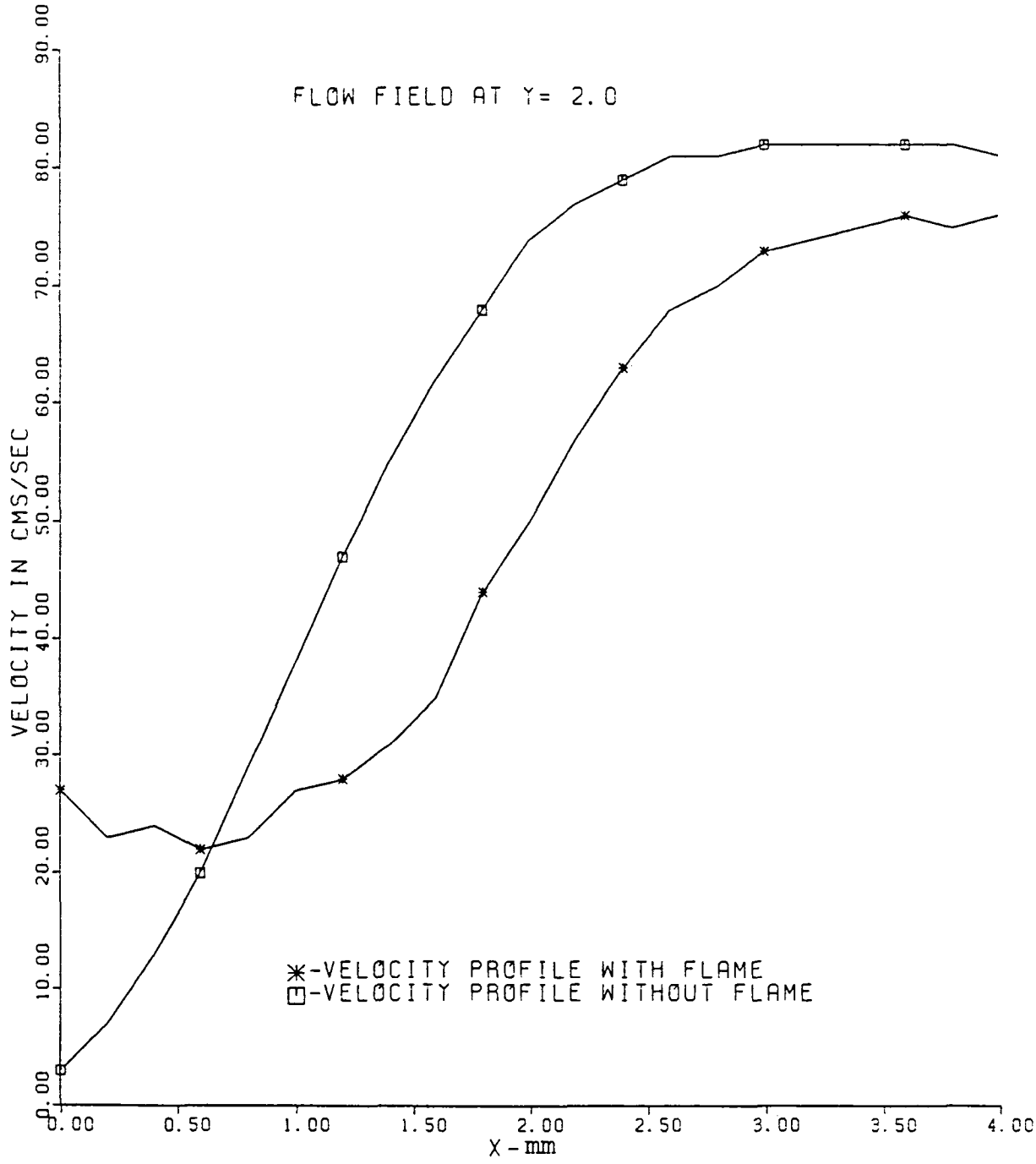

Fig.V-19. Velocity Profile of Methane-Air Mixture Along Flame Holder A.

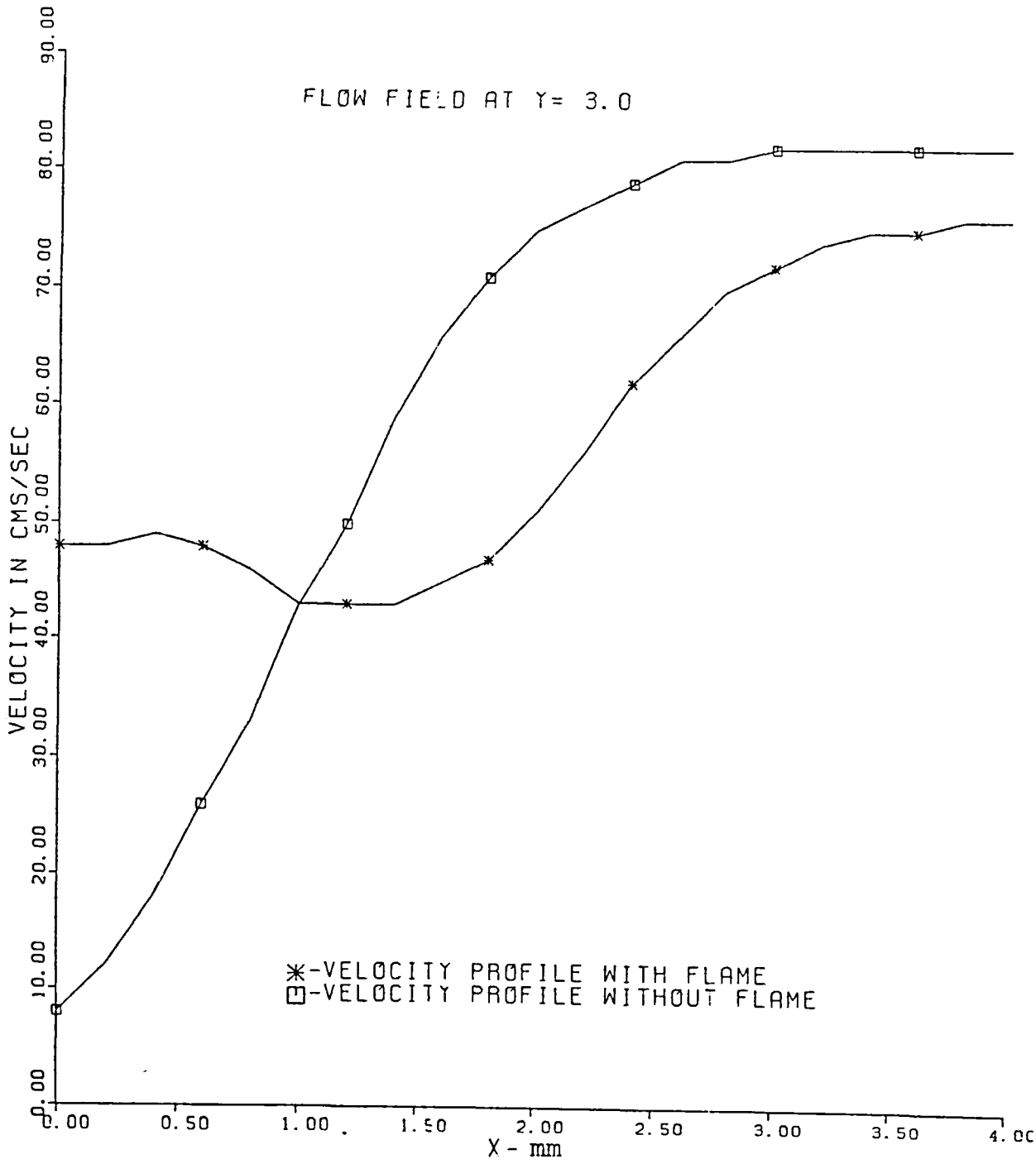

Fig.V-20. Velocity Profile of Methane-Air Mixture Along Flame Holder A.

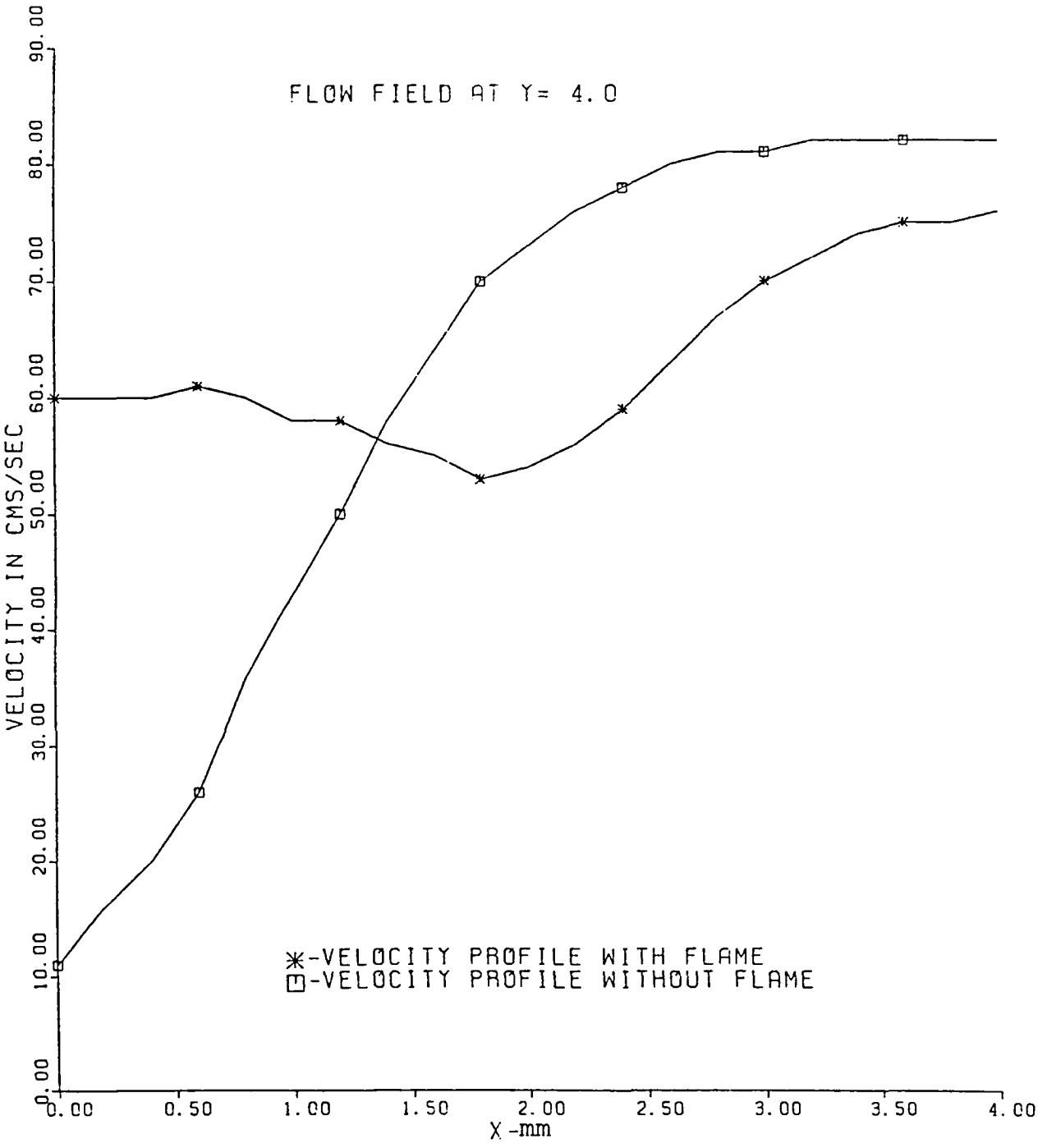

Fig.V-21. Velocity Profile of Methane-Air Mixture Along Flame Holder A.

the flame present are displaced and are lower than the velocity profiles without flame. The value of displacement seems to be minimum for the near blow-off limit flame and was observed to increase as the inverted flame was held further away from the blow-off limit. However if we look at the position of this displacement along the horizontal axis, it occurs for almost all Y positions, in an interval of X-axis between 1.2 mm and 2.0 mm. These displacements increase as one progresses upward along the Y-axis till one approaches the reaction zone where the velocity starts to increase. As one approaches the reaction zone of the flame in figure V-21, the flow velocity starts to accelerate near the trailing edge and attains its maximum velocity in the flame front. From figures V-18 to V-21, one can see the velocity profile downstream of the trailing edge. Here the points of intersection of velocity curves with and without flame are the maximum accelerated flow which represents the flame front. Since the spatial coordinates of these points with regard to the reference coordinate system are known, one can determine, with reasonable accuracy, the locus of flame front downstream of the trailing edge.

The velocity profile curves presented in the above figures show that at an approximate horizontal distance of 3.25 mm from the origin the approach flow velocity has reached its maximum value of U_o outside the boundary layer. The value of approach flow velocity, U_o outside the boundary layer in case when the

flame is present is lower and therefore it is obvious that the boundary layer thickness would be different depending on whether the flame is present or not.

Knowldge obtained from these velocity profiles and the schlieren and visible images can be presented in such a manner as to more explicitly correlate the position of the flame front and the preheat zone. In regard to this a visible light photograph of a methane flame was taken at the particular setting for flame holder A and it is presented in V-22. Knowing the position of the flame front, another form of representation is presented in figure V-23, where the magnitude of velocity vector in the vertical direction is shown, with the position of the flame front superimposed. Since the flow field is symmetric about the vertical axis, on the right hand side of the flame holder the flow field is shown with the flame present, while on the left side the flow field is shown without any flame. Each half of this figure covers an area of 4.0x1.8 square millimeters. The longest velocity vector represents a velocity of 74.0 cm per second. Everything else in this figure is to scale including the flame holder. Note that since the flow velocities are very subsonic the pressure of the flame is strongly felt upstream of the trailing edge. An important point to be noted in this figure is that only the vertical velocity components of the approach flow velocity are shown and the vector length corresponds to the magnitude of the velocity of the particles at that particular

Flame Holder A

Air Flow Rate = 0.36 liter/sec;
Methane Concentration = 6.25%

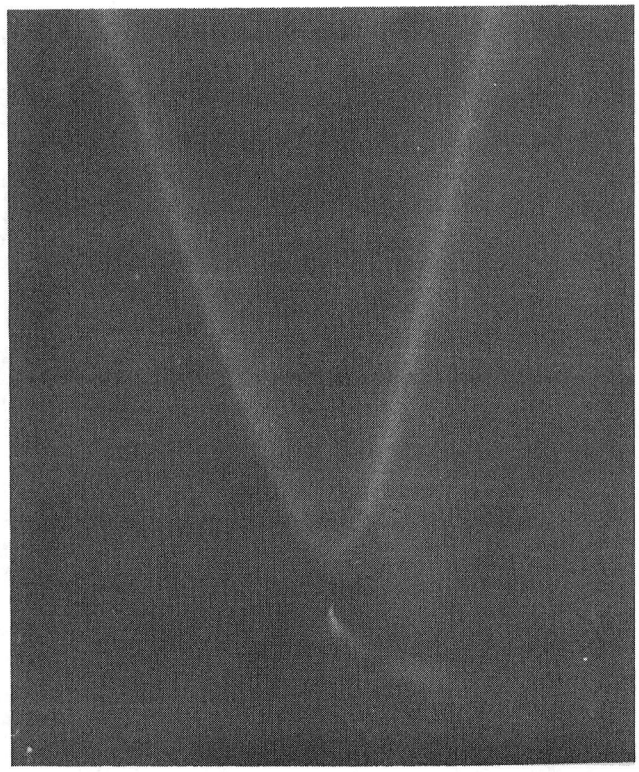

10 mm

Fig.V-22. Visible Light Picture of Methane-Air Flame with Particle Injection.

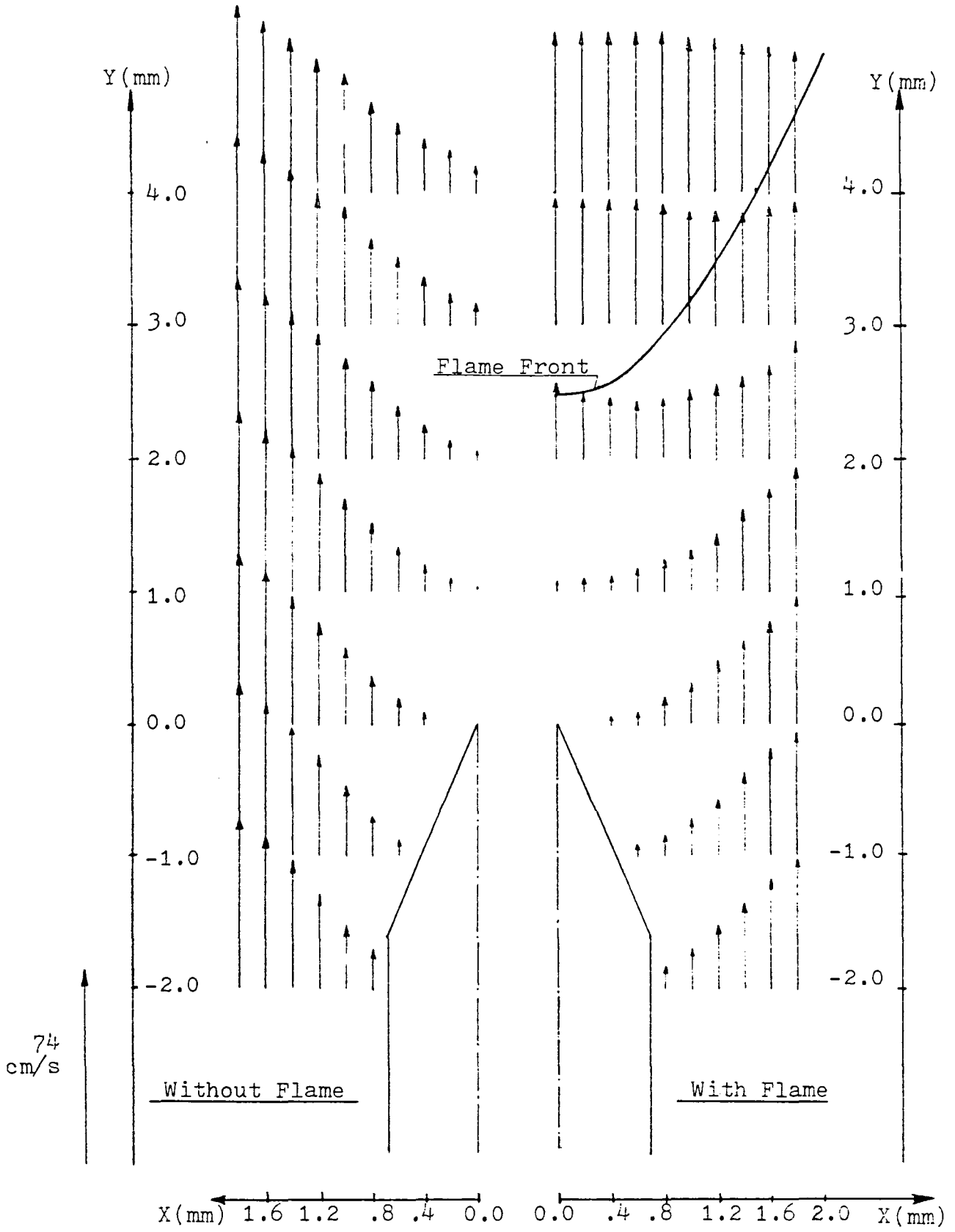

Fig.V-23. Vectorial Representation of Methane-Air Mixture With and Without Flame for Flame Holder A.

position in space. The base of the vectors drawn in this figure indicate the locations where the velocity was measured. As is shown in this figure the flow field with flame at Y > 1.0 mm, is totally different from that without the flame.

The velocity profile curves for all different vertical heights with and without flame are shown in figures V-24 and V-25 respectively. In these figures the different vertical heights are represented by numbering the curves to correspond to the vertical station, i.e the curve carrying the '0' marker represents the vertical station located at Y=-4.0 mm, similarly the vertical station at Y=4.0 is represented by the number 9. Table 5.2 contains the numbers of the curves corresponding to different vertical heights.

Three dimensional views of the profiles are presented in figures V-26 and V-27 with and without the flame respectively. Looking at figure V-26 one can see the origin of temperature rise where the flow velocity starts to increase downstream of the trailing edge, eventually reaching a maximum value in the reaction zone of the flame.

Table 5.2

Curve No.	Location at Y-axis
0	-4.0
1	-3.5
2	-3.0
3	-2.0
4	-1.0
5	0.0
6	1.0
7	2.0
8	3.0
9	4.0

Therefore one can reason that the region between the maximum of the curve to the point where it starts to increase, represents the preheat zone of the flame. This reasoning is only valid for the velocity profile curves at and above the vertical position of the flame base because only there is the flame front oriented exactly normal to to the approach flow direction.

The next flame holder that was used for the fuel methane is the flat edged flame holder, B. The air and fuel flow rates remain the same as for flame holder A. Here the velocity flow field was measured for values of Y starting from Y=-2.0 and going upto Y=3.0. The reason for using the flat edged flame holder was

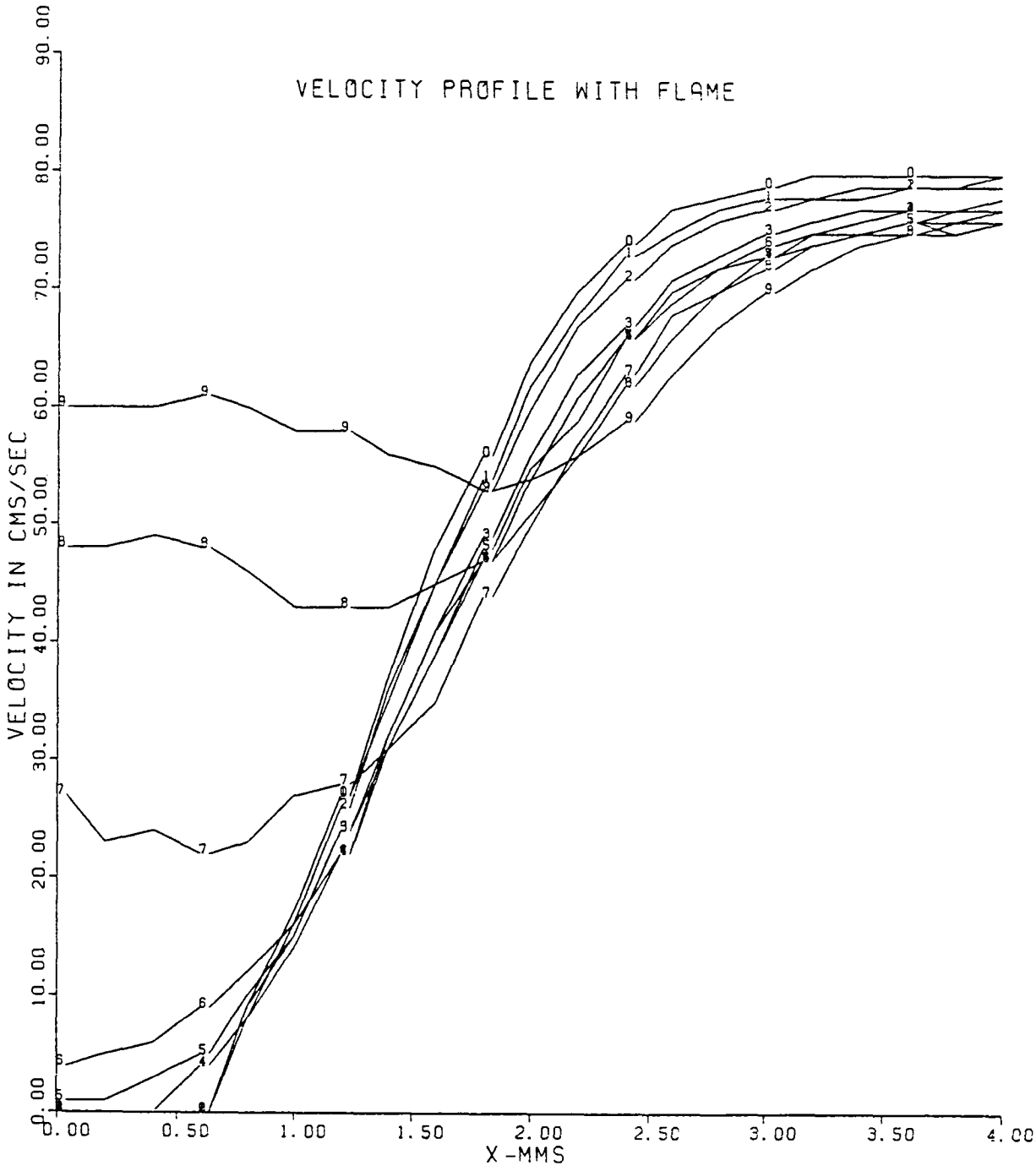

Fig.V-24. Velocity Profiles of Methane-Air Mixture at Different Vertical Locations Along Flame Holder A.

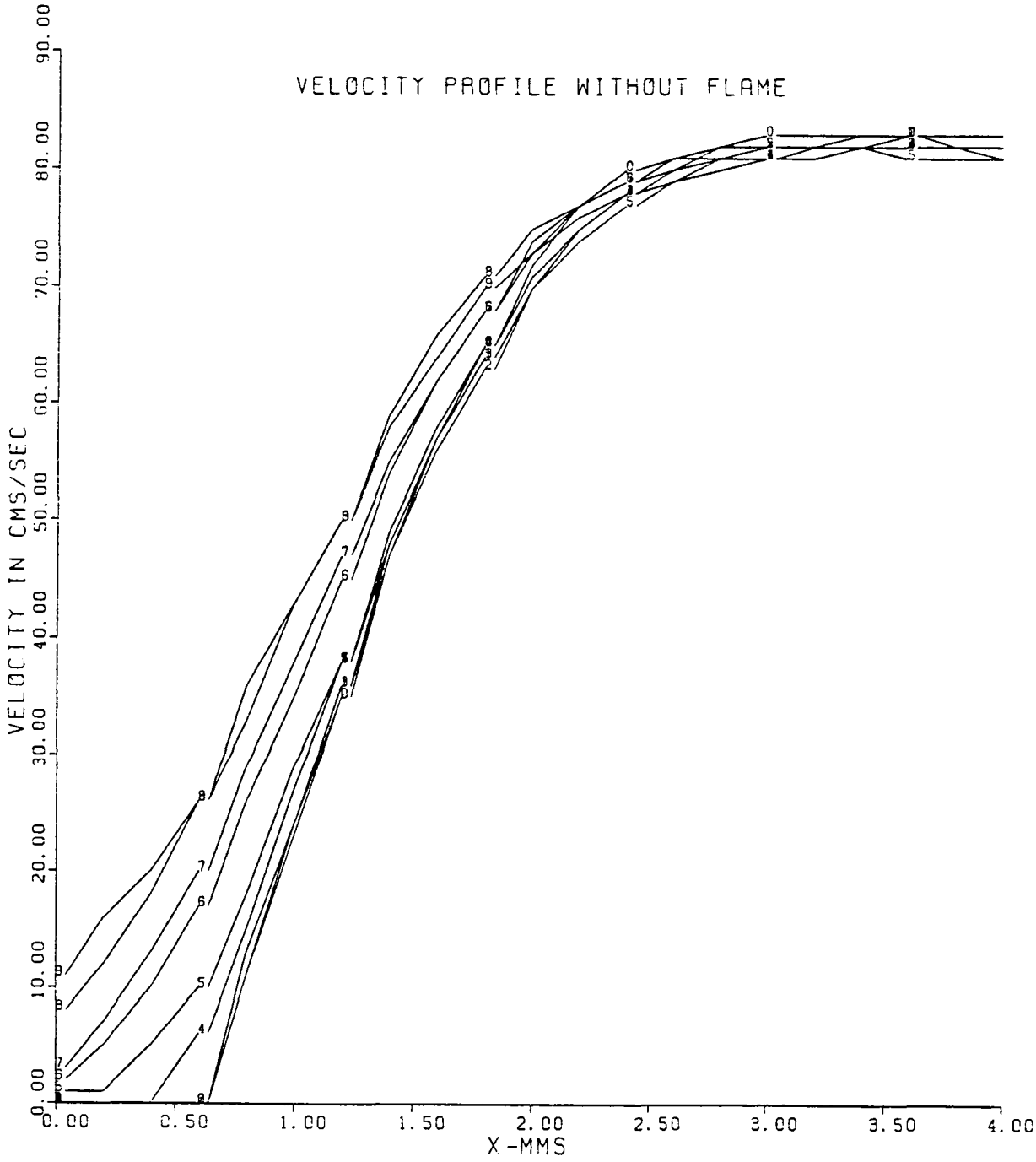

Fig.V-25. Velocity Profiles Of Methane-Air Mixture at Different Vertical Locations Along Flame Holder A.

Flame Holder A

Velocity Flow Field with Flame

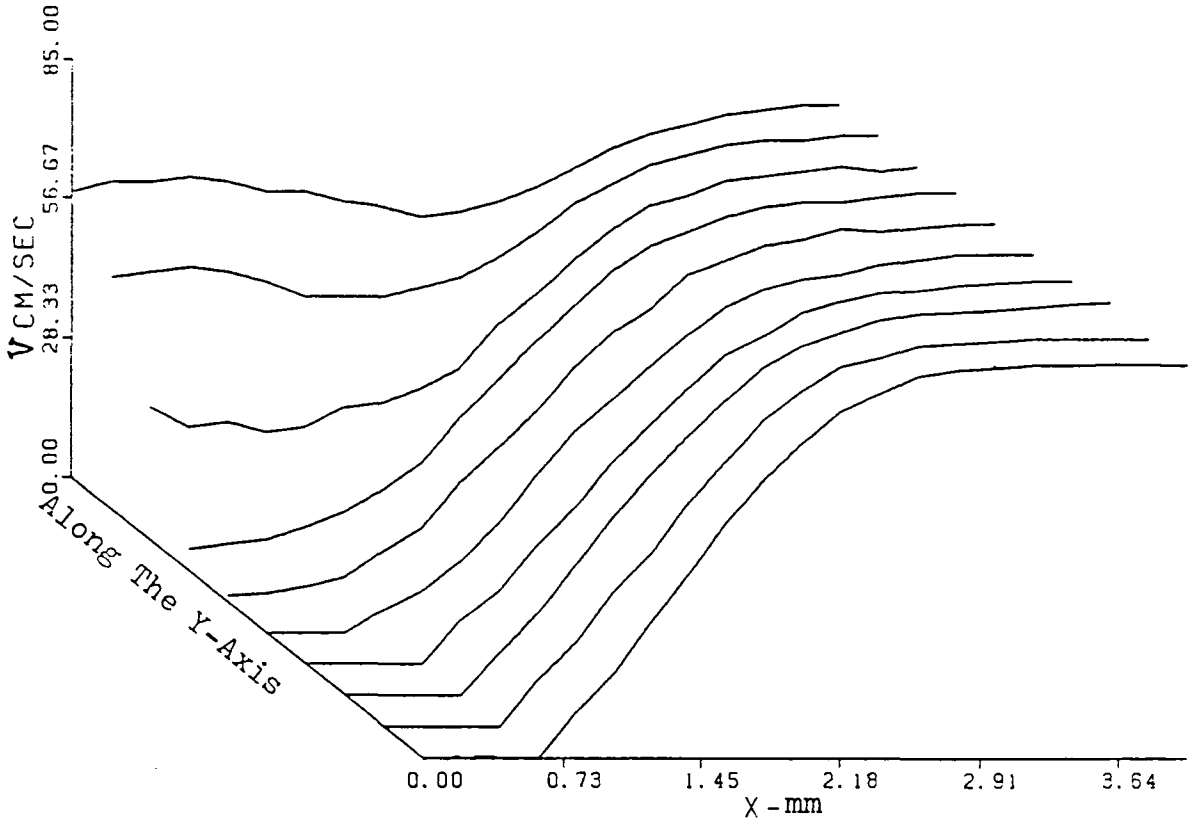

Fig.V-26. Three Dimensional View of Methane-Air Mixture Flow Field.

Flame Holder A

Velocity Flow Field Without Flame

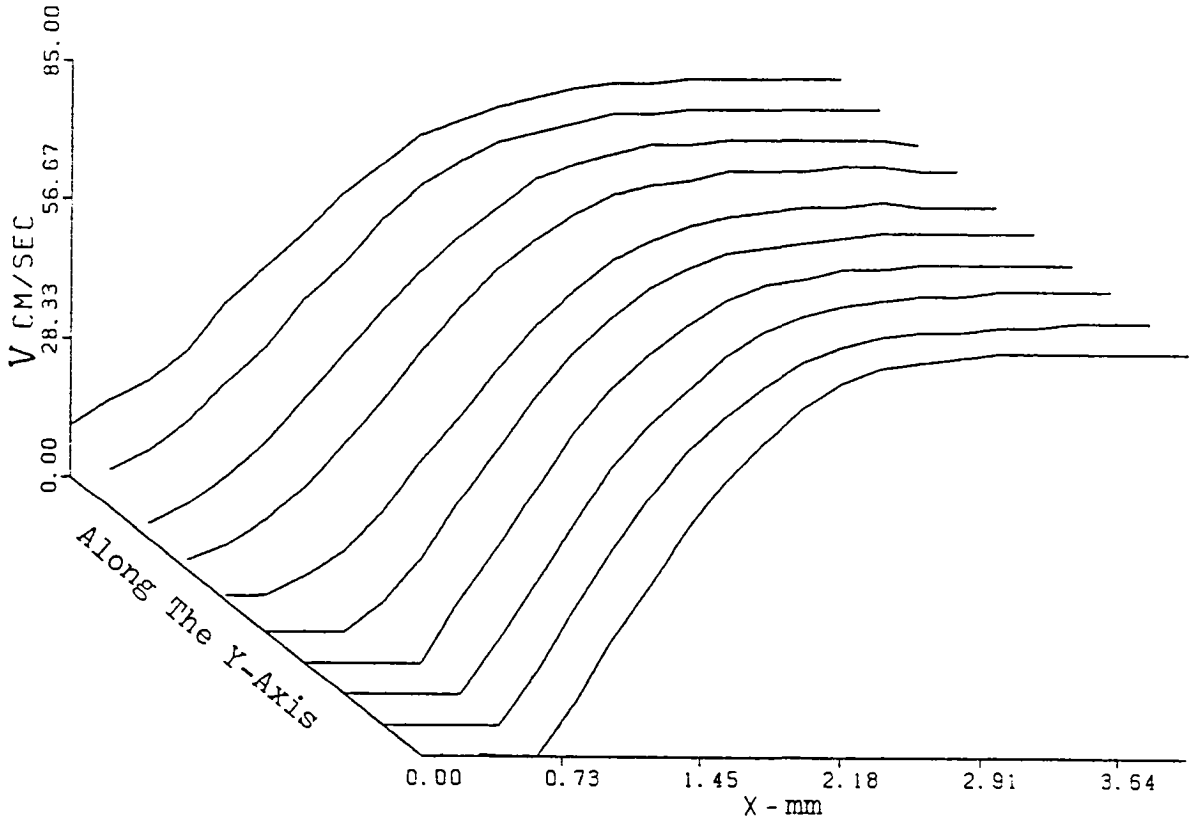

Fig.V-27. Three Dimensional View of Methane-Air Mixture Flow Field.

to observe its effects on the stability and blow-off limit of the flame. From the blow-off data presented earlier that one can see that no significant change in the blow-off behavior was observed. The curves for the velocity profiles with and without flame are shown in figure V-28 to V-31, along with the three dimensional flow field configuration. In the table 5.3 are given numbers of curves corresponding to different vertical heights.

Table 5.3

Curve No.	Location at Y-axis
0	-2.0
1	-1.0
2	0.0
3	1.0
4	2.0
5	3.0

It can be seen from curves numbered 3,4 and 5 that a dip is formed near the vertical axis of symmetry and the dip moves in the X direction as one moves up along Y-axis. The velocity increases at the dip as one moves towards the Y-axis (along curves 4 and 5), is due to the presence of the preheat zone, and the location where the velocity just acquires its maximum value, is the location of the reaction zone of the flame.

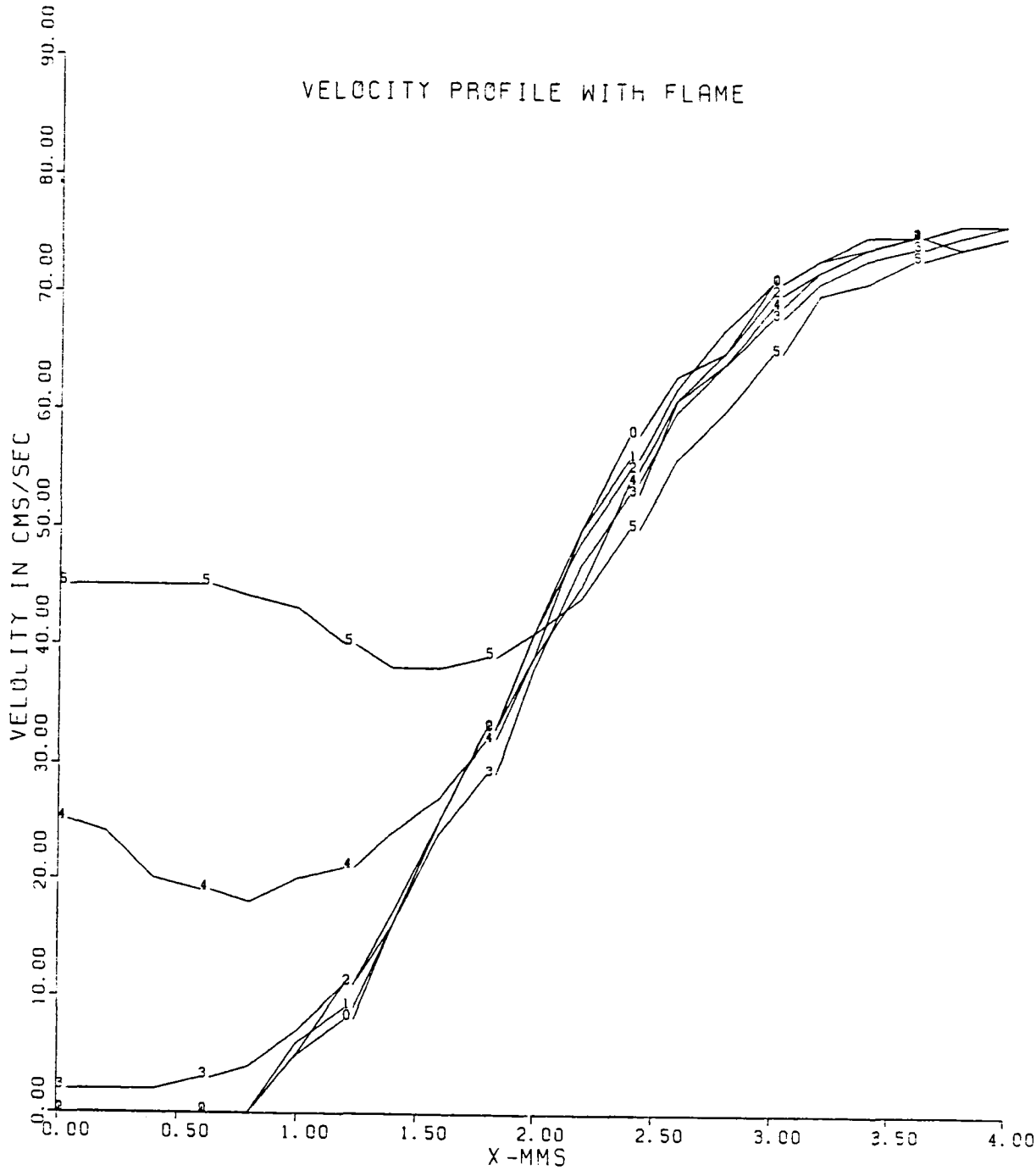

Fig.V-28. Velocity Profiles of Methane-Air Mixture at Different Vertical Locations Along Flame Holder B.

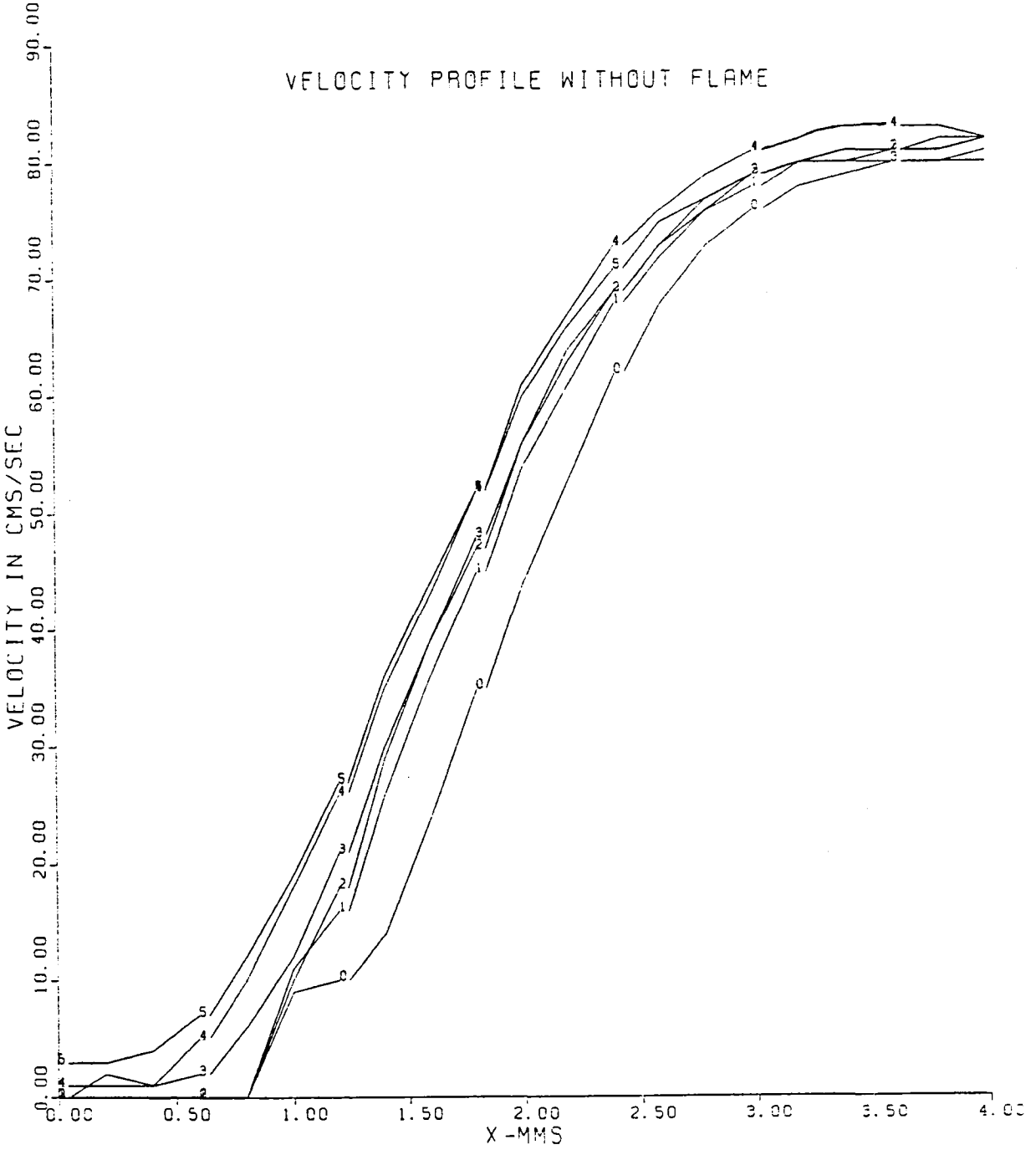

Fig.V-29. Velocity Profiles of Methane-Air Mixture at Different Vertical Locations Along Flame Holder B.

Flame Holder B

Velocity Flow Field With Flame

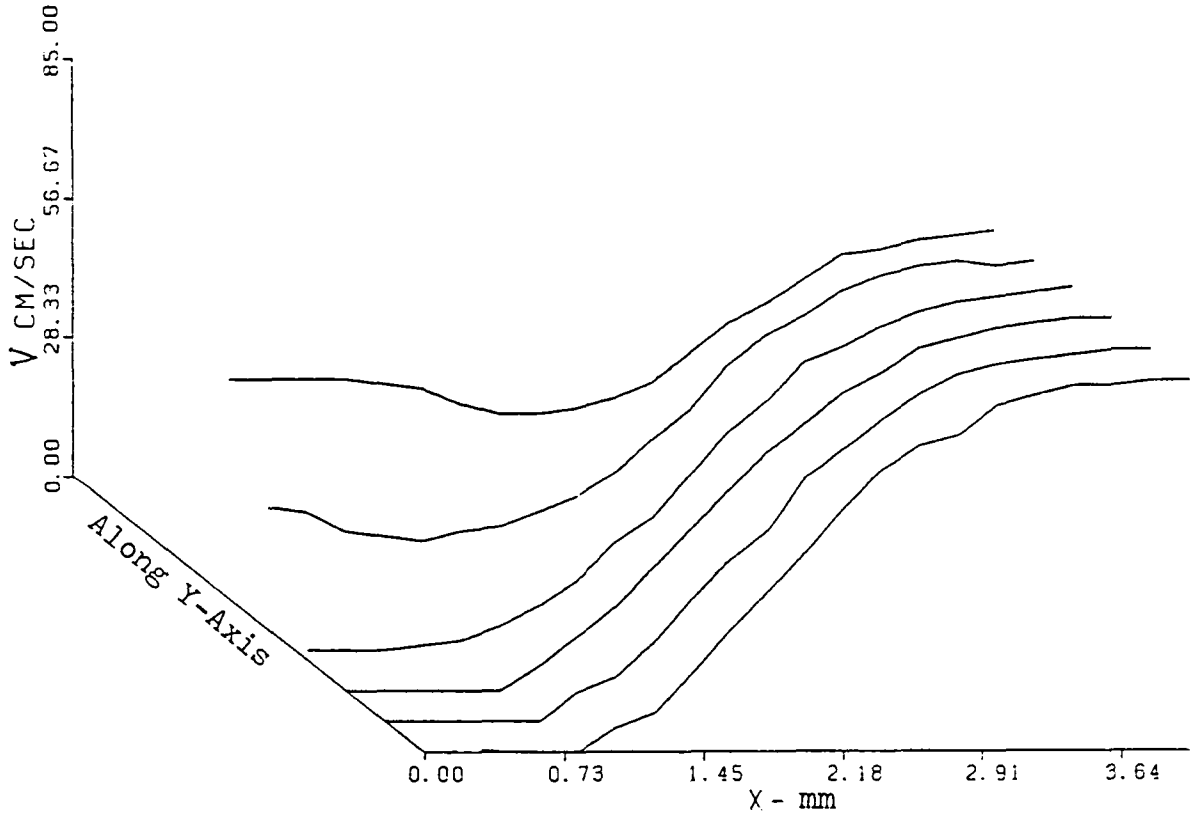

Fig.V-30. Three Dimensional View of Methane-Air Mixture Flow Field.

Flame Holder B

Velocity Flow Field Without Flame

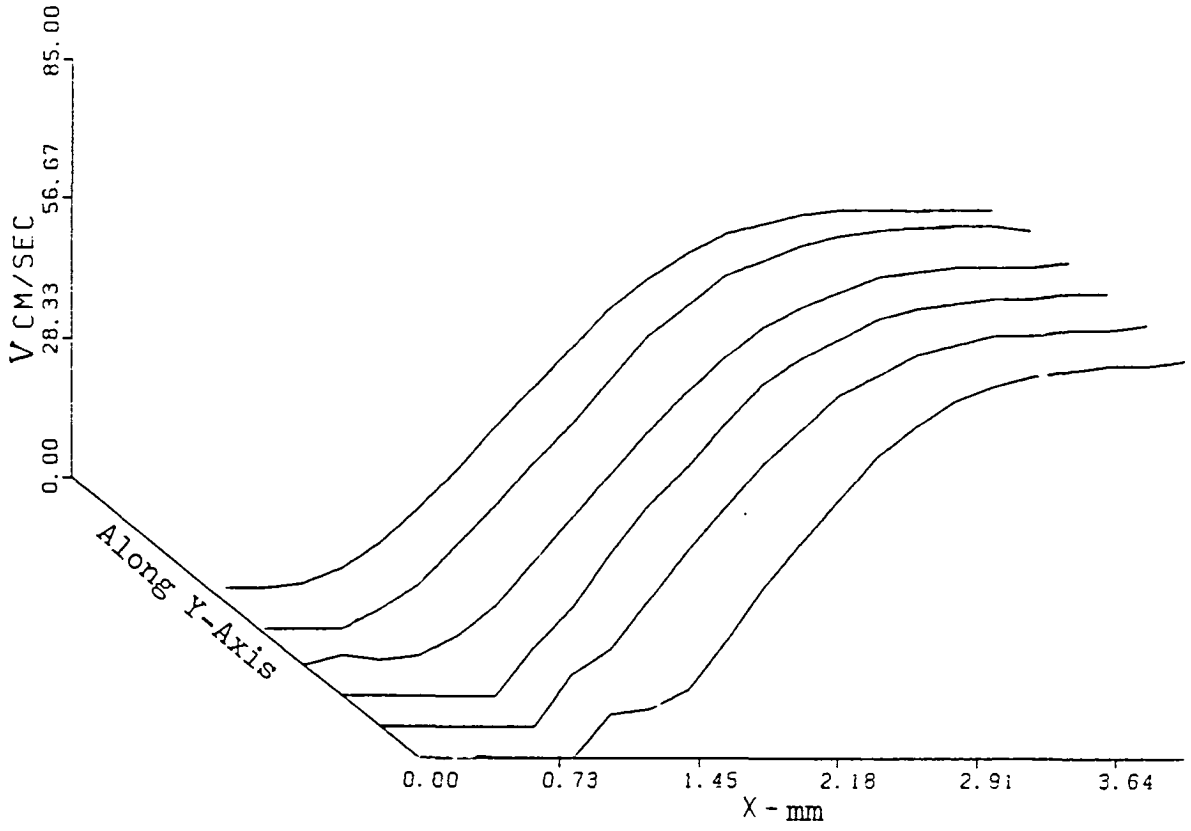

Fig.V-31. Three Dimensional View of Methane-Air Mixture Flow Field.

The flame holder referenced C was also used to further explore the effects of the thickness of the flame holder. In this case the flow rate had to be changed in order to keep the flame from blowing off. The air flow rate was kept the same as in previous cases but the fuel flow rate was increased to 0.025 liter/sec making the fuel concentration equal to 6.5%. Experimental data pertaining to this flame holder is presented in figures V-32 to V-33. Here the curves are numbered the same way as illustrated in table 5.2. Here again one observes a dip in the velocity profile curves above the trailing edge.

The next set of experimental data was taken for flame holder D. The air and fuel flow rates for methane were set at 0.4 and 0.028 liter/sec. The fuel concentration was calculated to be 6.5 %. The technique of taking the data for this flame holder was some-what different in manner. In this case the velocity components were measured in two directions, which were mutually perpendicular to each other. The configuration of this has already been shown and discussed in chapter IV. The two measured components were directed at 45 degrees to the right and left of the vertical axis. From the given magnitude and direction of these two orthogonal components, the resultant vectors in the (x,y) directions were calculated using a simple computer program. Hence, for this case the complete vectorial flow field was obtained with and without the flame. This was done for both the fuels methane and propane and these plots are

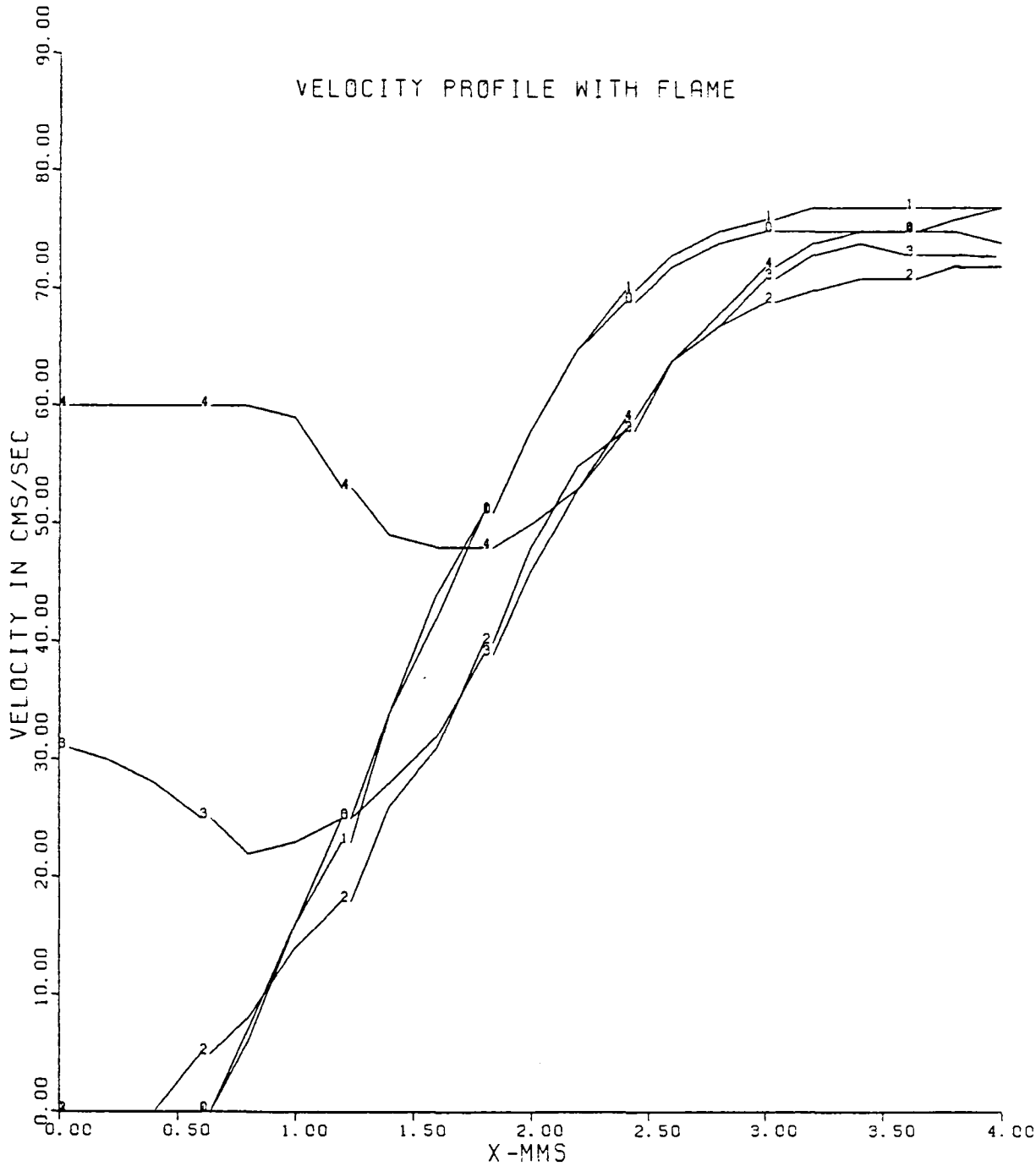

Fig.V-32. Velocity Profiles of Methane-Air Mixture at Different Vertical Locations Along Flame Holder C.

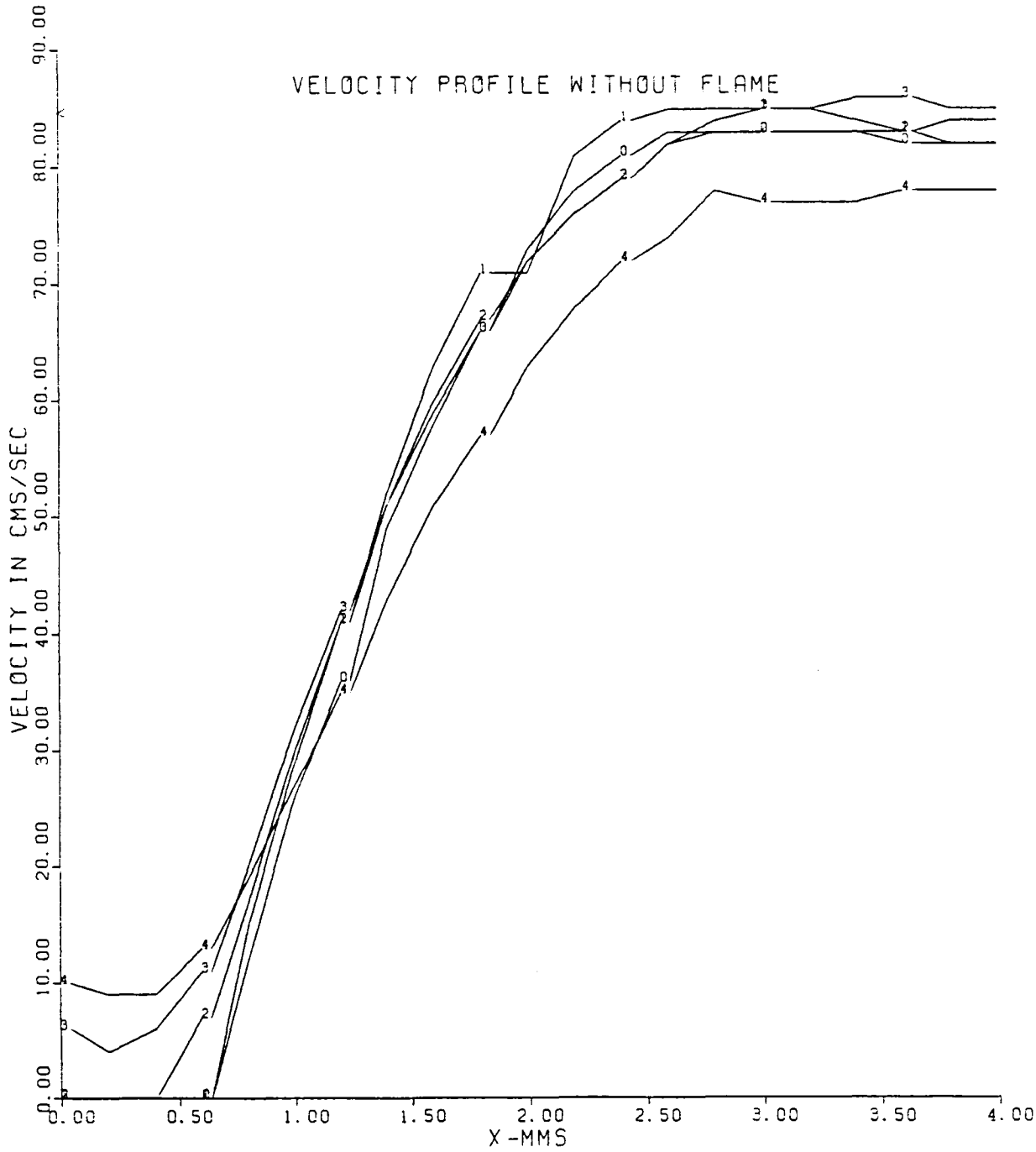

Fig.V-33. Velocity Profiles of Methane-Air Mixture at Different Vertical Locations Along Flame Holder C.

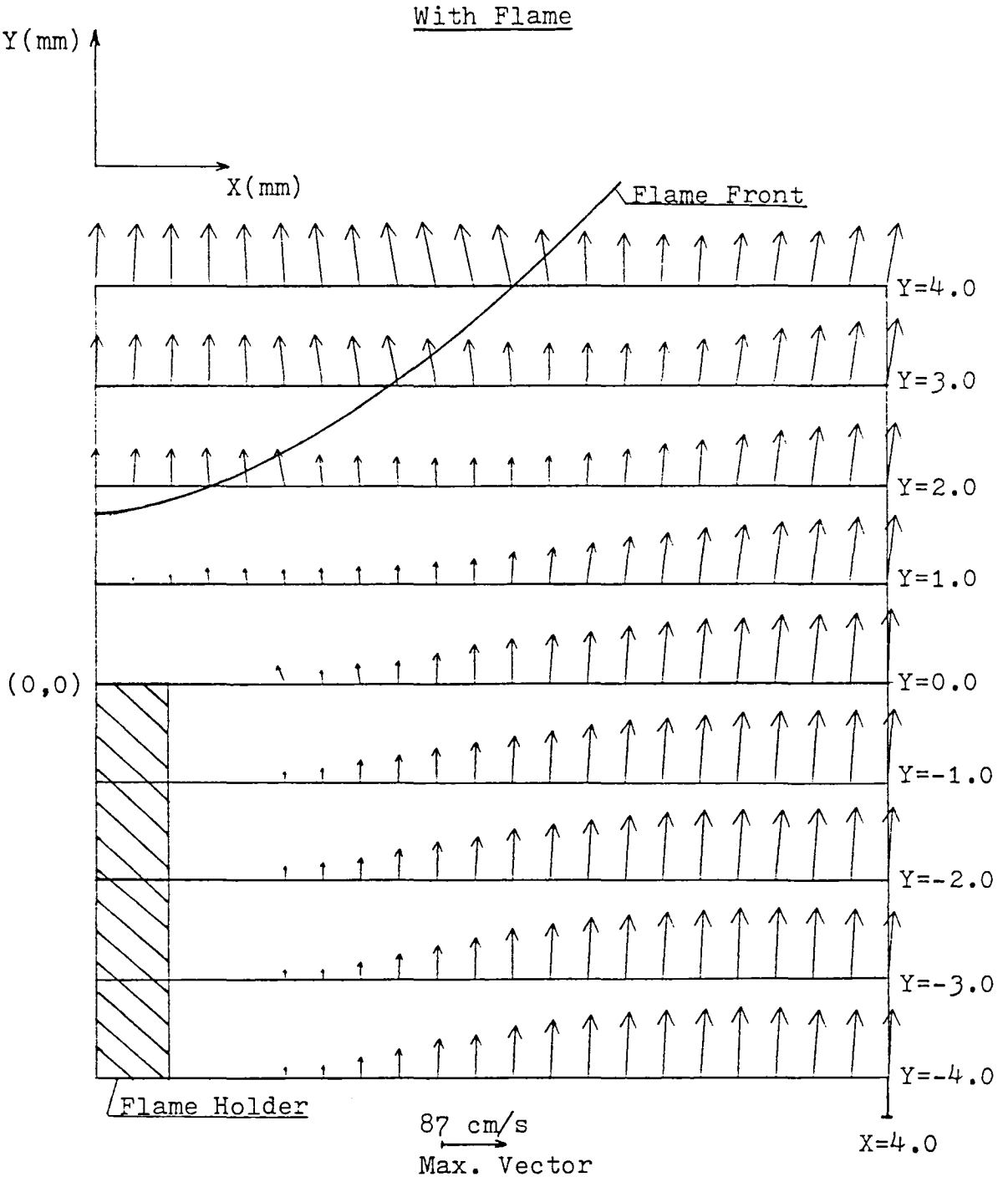

Fig.V-34. Vectorial Flow Field of Methane-Air Mixture Along Flame Holder D.

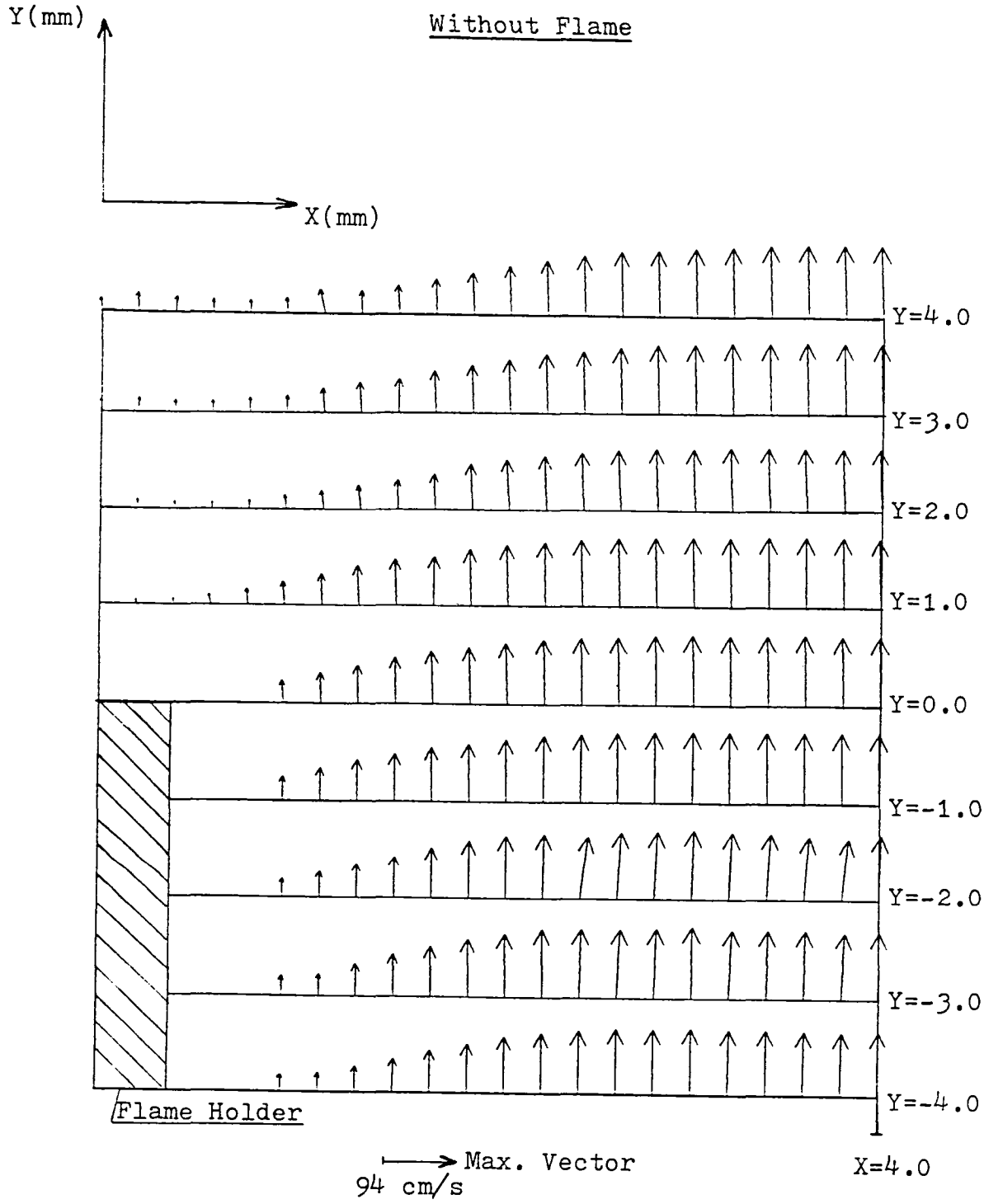

Fig.V-35. Vectorial Flow Field of Methane-Air Mixture Along Flame Holder D.

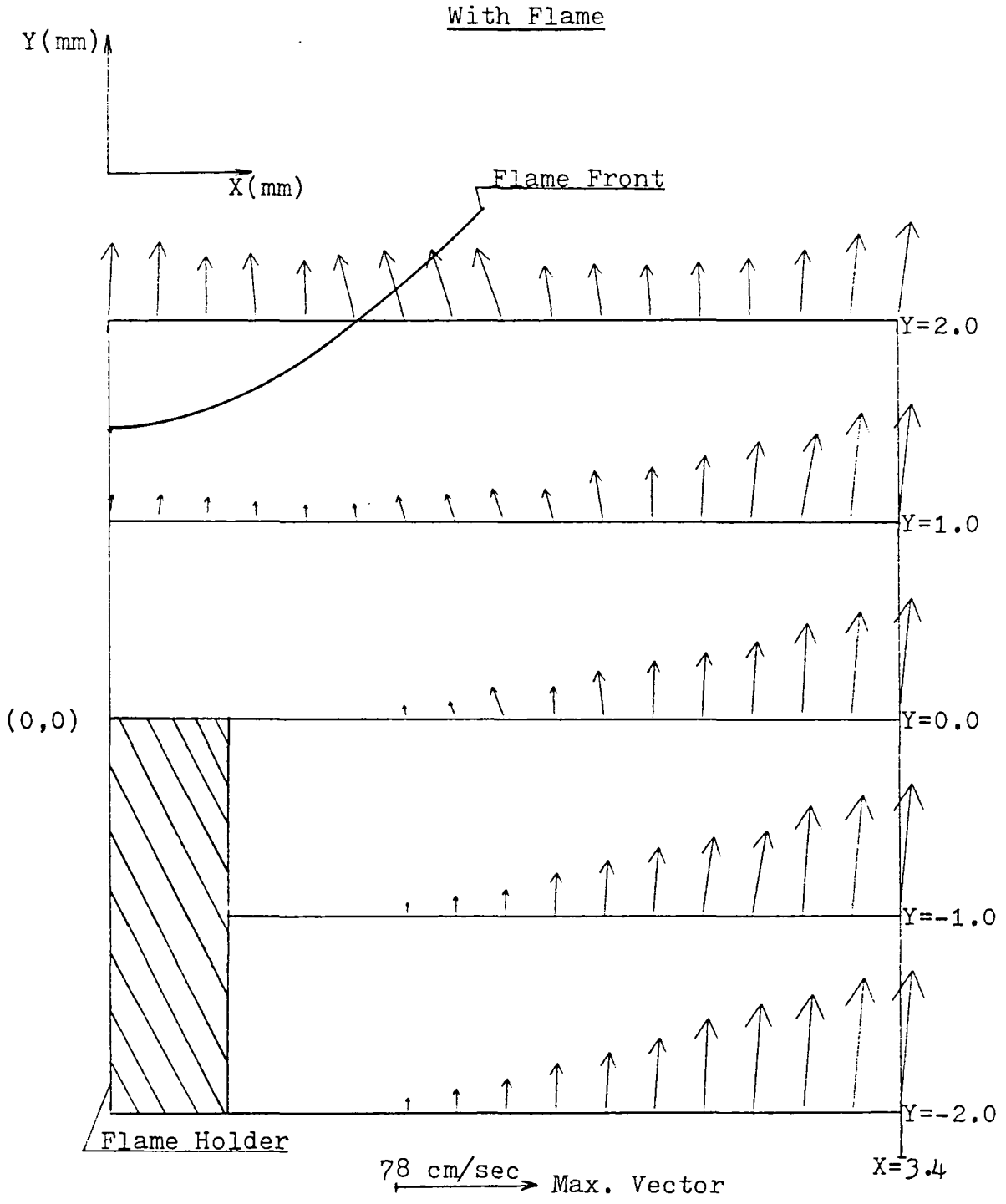

Fig.V-36. Vectorial Flow Field of Propane-Air Mixture Along Flame Holder D.

Without Flame

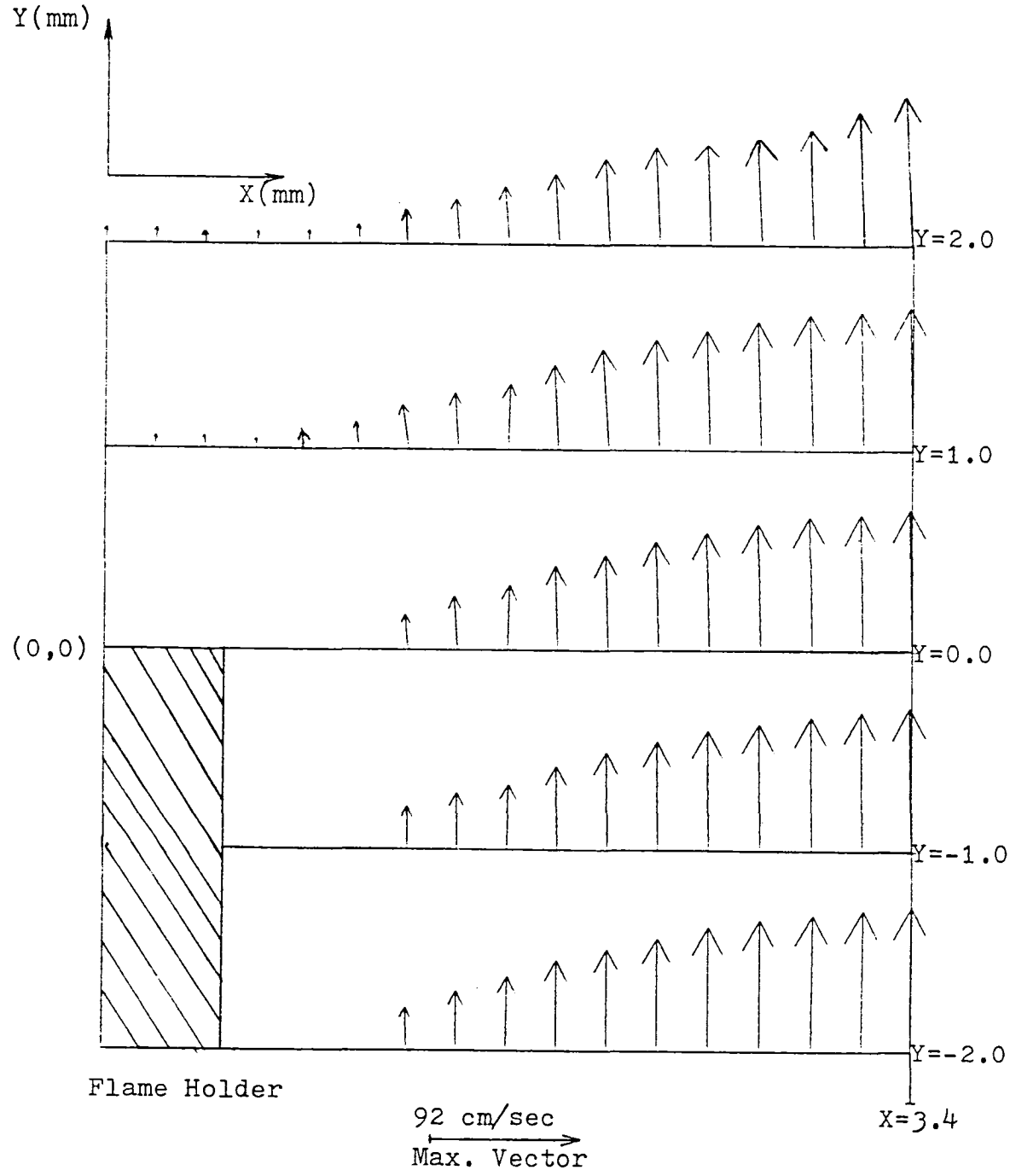

Fig.V-37. Vectorial Flow Field of Propane-Air Mixture Along Flame Holder D.

illustrated in figures V-34 to V-37. The air and fuel flow rates for propane were 0.44 and 0.0118 liters/sec and the fuel concentration calculated to be 2.61 %. On top of these figures are superimposed the position of the flame front which is known from the visible light photographs taken at these particular conditions. From the vectorial diagram a computer program was written to determine the streamlines of the flow field to show the deflection and widening of the stream tubes, as the flow enters the flame. These are illustrated in figures V-38 andV-39 for propane and methane respectively. Comparing vector flow field and streamlines for methane and propane, it is observed that the flow deflection due to the presence of the flame in the case of propane is more than it is for methane. The scales of these figures are given in the respective figures. The position and size of the flame holder is also scaled.

In the next phase of the experimental work the knife edged flame holder, A, was used with propane as fuel. A propane flame was stabilized at the trailing edge of the flame holder near the blow-off limit. The flow rates near the blow-off limit were the same as that for flamr holder D. The propane concentration was evaluated to be 2.61% and the equivalence ratio to be equal to 0.64.

The velocity profile curves for propane are presented in figures V-40 to V-44. Along the Y-axis data was taken at five

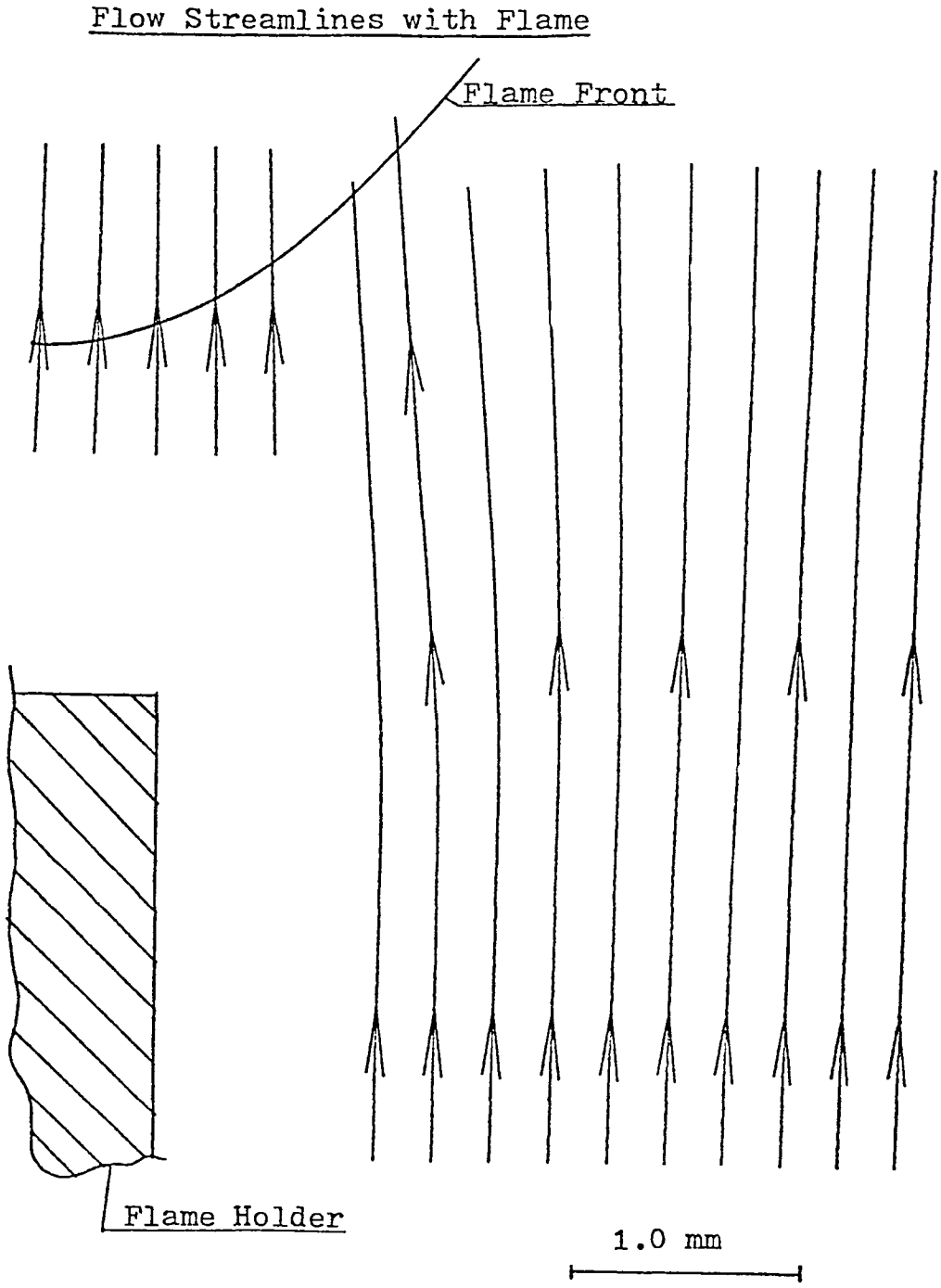

Fig.V-38. Streamlines Along Flame Holder D with Propane-Air Flame.

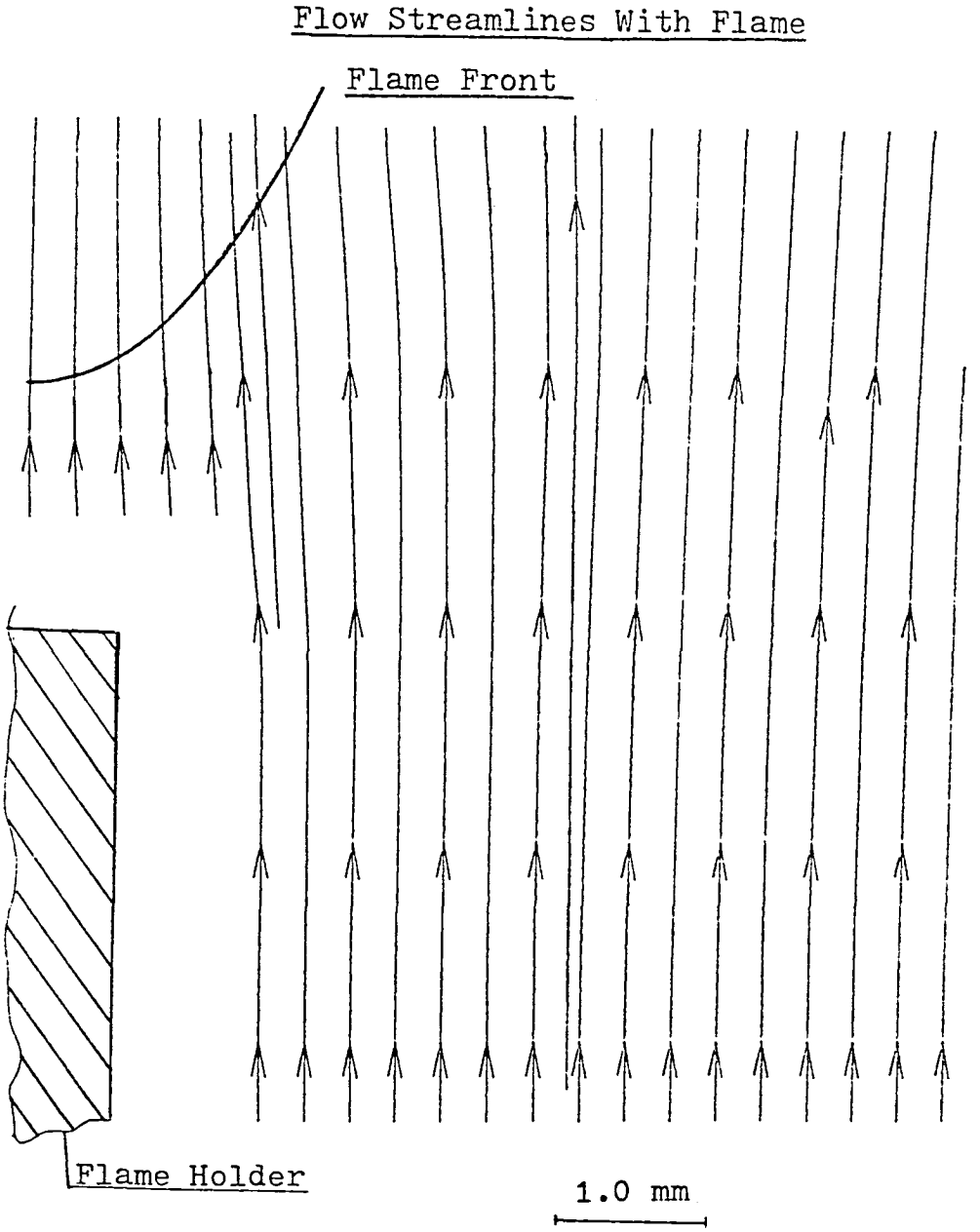

Fig.V-39. Streamlines Along Flame Holder D With Methane-Air Flame.

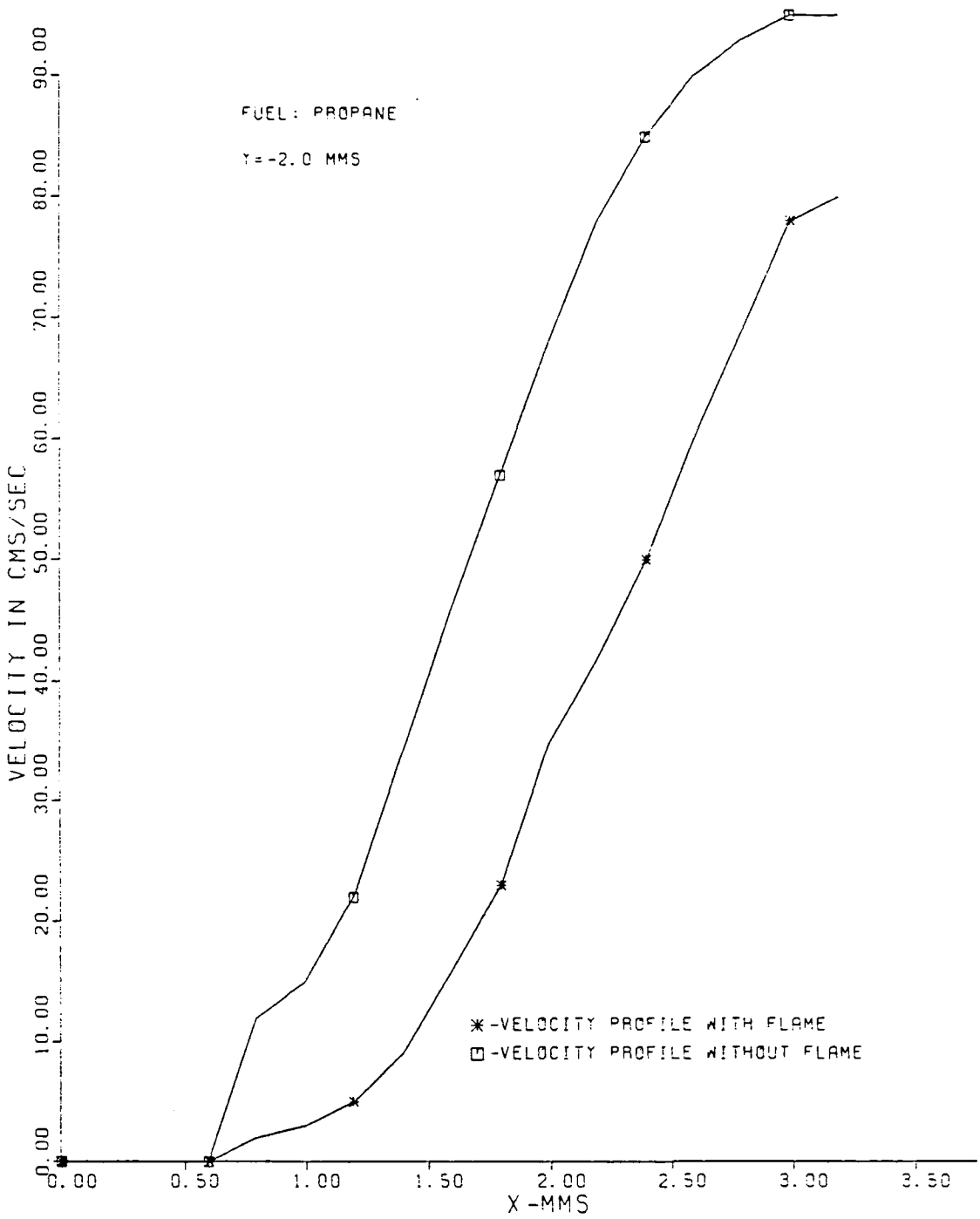

Fig.V-40. Velocity Profile of Propane-Air Mixture Along Flame Holder A.

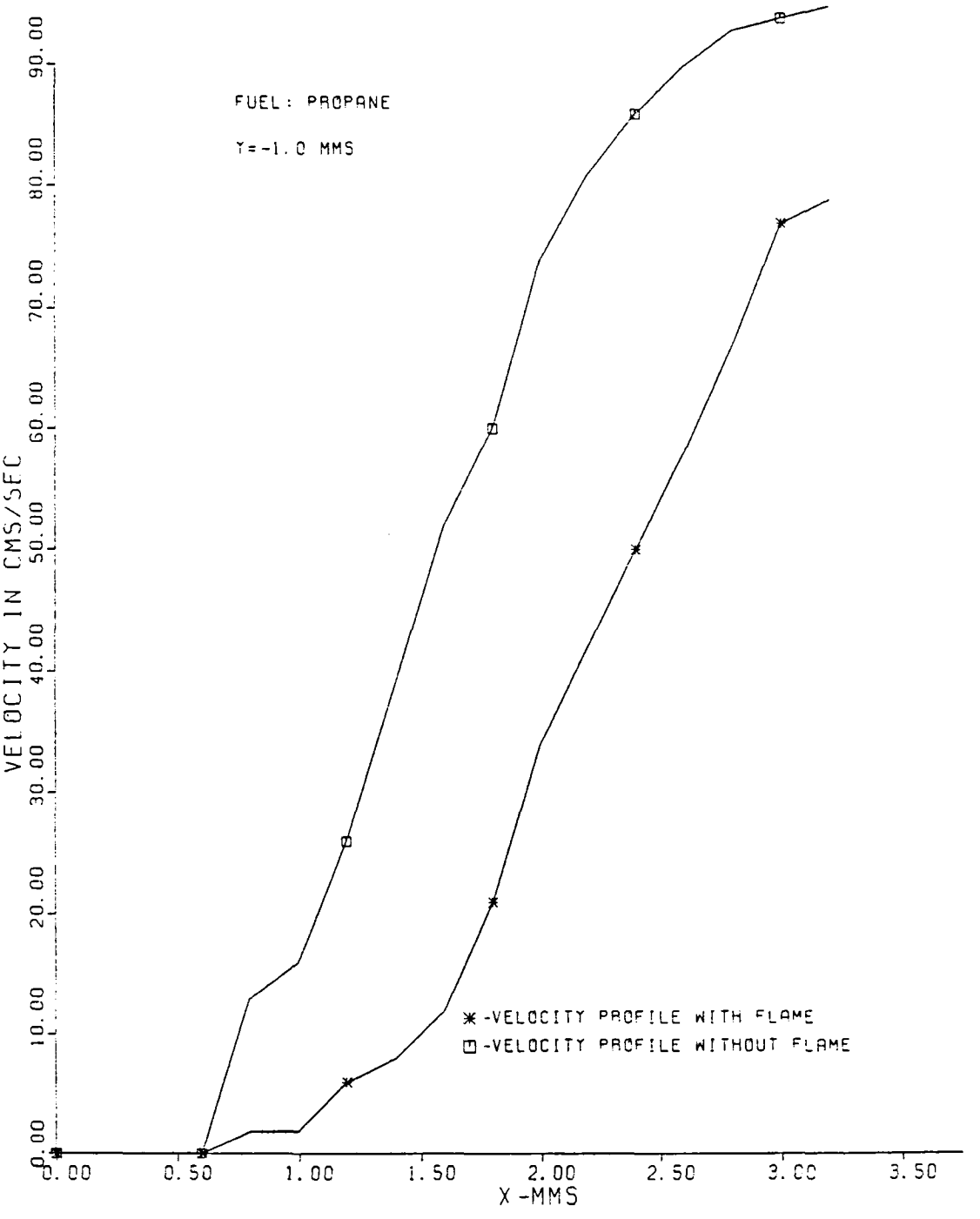

Fig.V-41. Velocity Profile of Propane-Air Mixture Along Flame Holder A.

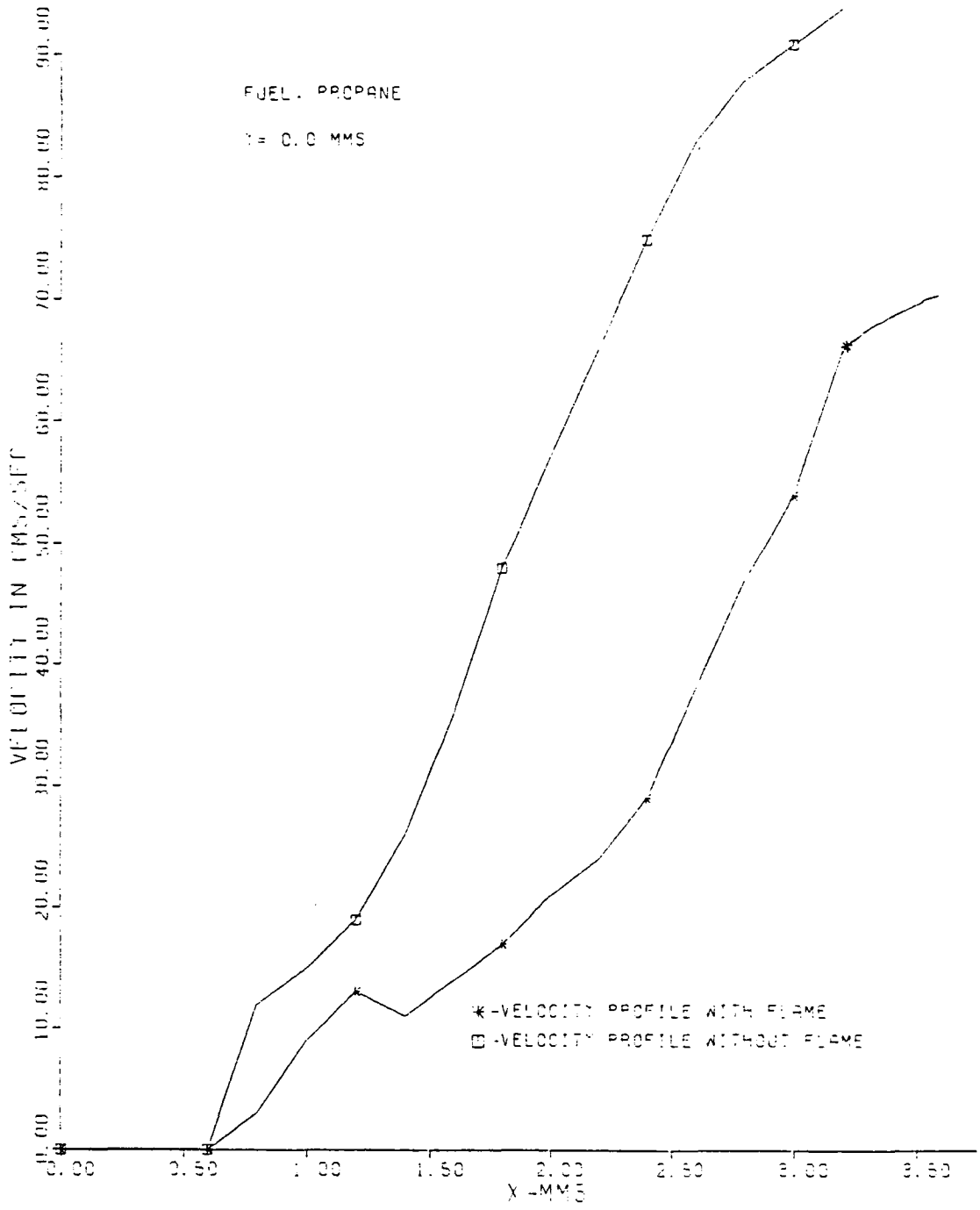

Fig.V-42. Velocity Profile of Propane-Air Mixture Along Flame Holder A.

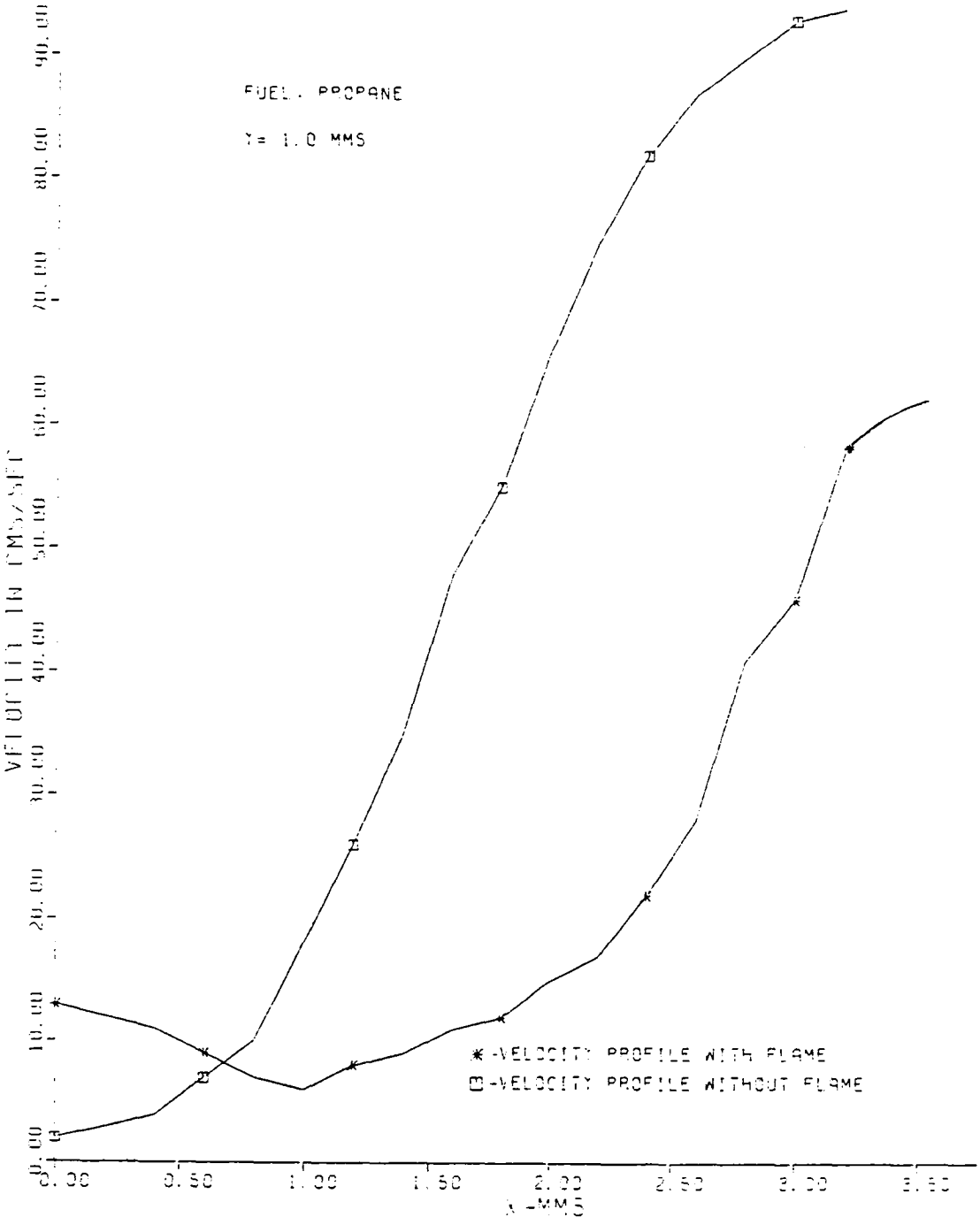

Fig.V-43. Velocity Profile of Propane-Air Mixture Along Flame Holder A.

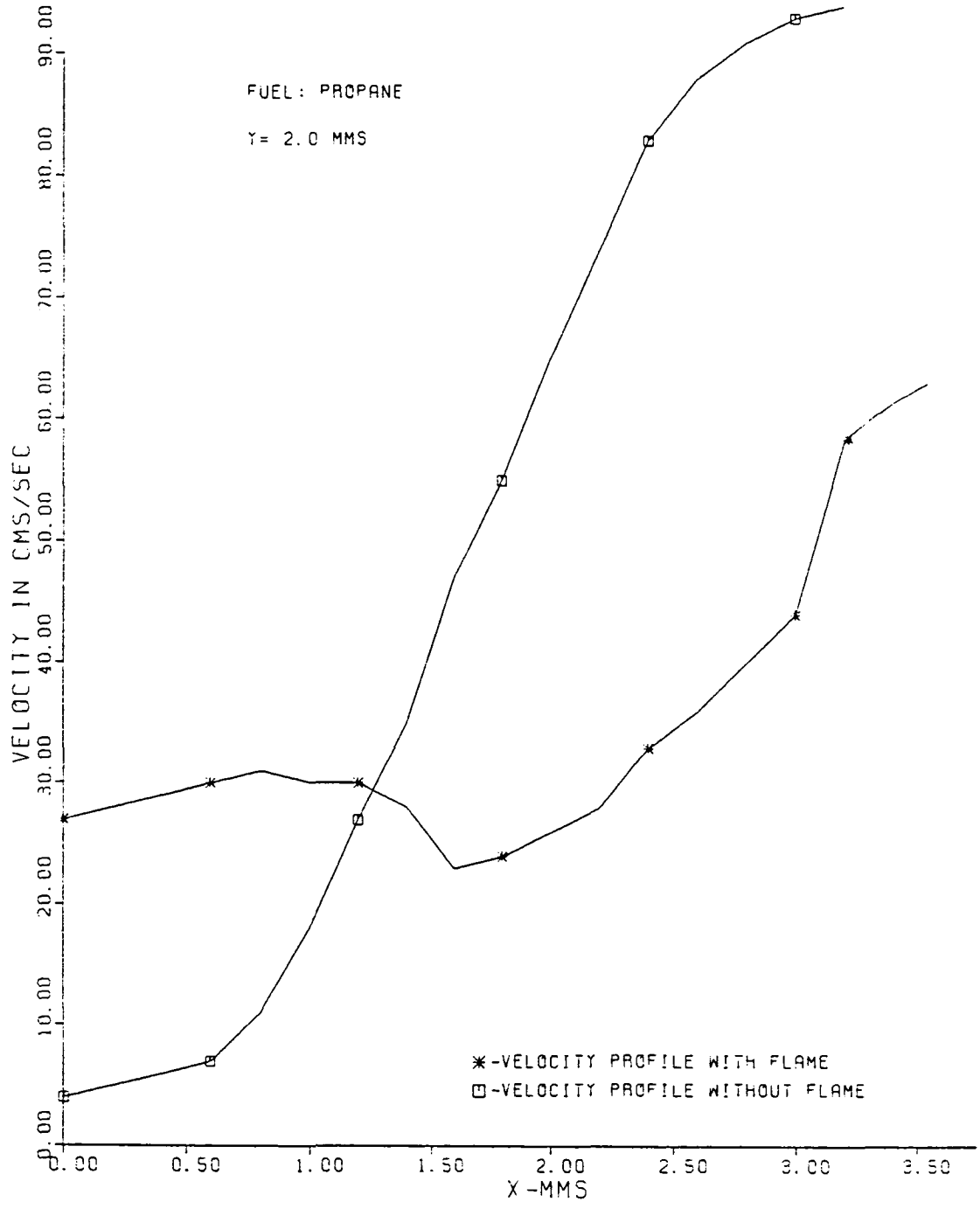

Fig.V-44. Velocity Profile of Propane-Air Mixture Along Flame Holder A.

different vertical locations starting from Y=-2.0 mm to Y=2.0 mm. In the horizontal direction data was taken from the origin of the reference coordinate system to X=3.2 mm. As in the case of methane the velocity profile with flame is displaced and the magnitude of the vertical velocity component in the boundary layer is retarded. The width of the low velocity region near the wall is again larger when the flame is present. The point along the horizontal axis where the maximum displacement occurs between these two curves is about 1.5 to 3.0 mm. The location of the point corresponding to the maximum displacement is a little larger than the value of 1.2 - 2.0 mm that was found.

Above the trailing edge of the flame holder at Y=1.0 mm, there occurs a bulge in the velocity profile curve when the flame is present. This bulge seems to shift to 1.55 mm at Y=2.0 mm. One could assume that at this point a localized perturbation occurs due to the back pressure because of the presence of flame. Generally it was found that velocity profile curves for propane were less smooth when compared to those for methane and that the blow-off phenomena for propane was very erractic and at times unpredictable.

In figure V-45 a visible light photograph similiar to that of methane flame is shown for the case of a propane flame. Thus knowing the position of the flame front it is drawn in figure V-46 together with the magnitude of the vertical velocity vectors

Flame Holder A

Air Flow Rate = 0.44 liter/sec;
Propane Concentration = 2.61%

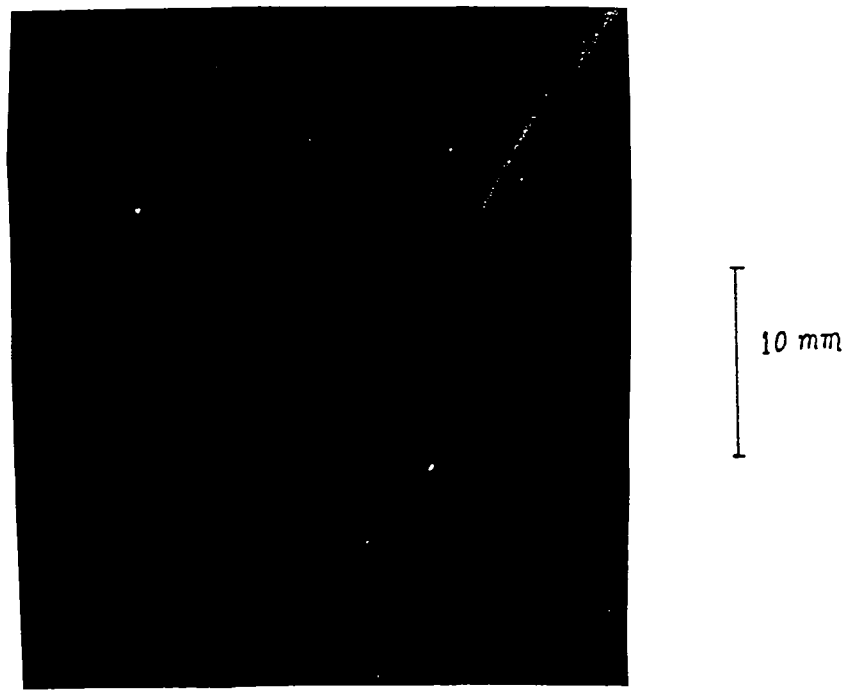

Fig.V-45. Visible Light Picture of Propane-Air Flame with Particle Injection.

Flame Holder A

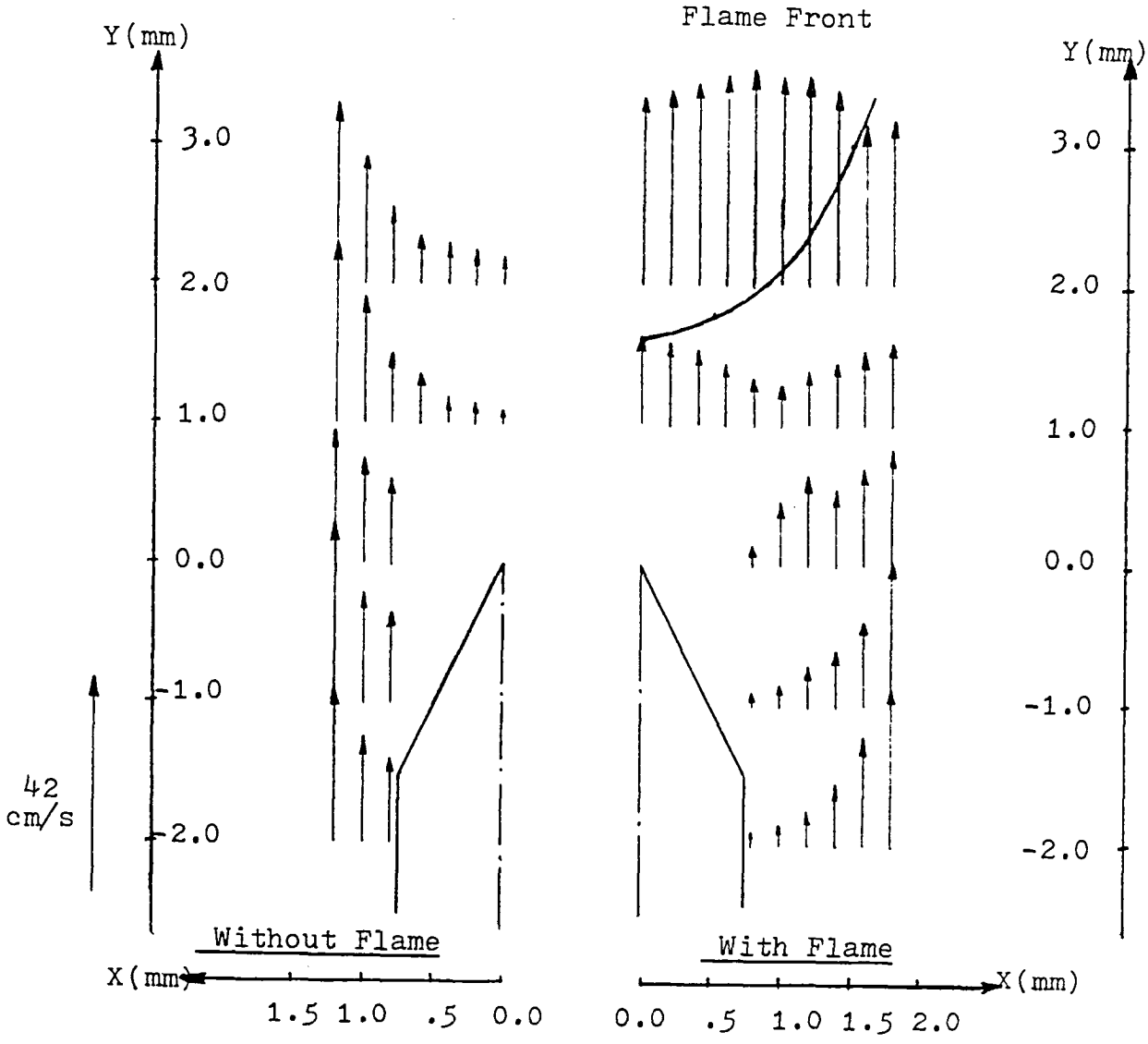

Fig.V-46. Vectorial Representation of Propane-Air Mixture With and Without Flame.

in the vicinty of the trailing edge of the flame holder A. Here the scale is little different from the similiar figure drawn for the case of methane. Everything sketched in figure V-46 is to scale. The length of the longest velocity vector represents a velocity of 42.0 cm/sec. From the position of the flame front predicted in this figure it can be said that the propane flame has a larger radius of curvature at its base than the methane flame.

Chapter 6

Interpretation of the Experimental Results and Conclusions

This concluding chapter is devoted to the interpretation of experimental results together with observations and conclusions which clarify the mechanism of flame holding.

Considering blow-off velocity curves versus fuel concentration (see figure V-1 to 4) obtained for various flame holders, it is apparent that variation in length of the flame holder does not alter the process of flame stabilization. On the other hand variation in thickness does affect the fuel-concentration at which the flame could possibly be stabilized, particularly for lean methane-air flames. At lower blow-off velocities for flame holder A and D (fig V-1a,4a), the methane fuel concentration is more or less the same but at higher blow-off velocities the methane flame could be stabilized at a leaner fuel concentration for flame holder A which is thicker than D. Also it is evident from the schlieren and visible light pictures that as the flow rate is increased, the radius of curvature of the base of the inverted flame decreases in the same manner for all the four flame holders.

The reason for a marked difference of methane fuel concentration at higher blow-off velocities can be explained by observing that these lean fuel-air mixtures are stoichiometrically unbalanced because the diffusivity of the deficient component (methane) exceeds that of the excess component (oxidizer). In such cases the mixture can stratify on entering the combustion wave which will lead to localized changes in mixture composition. This is illustrated in figure VI-1 which is a drawing of the position of the visible flame front stabilized over flame holder A and D at a blow-off velocity of 60.0 cm/sec. In the case of flame holder A the area upstream of the base of the inverted flame up to the trailing edge of the flame holder is greater than for holder D. This area is expressed as the product of the stand-off distance of the flame from the flame holder and the thickness of the flame holder, i.e d•t. The stand-off distance of the flame for both the flame holders was about the same as can be seen from the visible pictures. Hence the change in area is mainly due to the difference in thickness parameter of the flame holder and this causes a higher interdiffusion of the deficient more mobile methane into this region. Consequently at the holding point (along the centerline of the flame holder) the area of the reaction zone downstream of the trailing edge will have a higher concentration of methane (due to its higher diffusivity relative to that of the oxidizer). This increases the local methane concentration above that of the original mixture and thus enables

Methane-Air Flame

Blow-off Velocity=60cm/s

r_{crit}=1.6mm

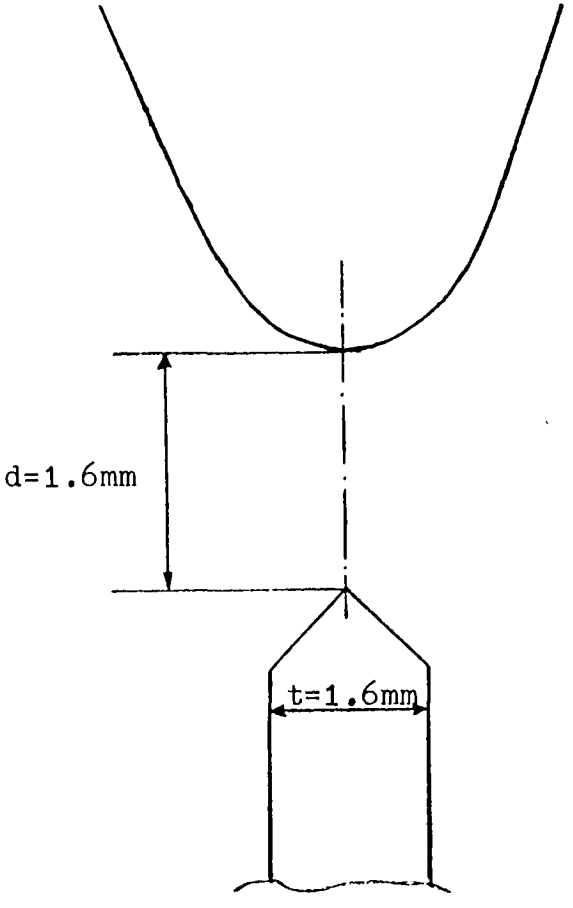

Flame Holder A

Blow-off Velocity=60.25cm/s

r_{crit}=1.6mm

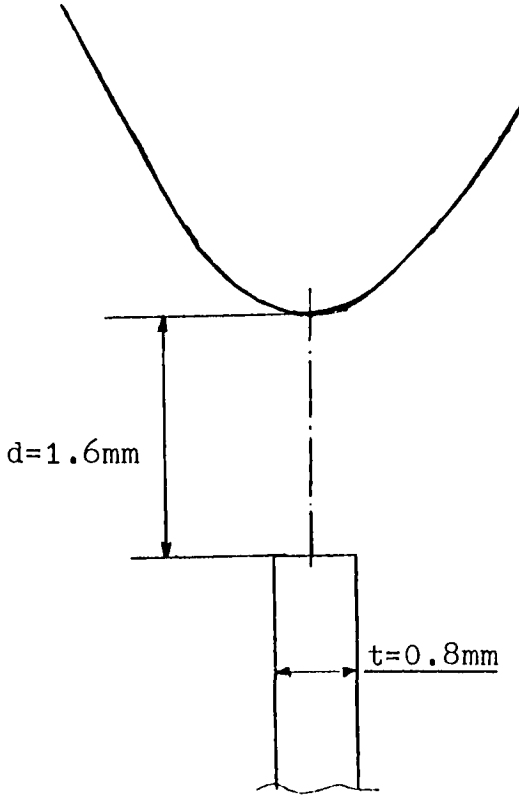

Flame Holder D

Fig.VI-1. Flame Holder Thickness Effect.

the flame to be stabilized at higher approach flow velocities or for leaner mixture composition at the same flow velocity. Another important aspect in this case is the fact that changes of composition occur because the concentration gradients are larger and not as parallel to the flow lines in the case of flame holder A, when compared to the streamlines downstream of flame holder D.

At incipient blow-off the radii of curvature of the base of inverted flames for methane and propane are markedly different from each other, though there is not much variation in radius from one flame to the other for each fuel. The radius of curvature at incipient blow-off taken from visible and schlieren pictures for flame holders A and D are plotted against blow-off velocities and presented in figure VI-2 and 3 respectively. These figures show that the radii of curvature do not change with flame holder for each fuel and approach flow velocity. It is also seen that there is a distinctive slope of proportionality for each fuel corresponding to a minimum radius of curvature r_{crit} at blow-off for each particular fuel concentration. There is a sharp decrease in the radius at higher blow-off velocities. This general trend is common for both the fuels. It is also observed that the radius of curvatures of the schlieren and visible light photographs tend to converge at higher blow-off velocities.

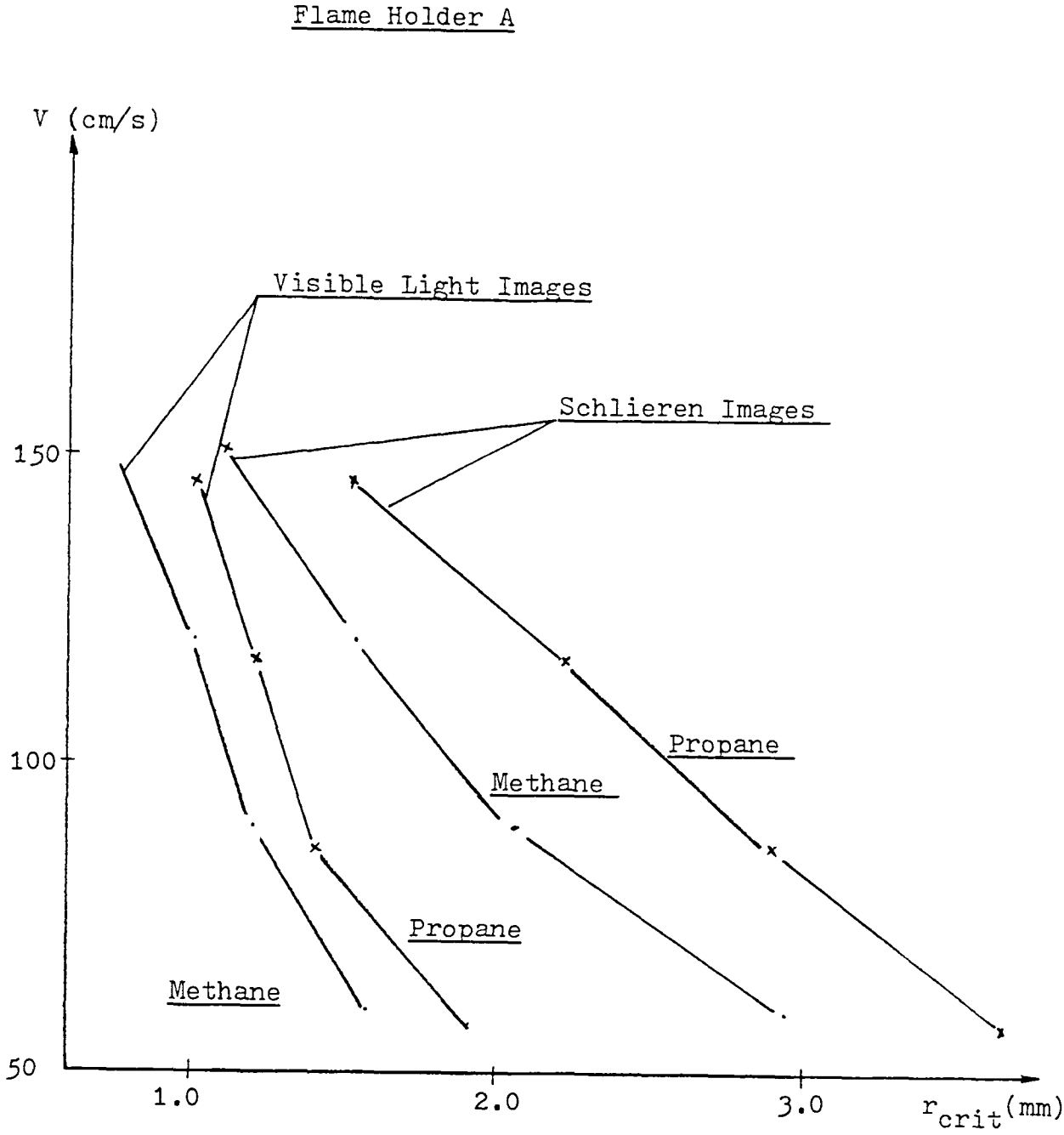

Fig.VI-2. The Radius of Curvature at Incipient Blow-Off.

Flame Holder D

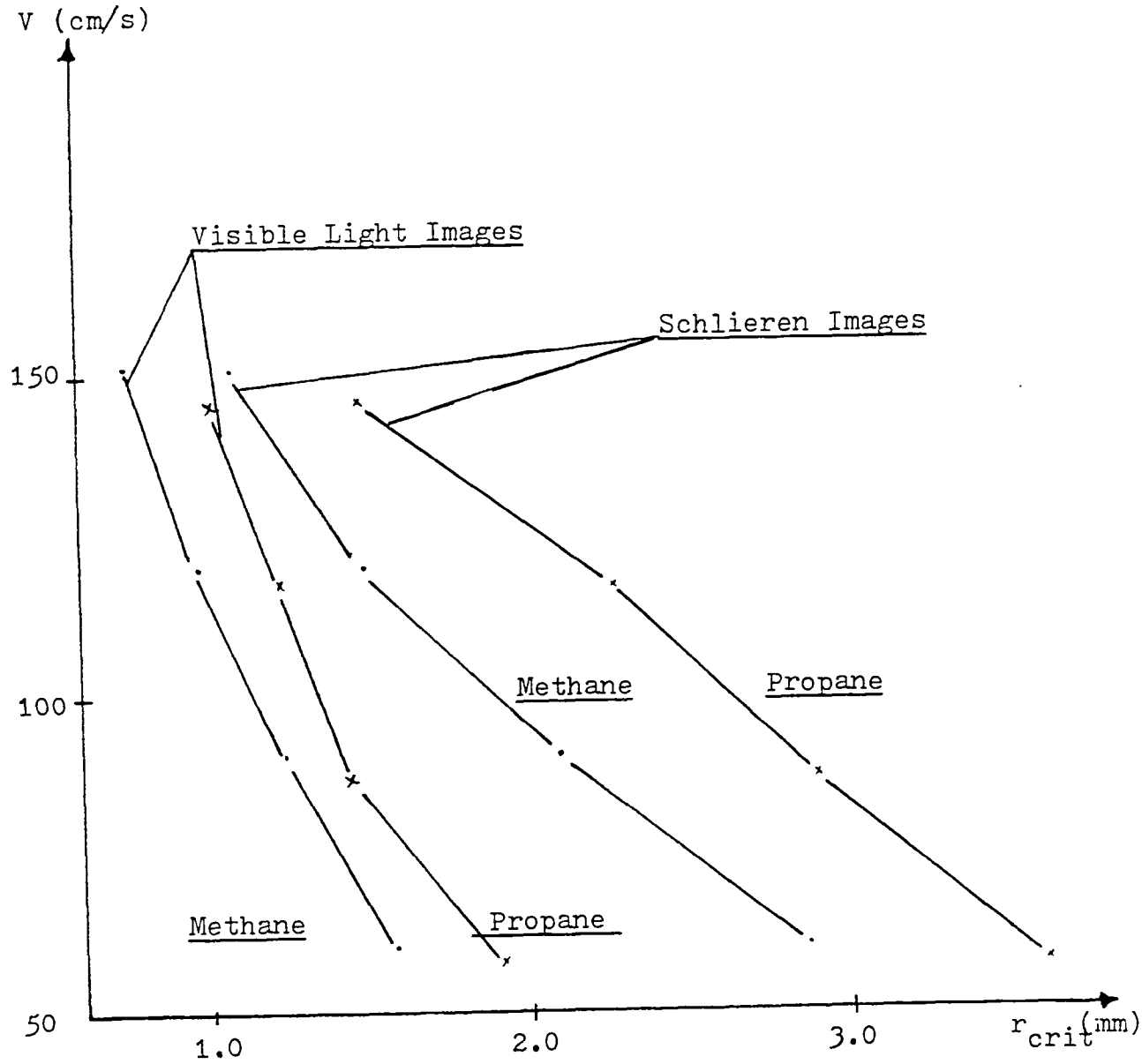

Fig.VI-3. The Radius of Curvature at Incipient Blow-Off.

It is interesting to observe the behavior of the product of the radius of curvature and blow-off velocity versus the equivalence ratio. Figure VI-4 shows this behavior for holder A for both the fuels. It is important to note that the product of r_{crit} and blow-off velocity ($r_{crit}.V$) is almost a constant for schlieren and visible light images for both the fuels. The values of equivalence ratio correspond to the values at which the pictures of the flame for both the fuels were taken. From this figure it is seen that values of $r_{crit}.V$ for the visible light image for both the fuels are much closer to each other and the slight variation of these values are similar for both the lean methane- and propane-air flames. On the other hand the values of $r_{crit}.V$ for schlieren image is significantly different for lean methane and lean propane flames. Also the size of the schlieren images (~ upstream distance between the edges of visible light and schlieren images) for methane and propane are different from each other and vary in the range of 1.15 and 0.9 mm for methane and propane respectively. This indicates that different controlling processes are occuring in the preheat zone for both the fuels which evidently affects the blow-off mechanism. It can be suggested that the Damköhler number,being the ratio of characteristic aerodynamic and chemical times, acquires qualitatively speaking a specific critical value in the preheat zone of the respective flames.

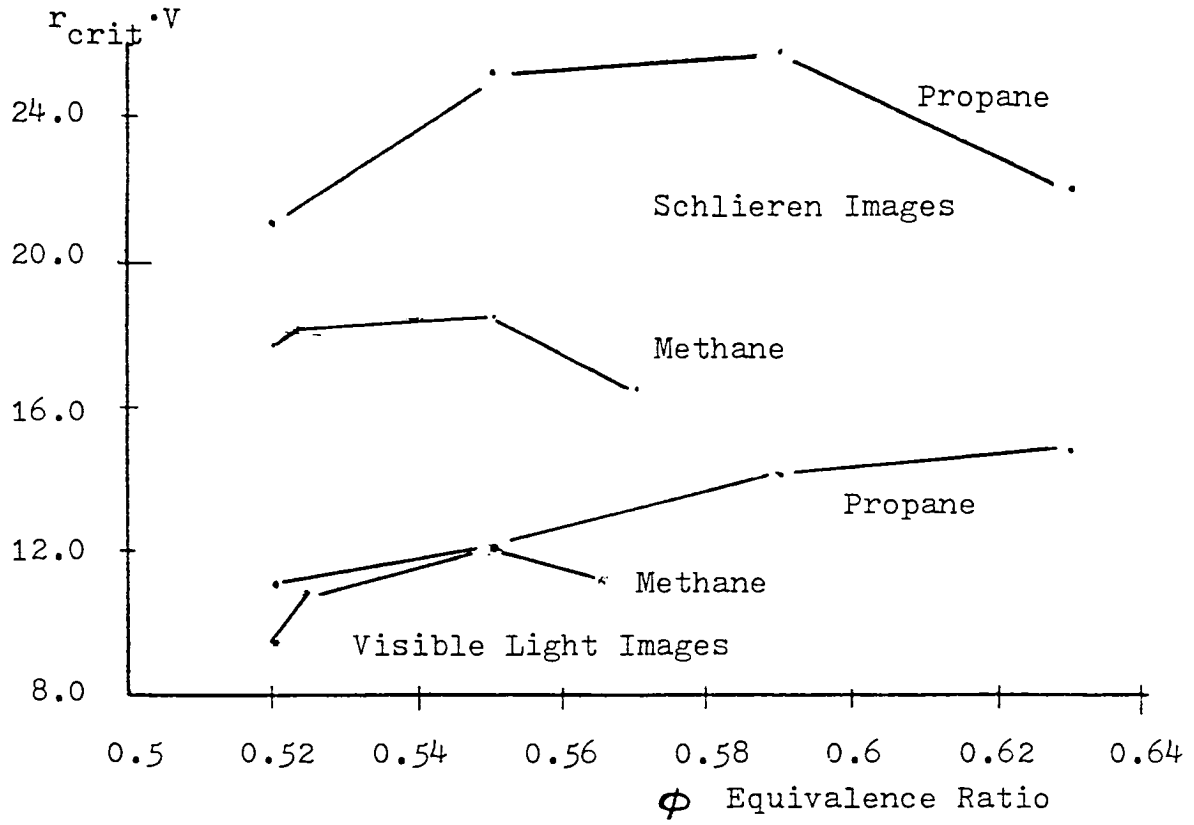

Fig.VI-4. Behavior of $r_{crit} \cdot V$ for Flame Holder A.

Referring to figures VI-2 and 3 it can be seen that the difference between the radii of curvature of schlieren and visible light pictures for higher blow-off velocity (in the range of 150 cm/sec) is:

$(r_{schl} - r_{visib})_{crit} = \sim 0.35$ for Methane

$(r_{schl} - r_{visib})_{crit} = \sim 0.50$ for propane

as compared to lower blow-off velocity, where the difference is:

$(r_{schl} - r_{visib})_{crit} = \sim 1.35$ for methane

$(r_{schl} - r_{visib})_{crit} = \sim 1.75$ for propane

From this one could suggest that propane-air flame is more spread out at the base and is liable to have wider interaction with the upstream flow which would result in the outflow of heat in the upstream direction and also increase the chances of the reaction to go to completion in the reaction zone. Also it can be assumed that smaller radius of curvature for methane must be due to incomplete reaction as was experimentally concluded by Tsuji and Yamaoka for their particular flow configuration. The above observations show as one would expect that the thickness of preheat region is of the order represented by the difference between the location of the schlieren image and the visible image, is decreasing at higher blow-off velocities i.e at higher fuel concentration.

The preheat zone thickness can be determined from the expression,

$$\eta_o = \frac{k}{\rho_m c_p S_u}$$

where k is the thermal conductivity of the mixture, c_p is the specific heat capacity of the mixture and ρ_m is the density of the mixture. These thermodynamic and transport properties for methane-air were calculated by using the subroutines prepared by L. D. Savage [41], in case of propane-air mixture the properties were calculated by the method described by R.B. Bird [42], as the transport properties for propane air mixture were not available in the above mentioned subroutines. The values of c_p , k and ρ_m are given below in table 6.1 for methane and propane. The values of transport and thermodynamic properties were evaluated at a temperature which was the average value of the unburnt mixture temperature and the adiabatic flame temperature. Thus the values of the equivalence ratio correspond to the case of flame holder A.

In figure VI-5 are plotted the values of η_o versus the blow-off velocities for both the fuels. One can clearly see the decrease in preheat zone thickness at higher blow-off velocities. This behavior clearly agrees with the variation of radius of curvature of the schlieren image versus blow-off velocity. It is worthwhile to note here that the decrease in η_o for the case of propane-air flame is less than methane-air flame as the blowing rate is increased.

Table 6.1

Φ	R (J/m.s.K)	ρ (kg/m³)	c_p (J/kg.K)	S_u^* (m/s)	η_o (mm)
			Methane-Air Mixture		
.52	0.0596	0.343	1700.3	0.105	0.97
.524	0.0598	0.341	1709.5	0.11	0.93
.55	0.06	0.328	1721.4	0.12	0.88
.57	0.0613	0.322	1727.6	0.135	0.82
			Propane-Air Mixture		
.52	0.0671	0.348	1632.4	0.215	0.55
.55	0.0678	0.333	1639.2	0.23	0.54
.59	0.0682	0.324	1648.2	0.24	0.53
.63	0.0687	0.318	1656.3	0.25	0.52

* The values of S_u were taken from [43, and 6] for methane and propane respectively.

Hence it can be assumed that the increase in blowing rate for the case of methane-air flame has a more profound effect on the preheat zone thickness and reaction kinetics of methane-air flame. It is known that at higher fuel concentrations η_o decreases and this is observed in figure VI-5, where higher blow-off velocities represent increase in fuel concentration. The variation of r_{crit} is in a way similiar to η_o in the sense that the former value also decreases with higher fuel concentration as does η_o. It is apparent from the above table that lean methane-air flame has a larger value of η_o than lean

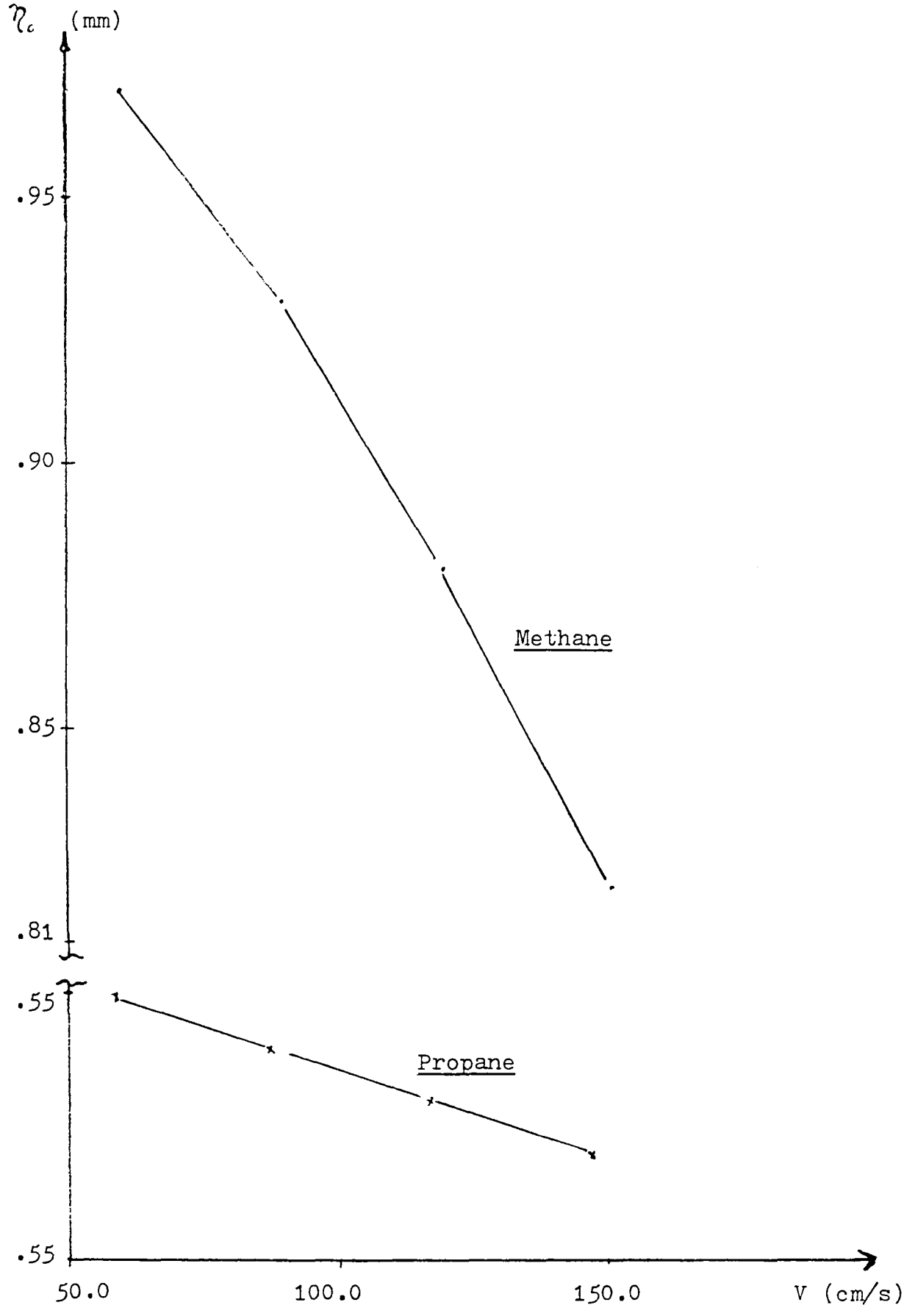

Fig.VI-5. η_o versus Blow-Off Velocity for Flame Holder A.

propane-air flame and it can be concluded for this case that the fuel deficient or more mobile reactant (methane) gets heated earlier (for a longer time) making the species move across the reaction zone faster, hence lower residence time in the reaction zone, and due to higher diffusivity change the concentration of the mixture locally in the preheat zone. The difference in preheat zone thickness for both the fuels can be attributed to different burning velocities for each fuel.

Since the approach flow fuel concentrations are known for each value of r_{crit} corresponding to particular blow-off velocities one can determine the normal adiabatic flame temperature [7]. The values of blow-off velocity versus the adiabatic flame temperature are plotted in figurw VI-6 for methane and propane. The variation in equivalence ratio for both the fuels is given in table 6.1, for which these temperatures are calculated. It is evident from figure VI-6 that flames near blow-off or to be more general, near extinction show a higher approach flow flame temperature for lean propane-air than lean methane-air flames. Preferential diffusion will cause the local methane flame temperature to be higher

Before making further interpretation of the experimental results pertaining to the process of flame blow-off or flame extinction, it is important to point out that the fuel oxidizer mixture can adequately be represented as a one-reactant system

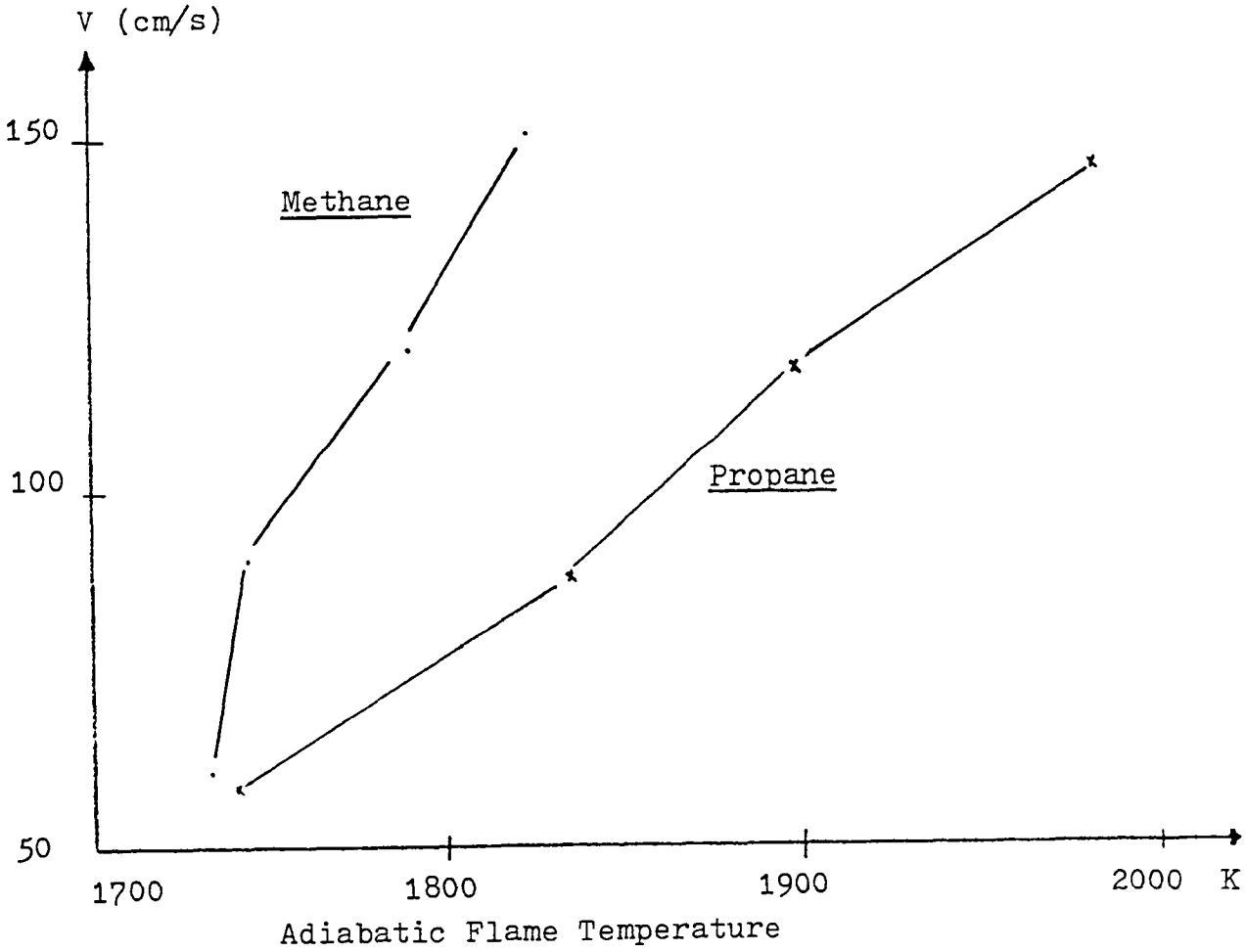

Fig.VI-6. Blow-Off Velocity vs Adiabatic Flame Temp.

controlled by the concentration of the deficient reactant. Thus for this system the relevant binary diffusion coefficient, D_{AB} , is that for the deficient reactant (say the fuel, methane or propane) and the inert. In this experimental study the binary diffusion coefficient of the deficient reactants with nitrogen are used as the diffusion coefficients, because the nitrogen concentration in all the mixtures used is much higher than the concentration of the other species.

As has been mentioned earlier in chapter III, diffusive transport is normal to the flame while convective transport is along the streamlines which are divergent relative to the flame. Thus the flame behavior, in particular its temperature, depends on the relative rates of heat and mass diffusion, which can be represented by the Lewis number,

$$Le = \frac{c_p \rho D_{AB}}{R}$$

From the definition of Lewis number it is obvious that for Le = 1.0 heat loss and mass gain occur at the same rate such that the flame temperature T_f is equal to the adiabatic flame temperature T_{ad} . In order to calculate the Lewis number one has to know the binary diffusion coefficient for the deficient reactant. The coefficient was calculated by the approximate method given by J.O. Hirschfelder, and R.B. Bird [44]. D_{AB} was found to be 0.112 cm^2/sec and 0.218 cm^2/sec for propane and methane respectively. Lewis number with respect to the equivalence ratio of both the fuels methane and propane are presented in table 6.2.

Table 6.2

Deficient Reactant	Equivalence Ratio	D_{AB} [cm^2/s]	Lewis Number
CH_4-Air	0.52	0.218	1.02
C_3H_8-Air	0.52	0.1125	0.53

The Lewis number of the deficient reactant of lean propane-air flame is much smaller than unity and this means outflow of heat by conduction from the reaction zone toward the unburnt mixture is not balanced by the inflow of the deficient reactant by diffusion from the unburnt mixture into the reaction zone. This eventually alters the picture in the sense that although the reaction is complete in that the deficient reactant (propane) is totally consumed in crossing the flame, the flame temperature is reduced (Le<1.0: $T_f < T_{ad}$) and the flame is blown off by the reduction in burning velocity at the centerline (stabilization point). The concentrations of the reactants have been experimentally determined by Tsuji [32] and it has been verified by them that the concentrations of the unburnt reactants for lean propane-air were near zero across the flame.

The above mentioned case corresponds to the deficient reactant which is less mobile one (higher diffusivity of the oxidizer). On the other hand if the deficient reactant is the

more mobile one as is the case for lean methane-air mixtures, when the Lewis number (table 6.2) is equal to 1.02. From the fact that Le $>$ 1.0, one can conclude that the inflow of the deficient reactant into the reaction zone slightly outweighs the outflow of heat from the reaction zone. In this case flame extinction can be attributed to a further increase in the blow-off velocity. This can be explained if one looks at the blow-off velocity versus fuel concentration in case of flame holder A for both the fuels methane and propane (figure V-1a,b) The blow-off velocity for methane at Φ =0.55 (fuel concentration = 5.44%) occurs at 120 cm/sec while for propane at ϕ =0.55 (fuel concentration =2.24%) occurs at 89 cm/sec (see figure VI-7). This shows that due to the increase in the blowing rate in the case of methane-air flame complete reaction is not possible because of the reduced residence time in the reaction zone and eventually extinction will occur. The fact that the flame extinction occurs as a result of incomplete combustion in the reaction zone can be verified by looking at the concentrations of reactants across the flame. The values of lean methane-air concentrations were found by Tsuji and Yamaoka [32] in their experimental work, and it is seen here that the concentration of the unburnt reactants is significant. Thus the reactions in the flame zone are not completed near the extinction limit. From the above remarks it may be concluded that complete reaction is not possible in case of lean methane-air flame as compared to lean propane-air flame and this factor over weighs the effect of

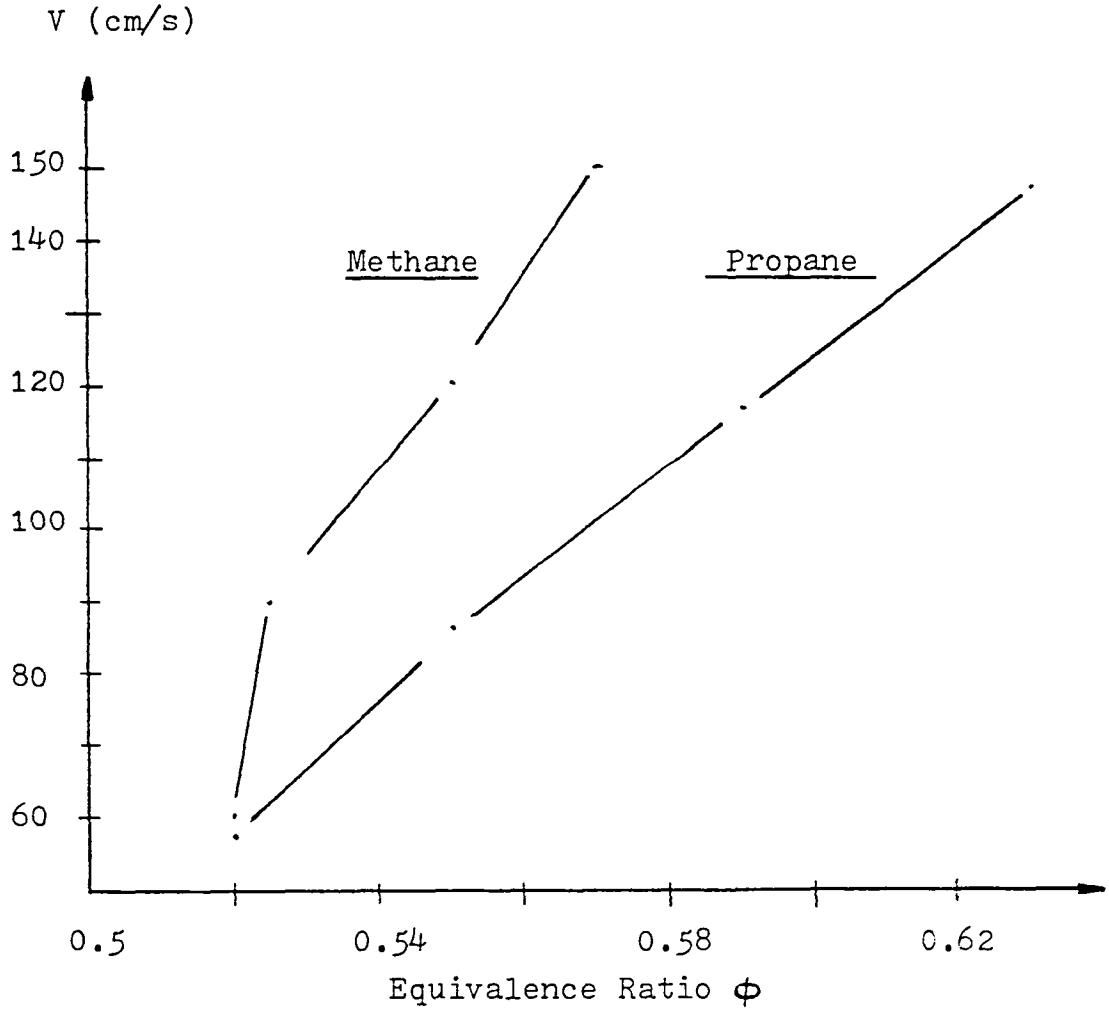

Fig.VI-7. Blow-Off Velocity vs Equivalence Ratio.

higher diffusion coefficient of the deficient reactant methane. But for the case of lean propane-air flame it can be concluded that reaction does go to completion and extinction is attributed mainly to stretch.

In view of the above considerations and in regard to the recent work of Tsuji and Yamaoka [32] and Ishizuka and Law [34], it is reasonable to conclude that there now exists convincing experimental evidence indicating that extinction of a premixed flame by positive stretch alone is possible only if the deficient species is also the less mobile one, i.e lean propane-air flame. But in case of lean methane-air flame a different factor affects the extinction, i.e incomplete combustion.

As has been discussed in the previous chapter, Laser Doppler Velocimetry techniques were used to determine the velocity flow field around the trailing edge of various sizes of flame holders. This kind of measurement enables one to determine the qualitative effects due to the flame presence in the flow field especially pertaining to effects on the boundary layer and in the vicinity of the trailing edge. The velocity profiles taken for all the flame holders showed a similiar trend irrespective of the type of flame holder being used. Thus it will be worthwhile to look at closely the LDV measurenments taken for both the flame holders A and D for both the fuels. The

velocity of the particles exiting from the burner outlet is laminar and one can estimate the boundary layer thickness which has not yet seperated from the flame holder with and without the presence of flame. In general the thickness of the boundary layer decreases with viscosity, or it decreases as the Reynolds number increases. In this two dimensional problem, U_o is referred to as the free stream velocity which coincides with the y direction, and all the linear dimensions are referred to a characteristic length, l which is the length of the flame holder (see figure IV-7). From the condition of equality of the friction and inertia forces in the laminar boundary layer

$$\mu \cdot \frac{U}{\delta^2} \sim \frac{\rho U^2}{y}$$

where μ is the viscosity of the mixture, δ is the boundary layer thickness and l is the variable distance from the leading edge. Thus for a laminar boundary layer

$$\delta = 5\sqrt{\mu l / \rho \cdot U}$$

where 5 is the numerical factor for the exact solution [45].

In order to determine the multicomponent viscosity of the reactive gas mixture of methane-air and propane-air, the semiempirical formula of Wilke [46] is used. The Chapman-Enskog theory has been extended to include multicomponent gas mixtures by Curtis and Hirschfelder [44], but for most purposes, Wilke's formula is quite adequate.

$$\mu_{mix} = \sum_{i=1}^{n} \frac{x_i \mu_i}{\sum_{j=1}^{n} x_j Z_{ij}}$$

$$Z_{ij} = \frac{1}{\sqrt{8}} \left(1 + \frac{M_i}{M_j}\right)^{-1/2} \left[1 + \left(\frac{\mu_i}{\mu_j}\right)^{1/2} \left(\frac{M_j}{M_i}\right)^{1/4}\right]$$

Here n is the number of components in the mixture; x_i and x_j are the mole fractions of components i and j; μ_i and μ_j are the viscosities of component i and j at room temperature and pressure, and M_i and M_j are the corresponding molecular weights. Note the Z_{ij} is dimensionless and, when i=j, $Z_{ij}=1$.

In table 6.3 are given the calculated values of boundary layer thickness from the above mentioned formula [45] at the trailing edge with and without the flame. In these calculations the density of the respective fuel-air mixture is calculated by using the following expression:

$$\sum_i \rho_i = \sum_i \frac{P_i}{R_i T_m} = \frac{P_m}{8314.3 \cdot T_m} \cdot \sum_i x_i M_i = \rho_m$$

The methane concentration in this case was 6.25% (ϕ =0.633) and propane concentration was 2.61% (ϕ =0.64).

Table 6.3

	δ [mm]	ν [cm^2 /sec]	U_o [cm/sec]
Methane-Air Mixture			
With Flame	2.6	0.152	73.0
Without Flame	2.4	0.152	81.2
Propane-Air Mixture			
With Flame	3.0	0.144	54.6
Without Flame	2.5	0.144	83.6

From the calculated boundary layer thickness it is clear that with the presence of flame the boundary layer thickness increases, and the particle velocity in the boundary layer is retarded. Comparing the calculated values of δ from table 6.3 with the LDV measurements of figure V-17 for methane and figure V-42 for propane, one finds similar values of δ with and without the flame. In the case when a propane-air flame is present one sees higher displacement of U_o because the radius of curvature of this flame is higher. This in effect causes the flame presence to be felt further upstream than for the case of a methane-air flame. It is obvious from these results that the presence of flame does affect the flow field in the manner that free stream velocity in the vicinity of the flame front is lowered due to the back pressure effect of the flame. The reason for the propane-air flame having a larger boundary layer thickness is related to the larger radius of curvature of the base of the flame. From this one can conclude that boundary layer thickness increases with radius of curvature of the base of the inverted flame, i.e $r_{crit} \sim \delta$. Therefore at blow-off, one would expect the boundary layer thickness to be minimum but still larger than when the flame is absent.

Looking back at figures V-38 and V-39, which show the deflection of streamlines due to the presence of propane-air and methane-air flames stabilized over flame holder D, one can measure the change in area of the streamlines before and after

the flame. Then with the help of equation of continuity, the density change across the flame can be evaluated, and from the equation of state the temperature downstream of the flame front determined. These calculations are presented below for methane- and propane-air mixtures. The fuel concentration for methane in this case was 6.5% (ϕ=0.67) and for propane was the same as for the flame holder A, i.e 2.61% (ϕ=0.64).

Calculation of Methane-air flame temperature

From figure V-39 (ϕ=0.67)

Density of the mixture ρ_m [kg/m^3] = 1.163

P_m = 101325 N/m^2]

R = 8314.3 J/Kgmole.K

T_m = 293 K

ρ_b = 0.1847 kg/m^3

T = P.M/ ρ.R = 1855 K

Calulation of Propane-air flame temperature

From Figure V-38 (ϕ=0.64)

Density of the mixture ρ_m [kg/m^3] = 1.216

P_m = 101325 N/m^2]

R = 8314.3 J/Kgmole.K

T_m =293 K

ρ_b = 0.198 kg/m^3

T =P.M/ ρ.R = 1800 K

Hence the calculated flame temperatures from V-38 and V-39 for methane and propane are 1855 K and 1800 K respectively. Comparing these values of flame temperature with the adiabatic flame temperature [7], one sees that due to higher diffusivity of deficient reactant methane into the reaction zone and also Le being slightly greater than 1.0 the flame temperature for methane-air flame is slightly higher than the adiabatic flame temperature (1845 K). On the other hand, in case of propane-air flame, the flame temperature is markedly lower than the adiabatic flame temperature (1900 K) because of Le<1.0. From these results it is seen that if the deficient reactant is the more mobile one as is the case for lean methane-air mixture, due to higher diffusivity the mixture concentration locally increases which leads to a corresponding increase in temperature. Such that blow-off (extinction) cannot be affected by stretch alone. Therefore inorder to achieve blow-off or extinction one has to allow the possibility of incomplete reaction due to the further increase in blowing rate leading to reduced residence time. On the other hand in case of lean propane-air flame the reaction is complete and there is no further increase in temperature and extinction occurs due to stretch alone.

In conclusion of this study it is reasonable to state that the present experiments have yielded convincing evidence of the blow-off mechanism of a stretched premixed flame. It can be said that blow-off is similiar to extinction of various kinds of

flames observed by other workers. One clearly sees that there are different mechanism operative at the time of extinction for lean propane and methane flames. Extinction occurs for lean propane-air flame inspite of the reaction going to completion and the disparity between the heat loss and the gain in mass diffusion in the reaction zone i.e Le<< 1.0 causes the flame to blow-off. Hence extinction by stretch alone is possible only when the deficient reactant is the less mobile one. On the other hand, if the limiting reactant is the more mobile one, then the controlling factor for blow-off is incomplete reaction due to higher blowing rate leading to reduced residence time in the reaction zone.

References

1. Lewis, B., von Elbe, G., Combustion, Flames and Explosions of Gases. Academic Press Inc. New York and London. 1961, Second Edition, Page 220.

2. Edmondson, H., Heap, M. P., Combustion and Flame, 14, 191 (1970).

3. Kawamura, T., Asato, K., Mazaki, T., Combustion and Flame, 45, 225, (1982).

4. Reed, S. B., Combustion and Flame, 11, 177, (1967).

5. Reed, S. B., Combustion and Flame, 17, 105, (1971).

6. Lewis, B., von Elbe, G., Combustion, Flames and Explosions of Gases. 1961. Page 389.

7. Computer package for calculation of adiabatic flame temperature written by Strehlow R. A., Dept. of Aeronautical Eng., Univ. of Illinois.

8. Fristorm, R. M., Westenberg, A. A., Flame Structure, McGraw-Hill Book Company, 1965, Page 93.

9. Mallard, E., Le Chatelier, H. L., Combustion des melanges gazeux explosifs. Ann. des Mines, ser, 8, 3:274-378.

10. Tanford, C., Pease, N., Journ. Chem. Physics, 15, 7, (1942).

11. Tanford, C., Pease, N., Journ. Chem. Physics, 13, 7, (1947).

12. Hirschfelder, J. O., Curtiss, C. F., Journ. Chem. Physics, 17, 11, (1949).

13. Streklow, R. A., Fundamentals of Combustion, Robert E. Kreiger Publishing Company, Huntington, New York (1979).

14. Friedman, R., Burke, E., Journ. Chem. Physics, 21, 4, (1953).

15. Smoot, L, D., Hecker, W. C., Williams, G. A., Combustion and Flame, 26, 3, (1976).

16. Levy, A., Weinberg, F. J., Combustion and Flame, 3, 229, (1959).

17. Fendell, F. E., Journ of Fluid Mechanics, 21, 281,

(1965).

18. Bush, W. B., Fendell, F. E., Combustion Science and Technology, 421, (1970).

19. Fendell, F. E., Journ. of Fluid Mechanics, 56, 81, (1972).

20. Karlovitz, B., Denniston, D. W., Knapschaefer, D. H., Wells, F. E., Fourth Symposium (International) on Combustion, The Combustion Institute, Pittsburgh, PA (1953).

21. Markstein, G. H., Non-Steady Flame Propagation, A Pergamon Press Book, The Macmillan Company New York (1964).

22. Lewis, B., von Elbe, G., Journ. Chemical Physics, 11, 75, (1942).

23. Elbe von, G., Menster, M., Journ. Chemical Physics, 13, 89, (1945).

24. Reed, S. B., "A unifying theory for the blow-off of aerated burner flames", Institute of Gas Engineering Journ., 8, 157, (1968).

25. Edmondson, H., Heap, M. P., " A precise test of the flame-stretch theory of blow-off", Twelfth Symposium (International) on Combustion, The Combustion Institute, Pittsburgh, PA (1969).

26. Edmondson, H., Heap, M. P., Combustion and Flame, 15, 179, (1970).

27. Kawamura, T., Asato, K., Mazaki, T., Hamaguchi, T., Kayanara, H., Combustion and Flame, 35, 109, (1979).

28. Melvin, A., Moss, J. B., Combustion Science and Technology 7, 189, (1973).

29. Haniff, M. S., Melvin, A., "The stabilizing region of premixed methane-air flames", Eighteenth Symposium (International) on Combustion, The Combustion Institute, Pittsburgh, PA (1981).

30. Sivashinsky, G. I., Acta Astranautica 4, 1207, (1977), Pergamon Press.

31. Tsuji, H., Prog. Energy Combust. Sci., 18, 93, (1982), Pergamon Press Ltd.

32. Tsuji, H., Yamaoka, I., "Structure and Extinction of Near-Limit flames in a stagnation flow", Nineteenth Symposium (International) on Combustion, The Combustion Institute (1982).

33. Sato, J., Tsuji, H., Combustion Science and Technology, 33, 193, (1983).

34. Ishizuka, S., Law, C. K., "An experimental study on extinction and stability of stretched flames", Nineteenth Symposium (International) on Combustion, The Combustion Institute, (1982).

35. Strehlow, R. A., Combustion Fundamentals McGraw-Hill Book Company, (In Print).

36. James, R. N., Babcock, W. R., Seifert, H. S., "A laser-doppler technique for the measurement of particle velocity", Journ. AIAA, 6, 160, (1968).

37. Kunii, D., Levespiel, O., Fluidization Engineering, Wiley, New York (1969).

38. Reuss, D., Doctoral Thesis, Dept. of Aeronautical and Astronautical Engineering, Univ of Illinois, (1979).

39. Guichard, J. C., Aerosol Generation Using Fluidized Beds, (Ed. Liu, B. Y. H.,) Academic Press, New York and London, (1976).

40. Durst, F., Kleine, R., " Velocity measurements in turbulent premixed flames by means of laser doppler anemometers", Univ. Karlsruhe, Sonderforschungsbereich 80, Report SFB 80/EM/10, (1973).

41. Savage, Jr. L. D., Combustion Lab., Dept., of Mech. Engineering, University of Illinois at Urbana-Champaign, (1980).

42. Bird, R. B., Stewart, W. E., Lightfoot, E. N., Transport Phenomena, John Wiley & Sons, Inc., (1960).

43. Andrews, G. E., Bradley, D., Combustion and Flame, 20, 77, (1973).

44. Hirschfelder, J. O., Curtiss, C. F., Bird, R. B., Molecular Theory of Gases and Liquids, John Wiley & Sons, (1954).

45. Schlichting, H., Boundary-Layer Theory, McGraw-Hill Book Company, Seventh Edition, (1970).

46. Wilke, C. R., Ind. Eng. Chem, 41,1345,(1949).

1. Report No.	2. Government Accession No.	3. Recipient's Catalog No.
NASA CR-3866		

4. Title and Subtitle	5. Report Date
The Mechanisms of Flame Holding in the Wake of a Bluff Body	March 1985
	6. Performing Organization Code

7. Author(s)	8. Performing Organization Report No.
Roger A. Strehlow and Sarmad Malik	None
	10. Work Unit No.

9. Performing Organization Name and Address	11. Contract or Grant No.
University of Illinois at Urbana-Champaign Urbana, Illinois 61801	NAG3-60
	13. Type of Report and Period Covered
	Contractor Report

12. Sponsoring Agency Name and Address	14. Sponsoring Agency Code
National Aeronautics and Space Administration Washington, D.C. 20546	505-31-42 (E-2382)

15. Supplementary Notes

Final report. Project Manager, Charles E. Baker, Aerothermodynamics and Fuels Division, NASA Lewis Research Center, Cleveland, Ohio 44135.

16. Abstract

In the present study the flame holding mechanism for lean methane- and lean propane-air flames is examined under conditions where the recirculation zone is absent. The main objective of this work is to study the holding process in detail in an attempt to determine the mechanism of flame holding and also the conditions where this mechanism is viable and when it fails and blow-off occurs. Inverted flames held in the wake of a flat strip were studied. Experiments with different sizes of flame holders have been performed. The velocity flow field was determined using a Laser Doppler Velocimetry technique. Equation of continuity was used to calculate the flame temperature from the change in area of flow streamlines before and after the flame. Observations of the inverted flame itself were obtained using schlieren and direct photography. Results show that there are different mechanisms operative at the time of blow-off for lean propane and methane flames. Blow-off or extinction occurs for lean propane-air flame in spite of the reaction going to completion and the disparity between the heat loss and the gain in mass diffusion in the reaction zone i.e., Le < 1.0 causes the flame to blow-off. For methane-air flame the controlling factor for blow-off is incomplete reaction due to higher blowing rate leading to reduced residence time in the reaction zone.

17. Key Words (Suggested by Author(s))	18. Distribution Statement
Combustion Flame stabilization	Unclassified - unlimited STAR Category 07

19. Security Classif. (of this report)	20. Security Classif. (of this page)	21. No. of pages	22. Price*
Unclassified	Unclassified	194	A09

*For sale by the National Technical Information Service, Springfield, Virginia 22161

NASA-Langley, 1985

National Aeronautics and
Space Administration

Washington, D.C.
20546

Official Business
Penalty for Private Use, $300

SPECIAL FOURTH CLASS MAIL
BOOK

Postage and Fees Paid
National Aeronautics and
Space Administration
NASA-451

NASA

POSTMASTER: If Undeliverable (Section 158
Postal Manual) Do Not Return